A Medicinal Chemistry Approach to Drug Repositioning in the Treatment of Tuberculosis and Malaria

Gurminder Kaur

University of Cape Town

August 2016

Supervisor: Signed by candidate Signature Removed

Student: Signed by candidate Signature Removed

A Medicinal Chemistry Approach to Drug Repositioning in the Treatment of Tuberculosis and Malaria

Thesis

Submitted to **University of Cape Town**

For the award of degree of

DOCTOR OF PHILOSOPHY

Supervised by:

Prof. Kelly Chibale

Submitted by:

Gurminder Kaur

Department of Chemistry, University of Cape Town, South Africa

Declaration

The work presented in the thesis entitled, "**A Medicinal Chemistry Approach to Drug Repositioning in the Treatment of Tuberculosis and Malaria**" has been done by me and not submitted elsewhere for award of any other degree. All the ideas and references have been duly acknowledged.

Gurminder Kaur Dated: 17 August 2016

Dedicated to

My loving parents

Acknowledgement

I am highly indebted to the Almighty who has given me strength to accomplish this big task.

It gives me immense pleasure to thank my supervisor, Professor Kelly Chibale, for his expertise and inspiring guidance throughout the period of my work. I am grateful to him for his constant support and encouragement, which has helped me to achieve this goal.

I acknowledge the contribution of Dr. Sergio Wittlin at the Swiss Tropical and Public Health Institute, Basel, Switzerland, Helena Boshoff at National Institute of Health, USA, Ms. Ronnett Seldon, Prof. Peter J. Smith, Ms. Carmen De Kock and Dr. Nigel Aminake Makoah at University of Cape Town, for biological testing of my compounds. Further, I wish to thank Peter Roberts for recording NMR spectra as well as for training and supporting me in the use of NMR spectrometers.

I am grateful to all my lab mates, members of the UCT Drug discovery and Development Centre (H3D), and members of chemistry department for providing friendly and supportive environment. Special thanks to Dr. Kawaljit Singh, Dr. Elumalai Pavadai and Ms. Karis Moxley for helping in my thesis write up and proofreading my drafts. I gratefully acknowledge the generous assistance provided by Mrs. Elaine Rutherfoord-Jones and Saroja Naicker. I also thank the administrative and support staff in the department of chemistry for making our work environment efficient and pleasant.

Last but not the least, I would like to thank my husband, my parents, my brother and my sisters. Without their patience, constant support, encouragement, faith and affection it would have not been possible for me to be where I am at present.

Abstract

Tuberculosis (TB) and malaria continue to be major public health concerns, globally claiming 2-3 million deaths every year. A number of efficacious drugs are available for the treatment of TB and malaria, which, through various combination therapies, are fully effective in treating these diseases. However, the wide spread resistance in *M. tuberculosis* (*Mtb*) and *P. falciparum*, the causative agents of TB and malaria, respectively, has made the existing therapies less effective. Thus novel agents able to circumvent drug resistance and other challenges associated with existing TB and malaria treatments are urgently needed.

The development of a new drug is a lengthy and costly process; therefore, approaches that can save both time and money need to be emphasised. Drug repositioning is one such approach that has been applied in this project. Drug repositioning basically involves a situation where a drug active in one disease is derivatised or used as a template for the synthesis of derivatives active in another disease. This approach has the potential to significantly shorten the drug discovery process.

This study focused on the repositioning of two drugs, the antibacterial agent fusidic acid and the antipsychotic agent metergoline, in TB and/or malaria via medicinal chemistry approaches. New semisynthetic derivatives of fusidic acid and metergoline were synthesized and evaluated for antimycobacterial activity against the H37Rv strain of *Mtb* and antiplasmodial activity against the NF54 strain of *P. falciparum*.

Fusidic acid derivatives were synthesized by performing various structural modifications at C-21 (SAR 1), C-3 (SAR 2) and C-16 (SAR 3) positions (Figure 1). C-21 derivatives were obtained by replacing the C-21 carboxyl group of fusidic acid with various bioisosteres. These replacements led to derivatives with inferior antimycobacterial activity ($MIC_{99} \geq 20$ µM) as compared to fusidic acid (MIC_{99} 0.6 µM).

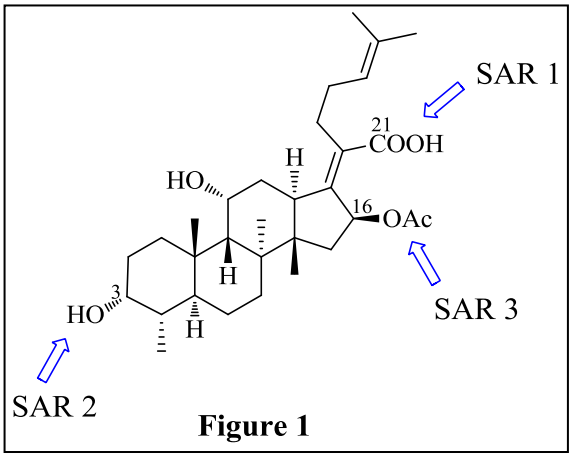

Figure 1

However, 2 out of these 28 compounds (**3.15** and **3.18**) displayed moderate activity (MIC_{99} 10 µM) and cytotoxicity (IC_{50} CHO 88.3 and 92.2 µM, respectively). On the other hand, most of these derivatives showed a 2-35 fold increase in antiplasmodial activity as compared to

fusidic acid (IC_{50} 59 μM) and were also found to be non-cytotoxic. The antimycobacterial and antiplasmodial data of C-21 fusidic acid derivatives suggest that the carboxylic acid group is essential for its antimycobacterial activity but not for antiplasmodial activity. The C-3 derivatives were obtained by replacing the C-3 hydroxyl group with various carboxylic and silicate esters as well as keto and oxime functionalities. C-3 derivatives exhibited more potent antimycobacterial activity as compared to C-21 derivatives, with 9 out of 14 derivatives displaying $MIC_{99} \leq 5$ μM. One of these derivative, the C-3 triisopropoxy silicate ester of fusidic acid (**3.42**, MIC_{99} 2.5 μM), demonstrated a superior *in vivo* (mouse) pharmacokinetic profile with higher concentrations achieved in blood, a longer half-life, and a lower clearance rate relative to fusidic acid. Similar to C-21 derivatives, structural modifications at the C-3 position also resulted in improved antiplasmodial activity as compared to fusidic acid. The C-16 derivatives were obtained by replacing the C-16 acetoxy group with methoxy and ethoxy groups. The antimycobacterial activity of the ethoxy derivative (MIC_{99} 0.8 μM) was found to be comparable to fusidic acid (MIC_{99} 0.6 μM). Seven miscellaneous derivatives with modifications at more than one diversity site of fusidic acid were also obtained. Antimycobacterial evaluation of these compounds indicated that the lipophilic side chain, carboxylic acid, and C-16 substitution are essential for antimycobacterial activity. Antiplasmodial evaluation revealed that C-3, C-11-diacetoxy fusidic acid methyl ester (**3.56**, IC_{50} 0.4 μM) has superior antiplasmodial activity with no cytotoxicity.

In addition, two separate *in silico* approaches were applied to fusidic acid. In one approach, a 3D-QSAR pharmacophore model was developed based on the antiplasmodial activity of 61 previously synthesized fusidic acid derivatives. This model was used as the 3D-structural search query to screen a fusidic acid-based combinatorial library. Eight virtual hit compounds were synthesized, including C-21 amide and C-3 ether fusidic acid derivatives. All synthesized hit compounds showed superior antiplasmodial activity relative to fusidic acid. Two C-21 amide derivatives (**4.7** and **4.8**) displayed significant activity against the CQ-sensitive NF54 strain (IC_{50} values of 0.3 μM and 0.7 μM, respectively) and the CQ-resistant K1 strain (IC_{50} 0.2 μM), and were also found to be non-cytotoxic. In another approach, 2D fingerprint and 3D shape similarity searches were performed on an in-house database using fusidic acid as the query compound. The database included 708 steroid-type natural products or their semi-synthetic derivatives with defined chemical structures and stereochemistry. This study was conducted with the aim of finding structurally similar compounds that may display similar biological activities as that of fusidic acid. Selected hit compounds were evaluated for

in vitro biological activity. Twelve out of 27 hit compounds displayed antiplasmodial activity (IC_{50} < 25 µM). However, these compounds did not show any antimycobacterial activity except **4.16** and **4.26** (MIC_{99} 80 µM).

Metergoline derivatives were synthesized by replacing the benzyl carbamate (CBz) group with various aromatic, heteroaromatic and aliphatic amide moieties (Figure 2). Nine out of 23 compounds exhibited antimycobacterial activity with MIC_{99} < 50 µM. The decanamide derivative of metergoline (**5.23**, MIC_{99} 9.4 µM, IC_{50} CHO 86.6 µM) was found to have a superior antimycobacterial activity and cytotoxicity profile relative to metergoline (MIC_{99} 25 µM, IC_{50} CHO 16.6 µM). Further, three derivatives, **5.3** (IC_{50} 1.3 µM), **5.9** (IC_{50} 2.5 µM) and **5.25** (IC_{50} 1.2 µM) were found to have slightly improved antiplasmodial activity relative to metergoline (IC_{50} 3.7 µM). Compound **5.25** was found to be the most active derivative with an encouraging selectivity index value of 13. The antimycobacterial and antiplasmodial data of metergoline and its derivatives suggest that the benzyl carbamate group of metergoline is not required for activity and its substitution with other moieties may result in compounds with improved antimycobacterial and / or antiplasmodial activity.

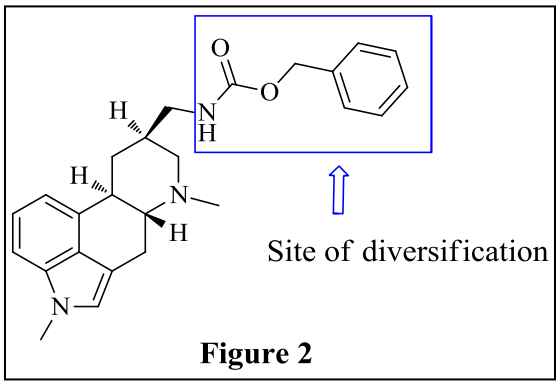

Figure 2

Overall, this work demonstrates the potential of fusidic acid and metergoline as a promising novel antimycobacterial and antiplasmodial templates for repositioning purposes.

Abbreviations

$(Ac)_2O$	Acetic anhydride
ACT	Artemisinin Combination Therapy
ADHD	Attention deficit hyperactivity disorder
Ag_2CO_3	Silver carbonate
AIDS	Acquired immunodeficiency syndrome
AMB	Amphotericin B
APCI	Atmospheric pressure chemical ionization
API	Atmospheric pressure ionization
AR	Analytical reagent
ATP	Adenosine triphosphate
AUC	Area under curve
$Bu4N^+Br^-$	Tetra butyl ammonium bromide
^{13}C	Carbon
CBr_4	Carbon tetrabromide
CBz	Benzyl carbamate
$CDCl_3$	Chloroform-d
CDI	1,1'-Carbonyldiimidazole
CD_3OD	Deuterated Methanol
CH_3I	Methyl iodide
CHO	Chinese Hamster Ovarian
CO_2	Carbon dioxide
COSY	Homonuclear correlation spectroscopy
CQ	Chloroquine
d	Density
2D	Two dimensional
3D	Three dimensional
DAD	Diode Array Detector
DCM	Dichloromethane
DIPEA	Diisopropylethylamine
DMAP	4-Dimethylaminopyridine
DMF	N,N-Dimethylformamide
DMSO	Dimethyl sulfoxide

DNA	Deoxyribonucleic acid
DOTS	Directly Observed Treatment, Short Course
DS-TB	Drug-Susceptible Tuberculosis
DR-TB	Drug-Resistant Tuberculosis
ECFC	Extended-connectivity fingerprints counts
ECFP	Extended-connectivity fingerprints
EDCI	1-Ethyl-3-(3-dimethylaminopropyl)carbodiimide
EF-G	Elongation factor G
EMB	Ethambutol
ESI	Electrospray ionisation
Et_3N	Triethylamine
EtOAc	Ethyl acetate
EtOH	Ethanol
FCFC	Functional-class extended-connectivity counts
FCFP	Functional-class fingerprints
FDA	Food and drug administration
FLC	Fluconazole
GDP	Guanosine 5′-diphosphate
GTP	Guanosine triphosphate
^1H	Proton
HCl	Hydrogen chloride
HEPES	4-(2-hydroxyethyl)-1-piperazineethanesulfonic acid
HIV	Human immunodeficiency virus
HOBt	Hydroxybenzotriazole
HPLC	High performance liquid chromatography
HTS	High-throughput screening
IC_{50}	Inhibitory concentration
IDM	Institute of Infectious Diseases and Molecular Medicine
INH	Isoniazid

J	Coupling constant
K_2CO_3	Potassium carbonate
KOH	Potassium hydroxide
LBVS	Ligand-based virtual screening
LCMS	Liquid chromatography–mass spectrometry
M	Molar
µM	Micro molar
MDL	Molecular design limited
MDR-TB	Multidrug-resistant tuberculosis
MHz	Mega hertz
MIC	Minimum inhibitory concentration
ml	milliliter
Mp	Melting point
MS	Mass spectroscopy
Mtb	Mycobacterium tuberculosis
MTT	3-(4,5-dimethylthiazol-2-yl)-2,5-diphenyltetrazoliumbromide
MW	Microwave
m/z	Mass over charge ratio
$NaBH_4$	Sodium borohydride
$NaHCO_3$	Sodium bicarbonate
NaOAc	Sodium acetate
NaOH	Sodium hydroxide
NH_4Cl	Ammonium chloride
NH_4OAc	Ammonium acetate
NIAID	National Institute of Allergy and Infectious Diseases
NIH	National Institute of Health
nM	Nano molar
NMR	Nuclear magnetic resonance
O_2	Oxygen
OAc	Acetoxy
PDA	Photodiode array

Pd/C	Palladium on carbon
PEG	Polyethylene glycol
P. falciparum	*Plasmodium falciparum*
PK	Pharmacokinetics
pH	Potential of hydrogen
PPh_3	Triphenylphosphine
PyBOP	Benzotriazol-1-yl-oxytripyrrolidinophosphonium hexafluorophosphate
QSAR	Quantitative structure–activity relationship
RBF	Round bottom flask
R_f	Retardation factor
RIF	Rifampicin
RMSD	Root mean square deviation
RNA	Ribonucleic acid
RPMI	Roswell Park Memorial Institute
SAR	Structure-activity relationship
SBVS	Structure-based virtual screening
SI	Selectivity Index
$SiCl_4$	Silicon tetrachloride
$Si(OH)_4$	Orthosilicic acid
SM	Streptomycin
TAACF	Tuberculosis Antimicrobial Acquisition Coordinating Facility
TB	Tuberculosis
TBTU	*N*,*N*,*N*′,*N*′-Tetramethyl-O-(benzotriazol-1-yl)uronium tetrafluoroborate
Tc	Tanimoto coefficient
THF	Tetrahydrofuran
TLC	Thin layer chromatography
TMS	Tetramethyl silane
T3P	n-Propanephosphonic acid anhydride
UK	United Kingdom

USA	United states of America
UV	Ultra violet
v/v	Volume by volume ratio
WHO	World health organization
w/v	Weight over volume ratio
XDR-TB	Extensively drug-resistant tuberculosis

Table of content

Publications

(1) Singh, K.; Kaur, G.; Mjambili, F.; Smith, P. J.; Chibale, K. Synthesis of Metergoline Analogues and Their Evaluation as Antiplasmodial Agents. *Med.Chem.Commun.* **2014**, *5*, 165-170.

(2) Kaur, G.; Singh, K.; Pavadai, E.; Njoroge, M.; Espinoza-moraga, M.; Kock, C. De; Smith, P. J.; De, S. W.; Chibale, K. Synthesis of Fusidic Acid Bioisosteres as Antiplasmodial Agents and Molecular Docking Studies in the Binding Site of Elongation Factor-G. *Med.Chem.Commun.* **2015**, *6*, 2023–2028.

Chapter 1

Introduction

Tuberculosis (TB) and malaria still remain among the major causes of death worldwide, particularly in developing countries. In spite of a number of drugs developed for TB and malaria, treatments are still challenged by drug resistance, extended treatment duration (TB), toxicity profile, and side effects that make these drugs unsatisfactory. Therefore, new drugs are needed that can successfully combat the aforementioned challenges.

This chapter provides a brief introduction of TB and malaria. It also describes currently used anti-TB and antimalarial drugs, existing TB and malaria treatment regimens, as well as challenges associated with these treatments. New pipeline drugs developed to combat the current treatment challenges are also briefly described.

1.1 Tuberculosis (TB)

1.1.1 Disease and epidemiology

TB is a contagious airborne disease responsible for ill health among millions of people each year. TB ranks as the second leading cause of death from an infectious disease worldwide, after the human immunodeficiency virus (HIV). According to the latest World Health Organization (WHO) report on TB[1] collected from 205 countries and territories, an estimated 9.6 million people developed TB in 2014 and 1.5 million died from the disease, 0.4 million of whom were HIV-positive. Further, the highest occurrence of TB cases (86%) was reported in Asia and the African region, while smaller proportions of cases also occurred in the Eastern Mediterranean (8%), European (3%) and American (3%) regions. Figure 1.1 shows the global estimated TB incidences in 2014.

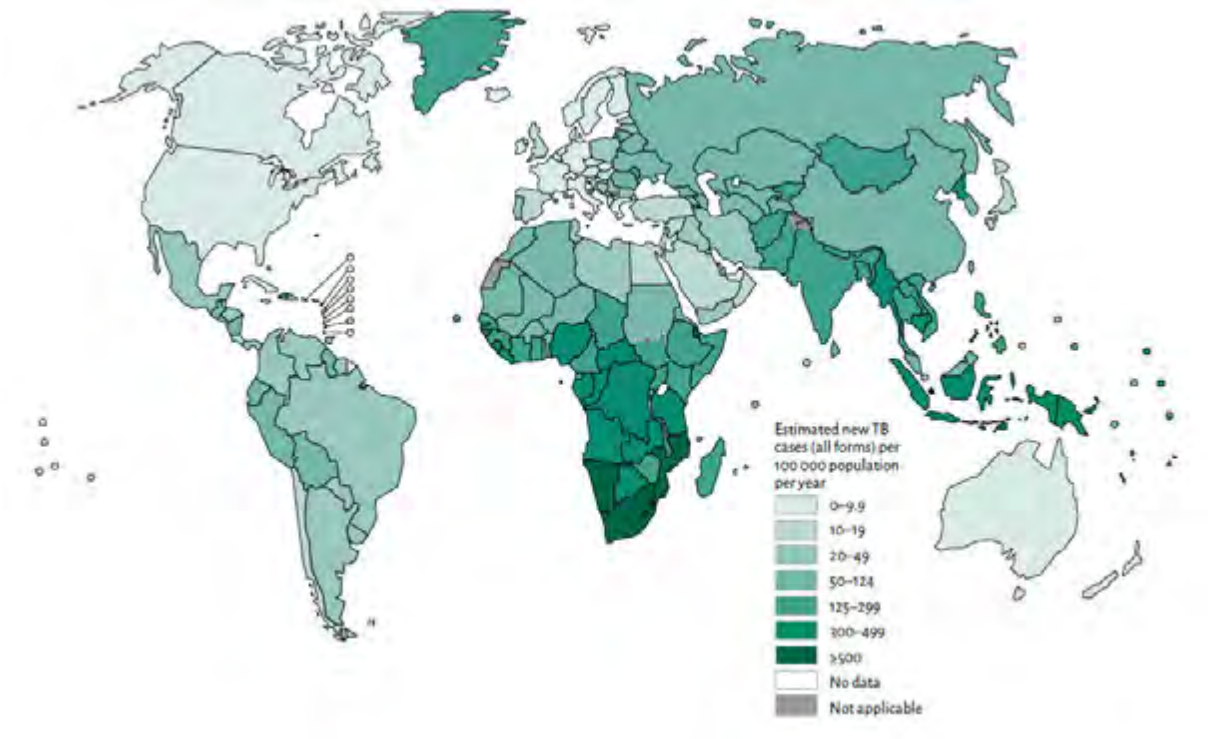

Figure 1.1: Global estimated TB incidences in 2014[1]

TB infections in humans are primarily caused by *Mycobacterium tuberculosis* (*Mtb*), which was discovered by Robert Koch in 1882. *Mtb* is a slow growing, aerobic, non-motile, rod-shaped bacterium (Figure 1.2). This gram-positive bacterium is enclosed by a thick and impermeable cell wall which is made up of peptidoglycans, arabinogalactans, and unusual lipids such as mycolic acids, with an outer cover of non-covalently linked proteins and polysaccharides. This unusual cell wall structure is believed to be the potential cause of *Mtb* virulence and dormancy.[2,3]

Figure 1.2: Typical rod-shaped cells of *Mtb*[4]

TB typically affects the lungs (pulmonary TB) but the bacterium can also enter the blood stream and infect other parts of the body (non-pulmonary TB), which occurs in over 15% of patients. TB in the human body resides either as active TB or latent TB. Active TB is contagious, symptomatic and can cause the death of a person if not treated at the right time with appropriate medication. Symptoms of active TB include fever, loss of weight and appetite, as well as organ specific symptoms such as lung pain and coughing up blood/sputum. TB can also lie dormant where the human immune system keeps it under control without completely eliminating it. This is called latent TB, which is non-contagious and asymptomatic. TB resides as latent TB in 90-95% of infected individuals and only 5-10% develop active TB at some stage of their lives.[5,6] Co-infection with HIV further complicates TB. HIV infection makes the individual more susceptible to TB infection and can also activate a latent infection. This co-infection causes both TB and HIV to progress more rapidly. [7–9]

1.1.2 Transmission and pathogenesis

Through coughing and sneezing by an individual with active TB, *Mtb* is released into the air in the form of aerosols. These *Mtb* containing aerosols can then be inhaled by other individuals.[10] Lungs are the primary site of infection where *Mtb* bacilli are phagocytized by alveolar macrophages. These cells are programmed to combat microbial intruders and to, ultimately, destroy them. However, some *Mtb* bacilli manage to escape eradication by macrophages and survive within these cells.[11,12] *Mtb* multiplies in these cells and is released upon death of the macrophages. These bacilli may spread by way of lymphatic channels or through the bloodstream to more distant tissues and organs (including areas of the body in which TB is most likely to develop such as regional lymph nodes, apex of the lung, kidneys, brain and bone). This process of dissemination primes the immune system for a systemic response in which the infected macrophages together with T-lymphocytes and other mononuclear cells mature into a solid granuloma, the hallmark of TB.[13]

It is believed that granulomas are structured clusters consisting of *Mtb* infected macrophages surrounded by different types of immune cells, in particular macrophages and T-lymphocytes. The pathogen is controlled at this stage by the immune system in immuno-competent individuals. *Mtb* is more likely to lie in a dormant (latent infection) state in a solid granuloma and does not spread further as a result of which latent TB infection is established in immune-competent individuals with a life-long risk of reactivation. However, in the presence of a

weakened immune system, macrophages are unable to capture *Mtb* bacilli in the form of a solid granuloma as a result of which *Mtb* bacilli multiply at higher rates leading to the development of active disease (Figure 1.3).[3]

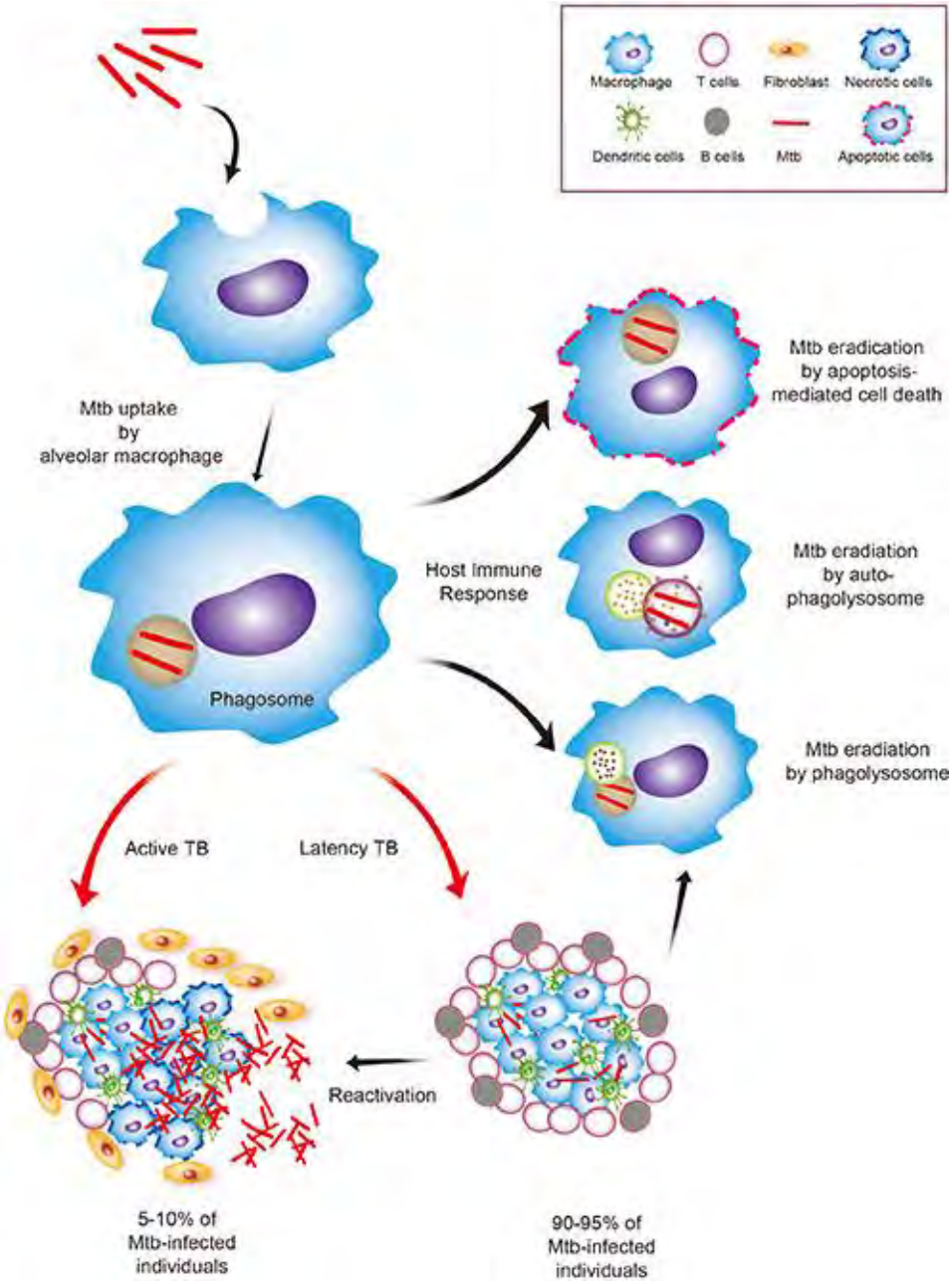

Figure 1.3: A schematic diagram showing the action of the host immune system against infection of *Mtb*[14]

1.1.3 Anti-TB Drugs

There are more than 20 drugs currently used in the treatment of TB. The WHO has classified the available TB drugs into five groups based on efficacy, potency, drug class and experience

of use (Figure 1.4). TB can be cured completely with a combination of these TB drugs if there is patient compliance.

Group 1:	Isoniazid (INH), Rifampicin (RIF), Rifabutin, Rifapentine, Ethambutol (EMB), Pyrazinamide (PZA)
Group 2:	Aminoglycosides {Streptomycin (SM), Kanamycin, Amikacin}, Polypeptide (Capreomycin)
Group 3:	Fluoroquinolones (Levofloxacin, Moxifloxacin, Gatifloxacin, Ofloxacin)
Group 4:	Ethionamide, Prothionamide, D-Cycloserine, Terizidone, *p*-Aminosalicylic acid
Group 5:	Bedaquiline (TMC-207), Delamanid (OPC-67683), Linezolid, Clofazimine, Amoxicillin/Clavulanate, Imipenem/Cilastatin, Meropenem, Thioacetazone, Clarithromycin

Figure 1.4: Classification of anti-TB drugs[15]

All group 1 drugs, as well as streptomycin from group 2, are used as first-line drugs for the treatment of TB. Active TB infection that can be treated with these drugs is called drug-susceptible TB (DS-TB). These drugs were discovered between the 1950s and 1960s and since then have been used successfully in the treatment of DS-TB. Two new RIF analogues, rifabutin and rifapentine, have also been developed and can be used as an alternative to RIF. All these drugs are administered orally except streptomycin which is given intramuscularly or intravenously. Chemical structures of the first-line drugs are displayed in Figure 1.5.

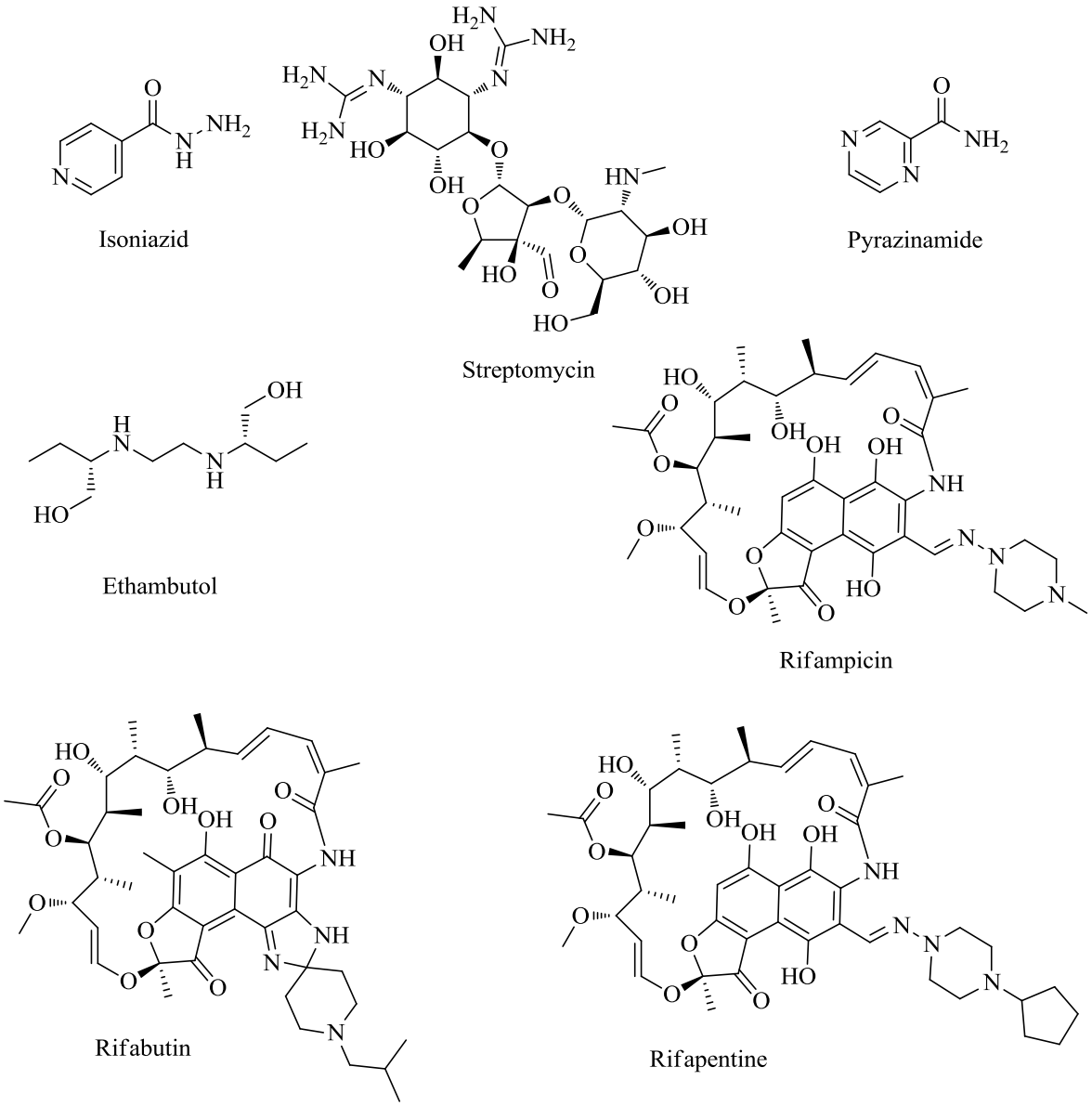

Figure 1.5: First-line anti-TB drugs

Drugs placed in groups 2 (except SM), 3 and 4 in Figure 1.4 are second-line drugs in TB and are used to treat drug-resistant TB (DR-TB). These consist of orally administered fluoroquinolones, injectable drugs such as kanamycin, amikacin, capreomycin, and oral bacteriostatic drugs such ethionamide, prothionamide, D-cyclocerine, teridizone and para-amino salicylic acid. Structures of the second-line drugs are displayed in Figure 1.6.

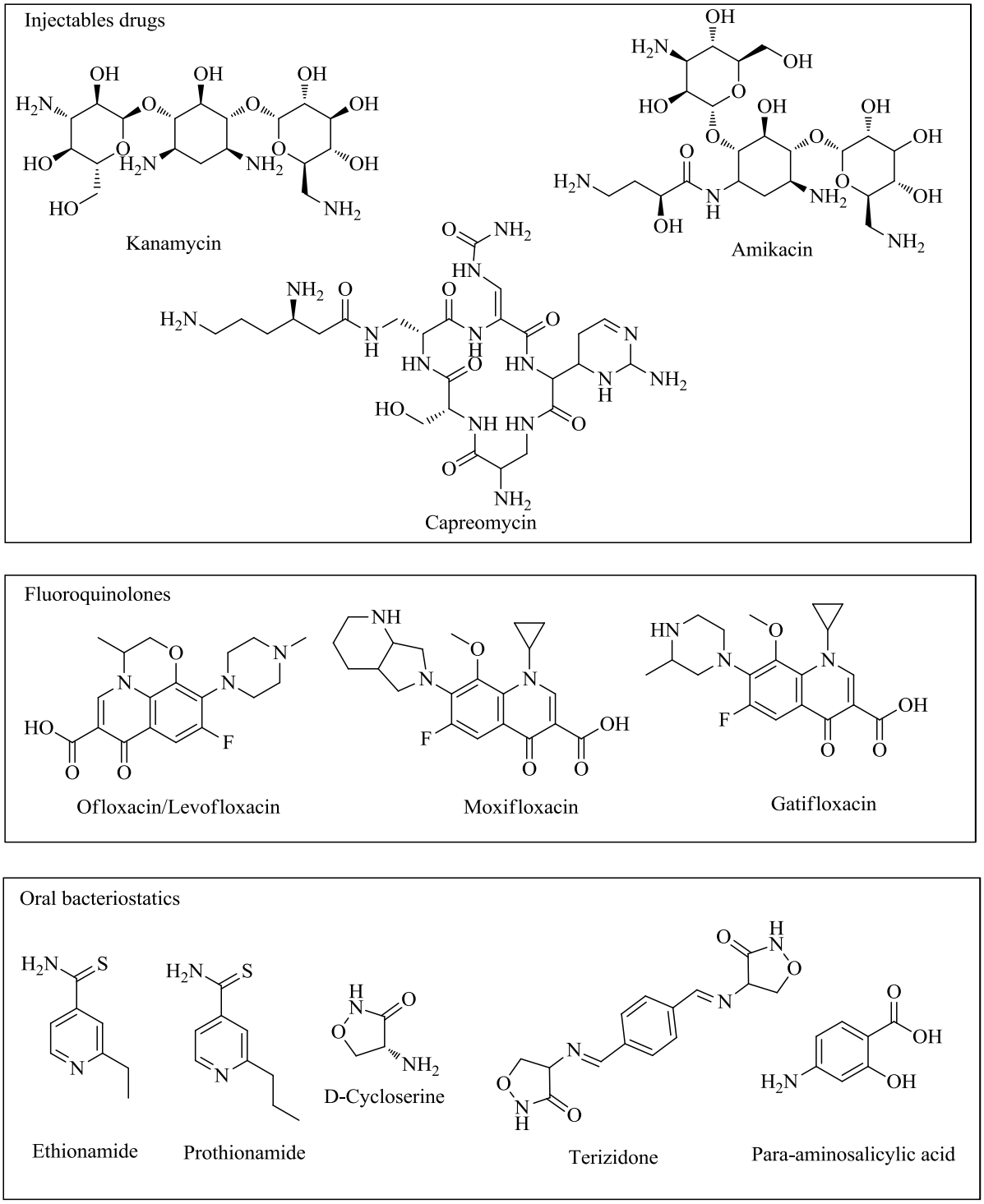

Figure 1.6: Second-line anti-TB drugs

Poor management of chemotherapy and poor patient compliance have contributed to the appearance of drug-resistant strains of *Mtb* [multi drug-resistant (MDR) and extensively drug-resistant (XDR) TB].[16] According to the latest WHO report, 3.3% of new and 20% of previously treated TB cases have MDR-TB and 9.7% of MDR-TB patients have XDR-TB.[1] DR-TB is called MDR-TB when it is resistant to at least INH and RIF, the two most

important first-line drugs used in the treatment of TB.[17] DR-TB is called XDR-TB when it is resistant to INH and RIF as well as any of the fluoroquinolones and the injectable drugs (amikacin, kanamycin or capreomycin).[17]

Group 5 in Figure 1.4 comprises third-line anti-TB drugs which can be used to treat DR-TB if recommended drugs cannot be provided for some reason. Many of these drugs such as linezolid, amoxicillin, imipenem, meropenem and clofazimine are already in use to treat other bacterial infections. However, there is limited data available concerning their efficacy in TB and/or long-term safety in humans. Therefore, these drugs are not recommended by the WHO for routine use. Most of these drugs, with the exception of bedaquiline and delamanid, are not registered for treatment, making their use 'off-label'. Chemical structures of third-line drugs are presented in Figure 1.7.

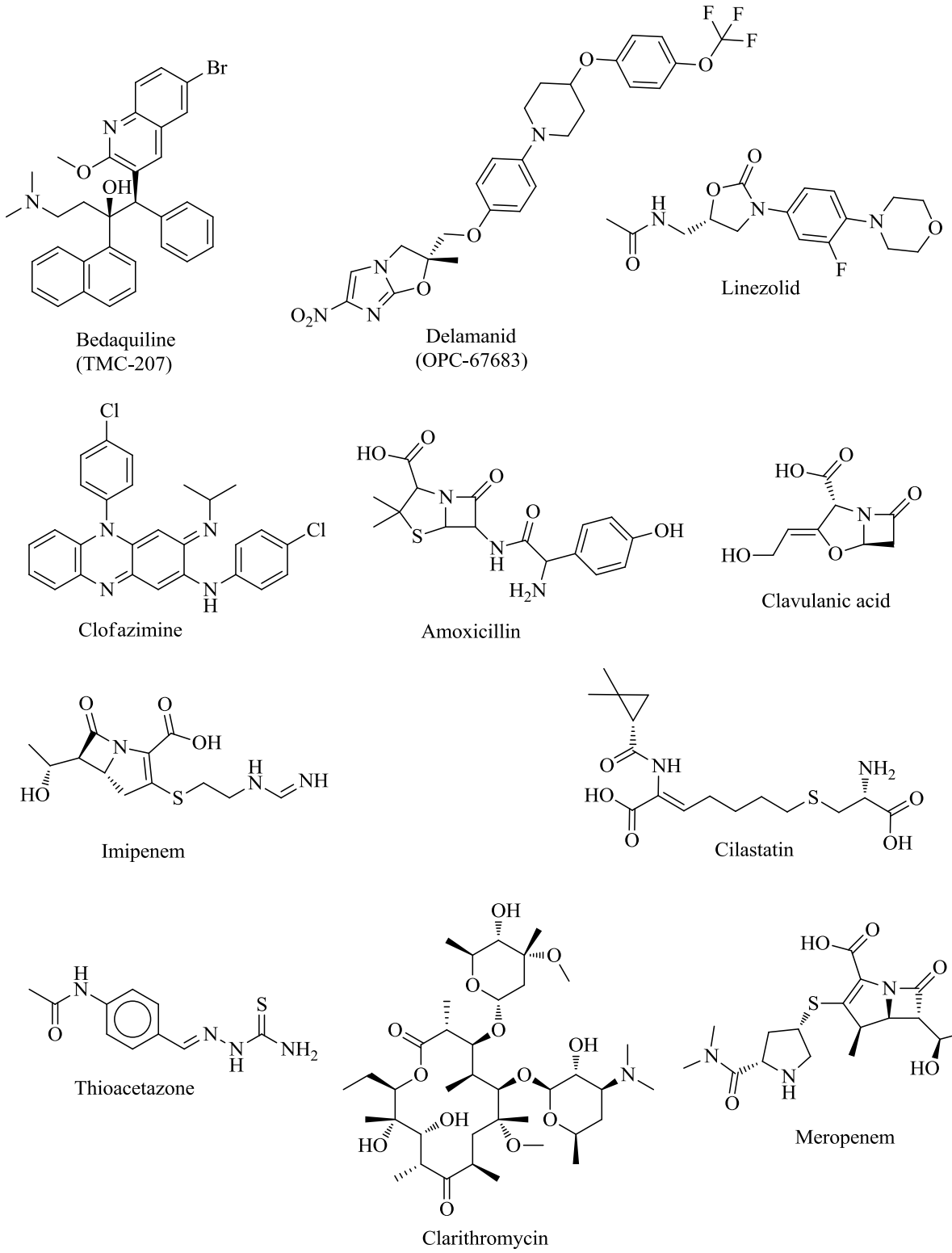

Figure 1.7: Third-line anti-TB drugs

A brief description of the mechanisms of action of the above-mentioned anti-TB drugs and *Mtb* genes involved in drug resistance is given in Table 1.1.

Table 1.1: Anti-TB drugs, their mode of action and main *Mtb* genes involved in resistance

Drug	Mechanism of Action	*Mtb* genes	References
First-line drugs			
Orally administered			
Isoniazid	Prodrug which is activated by *Mtb* catalase-peroxidase encoded by the *katG* gene and targets Enoyl-[acyl-carrier-protein] reductase (InhA) resulting in inhibition of mycolic acid synthesis.	*katG, inhA*	[18–21]
Rifampicin Rifabutin, Rifapentine	Inhibit *Mtb* RNA synthesis by binding to the β-subunit of the *Mtb* RNA polymerase.	*rpoB*	[22–24]
Ethambutol	Inhibits arabinosyl transferase, encoded by *embB* gene, an enzyme involved in the synthesis of arabinogalactan of cell wall.	*embB*	[25–27]
Pyrazinamide	Prodrug is activated by pyrazinamidase encoded by *pncA* gene into pyrazinoic acid which after initial efflux from the cell gets reabsorbed under acidic pH and accumulates in the membrane, disturbing membrane potential.	*pncA*	[28–32]
Injectable			
Streptomycin	Binds to the 30S subunit of the ribosome at the ribosomal protein S12 and the 16S rRNA, thereby inhibiting protein synthesis	*rpsL* and *rrs* encoding for S12 and 16S rRNA, respectively	[33–35]

Table 1.1: Continued…

Second-line drugs			
Injectable			
Kanamycin Amikacin	Binds to 16S rRNA of 30S ribosome subunit resulting in inhibition of protein synthesis.	*rrs*	[36,37]
Capreomycin	Binds to intersubunit bridge B2a between 30S and 50S ribosomal subunits, inhibits protein synthesis.	*tlyA* encoding rRNA 2-O′ methyltransferase	[38]
Fluoroquinolones (FQs)			
Levofloxacin, Moxifloxacin, Gatifloxacin Ofloxacin	Inhibit DNA gyrase (topoisomerase II) and topoisomerase IV, thereby blocking DNA replication and transcription.	*gyrA*	[39,40]
Oral bacteriostatic			
Ethionamide Prothionamide	Prodrug which is activated by flavin monooxygenase encoded by *etaA* or *ethA* and targets Enoyl-[acyl-carrier-protein] reductase (InhA) thereby inhibiting mycolic acid synthesis.	*etaA* or *ethA*, *inhA*	[41–44]
D-Cycloserine Terizidone	Inhibit d-alanine racemase (AlrA) and d-alanine:d-alanine ligase (Ddl) involved in the synthesis of peptidoglycan of *Mtb* cell wall.	Over expression of *alrA, Ddl genes*	[45,46]
p-Aminosalicylic acid	Inhibit folic acid biosynthesis and uptake of iron.	*thyA,*	[47]

Table 1.1: Continued…

Third-line drugs		
Bedaquiline (TMC-207)	Inhibits mycobacterial ATP (adenosine 5'-triphosphate) synthase, an enzyme that is essential for the generation of energy in *Mtb*.	[48]
Delamanid (OPC-67683)	Prodrug which is activated by an F420-deazaflavin dependent nitroreductase and thereby inhibits the synthesis of mycobacterial cell wall components: methoxy mycolic acid and ketomycolic acid.	[49,50]
Linezolid	Binds to the 23S rRNA of 50S ribosome subunit, inhibits protein synthesis.	[51]
Clofazimine	Appears to kill *Mtb* through prodrug action that involves a redox cycling pathway. As demonstrated in *M. smegmatis*, the drug is reduced by NDH-2 enzyme (NADH:quinone oxidoreductase) and produces reactive oxygen species upon subsequent reoxidation by O_2	[52]
Amoxicillin/Clavulanate	Inhibits peptidoglycan synthesis.*	[53]
Imipenem/Cilastatin	Inhibits peptidoglycan synthesis.*	[54]
Meropenem	Inhibits peptidoglycan synthesis.*	[54]
Thioacetazone	Inhibits mycolic acid synthesis.*	[55]
Clarithromycin	Inhibits protein synthesis by binding to the 23S rRNA of 50S ribosomal subunit.*	[56]

* Proposed mechanism of action in *Mtb* based on the mechanism of action in bacteria

1.1.4 Treatment

The current anti-TB therapy recommended by the WHO is called DOTS (directly observed treatment, short course). It requires the administration of four drugs: Isoniazid (INH), Rifampicin (RIF), Pyrazinamide (PZA) and Ethambutol (EMB) or Streptomycin (SM). These drugs may possess bactericidal and/or sterilizing activity individually to varying degrees, but, in combination, are highly effective against all populations (fast-replicating, slow-replicating and non-replicating or dormant) of *Mtb*. All these drugs (INH, RIF, PZA, EMB or SM) are administered for the first two months of treatment followed by four months of treatment with a combination of INH and RIF. These drugs destroy *Mtb* in all growth stages in the initial two

months of treatment. In the additional four months, RIF kills any residual dormant bacilli and INH kills any RIF-resistant mutants that commence replication.[57] This regimen is more than 40 years old and is currently implemented for the treatment of pulmonary TB and most forms of extra-pulmonary TB, regardless of HIV status.[1,5]

Treatment of latent TB infection (LTBI) is essential to control and eliminate TB as it considerably reduces the risk of progress of TB infection to disease. Recommended latent TB treatment includes (1) INH at a dose of 300 mg daily for at least 6 months and preferably for 9 months; or (2) INH and rifapentine each at a dose of 900 mg weekly for 3 months; or (3) RIF at a dose of 600 mg daily for 4 months. INH at a dose of 300 mg for 9 months is highly effective and is the preferred regimen for HIV-infected people taking antiretroviral medication, and children aged 2–11 years. INH and rifapentine, each at a dose of 900 mg weekly for 3-4 months, is another effective regimen option for otherwise healthy patients aged ≥ 12 years.[5]

The WHO guidelines recommend the following 5-agent treatment regimen for MDR-TB: Pyrazinamide (PZA); a fluoroquinolone; a parenteral agent (typically amikacin or kanamycin); ethionamide (or prothionamide); and either D-cycloserine or *p*-aminosalicylic acid, with preference for D-cycloserine. Such therapy should be administered for at least 20 months in patients who have not received previous treatment for MDR-TB and for up to 30 months in those who have received previous treatment. Because of limited data, there is no separate recommended treatment regimen for XDR-TB. A regimen similar to MDR-TB is used for patients with XDR-TB.[5,15]

1.1.5 Challenges

There are several major challenges associated with current TB treatment.[6,58] The cure rates with the standard first-line regimen are quite high (exceeding 90%) when delivered under DOTS, a program promoted by WHO. This includes direct observation of patient consumption of the TB medications by trained personnel. However, there is poor patient compliance due to many factors such as the cost of drugs, side effects, long treatment duration and the number of drug doses required. This has led to suboptimal responses (failure and relapse), the emergence of resistance (MDR- and XDR-TB), and continuous spread of the disease. Second-line drugs which are used to treat MDR- and XDR-TB are not available everywhere especially in poor nations and are less effective, more expensive, more toxic, and require a longer treatment duration than first-line drugs.

The frequent co-infection of TB in HIV patients further complicates the selection of an appropriate treatment regimen. Additional pill burden of anti-TB drugs with HIV medications diminishes compliance in patients. Another major concern in the treatment of TB/HIV co-infections is the drug-drug interaction involving RIF and the antiretroviral protease inhibitors. RIF is a potent cytochrome P450 3A4 enzyme inducer. Administering RIF along with antiretroviral protease inhibitors increases the metabolism of these protease inhibitors resulting in decreased therapeutic concentrations.[59,60] Consequently, RIF should not be used in HIV patients who are under treatment with protease inhibitors. In addition to HIV, patients with diabetes are at increased risk of developing active TB, and have higher rates of treatment failure and death, even when placed on appropriate TB treatment.[61–63]

Treatment of latent TB infection is equally important as it may substantially reduce the risk of developing active TB. However, the most preferred prophylactic treatment of latent TB (9-month with 300 mg isoniazid daily) is quite long and shows poor adherence.

The above-mentioned challenges emphasize the urgent need to develop new anti-TB drugs which can shorten the duration of TB treatment, reduce dosing frequency, have an acceptable toxicity profile, target MDR and XDR strains, be co-administered with HIV drugs, and be effective against latent TB.

1.1.6 New anti-TB drugs in the pipeline

Many novel compounds or repurposed drugs have been revealed in the past few decades with anti-TB activity and some of them have reached clinical trial stages. Figure 1.8 displays the current progress of anti-TB agents or drugs at various preclinical and clinical stages.

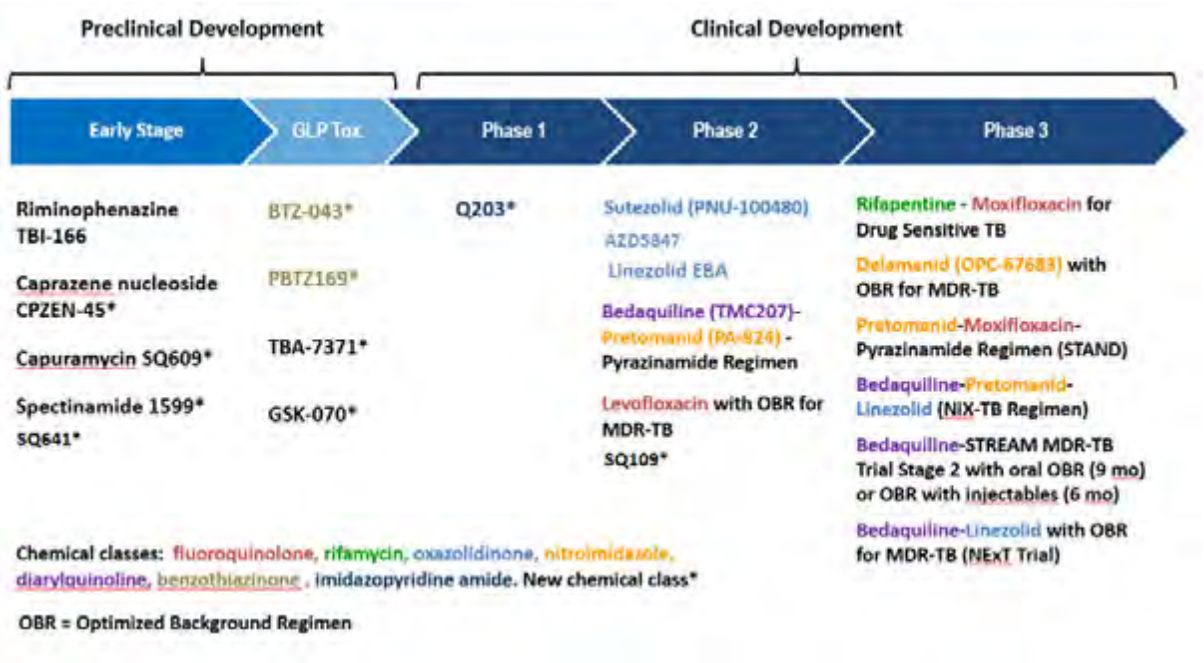

Figure 1.8: Current progress of anti-TB agents or drugs at preclinical and clinical stages [64]

For the first time in more than 40 years, two new anti-TB drugs, bedaquiline and delamanid, have been approved for MDR-TB. However, both drugs have only received conditional approval[65–67]and can be used as a part of combination regimen for treating adult pulmonary MDR-TB only when MDR-TB is in severe form or when other recommended regimens cannot be provided. Bedaquiline (or TMC-207, Figure 1.7) is a diarylquinoline with a novel mechanism of action and acts on both replicating and dormant mycobacteria. It specifically inhibits mycobacterial ATP (adenosine 5'-triphosphate) synthase, an enzyme that is essential for the generation of energy in *Mtb*.[48] Delamanid (Figure 1.7) is a nitroimidazole prodrug, which is activated by an F_{420}-deazaflavin dependent nitroreductase. It acts by inhibiting the synthesis of mycobacterial cell wall components methoxy mycolic acid and ketomycolic acid.[49,50] The approval of bedaquline and delamanid is based on limited phase II clinical data in patients with pulmonary MDR-TB and on a review of the safety data gathered in these studies. Various safety and efficacy trials of delamanid and bedaquiline when added to short MDR-TB regimens of nine and six month's duration are going on in Phase III.[68–70] Delamanid, due to its manageable side effects,[50] is also being evaluated against MDR-TB in children.[71]

Pretomanid or PA-824 (Figure 1.9), like delamanid, is another nitroimidazole prodrug that requires intracellular activation by an F_{420}-deazaflavin-dependent nitroreductase. Activation produces a des-nitro metabolite that generates reactive nitrogen species (including NO)

leading to a decrease in intracellular ATP causing anaerobic killing (similar to the action of cyanide).[72] Besides being effective in anaerobic conditions, PA-824 also kills aerobically by inhibiting cell wall mycolic acid biosynthesis.[73] With its dual mode of action, the drug is effective against drug- susceptible and drug- resistant TB.

Three pretomanid-containing combination regimens are in phase II and III clinical trials for the treatment of both drug- susceptible and drug- resistant TB.[1,64] In one regimen, pretomanid in combination with moxifloxacin and PZA has shown active bactericidal activity in phase II trials over two months against both drug-susceptible and MDR-TB. The bactericidal activity was found to be significantly superior when compared with the standard combination therapy (INH, RIF, PZA, EMB) against drug-susceptible TB. The regimen has now advanced to the phase III clinical trial stage. Another regimen containing pretomanid, bedaquiline and linezolid, is in phase III for evaluation of safety and efficacy against XDR-TB. A pretomaind-bedaquiline-PZA combination is also being tested in phase II against drug-susceptible TB and against drug-resistant TB with addition of moxifloxacin.

Rifapentine (Figure 1.5), a RIF derivative, displays better pharmacokinetic properties relative to RIF such as increased half-life and decreased CYP3A4 induction. Rifapentine has been shown as a potential substitute for RIF.[74,75] A new combination containing rifapentine and moxifloxacin is also in phase III clinical trials to assess the efficacy of this regimen for less than two months in patients with drug-susceptible TB.[76]

The ethylenediamine derivative SQ109 (Figure 1.9) is structurally related to EMB but has a different mechanism of action thereby displaying activity against EMB-resistant *Mtb* strains. This drug targets the *Mtb* transmembrane transporter protein encoded by the mycobacterial membrane protein large 3 (*MmpL3*) gene, and interferes with cell wall assembly.[77] SQ109 is currently in phase II clinical trials. Other phase II candidates are the oxazolidinones: linezolid, its thiomorpholine analogue PNU-100480 (sutezolid) and AZD5847, which inhibit protein biosynthesis via binding to the 23S rRNA of the 50S ribosome subunit.

Many drugs have progressed to the preclinical development stage (Figure 1.9). These include a caprazamycin derivative CPZEN-45, two DprE1 inhibitors benzothiazinones (BTZ043 and PBTZ169), a spectinomycin derivative 1599, a dipiperidine derivative SQ609, a capuramycin derivative SQ641, a DprE1 Inhibitor TBA-7371, a leucyl-tRNA synthetase inhibitor GSK-070 and a riminophenazine derivative TBI-166.[64] An imidazopyridine Q203 has advanced to

the phase I stage for the evaluation of safety, tolerability and pharmacokinetics of single doses of Q203 in healthy volunteers.[78] Figure 1.10 summarizes targets of existing anti-TB drugs (purple) as well as those of current pipeline drugs (red).

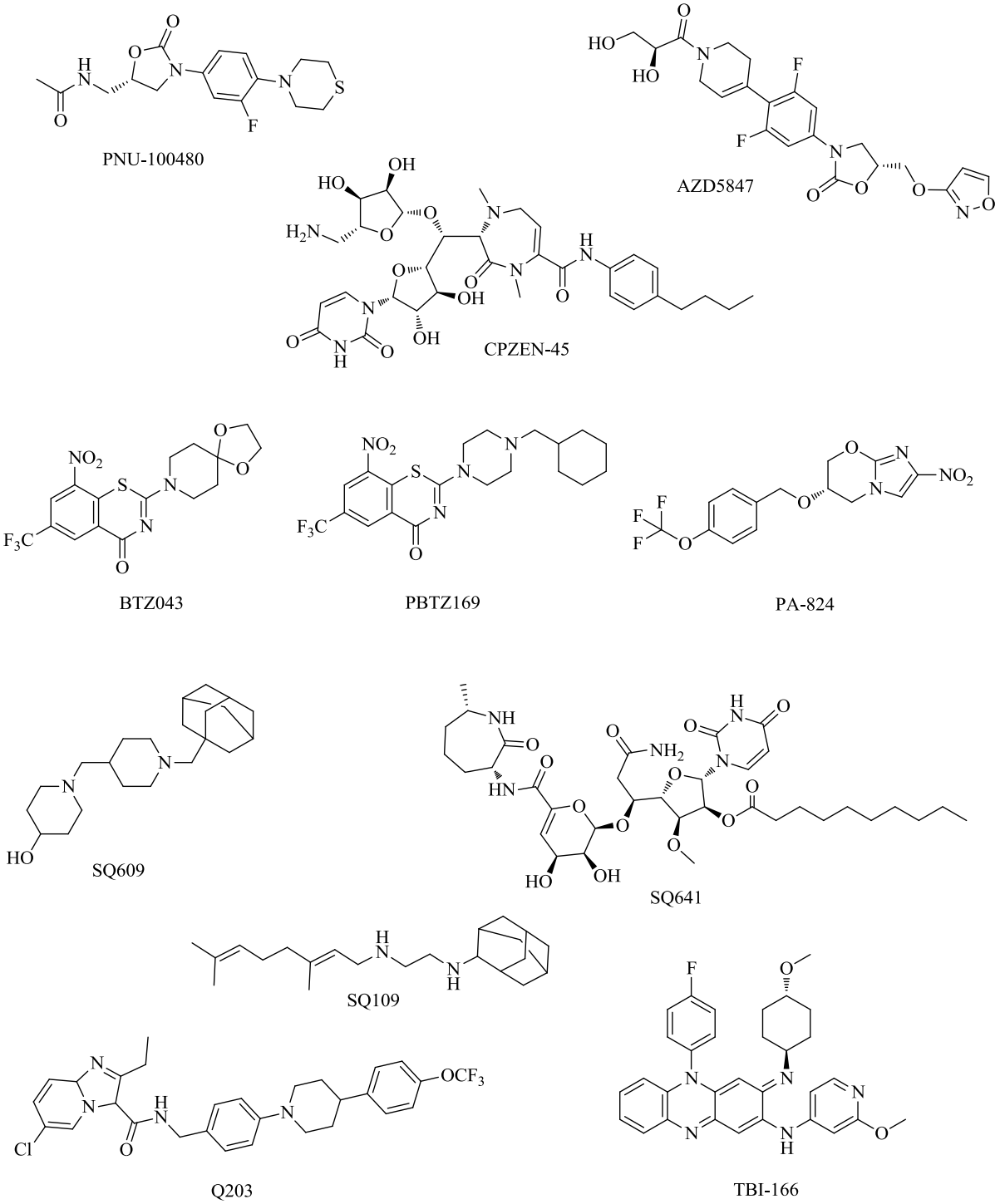

Figure 1.9: Chemical structures of clinical and preclinical candidates for the treatment of TB

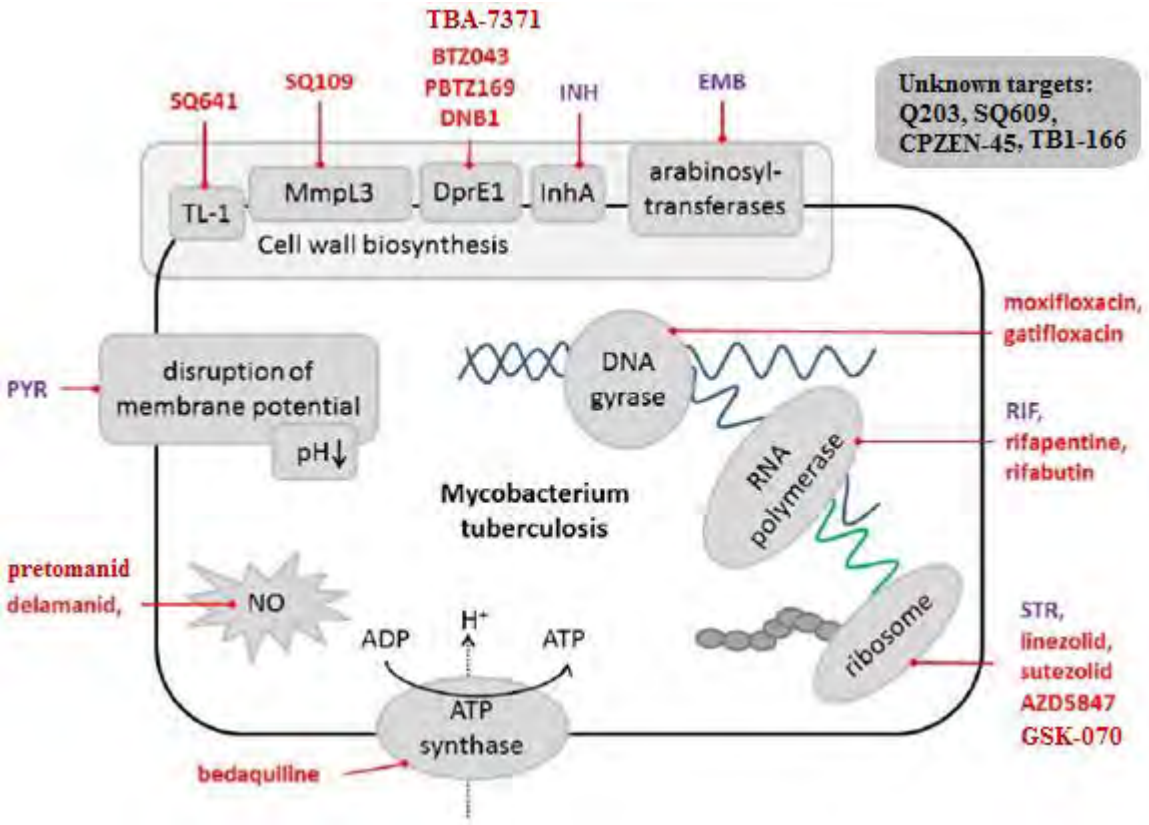

Figure 1.10: Targets of existing (purple) and pipelined (red) anti-TB drugs[79]

In summary, TB is occurring in more than 200 countries worldwide, killing one and half million people each year. Current TB treatment is faced with many challenges such as poor patient compliance due to administration of multiple drugs and longer treatment durations, emergence of *Mtb* resistant strains, and TB/HIV co-infections. New anti-TB drugs with novel mechanisms of action are thus needed to overcome these challenges and to achieve global control of TB.

1.2 Malaria

1.2.1 Disease and epidemiology

Malaria is transmitted in nearly 100 countries worldwide. According to latest estimates released by WHO,[80] around 214 million cases of malaria occurred in 2015 and the disease led to nearly half a million deaths worldwide. Malaria is most prevalent in Africa which alone accounted for 88% of all malaria cases and 90% of all malaria deaths in 2015. The remaining cases of malaria have been reported in South-East Asia and the Eastern Mediterranean Regions with 10% and 2% of all malaria cases, respectively.

Malaria in humans is transmitted by the bite of a female *Anopheles* mosquito infected by a parasite called *Plasmodium*.[81] Five *Plasmodium* species are responsible for causing malaria in

humans. These are *P. falciparum, P. vivax*, *P. ovale, P. malariae* and *P. knowlesi*.[82] *P. falciparum*, among these, is the most virulent and is mainly found in Africa where it is the primary cause of malaria morbidity and mortality. In regions outside Africa, South-East Asia and South America, substantial cases of infections occur due to *P. vivax* species.[80] The virulence of *P. vivax* is due to the dormant liver stage of the parasite that can later activate and cause the disease months after the mosquito bite. Infections due to *P. malariae* and *P. ovale* are less common. *P. malariae* is located worldwide in Africa, South-East Asia and South America while *P. ovale* infections mainly occur in Africa. Similar to *P. vivax*, *P. ovale* also produces dormant liver stage parasites causing malaria months after the mosquito bite. *P. knowlesi* causes malaria mainly among monkeys but cases of human infections have been reported in certain forested areas of South-East Asia in recent years.[80,83]

Malaria can be uncomplicated or severe malaria based on the parasite burden in the host. Uncomplicated malaria can be caused by all the above five *Plasmodium* species. Symptoms of uncomplicated malaria are non-specific and frequently include fever, and chills accompanied by headache, fatigue, abdominal discomfort, muscle and joint aches and vomiting. These symptoms should be diagnosed quickly if a person is living or has travelled to a malaria endemic region. Severe malaria is caused only by *P. falciparum*. In the absence of prompt treatment, the parasite burden continues to grow and uncomplicated malaria can progress to severe malaria. The main symptoms of severe malaria include coma (cerebral malaria), severe anaemia, hypoglycaemia, metabolic acidosis, acute renal failure or acute pulmonary oedema. Severe malaria is diagnosed when one of these symptoms occur with no other obvious cause accompanied by the presence of *P. falciparum* parasites in that region.

1.2.2 Transmission and Pathology

The life cycle of the *Plasmodium* parasite is divided between the female *Anopheles* mosquito and human (Figure 1.11).[84,85] The *Plasmodium* parasites are found as "sporozoites" in the salivary glands of an infected mosquito. When the mosquito bites a human, the sporozoites are released into the human's bloodstream. Sporozoites are rapidly taken up by the liver cells, where they multiply and develop into schizonts over the next one or two weeks.[86] This is called the exoerythrocytic stage of infection and is asymptomatic. This process occurs with all *Plasmodium* species, except with *P. vivax* and *P. ovale* which can become dormant in the liver as 'hypnozoites' and cause malaria by invading the bloodstream weeks or even years later, causing clinical symptoms of malaria without a recent mosquito bite.[87–89]

Schizonts rupture to release merozoites into the bloodstream where they invade erythrocytes.[86] Within the erythrocytes, merozoites successively mature from ring forms to trophozoites and then to multinucleated schizonts (over 48 hours for *P. falciparum*, *P. vivax* and *P. ovale*, 72 hours for *P. malariae* and 24 hours for *P. knowlesi*).[90] These schizonts then rupture and release more merozoites in the blood which then infect more blood cells. This cycle of asexual multiplication is repeated and is known as the erythrocytic stage of the infection. Rupturing of schizonts releases parasites and host cellular material into the blood stream. This activates macrophages to release pro-inflammatory cytokines which cause fever and other pathological effects.

Within some infected blood cells, *Plasmodium* enters a sexual multiplication cycle. The merozoites develop into sexual forms of the parasite called gametocytes. Gametocyte-containing blood cells circulate in the bloodstream. When a mosquito feeds on infected human blood, it ingests the blood cells which burst in the mosquito's gut, thus releasing the gametocytes. These then develop further into mature sex cells called gametes. Male and female gametes fuse to form diploid zygotes, which develop into actively moving ookinetes that burrow into the mosquito midgut wall and form oocysts. Growth and division of each oocyst produces thousands of active haploid forms called sporozoites. After one or two weeks (time frame depends on *Plasmodium* species), the oocyst bursts and releases sporozoites into the body cavity of the mosquito, from where they travel to and invade the mosquito's salivary glands. The cycle of human infection re-starts when the mosquito bites again.[85,91,92]

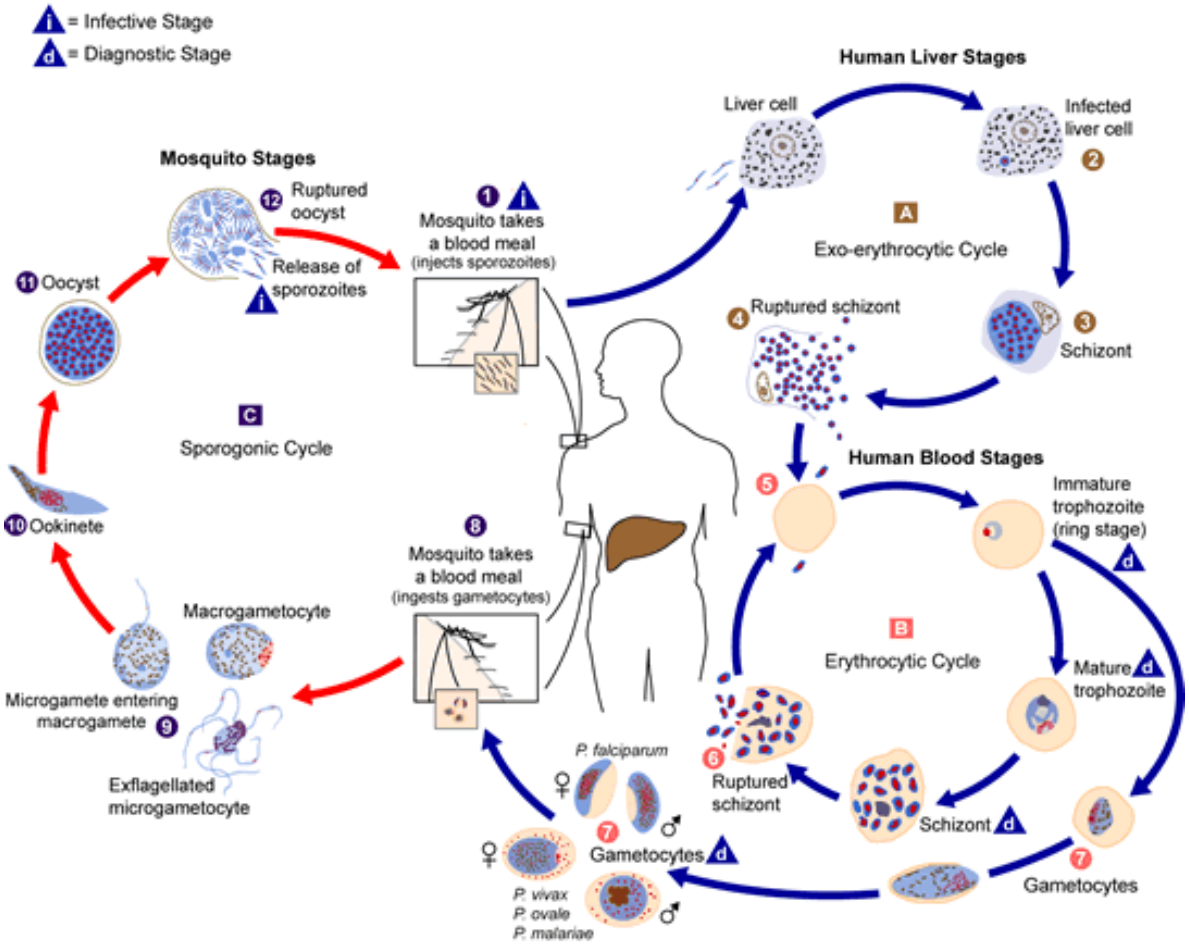

Figure 1.11: Life cycle of *Plasmodium* parasite[93]

Upon invasion of the erythrocytes, the parasite degrades and consumes intracellular components, primarily haemoglobin. The parasite degrades haemoglobin in the food vacuole into heme (iron porphyrin) and globulin (protein), which are important sources of iron and amino acids, respectively, and are utilised in the synthesis of various parasitic proteins. Heme as such is toxic for the parasite as it can generate free radicals and reactive oxygen species which can degrade plasmodial proteins, lipids and DNA molecules. Therefore, *Plasmodium* detoxifies this iron-rich compound by polymerising it into the crystalline hemozoin (malaria pigment). Quine, chloroquine (CQ), mefloquine and other related drugs target the parasite through inhibition of hemozoin formation.

1.2.3 Antimalarial drugs

Total eradication of malaria can potentially be achieved by the effective prevention and treatment of malaria. Prevention of malaria can be further achieved by 1) control of the vector mosquito *Anopheles* and 2) chemoprophylaxis and chemoprevention. Deployment of long-lasting-insecticide-treated mosquito nets, application of mosquito repellents to the skin,

spraying of the user-friendly insecticides in houses, buildings and agriculture in areas of moderate or high transmission have all substantially contributed to the decrease in malaria morbidity and mortality, by controlling the bite of vector mosquito *Anopheles*. Once the clinical symptoms develop and the patient is diagnosed with malaria, treatment of the disease becomes necessary with the available antimalarial drugs. The available antimalarial drugs can be classified as following.

1. Quinolines: Quinine, CQ, piperaquine, amodiaquine, mefloquine, primaquine
2. Aryl amino alcohols: halofantrine, lumenfantrine
3. Sulfones and sulfonamides: Dapsone and sulfadoxine (Type 1 antifolates)
4. Guanidines and diaminopyrimidines: Proguanil, chloroproguanil, pyrimethamine (Type 2 antifolates)
5. Naphthoquinones: Atovaquone
6. Artemisinin derivatives or peroxides: artemether, arteether, artesunate, artelinic acid
7. Antibiotics: Tetracycline, doxycycline, clindamycin

Another way of classifying the above-mentioned antimalarial drugs is based on the specific stage of the *Plasmodium* life cycle at which the drug shows its antimalarial action. Drugs that eliminate developing or dormant liver forms, such as primaquine, are called tissue schizonticides. Drugs that act on the blood forms of the parasite (erythrocytic parasites) and thereby terminate clinical attacks of malaria are called blood schizonticides. These are the most important drugs in anti-malarial chemotherapy. All above-mentioned drugs except primaquine possess this activity. *P. vivax* and *P. Ovale* infections not only require the cure of blood stage infection but also require the prevention of relapse by the killing of hypnozoites and therefore need both tissue schizonticides and blood schizonticides. This treatment method is known as radical cure of malaria. Drugs that kill sexual stages of the parasite i.e. gametocytes and prevent transmission are called gametocides. Complete and effective treatment of malaria requires drugs with activity at all growth stages of the parasite. Figure 1.12 displays the chemical structures of currently used antimalarial drugs.

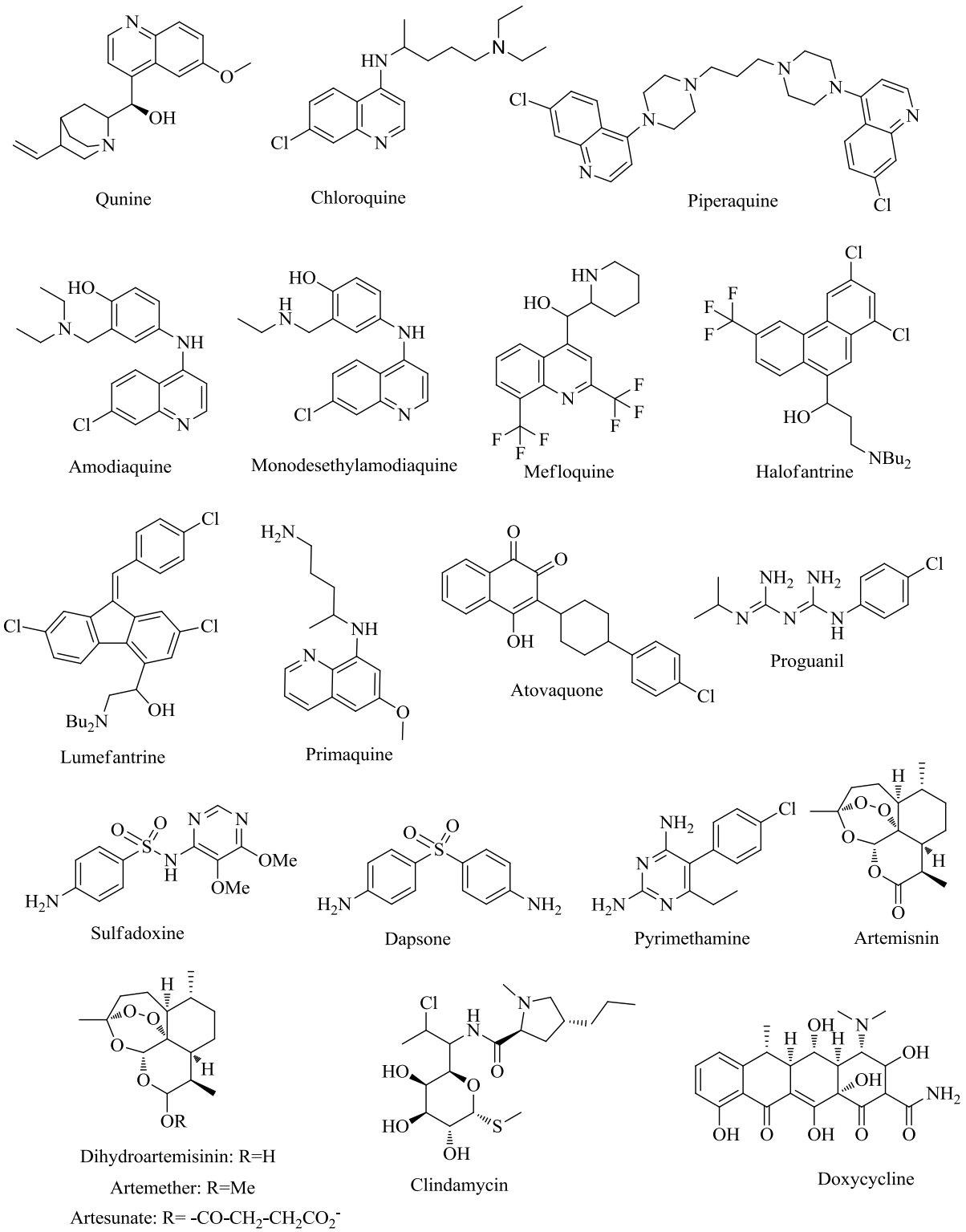

Figure 1.12: Chemical structures of currently used antimalarial drugs

Quinine is one of the oldest antimalarial agents. It was first isolated from the cinchona tree in 1820. Quinine was later replaced with a safer drug, a 4-aminoquinoline: CQ, and is now used to treat severe cases of malaria.[94] CQ was introduced in the 1940s and resistance emerged approximately 10 years after its introduction. CQ is also used as the first-line treatment of *P.*

vivax infections; however, the prevalence of CQ-resistant *P. vivax* is increasing. Nevertheless, the efficacy, affordability and safety, even during pregnancy, made it the gold standard treatment of malaria for many years.[95] CQ is still used as first-line drug in most African countries. Amodiaquine is another 4-aminoquinoline which has been in use for more than 70 years. Amodiaquine has a short half-life of 3 h, thus the antimalarial activity is thought to be exerted by the primary metabolite, monodesethylamodiaquine, which has a half-life of 9-18 days.[96] The 4-methanol quinoline: mefloquine and the two aryl amino alcohols: halofantrine and lumenfantrine are used to treat CQ-resistant malaria.

All the above-mentioned quinolines and aryl amino alcohols are blood schizontocides and are used in the treatment of clinical infections due to *P. falciparum*.[97]The 8-aminoquinoline primaquine, which is a tissue schizontocide, is not used in curing *P. falciparum* malaria but it is the only approved therapy for the treatment of *P. vivax* dormant liver stages.[98]

CQ, due to its weakly basic nature (pKa values at 8.1 and 10.2), can diffuse freely across membranes at the neutral pH of the blood. However, due to the acidic nature of the parasite's food vacuole, it becomes diprotonated and trapped inside this compartment. This allows CQ to accumulate in large quantities in the food vacuole where it binds to heme dimer and prevents polymerisation of heme into hemozoin, resulting in death of the parasite. Mechanisms of action of other quinolines and aryl amino alcohols are not much clear. However, they all have been proposed to inhibit heme detoxification based on the similarity in their chemical structures and some *in vitro* studies.[97,99,100]

Atovaquone is a hydroxynaphthoquinone analogue and is used in combination with proguanil as 'Malarone', mainly as a prophylactic medication for tourists. Atovaquone has been shown to inhibit the respiratory chain of plasmodial mitochondria at the cytochrome bc1 complex by mimicking the natural substrate, ubiquinone. [101,102]

The antifolate drugs inhibit two key enzymes in the folate biosynthesis pathway in plasmodia and are accordingly classified as type 1 and type 2 antifolate drugs depending upon the enzyme they inhibit. Type 1 antifolates inhibit the dihydropteroate synthase enzyme (*Pf*DHPS) and include sulfadoxine and dapsone. Type 2 antifolates inhibit the dihydrofolate reductase enzyme (*Pf*DHFR) and include pyrimethamine and proguanil. Antifolate drugs are highly effective when used in combination. The drug combination sulfadoxine-pyrimethamine, named as 'Fansidar', was introduced in 1970s after the emergence of CQ-

resistant parasites and was highly effective, cheap and well-tolerated with good compliance rates due to being administered in a single dose. However, resistance of *Plasmodium* to these antifolates emerged quickly after their introduction. Therefore, the sulfadoxine-pyrimethamine combination is now primarily used as an intermittent preventative malaria treatment during pregnancy and to a lesser extent for the treatment of malaria infection. The other combination dapsone-proguanil, named as 'Lapdap', is no longer recommended as dapsone causes hemolysis in G6PD-deficient patients.[103]

The most recent and effective class of antimalarial drugs is the peroxides, which include artemisinin and its derivatives (dihydroartemisinin, artemether, arteether, artesunate and artelinic acid). They have tissue, blood-schizontocidal and gametocidal activity and therefore eliminate all stages of the parasite. Artemisinin is a natural product isolated from the *Artemisia annua* plant (Chinese wormwood). Artemisinins display a unique trioxane structure with an endoperoxide bond that is mandatory for antimalarial activity. The mechanism of action of artemisinin is not fully understood but the prevailing theory is that the endoperoxide bridge is cleaved reductively by Fe(II) of heme proteins, leading to the formation of reactive carbon radicals that subsequently alkylate essential biomolecules.[104,105]

Antibiotics such as tetracycline, doxycycline and clindamycin are quite effective, albeit slow-acting antimalarials. Due to their slow action, these antibiotics are used in combination with more rapidly acting drugs like quinine. These antibiotics target the parasite apicoplast, a nonphotosynthetic plastid organelle, unique to plasmodia and other apicomplexan parasites. In *Plasmodium* species, the apicoplast appears to be essential for the synthesis of fatty acids, isoprenoids and heme.[106] The apicoplast expresses its own genome, which encodes a small set of genes (approximately 30). The apicoplast proteome is thus supplemented by as many as 500 nucleus-encoded apicoplast-targeted proteins. Antibiotics disrupt the apicoplast translation machinery during the first replication cycle delivering non-functional apicoplasts into the progeny during the second cycle. This results in the interruption import or export of new nuclear and apicoplast-encoded proteins during the second cycle, resulting in death of the parasites. However, during this first cycle, these antibiotics do not affect the apicoplast metabolic functions, especially those catalyzed by nuclear-encoded proteins, since they are already present in the apicoplast at the time of the antibacterial exposure. This explains the delayed death effect (DDE) of these antibiotics.[107,108]

1.2.4 Treatment

The WHO has provided guidelines for treating *P. falciparum* malaria based on the severity of the disease which can be uncomplicated or severe *P. falciparum* malaria.[109]

Following artemisinin combination therapies (ACTs) are recommended for the treatment of uncomplicated *P. falciparum* malaria over a period of three days:

1. Artemether plus lumefantrine
2. Artesunate plus amodiaquine
3. Artesunate plus mefloquine
4. Dihydroartemisinin plus piperaquine
5. Artesunate plus sulfadoxine-pyrimethamine

ACT can be orally administered to all children and adults except pregnant women in their first trimester. Seven day treatment of quinine plus clindamycin has been recommended for pregnant women in the first trimester. ACT therapy is also recommended in uncomplicated malaria caused by species other than *P. falciparum*. Patients with *P. vivax* or *P. ovale* infections should be given a primaquine treatment after ACT to eradicate hypnozoites.

Severe *P. falciparum* malaria treatment is started with intravenous or intramuscular injection of artesunate for at least 24 h and until the patient can tolerate oral medication. After the patient has received parenteral therapy and is now able to tolerate oral medication, treatment is completed with 3 days of ACT. Use of intramuscular artemether is recommended if artesunate is unavailable and intramuscular quinine dihydrochloride when both artesunate and artemether are unavailable. This treatment of severe malaria is given regardless of adults, infants or pregnant women.

1.2.5 Challenges

P. falciparum has developed resistance to quinolines and related analogues, to antifolates, to inhibitors of electron transport and, more recently, to artemisinins.[97,110–113] Therefore, new medicinal agents with novel mechanisms of action are needed to overcome the problem of resistance.

ACTs are the current standard of care for uncomplicated malaria. Artemisinin and its derivatives have a fast onset of action but short half-lives ($t_{1/2}$ = 0.5-4 h) and rapid clearance. Therefore, artemisinins are combined with slow-clearing drugs like lumefantrine ($t_{1/2}$ = 3-4

days) and piperaquine ($t_{1/2}$ = 8-16 days) to kill residual parasites. New drugs are needed, which possess potencies similar to artemisinins but with longer half-lives.

For complete eradication of malaria, drugs are needed that can eliminate liver stage hypnozoites, block transmission of the parasite by acting on gametocytes and are active in the mosquito stages of the parasite. Primaquine is the only drug approved to eliminate hypnozoites and is also active against mature gametocytes. There is no drug currently registered to target mosquito stages. Patient compliance to the current treatment is poor due to multiple doses, adverse reactions, costliness and unavailability of the drugs in poor communities.

In order to overcome the above-mentioned challenges, new drugs should be efficacious against drug-resistant strains, provide cure within a reasonable time (ideally three days or less) to ensure good compliance, be safe, be suitable for small children and pregnant women, have appropriate formulations for oral use and, above all, be affordable.

1.2.6 Antimalarials in the pipeline

As of March 2016, there are 9 antimalarial compounds being evaluated in humans for safety, pharmacokinetics and efficacy. In addition, 9 compounds are in preclinical studies for their evaluation as potential candidates to go further in human trials. Most of these compounds possess novel mechanisms of action and thus evade drug resistance (Figure 1.13 and 1.14). A brief description of these preclinical and clinical candidates is given below.

Primaquine is the only available drug so far that can prevent relapse due to *P. vivax* malaria. A new 8-aminoquinoline named tafenoquine has been developed that has shown activity against *P.vivax* life cycle including dormant forms. The drug is in Phase III trials to investigate a single dose treatment for relapsing *P. vivax* malaria.[114]

Figure 1.13: Global pipeline of preclinical and clinical antimalarial candidates[115]

The problem of short half-lives for artemisinins can be overcome by improving both metabolic stability and aqueous solubility. A new endoperoxide OZ439, has been developed, which show greater metabolic stability and improved aqueous solubility. OZ439 is a 1,2,4-trioxolane analogue containing adamantyl and 4-morpholinoethoxyphenylcyclohexyl moieties. This drug maintains activity across all asexual blood stages of the parasite such as rings, trophozoites and schizonts. This compound has a half-life of 25-30 h which has not been achieved with any other artemisinin derivative. The extended half-life and better solubility has improved the oral pharmacokinetic profile of OZ439.[116] OZ439 has completed phase IIa trials for acute, uncomplicated malaria in patients with *P. falciparum* or *P. vivax* malaria monoinfection[117,118] and is currently in phase IIb studies to determine the efficacy in combination with piperaquine for uncomplicated *P. falciparum* malaria.[119] CDRI 97/78 is another 1,2,4-trioxolane derivative which has been found to be safe with an average half-life of 5 h, in a single ascending dose safety and pharmacokinetics study conducted in healthy

volunteers.[120] CDRI 97/78 exerts its action by rapidly converting into its active alcohol metabolite arising from hydrolysis or metabolism of the ester group.

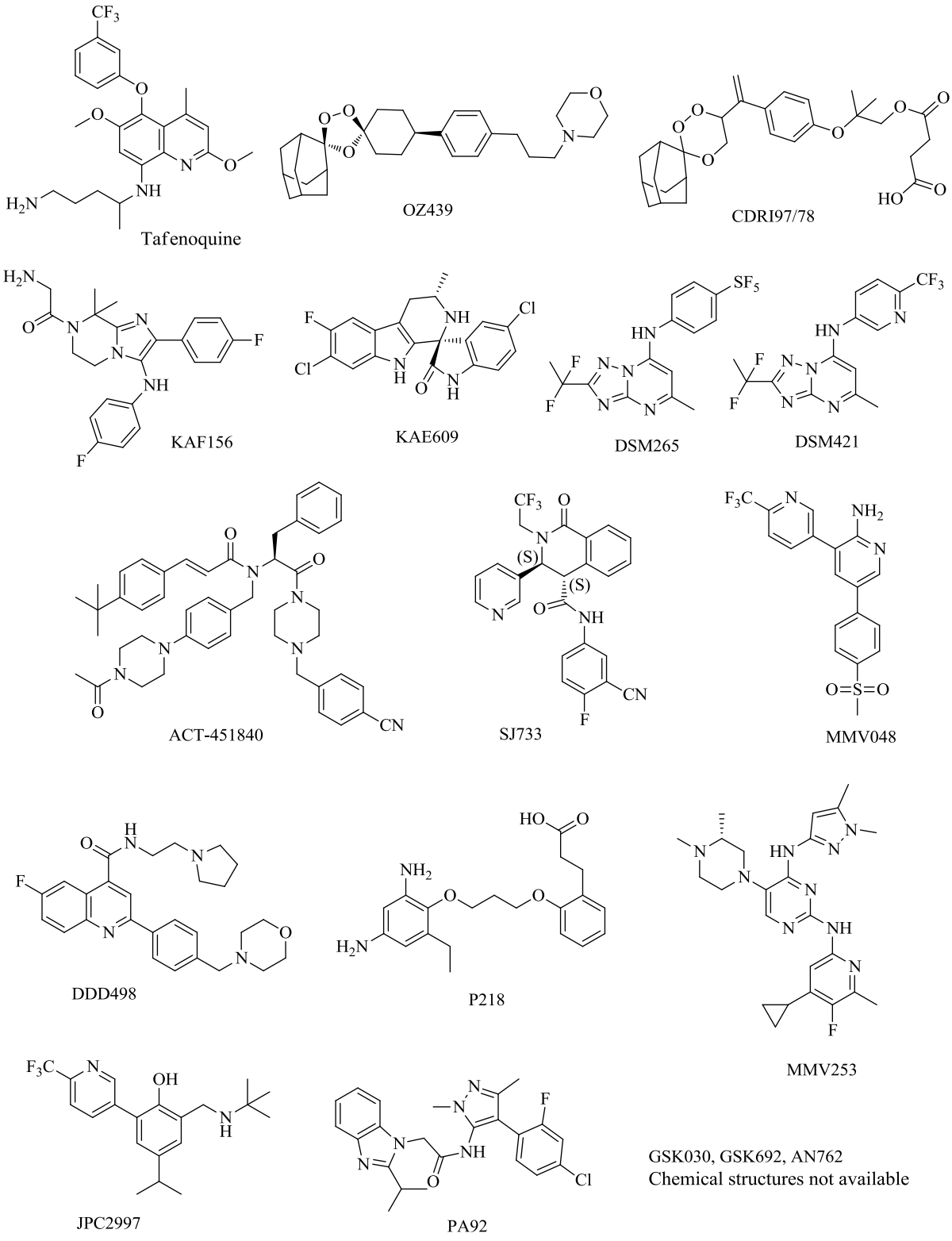

Figure 1.14: Chemical structures of preclinical and clinical antimalarial candidates

Two novel molecules developed by Novartis, a spiroindolone KAE609 and an imidazolopiperazine KAF156, are also in phase II trials to assess safety and efficacy in *P. falciparum* or *P. vivax* malaria monoinfection.[121] KAE609 inhibits the P-type cation transporter ATPase 4 (*Pf*ATP4), which regulates sodium concentration in the parasite [122] while KAF156 targets the *P. falciparum* cyclic amine resistance locus (*Pf*carl) gene that encodes a transmembrane protein believed to play a role in protein folding within the endoplasmic reticulum.[123] Further, KAF156 was found to be completely protective as a single oral dose of 10 mg/kg when administered prophylactically in a sporozoite challenge mouse model.[123] Based on this preclinical study, sporozoite challenge study in human volunteers is ongoing in order to evaluate the potential of KAF156 as a chemoprophylactic agent in malaria.[115]

A triazolopyrimidine derivative DSM265 is one more candidate in phase II. DSM265 is a selective inhibitor of *P. falciparum* dihydroorotate dehydrogenase (DHODH). DHODH is involved in the biosynthesis of pyrimidines, which are important components of DNA and RNA. DSM265, thus, has the potential to prevent and cure malaria by targeting the ability of the parasite to replicate both in liver and blood stages.[124] DSM 412, obtained by replacing the SF_5-phenyl group of DSM265 with a CF_3-pyridyl, is another member of this series which has reached preclinical trials.

Other preclinical and clinical candidates include a *P. falciparum* phosphatidylinositol 4-kinase (*Pf*PI4K) inhibitor MMV048, a peptidomimetic protease inhibitor ACT-451840, three *Pf*ATP4 enzyme inhibitors SJ733, PA92 and GSK030, a *P. falciparum* dihydrofolate reductase (*Pf*DHFR) inhibitor P218, a *P. falciparum* eukaryotic elongation factor 2 (*Pf*eEF2) inhibitor DDD498, a V-type H+ ATPase inhibitor MMV 253, and three candidates, JPC2997, AN762 and GSK692, with unknown mechanisms of action.[115]

In summary, malaria is being transmitted worldwide in nearly 100 countries causing half a million deaths each year. The emergence of resistant strains of *P. falciparum* has hindered current antimalarial treatment and global control of the disease. New drugs with novel mechanisms of action are required to overcome resistance and contribute to the eradication agenda.

1.3 Conclusion

The high epidemiology of TB and malaria, and emerging drug resistance in both diseases necessitates the discovery of new agents with novel mechanisms of action. This project, therefore, seeks to contribute to this aspect and is an attempt to identify novel agents effective against TB and / or malaria using approaches underpinned by medicinal chemistry.

Chapter 2 provides a discussion of drug repositioning/ repurposing as an approach to fast-track the process of drug discovery and development, and its application in the field of chemotherapy for TB and malaria.

1.4 References

(1) World Health Organization. *Global Tuberculosis Report*; 2015.

(2) Kieser, K. J.; Rubin, E. J. How Sisters Grow Apart: Mycobacterial Growth and Division. *Nat. Rev. Microbiol.* **2014**, *12*, 550–562.

(3) Gengenbacher, M.; Kaufmann, S. H. E. Mycobacterium Tuberculosis: Success through Dormancy. *FEMS Microbiol. Rev.* **2012**, *36*, 514–532.

(4) Tuberculosis (TB) Cause https://www.niaid.nih.gov/topics/tuberculosis/understanding/pages/cause.aspx.

(5) Zumla, A.; Raviglione, M.; Hafner, R.; Fordham von Reyn, C. Tuberculosis. *N. Engl. J. Med.* **2013**, *368*, 745–755.

(6) Koul, A.; Arnoult, E.; Lounis, N.; Guillemont, J.; Andries, K. The Challenge of New Drug Discovery for Tuberculosis. *Nature* **2011**, *469*, 483–490.

(7) Rosas-Taraco, A. G.; Arce-Mendoza, A. Y.; Caballero-Olín, G.; Salinas-Carmona, M. C. Mycobacterium Tuberculosis Upregulates Coreceptors CCR5 and CXCR4 While HIV Modulates CD14 Favoring Concurrent Infection. *AIDS Res. Hum. Retroviruses* **2006**, *22*, 45–51.

(8) Goletti, D.; Weissman, D.; Jackson, R. W.; Graham, N. M.; Vlahov, D.; Klein, R. S.; Munsiff, S. S.; Ortona, L.; Cauda, R.; Fauci, a S. Effect of Mycobacterium Tuberculosis on HIV Replication. Role of Immune Activation. *J. immunol.* **1996**, *157*, 1271–1278.

(9) Mariani, F.; Goletti, D.; Ciaramella, A.; Martino, A.; Colizzi, V.; Fraziano, M. Macrophage Response to Mycobacterium Tuberculosis during HIV Infection: Relationships between Macrophage Activation and Apoptosis. *Curr. Mol. Med.* **2001**, *1*, 209–216.

(10) Kaufmann, S. H. How Can Immunology Contribute to the Control of Tuberculosis? *Nat. Rev. Immunol.* **2001**, *1*, 20–30.

(11) Russell, D. G. Mycobacterium Tuberculosis: Here Today, and Here Tomorrow. *Nat. Rev. Mol. Cell Biol.* **2001**, *2*, 569–577.

(12) Vandal, O. H.; Nathan, C. F.; Ehrt, S. Acid Resistance in Mycobacterium Tuberculosis. *J. Bacteriol.* **2009**, *191*, 4714–4721.

(13) Ramakrishnan, L. Revisiting the Role of the Granuloma in Tuberculosis. *Nat. Rev. Immunol.* **2012**, *12*, 352–366.

(14) Yuk, J.-M.; Jo, E.-K. Host Immune Responses to Mycobacterial Antigens and Their Implications for the Development of a Vaccine to Control Tuberculosis. *Clin. Exp. Vaccine Res.* **2014**, *3*, 155–167.

(15) World Health Organization. *Companion Handbook to the WHO Guidelines for the Programmatic Management of Drug-Resistant Tuberculosis*; 2014.

(16) Zhang, Y.; Yew, W. Mechanisms of Drug Resistance in Mycobacterium Tuberculosis. *Int. J. Tuberc. Lung Dis.* **2009**, *13*, 1320–1330.

(17) Caminero, J. a.; Sotgiu, G.; Zumla, A.; Migliori, G. B. Best Drug Treatment for Multidrug-Resistant and Extensively Drug-Resistant Tuberculosis. *Lancet Infect. Dis.* **2010**, *10*, 621–629.

(18) Rozwarski, D. a; Grant, G. a; Barton, D. H.; Jacobs, W. R.; Sacchettini, J. C. Modification of the NADH of the Isoniazid Target (InhA) from Mycobacterium Tuberculosis. *Science* **1998**, *279*, 98–102.

(19) Zhang, Y.; Heym, B.; Allen, B.; Young, D.; Cole, S. The Catalase-Peroxidase Gene and Isoniazid Resistance of Mycobacterium Tuberculosis. *Nature* **1992**, *358*, 591–593.

(20) Rawat, R.; Whitty, A.; Tonge, P. J. The Isoniazid-NAD Adduct Is a Slow, Tight-Binding Inhibitor of InhA, the Mycobacterium Tuberculosis Enoyl Reductase: Adduct Affinity and Drug Resistance. *Proc. Natl. Acad. Sci. U.S.A.* **2003**, *100*, 13881–13886.

(21) Yu, S.; Girotto, S.; Lee, C.; Magliozzo, R. S. Reduced Affinity for Isoniazid in the S315T Mutant of Mycobacterium Tuberculosis KatG Is a Key Factor in Antibiotic Resistance. *J. Biol .Chem.* **2003**, *278*, 14769–14775.

(22) Telenti, a; Imboden, P.; Marchesi, F.; Lowrie, D.; Cole, S.; Colston, M. J.; Matter, L.; Schopfer, K.; Bodmer, T. Detection of Rifampicin-Resistance Mutations in Mycobacterium Tuberculosis. *Lancet* **1993**, *341*, 647–650.

(23) Williams, D. L.; Spring, L.; Collins, L.; Miller, L. P.; Heifets, L. B.; Gangadharam, P. R.; Gillis, T. P. Contribution of rpoB Mutations to Development of Rifamycin Cross-Resistance in Mycobacterium Tuberculosis. *Antimicrob. Agents Chemother.* **1998**, *42*, 1853–1857.

(24) Bodmer, T.; Zürcher, G.; Imboden, P.; Telenti, A. Mutation Position and Type of Substitution in the Beta-Subunit of the RNA Polymerase Influence in-Vitro Activity of

Rifamycins in Rifampicin-Resistant Mycobacterium Tuberculosis. *J. Antimicrob. Chemother.* **1995**, *35*, 345–348.

(25) Mikusová, K.; Slayden, R. a; Besra, G. S.; Brennan, P. J. Biogenesis of the Mycobacterial Cell Wall and the Site of Action of Ethambutol. *Antimicrob. Agents Chemother.* **1995**, *39*, 2484–2489.

(26) Sreevatsan, S.; Stockbauer, K. E.; Pan, X.; Kreiswirth, B. N.; Moghazeh, S. L.; Jacobs, W. R.; Telenti, A.; Musser, J. M. Ethambutol Resistance in Mycobacterium Tuberculosis: Critical Role of embB Mutations. *Antimicrob. Agents Chemother.* **1997**, *41*, 1677–1681.

(27) Ramaswamy, S. V; Amin, a G.; Göksel, S.; Stager, C. E.; Dou, S. J.; El Sahly, H.; Moghazeh, S. L.; Kreiswirth, B. N.; Musser, J. M. Molecular Genetic Analysis of Nucleotide Polymorphisms Associated with Ethambutol Resistance in Human Isolates of Mycobacterium Tuberculosis. *Antimicrob. Agents Chemother.* **2000**, *44*, 326–336.

(28) Konno, K.; Feldmann, F. M.; McDermott, W. Pyrazinamide Susceptibility and Amidase Activity of Tubercle Bacilli. *Am. Rev. Respir. Dis.* **1967**, *95*, 461–469.

(29) Palomino, J.; Martin, A. Drug Resistance Mechanisms in Mycobacterium Tuberculosis. *Antibiotics* **2014**, *3*, 317–340.

(30) Juréen, P.; Werngren, J.; Toro, J. C.; Hoffner, S. Pyrazinamide Resistance and pncA Gene Mutations in Mycobacterium Tuberculosis. *Antimicrob. Agents Chemother.* **2008**, *52*, 1852–1854.

(31) Scorpio, A.; Lindholm-Levy, P.; Heifets, L.; Gilman, R.; Siddiqi, S.; Cynamon, M.; Zhang, Y. Characterization of pncA Mutations in Pyrazinamide-Resistant Mycobacterium Tuberculosis. *Antimicrob. Agents Chemother.* **1997**, *41*, 540–543.

(32) Scorpio, A.; Zhang, Y. Mutations in pncA, a Gene Encoding Pyrazinamidase/nicotinamidase, Cause Resistance to the Antituberculous Drug Pyrazinamide in Tubercle Bacillus. *Nat. Med.* **1996**, *2*, 662–667.

(33) Finken, M.; Kirschner, P.; Meier, A.; Wrede, A.; Böttger, E. C. Molecular Basis of Streptomycin Resistance in Mycobacterium Tuberculosis: Alterations of the Ribosomal Protein S12 Gene and Point Mutations within a Functional 16S Ribosomal RNA Pseudoknot. *Mol. Microbiol.* **1993**, *9*, 1239–1246.

(34) Honoré, N.; Cole, S. T. Streptomycin Resistance in Mycobacteria. *Antimicrob. Agents Chemother.* **1994**, *38*, 238–242.

(35) Nair, J.; Rouse, D. a.; Bai, G. H.; Morris, S. L. The rpsL Gene and Streptomycin Resistance in Single and Multiple Drug-Resistant Strains of Mycobacterium Tuberculosis. *Mol. Microbiol.* **1993**, *10*, 521–527.

(36) Alangaden, G. J.; Kreiswirth, B. N.; Aouad, A.; Khetarpal, M.; Igno, F. R.; Moghazeh, S. L.; Manavathu, E. K.; Lerner, S. A. Mechanism of Resistance to Amikacin and

Kanamycin in Mycobacterium Tuberculosis. *Antimicrob. Agents Chemother.* **1998**, *42*, 1295–1297.

(37) Suzuki, Y.; Katsukawa, C.; Tamaru, A.; Abe, C.; Makino, M.; Mizuguchi, Y.; Taniguchi, H. Detection of Kanamycin-Resistant Mycobacterium Tuberculosis by Identifying Mutations in the 16S rRNA Gene. *J. Clin. Microbiol.* **1998**, *36*, 1220–1225.

(38) Johansen, S. K.; Maus, C. E.; Plikaytis, B. B.; Douthwaite, S. Capreomycin Binds across the Ribosomal Subunit Interface Using tlyA-Encoded 2'-O-Methylations in 16S and 23S rRNAs. *Mol. Cell* **2006**, *23*, 173–182.

(39) Aubry, A.; Pan, X.-S.; Fisher, L. M.; Jarlier, V.; Cambau, E. Mycobacterium Tuberculosis DNA Gyrase: Interaction with Quinolones and Correlation with Antimycobacterial Drug Activity. *Antimicrob. Agents Chemother.* **2004**, *48*, 1281–1288.

(40) Maruri, F.; Sterling, T. R.; Kaiga, A. W.; Blackman, A.; Van Der Heijden, Y. F.; Mayer, C.; Cambau, E.; Aubry, A. A Systematic Review of Gyrase Mutations Associated with Fluoroquinolone-Resistant Mycobacterium Tuberculosis and a Proposed Gyrase Numbering System. *J. Antimicrob. Chemother.* **2012**, *67*, 819–831.

(41) Baulard, A. R.; Betts, J. C.; Engohang-Ndong, J.; Quan, S.; McAdam, R. a.; Brennan, P. J.; Locht, C.; Besra, G. S. Activation of the pro-Drug Ethionamide Is Regulated in Mycobacteria. *J. Biol. Chem.* **2000**, *275*, 28326–28331.

(42) Banerjee, A.; Dubnau, E.; Quemard, A.; Balasubramanian, V.; Um, K. S.; Wilson, T.; Collins, D.; de Lisle, G.; Jacobs, W. R. inhA, a Gene Encoding a Target for Isoniazid and Ethionamide in Mycobacterium Tuberculosis. *Science* **1994**, *263*, 227–230.

(43) Brossier, F.; Veziris, N.; Truffot-Pernot, C.; Jarlier, V.; Sougakoff, W. Molecular Investigation of Resistance to the Antituberculous Drug Ethionamide in Multidrug-Resistant Clinical Isolates of Mycobacterium Tuberculosis. *Antimicrob. Agents Chemother.* **2011**, *55*, 355–360.

(44) Morlock, G. P.; Metchock, B.; Sikes, D.; Crawford, J. T.; Cooksey, R. C. ethA, inhA, and katG Loci of Ethionamide-Resistant Clinical Mycobacterium Tuberculosis Isolates. *Antimicrob. Agents Chemother.* **2003**, *47*, 3799–3805.

(45) Cáceres, N. E.; Harris, N. B.; Wellehan, J. F.; Feng, Z.; Kapur, V.; Barletta, R. G. Overexpression of the D-Alanine Racemase Gene Confers Resistance to D-Cycloserine in Mycobacterium Smegmatis. *J. Bacteriol.* **1997**, *179*, 5046–5055.

(46) Feng, Z.; Barletta, R. G. Roles of Mycobacterium Smegmatis D-ala:D-Ala Ligase and D-Ala Racemase in the Mechanisms of Action of and Resistance to the Peptidoglycan Inhibitor D-Cycloserine. *Antimicrob. Agents Chemother.* **2003**, *47*, 283–291.

(47) Rengarajan, J.; Sassetti, C. M.; Naroditskaya, V.; Sloutsky, A.; Bloom, B. R.; Rubin, E. J. The Folate Pathway Is a Target for Resistance to the Drug Para-Aminosalicylic Acid (PAS) in Mycobacteria. *Mol. Microbiol.* **2004**, *53*, 275–282.

(48) Andries, K.; Verhasselt, P.; Guillemont, J.; Göhlmann, H. W. H.; Neefs, J.-M.; Winkler, H.; Van Gestel, J.; Timmerman, P.; Zhu, M.; Lee, E.; Williams, P.; de Chaffoy, D.; Huitric, E.; Hoffner, S.; Cambau, E.; Truffot-Pernot, C.; Lounis, N.; Jarlier, V. A Diarylquinoline Drug Active on the ATP Synthase of Mycobacterium Tuberculosis. *Science* **2005**, *307*, 223–227.

(49) Zumla, A.; Nahid, P.; Cole, S. T. Advances in the Development of New Tuberculosis Drugs and Treatment Regimens. *Nat. Rev. Drug discov.* **2013**, *12*, 388–404.

(50) Xavier, A. S.; Lakshmanan, M. Delamanid: A New Armor in Combating Drug-Resistant Tuberculosis. *J. Pharmacol .Pharmacother.* **2014**, *5*, 222–224.

(51) Da Silva, P. E. A.; Palomino, J. C. Molecular Basis and Mechanisms of Drug Resistance in Mycobacterium Tuberculosis: Classical and New Drugs. *J. Antimicrob. Chemother.* 2011, pp 1417–1430.

(52) Yano, T.; Kassovska-Bratinova, S.; Shin Teh, J.; Winkler, J.; Sullivan, K.; Isaacs, A.; Schechter, N. M.; Rubin, H. Reduction of Clofazimine by Mycobacterial Type 2 NADH: Quinone Oxidoreductase: A Pathway for the Generation of Bactericidal Levels of Reactive Oxygen Species. *J. Biol.Chem.* **2011**, *286*, 10276–10287.

(53) Williamson, R.; Collatz, E.; Gutmann, L. Mechanisms of Action of Beta-Lactam Antibiotics and Mechanisms of Non-Enzymatic Resistance. *Presse med.* **1986**, *15*, 2282–2289.

(54) Dubée, V.; Triboulet, S.; Mainardi, J. L.; Ethève-Quelquejeu, M.; Gutmann, L.; Marie, A.; Dubost, L.; Hugonnet, J. E.; Arthur, M. Inactivation of Mycobacterium Tuberculosis L,D-Transpeptidase Ldt Mt1 by Carbapenems and Cephalosporins. *Antimicrob. Agents Chemother.* **2012**, *56*, 4189–4195.

(55) Alahari, A.; Trivelli, X.; Guérardel, Y.; Dover, L. G.; Besra, G. S.; Sacchettini, J. C.; Reynolds, R. C.; Coxon, G. D.; Kremer, L. Thiacetazone, an Antitubercular Drug That Inhibits Cyclopropanation of Cell Wall Mycolic Acids in Mycobacteria. *PLoS ONE* **2007**, *2*.

(56) Kanoh, S.; Rubin, B. K. Mechanisms of Action and Clinical Application of Macrolides as Immunomodulatory Medications. *Clin. Microbiol. Rev.* 2010, pp 590–615.

(57) Mitchison, D. A. Role of Individual Drugs in the Chemotherapy of Tuberculosis. *Int. J.Tuberc. Lung Dis.* **2000**, *4*, 796–806.

(58) Laurenzi, M.; Ginsberg, A.; Spigelman, M. Challenges Associated with Current and Future TB Treatment. *Infect. Disord. Drug Targets* **2007**, *7*, 105–119.

(59) L'homme, R. F.; Nijland, H. M. J.; Gras, L.; Aarnoutse, R. E.; van Crevel, R.; Boeree, M.; Brinkman, K.; Prins, J. M.; Juttmann, J. R.; Burger, D. M. Clinical Experience with the Combined Use of Lopinavir/ritonavir and Rifampicin. *AIDS* **2009**, *23*, 863–865.

(60) Chen, J.; Raymond, K. Roles of Rifampicin in Drug-Drug Interactions: Underlying Molecular Mechanisms Involving the Nuclear Pregnane X Receptor. *Ann. Clin. Microbiol. Antimicrob.* **2006**, *5*, 3.

(61) Jeon, C. Y.; Murray, M. B. Diabetes Mellitus Increases the Risk of Active Tuberculosis: A Systematic Review of 13 Observational Studies. *PLoS Med.* **2008**, *5*, 1091–1101.

(62) Baker, M. A.; Harries, A. D.; Jeon, C. Y.; Hart, J. E.; Kapur, A.; Lönnroth, K.; Ottmani, S.-E.; Goonesekera, S. D.; Murray, M. B. The Impact of Diabetes on Tuberculosis Treatment Outcomes: A Systematic Review. *BMC Med.* **2011**, *9*, 1–15.

(63) Baghaei, P.; Marjani, M.; Javanmard, P.; Tabarsi, P.; Masjedi, M. R. Diabetes Mellitus and Tuberculosis Facts and Controversies. *J. diabetes Meta. Disord.* **2013**, *12*, 1–8.

(64) Drug Pipeline http://www.newtbdrugs.org/pipeline.php (accessed Jul 10, 2016).

(65) FDA News Release http://www.fda.gov/NewsEvents/Newsroom/PressAnnouncements/ucm333695.htm.

(66) SIRTURO® (bedaquiline) Receives Conditional Approval in the European Union for the Treatment of Multi-Drug Resistant Tuberculosis http://www.investor.jnj.com/releasedetail.cfm?ReleaseID=831021.

(67) World Health Organization. WHO Interim Guidance on the Use of Delamanid in the treatment of MDR-TB. www. who.int/tb/features_archive/delamanid/en/ (accessed Dec 13, 2015).

(68) STREAM stage 2 clinical study enrols patients in first trial to include bedaquiline to test shortened MDR-TB treatment regimens http://www.theunion.org/news-centre/features/stream-video (accessed Jul 10, 2016).

(69) Bedaquiline with OBR for MDR-TB (STREAM MDR Trial) http://www.newtbdrugs.org/project.php?id=141 (accessed Jul 10, 2016).

(70) Delamanid with OBR for MDR-TB http://www.newtbdrugs.org/project.php?id=136 (accessed Jul 10, 2016).

(71) ClinicalTrials.gov Identifier NCT01859923 https://clinicaltrials.gov/ct2/show/study/NCT01859923.

(72) Singh, R.; Manjunatha, U.; Boshoff, H. I. M.; Ha, Y. H.; Niyomrattanakit, P.; Ledwidge, R.; Dowd, C. S.; Lee, I. Y.; Kim, P.; Zhang, L.; Kang, S.; Keller, T. H.; Jiricek, J.; Barry, C. E. PA-824 Kills Nonreplicating Mycobacterium Tuberculosis by Intracellular NO Release. *Science* **2008**, *322*, 1392–1395.

(73) Stover, C. K.; Warrener, P.; VanDevanter, D. R.; Sherman, D. R.; Arain, T. M.; Langhorne, M. H.; Anderson, S. W.; Towell, J. a; Yuan, Y.; McMurray, D. N.; Kreiswirth, B. N.; Barry, C. E.; Baker, W. R. A Small-Molecule Nitroimidazopyran Drug Candidate for the Treatment of Tuberculosis. *Nature* **2000**, *405*, 962–966.

(74) Dorman, S. E.; Goldberg, S.; Stout, J. E.; Muzanyi, G.; Johnson, J. L.; Weiner, M.; Bozeman, L.; Heilig, C. M.; Feng, P. J.; Moro, R.; Narita, M.; Nahid, P.; Ray, S.; Bates, E.; Haile, B.; Nuermberger, E. L.; Vernon, A.; Schluger, N. W. Substitution of Rifapentine for Rifampin during Intensive Phase Treatment of Pulmonary Tuberculosis: Study 29 of the Tuberculosis Trials Consortium. In. *J. Infect. Dis.*; **2012**; Vol. 206, pp 1030–1040.

(75) Dorman, S. E.; Savic, R. M.; Goldberg, S.; Stout, J. E.; Schluger, N.; Muzanyi, G.; Johnson, J. L.; Nahid, P.; Hecker, E. J.; Heilig, C. M.; Bozeman, L.; Feng, P. J. I.; Moro, R. N.; MacKenzie, W.; Dooley, K. E.; Nuermberger, E. L.; Vernon, A.; Weiner, M. Daily Rifapentine for Treatment of Pulmonary Tuberculosis: A Randomized, Dose-Ranging Trial. *Am. J. Respir. Crit. Care Med.* **2015**, *191*, 333–343.

(76) Rifapentine-Moxifloxacin for DS-TB http://www.newtbdrugs.org/project.php?id=154 (accessed Jul 10, 2016).

(77) Tahlan, K.; Wilson, R.; Kastrinsky, D. B.; Arora, K.; Nair, V.; Fischer, E.; Barnes, S. W.; Walker, J. R.; Alland, D.; Barry, C. E.; Boshoff, H. I. SQ109 Targets MmpL3, a Membrane Transporter of Trehalose Monomycolate Involved in Mycolic Acid Donation to the Cell Wall Core of Mycobacterium Tuberculosis. *Antimicrob. Agents Chemother.* **2012**, *56*, 1797–1809.

(78) Q203-Novel Anti-TB Agent http://www.newtbdrugs.org/project.php?id=176 (accessed Jul 10, 2016).

(79) Rudolph, A. I. Antitubercular Benzothiazinones : Synthesis , Activity , Properties and SAR, Martin-Luther-Universität Halle-Wittenberg, 2014.

(80) World Health Organization. *Global Malaria Report*; 2015.

(81) Cox, F. E. History of the Discovery of the Malaria Parasites and Their Vectors. *Parasit. Vectors* **2010**, *3*, 5.

(82) Greenwood, B. M.; Fidock, D. A.; Kyle, D. E.; Kappe, S. H. I.; Alonso, P. L.; Collins, F. H.; Duffy, P. E. Malaria: Progress, Perils, and Prospects for Eradication. *J. Clin. Invest.* **2008**, *118*, 1266–1276.

(83) White, N. J. Plasmodium Knowlesi: The Fifth Human Malaria Parasite. *Clin. Infect. Dis.* **2008**, *46*, 172–173.

(84) Kar, S.; Kar, S. Control of Malaria. *Nat. Rev. Drug discov.* **2010**, *9*, 511–512.

(85) National Institute of Allergy and Infectioes Diseases,understanding Malaria http://www.niaid.nih.gov/topics/Malaria/understandingMalaria/Pages/default.aspx.

(86) Garnham, P. C. C. *Malaria Parasites and Other Haemosporidia.*; Oxford : Blackwell Scientific Publications, 1966.

(87) Imwong, M.; Snounou, G.; Pukrittayakamee, S.; Tanomsing, N.; Kim, J. R.; Nandy, A.; Guthmann, J.; Nosten, F.; Carlton, J.; Looareesuwan, S.; Nair, S.; Sudimack, D.;

Day, N. P. J.; Anderson, T. J. C.; White, N. J. Relapses of Plasmodium Vivax Infection Usually Result from Activation of Heterologous Hypnozoites. *J. Infect. Dis.* **2007**, *195*, 927–933.

(88) Hulden, L.; Hulden, L. Activation of the Hypnozoite: A Part of Plasmodium Vivax Life Cycle and Survival. *Malar. J.* **2011**, *10*, 90.

(89) Richter, J.; Franken, G.; Mehlhorn, H.; Labisch, A.; Häussinger, D. What Is the Evidence for the Existence of Plasmodium Ovale Hypnozoites? *Parasitol. Res.* **2010**, *107*, 1285–1290.

(90) Garnham, P. C. C. Malaria Parasites of Man: Life-Cycles and Morphology (excluding Ultrastructure). In *Malaria: principles and practice of malariology.*; Wernsdorfer, W.H.;McGregor, I., Ed.; Churchill Livingstone, Edinburgh, 1988; pp 61–96.

(91) Cox, F. E. History of the Discovery of the Malaria Parasites and Their Vectors. *Parasit. Vectors* **2010**, *3*, 1–9.

(92) White, N. J. Plasmodium Species (malaria). In *Antimicrobial therapy and vaccines*; V. Yu, R. Weber, and D. R., Ed.; Apple Trees Productions LLC. New York, New York, USA, 2002; pp 1609–1634.

(93) Malaria:Biology. https://www.cdc.gov/malaria/about/biology/ (accessed Jul 12, 2016).

(94) Butler, a. R.; Khan, S.; Ferguson, E. A Brief History of Malaria Chemotherapy. *J. R. Coll. Physicians Edinb.* **2010**, *40*, 172–177.

(95) AlKadi, H. O. Antimalarial Drug Toxicity: A Review. *Chemotherapy* **2007**, *53*, 385–391.

(96) Mariga, S. T.; Gil, J. P.; Sisowath, C.; Wernsdorfer, W. H.; Bjorkman, A. Synergism between Amodiaquine and Its Major Metabolite, Desethylamodiaquine, against Plasmodium Falciparum in Vitro. *Antimicrob. Agents Chemother.* **2004**, *48*, 4089–4096.

(97) Petersen, I.; Eastman, R.; Lanzer, M. Drug-Resistant Malaria: Molecular Mechanisms and Implications for Public Health. *FEBS Lett.* **2011**, *585*, 1551–1562.

(98) Baird, J. K.; Hoffman, S. L. Primaquine Therapy for Malaria. *Clin. Infect. Dis.* **2004**, *39*, 1336–1345.

(99) Müller, I. B.; Hyde, J. E. Antimalarial Drugs: Modes of Action and Mechanisms of Parasite Resistance. *Future Microbiol.* **2010**, *5*, 1857–1873.

(100) Olliaro, P. Mode of Action and Mechanisms of Resistance for Antimalarial Drugs. *Pharmacol. Ther.* **2001**, *89*, 207–219.

(101) Vaidya, A. B.; Lashgari, M. S.; Pologe, L. G.; Morrisey, J. Structural Features of Plasmodium Cytochrome B That May Underlie Susceptibility to 8-Aminoquinolines and Hydroxynaphthoquinones. *Mol. Biochem. Parasitol.* **1993**, *58*, 33–42.

(102) Fry, M.; Pudney, M. Site of Action of the Antimalarial Hydroxynaphthoquinone, 2-[trans-4-(4'-Chlorophenyl) Cyclohexyl]-3-Hydroxy-1,4-Naphthoquinone (566C80). *Biochem. Pharmacol.* **1992**, *43*, 1545–1553.

(103) Luzzatto, L. The Rise and Fall of the Antimalarial Lapdap: A Lesson in Pharmacogenetics. *Lancet* **2010**, *376*, 739–741.

(104) O'Neill, P. M.; Barton, V. E.; Ward, S. A. The Molecular Mechanism of Action of Artemisinin—The Debate Continues. *Molecules* **2010**, *15*, 1705–1721.

(105) Cui, L.; Su, X. Discovery, Mechanisms of Action and Combination Therapy of Artemisinin. *Expert Rev. Anti Infect. Ther* **2009**, *7*, 999–1013.

(106) Pradel, G.; Schlitzer, M. Antibiotics in Malaria Therapy and Their Effect on the Parasite Apicoplast. *Curr. Mol. Med.* **2010**, *10*, 335–349.

(107) Tan, K. R.; Magill, A. J.; Parise, M. E.; Arguin, P. M. Doxycycline for Malaria Chemoprophylaxis and Treatment: Report from the CDC Expert Meeting on Malaria Chemoprophylaxis. *Am. J.Trop. Med. Hyg.* **2011**, *84*, 517–531.

(108) Dahl, E. L.; Rosenthal, P. J. Multiple Antibiotics Exert Delayed Effects against the Plasmodium Falciparum Apicoplast. *Antimicrob. Agents Chemother.* **2007**, *51*, 3485–3490.

(109) World Health Organization. *Guidelines For The Treatment of Malaria, 3rd Edition*; **2015**.

(110) Wellems, T. E.; Plowe, C. V. Chloroquine-Resistant Malaria. *J. Infect. Dis.* **2001**, *184*, 770–776.

(111) Bosman, P.; Stassijns, J.; Nackers, F.; Canier, L.; Kim, N.; Khim, S.; Alipon, S. C.; Chuor Char, M.; Chea, N.; Dysoley, L.; Van den Bergh, R.; Etienne, W.; De Smet, M.; Ménard, D.; Kindermans, J.-M. Plasmodium Prevalence and Artemisinin-Resistant Falciparum Malaria in Preah Vihear Province, Cambodia: A Cross-Sectional Population-Based Study. *Malar. J.* **2014**, *13*, 394.

(112) Wongsrichanalai, C.; Meshnick, S. R. Declining Artesunate-Mefloquine Efficacy against Falciparum Malaria on the Cambodia-Thailand Border. *Emerg. Infect. Dis.* **2008**, *14*, 716–719.

(113) Cottrell, G.; Musset, L.; Hubert, V.; Le Bras, J.; Clain, J. Emergence of Resistance to Atovaquone-Proguanil in Malaria Parasites: Insights from Computational Modeling and Clinical Case Reports. *Antimicrob. Agents Chemother.* **2014**, *58*, 4504–4514.

(114) Press Release. GSK and MMV announce start of phase III programme of tafenoquine for Plasmodium vivax malaria. https://us.gsk.com/en-us/media/press-releases/2014/gsk-and-mmv-announce-start-of-phase-iii-programme-of-tafenoquine-for-plasmodium-vivax-malaria/.

(115) Interactive R&D portfolio. http://www.mmv.org/research-development/interactive-rd-portfolio (accessed Jul 12, 2016).

(116) Moehrle, J. J.; Duparc, S.; Siethoff, C.; van Giersbergen, P. L. M.; Craft, J. C.; Arbe-Barnes, S.; Charman, S. a.; Gutierrez, M.; Wittlin, S.; Vennerstrom, J. L. First-in-Man Safety and Pharmacokinetics of Synthetic Ozonide OZ439 Demonstrates an Improved Exposure Profile Relative to Other Peroxide Antimalarials. *Br. J. Clin. Pharmacol.* **2013**, *75*, 535–548.

(117) Phyo, A. P.; Jittamala, P.; Nosten, F. H.; Pukrittayakamee, S.; Imwong, M.; White, N. J.; Duparc, S.; Macintyre, F.; Baker, M.; Möhrle, J. J. Antimalarial Activity of Artefenomel (OZ439), a Novel Synthetic Antimalarial Endoperoxide, in Patients with Plasmodium Falciparum and Plasmodium Vivax Malaria: An Open-Label Phase 2 Trial. *Lancet Infect. Dis.* **2015**.

(118) ClinicalTrials.gov Identifier NCT01213966 https://clinicaltrials.gov/ct2/show/study/NCT01213966.

(119) ClinicalTrials.gov Identifier NCT02083380 https://clinicaltrials.gov/ct2/show/NCT02083380.

(120) Shafiq, N.; Rajagopalan, S.; Kushwaha, H. N.; Mittal, N.; Chandurkar, N.; Bhalla, A.; Kaur, S.; Pandhi, P.; Puri, G. D.; Achuthan, S.; Pareek, A.; Singh, S. K.; Srivastava, J. S.; Gaur, S. P.; Malhotra, S. Single Ascending Dose Safety and Pharmacokinetics of CDRI-97/78: First-in-Human Study of a Novel Antimalarial Drug. *Malar. Res. Treat.* **2014**, *2014*, 372521.

(121) Held, J.; Jeyaraj, S.; Kreidenweiss, A. Antimalarial Compounds in Phase II Clinical Development. *Expert Opin. Investig. Drugs* **2015**, *24*, 363–382.

(122) Rottmann, M.; McNamara, C.; Yeung, B. K. S.; Lee, M. C. S.; Zou, B.; Russell, B.; Seitz, P.; Plouffe, D. M.; Dharia, N. V; Tan, J.; Cohen, S. B.; Spencer, K. R.; González-Páez, G. E.; Lakshminarayana, S. B.; Goh, A.; Suwanarusk, R.; Jegla, T.; Schmitt, E. K.; Beck, H.-P.; Brun, R.; Nosten, F.; Renia, L.; Dartois, V.; Keller, T. H.; Fidock, D. a; Winzeler, E. a; Diagana, T. T. Spiroindolones, a Potent Compound Class for the Treatment of Malaria. *Science* **2010**, *329*, 1175–1180.

(123) Kuhen, K. L.; Chatterjee, A. K.; Rottmann, M.; Gagaring, K.; Borboa, R.; Buenviaje, J.; Chen, Z.; Francek, C.; Wu, T.; Nagle, A.; Barnes, S. W.; Plouffe, D.; Lee, M. C. S.; Fidock, D. A.; Graumans, W.; van de Vegte-Bolmer, M.; van Gemert, G. J.; Wirjanata, G.; Sebayang, B.; Marfurt, J.; Russell, B.; Suwanarusk, R.; Price, R. N.; Nosten, F.; Tungtaeng, A.; Gettayacamin, M.; Sattabongkot, J.; Taylor, J.; Walker, J. R.; Tully, D.; Patra, K. P.; Flannery, E. L.; Vinetz, J. M.; Renia, L.; Sauerwein, R. W.; Winzeler, E. A.; Glynne, R. J.; Diagana, T. T. KAF156 Is an Antimalarial Clinical Candidate with Potential for Use in Prophylaxis, Treatment, and Prevention of Disease Transmission. *Antimicrob. Agents Chemother.* **2014**, *58*, 5060–5067.

(124) Phillips, M. A.; Lotharius, J.; Marsh, K.; White, J.; Dayan, A.; White, K. L.; Njoroge, J. W.; El Mazouni, F.; Lao, Y.; Kokkonda, S.; Tomchick, D. R.; Deng, X.; Laird, T.; Bhatia, S. N.; March, S.; Ng, C. L.; Fidock, D. A.; Wittlin, S.; Lafuente-Monasterio,

M.; Benito, F. J. G.; Alonso, L. M. S.; Martinez, M. S.; Jimenez-Diaz, M. B.; Bazaga, S. F.; Angulo-Barturen, I.; Haselden, J. N.; Louttit, J.; Cui, Y.; Sridhar, A.; Zeeman, A.-M.; Kocken, C.; Sauerwein, R.; Dechering, K.; Avery, V. M.; Duffy, S.; Delves, M.; Sinden, R.; Ruecker, A.; Wickham, K. S.; Rochford, R.; Gahagen, J.; Iyer, L.; Riccio, E.; Mirsalis, J.; Bathhurst, I.; Rueckle, T.; Ding, X.; Campo, B.; Leroy, D.; Rogers, M. J.; Rathod, P. K.; Burrows, J. N.; Charman, S. A. A Long-Duration Dihydroorotate Dehydrogenase Inhibitor (DSM265) for Prevention and Treatment of Malaria. *Sci. Transl. Med.* **2015**, *7*, 296ra111.

Chapter 2

Drug Repositioning/Repurposing

As explained in chapter 1, there is a need for the development of novel agents to overcome drug resistance and other challenges associated with the treatment of TB and malaria. The development of a new drug is a lengthy and costly process; therefore, the need for approaches that can save both time and money has been emphasised within this area of research. Drug repositioning and/or repurposing is one such approach. This chapter describes the application of drug repositioning within the context.

2.1 Drug repositioning/repurposing as an approach in drug discovery

The development of a new drug begins with the discovery of new hits. These hits are optimized by medicinal chemistry approaches to find new drug candidates which are then tested in various preclinical and clinical trials before entering the market. This process is quite lengthy and typically takes 12-14 years or sometimes even longer, and involves immense effort and money. Therefore, efforts to accelerate the drug discovery process have been the focus within this field of research.

One of the strategies to accelerate the drug development process is called drug repositioning or repurposing.[1] The two terms 'repositioning' and 'repurposing' have been used interchangeably but their individual meanings are different. "Drug repurposing" is applied to existing drugs, which can be used for a new indication without any chemical modification. Changes are made by optimising only the doses in preclinical and clinical stages. On the other hand, 'drug repositioning' is a broader term and refers to the chemical modification of a pre-existing drug. This term can also be applied to drugs, which have been rescued from phase III or IV clinical stages. Briefly, drug repositioning/repurposing allows pre-existing drugs to be used for indications that were not their initial target. The benefit of applying such an approach is that the pharmacokinetic and safety profiles of these drugs are already known and, therefore, this substantially reduces the money and time involved in new drug development. Several examples can be found in medicine history that supports this concept. For example, as described in Table 2.1, methotrexate was initially used to treat cancer but has also been shown to be useful in the treatment of rheumatoid arthritis; minoxidil was initially used in the treatment for hypertension but subsequently used to treat hair loss; sildenafil was successfully repurposed from a drug prescribed for hypertension to a drug now prescribed for erectile

dysfunction; thalidomide was initially developed as a sedative, analgesic and antiemetic to treat morning sickness and is now successfully used in the treatment of multiple myeloma.[1,2]

Table 2.1: Examples of drug repositioning/repurposing[2]

Drug	Original indication	New indication	Year*
Amphetamine	Stimulant	Hyperkinesis in children (attention deficit hyperactivity disorder, ADHD)	1943
Allopurinol	Tumor lysis syndrome	Gout	1967
Zidovudine	Cancer	HIV/AIDS	1985
Minoxidil	Hypertension	Hair loss (Alopecia)	1988
Bupropion	Depression	Smoking cessation	1997
Sibutramine	Depression	Obesity	1997
Finasteride	Benign prostatic hyperplasia	Alopecia	1997
Methotrexate	Cancer	Rheumatoid arthritis	1999
Fluoxetine	Depression	Premenstrual dysphoric disorder	2000
Atomoxetine	Parkinson's disease	ADHD	2002
Thalidomide	Morning sickness	Multiple myeloma	2003
Cymbalta	Depression	Diabetic peripheral neuropathy	2004
Topiramate	Epilepsy	Migraine	2004
Paclitaxel	Cancer	Restenosis	2004
Sildenafil	Angina	Erectile dysfunction	2005
Requip	Parkinson's disease	Restless legs	2005
Lumigan	Glaucoma	Hypotrichosis simplex	2009
Dapoxetine	Analgesia and depression	Premature ejaculation	2009
Milnacipran	Depression	Fibromyalgia syndrome	2009
Phentolamine	Hypertension	Dental anesthesia reversal agent	2009
Lidocaine	Local anesthetic	Arrhythmia	2010
Mifepristone	Pregnancy termination	Cushing's syndrome	2012

** Year of first approval in new indication*

Many drugs display off-target activity that often results in undesirable side effects. A drug can affect multiple targets or an individual target can be involved in multiple biological pathways. In addition, similarities in biochemical pathways, cell biology and biological processes can also be seen in different diseases. Knowledge of additional targets of a drug, the role of these targets in different biological pathways, as well as similarity in cell biology and biological processes in different diseases can help researchers identify potential drug candidates for repositioning/repurposing.

Based on the above discussion, there are two basic approaches for drug repositioning/repurposing (Figure 2.1): (1) discovering a new target for a known drug, (ii) discovering the role of a known target in a new indication.

A simple and common procedure, which is usually followed to identify potential drug candidates for repositioning is the phenotypic whole cell screening against an indication, followed by target investigation.

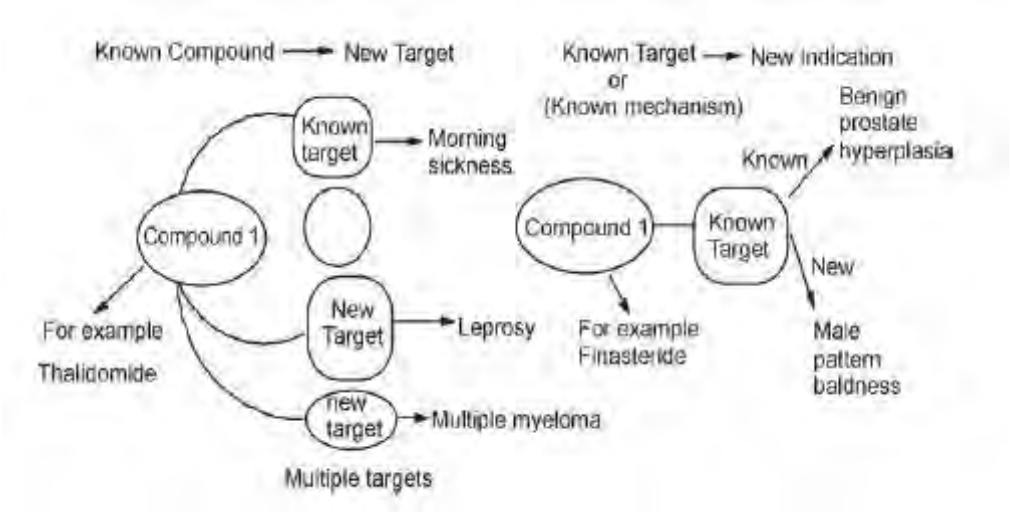

Figure 2.1: Approaches for drug repositioning/repurposing.[3]

2.2 Drug repositioning/repurposing in tuberculosis (TB)

Many drugs have either been, or shown the potential to be, repositioned in TB. Some of these drugs are merely the outcomes of expansion of their antibacterial spectrum while others have come from totally different indications.

The best example of drug repositioning for TB exists in the form of fluoroquinolones (Figure 2.2).[4,5] Fluoroquinolones are DNA gyrase inhibitors and were originally introduced for the treatment of several bacterial infections, for example, bone and joint infections, skin infections, urinary tract infections, serious ear infections, bronchitis, and pneumonia. Fluoroquinolones have been successfully included in the WHO recommended treatment regimen for MDR-TB. All fluoroquinolones currently in use are synthetic derivatives of the parent compound nalidixic acid, which was discovered as a by-product during purification of the antimalarial drug chloroquine in 1962[6] and has been used to treat urinary tract infections.[7] New fluoroquinolones have been obtained through structural modifications of nalidixic acid (Figure 2.2), yielding far more potent and broad-spectrum antibiotics.[8]

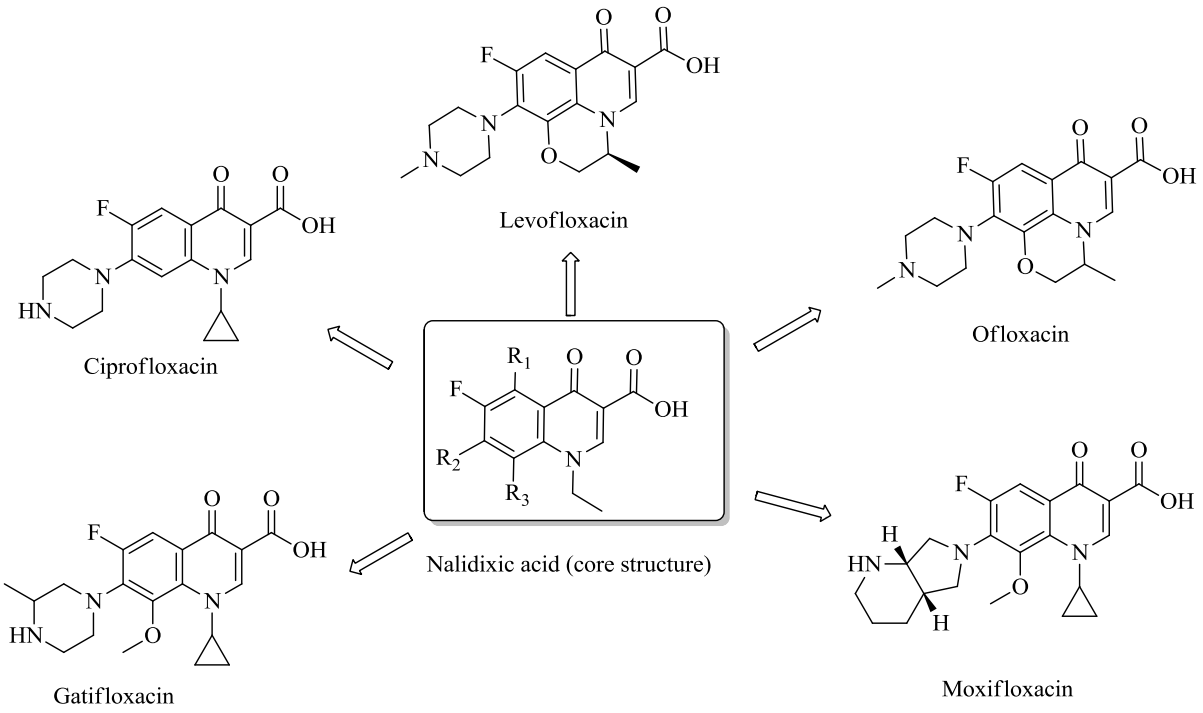

Figure 2.2: Chemical structures of repositioned fluoroquinolones for the treatment of TB

Since the successful repositioning of fluoroquinolones, many other antibiotics have been explored in TB. Linezolid (Figure 2.3), a third-line anti-TB drug, belongs to oxazolidinone class of antibiotics and is a protein synthesis inhibitor. Linezolid was originally introduced for the treatment of various infections caused by methicillin-, vancomycin- and penicillin-resistant bacterial strains.[9] The broad-spectrum activity of linezolid was then explored in TB bacteria. After successful *in vitro* and *in vivo* evaluations in the mouse model, linezolid was also found efficacious and tolerable in MDR-TB patients. Due to toxicity issues, such as anaemia, and peripheral and optic neuropathy,[10] the use of linezolid is limited to selected cases of drug-resistant TB when fewer treatment options are available. The high efficacy of linezolid led researchers to investigate the oxazolidinone class of antibiotics. Newer oxazolidinone derivatives PNU-100480 and AZD5847 with superior *in vitro* activity and *in vivo* efficacy[11,12] have been developed and are expected to possess superior safety profiles compared to linezolid. Likewise, two newly-developed candidates PA-824 and OPC-67683 (Figure 2.3) have been repositioned from the antibiotic metronidazole. These drugs possess activity against both anaerobic and aerobic *Mtb* through a dual mechanism of action, as follows: (i) killing anaerobic *Mtb* by generating reactive nitrogen species during activation by a F420-deazaflavin dependent nitroreductase; and, (ii) killing aerobic *Mtb* by inhibiting cell wall mycolic acid biosynthesis.[13,14] The precursor metronidazole, itself is highly active

against *Mtb*[15] and has been reported to prevent reactivation of latent TB in the macaques model.[16]

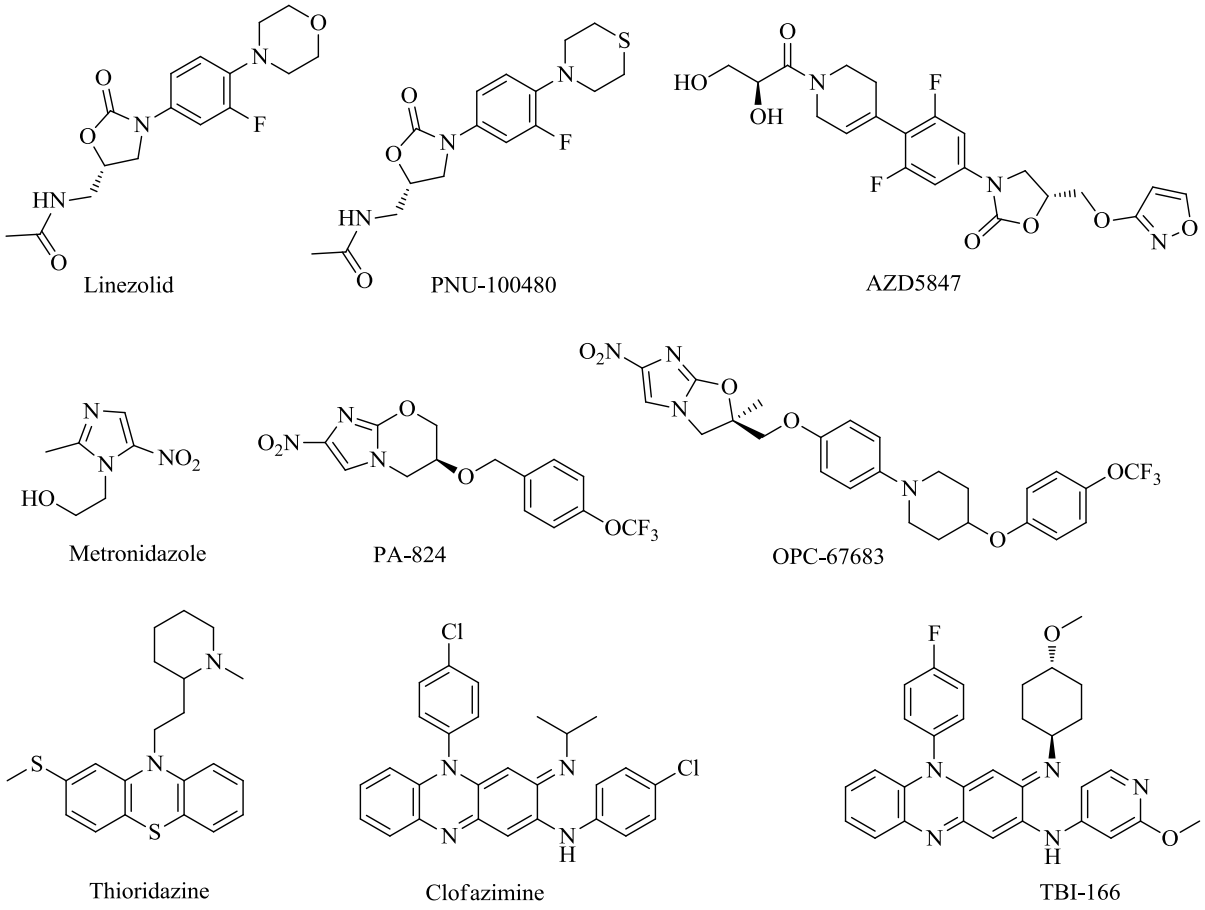

Figure 2.3: Chemical structures of repositioned anti-TB drugs and potential repositioning candidates

The anti-leprosy drug clofazimine (Figure 2.3) is successful in treating MDR- and XDR-TB. Clofazimine is a riminophenazine derivative that appears to kill *Mtb* by affecting intracellular redox cycling.[17] In addition, clofazimine has also been shown to reverse the inhibitory effect of *Mtb* on the phagocyte's intracellular killing mechanisms.[18] Although the efficacy and role of clofazimine is not fully established, the regimens including clofazimine are able to shorten the treatment of MDR- and XDR-TB.[19] In addition to clofazimine, many riminophenazine derivatives possess high bactericidal and sterilizing activity against TB both *in vitro* and *in vivo* in mouse models of TB. However, the unwelcome skin pigmentation caused by the use of riminophenazines hinders the development of this class of drugs.[20,21] Efforts have been made to identify riminophenazine derivatives with improved physicochemical and pharmacokinetic properties that will avoid discoloration of the skin, but fight TB with efficacy that is similar to clofazimine. One such derivative, TB1-166, is in preclinical trials.[22]

Thioridazine (Figure 2.3) is an antipsychotic drug that has also shown promising *in vitro* and *in vivo* (mouse model) activity against MDR- and XDR-TB.[23] It also possess *in vitro* activity against dormant forms of *Mtb* suggesting that it could also be used for latent TB therapy, either alone or in combination with existing anti-TB drugs.[24]

In addition to the above drugs, many other drugs have been identified with promising *in vitro* activity against sensitive as well as resistant *Mtb* strains (Figure 2.4). For example, a novel candidate and anti-helminthic drug, pyrvinium pamoate, possesses strong inhibitory effects (MIC 310 nM) against the H37Rv strain of *Mtb*.[25] Disulfiram, which has been in use since the 1940s to treat chronic alcoholism, has shown complete inhibition of H37Rv growth at 5.26 μM. The drug has also shown the same level of inhibition against clinical isolates and MDR and XDR strains of *Mtb*, and remarkable bactericidal activity in an *in vivo* experiment on guinea pigs.[26] A trimethoprim-sulfamethoxazole combination (Co-trimoxazole), which is used as a prophylactic agent to treat non-tuberculosis bacterial infections in HIV-infected patients, has been found active against 100 wild type, MDR and XDR *Mtb* isolates with *in vitro* MIC distribution ranging from 0.125/2.4 to 2/38 μg/ml.[27] The anti-protozoal drug nitazoxanide is active against replicating and non-replicating forms of *Mtb*. Since any attempt to raise resistant mutant *Mtb* strains for this drug failed, the drug is thought to have a novel mechanism of action through which it bypasses resistance. [28] The antimalarial drug mefloquine has been shown to be active *in vitro* with an average MIC of 21 μM against more than hundred sensitive and resistant *Mtb* strains.[29] The drug has also shown good activity in macrophages.[30]

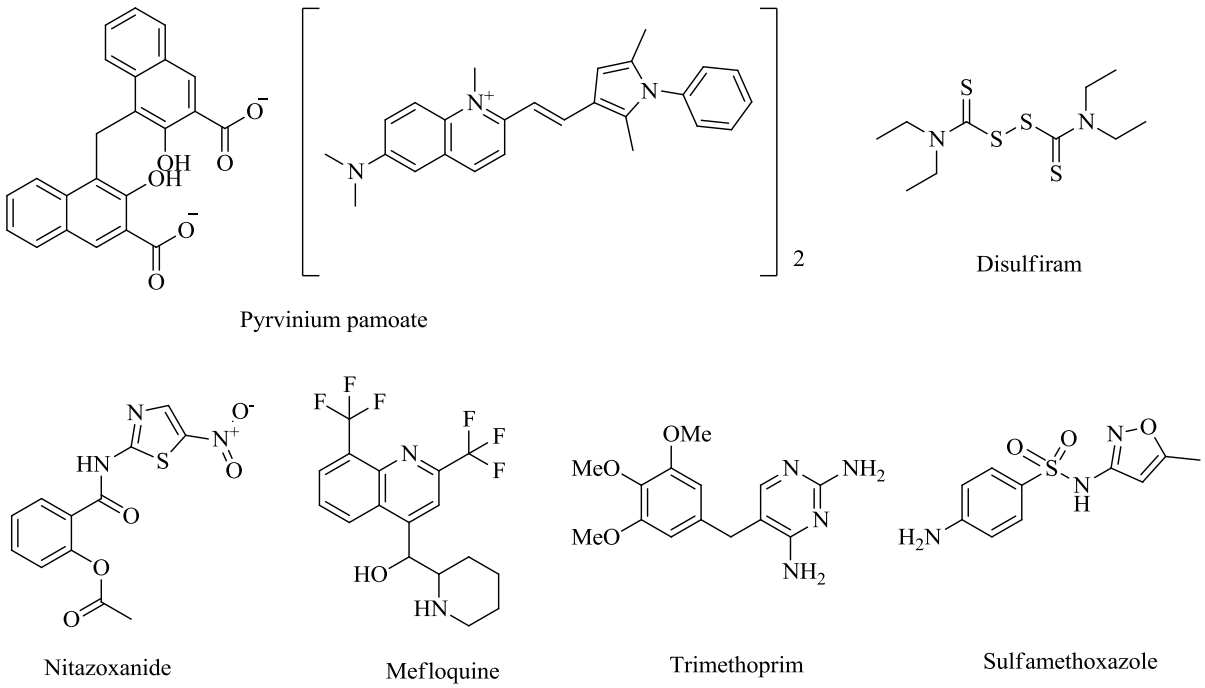

Figure 2.4: Chemical structures of new promising candidates with effective *in vitro* activity against *Mtb*

2.3 Drug repositioning/repurposing in malaria

There are examples in malaria which show that the drug repositioning approach has made useful contributions to antimalarial drug development. Several broad spectrum antibiotics are effective antimalarial drugs in certain settings. For example, a synthetically derived tetracycline doxycycline, which has been in use as a broad spectrum antibiotic since 1967, has been successfully repositioned for chemoprophylaxis and treatment of malaria. Likewise clindamycin, a lincosamide antibiotic, which was originally used for acne treatment and numerous other applications since 1940, is now used clinically for the treatment of malaria These antibiotics, due to their delayed death effect[31] (killing *Plasmodium* parasites in the second replication cycle which leads to delayed clearance of the parasite), are usually combined with rapid-acting standard antimalarials such as chloroquine (CQ) and quinine during treatment.

A number of sulphonamide-containing drugs are in the clinic for the treatment of a wide range of human diseases, including kidney disease, glaucoma, epilepsy, obesity and cancer.[32] Sulphonamides that target the folate biosynthesis pathway in bacteria have been evaluated as antimalarials since the same pathway is also present in *Plasmodia*. One such sulphonamide, sulphadoxine, originally developed as an antibacterial, has been used in combination therapy to treat *P. falciparum* infections. Sulfadoxine in combination with pyrimethamine, under the

name 'Fansidar', is used as an intermittent preventive treatment of malaria during pregnancy. This combination is also used in the treatment of uncomplicated malaria in combination with artesunate.[33] Likewise, another sulphonamide, sulfamethoxazole, in combination with trimethoprim, under the name 'Co-trimoxazole',[34] is currently recommended by the WHO as prophylaxis against opportunistic infections (malaria and several bacterial infections) in HIV-infected patients.[35,36]

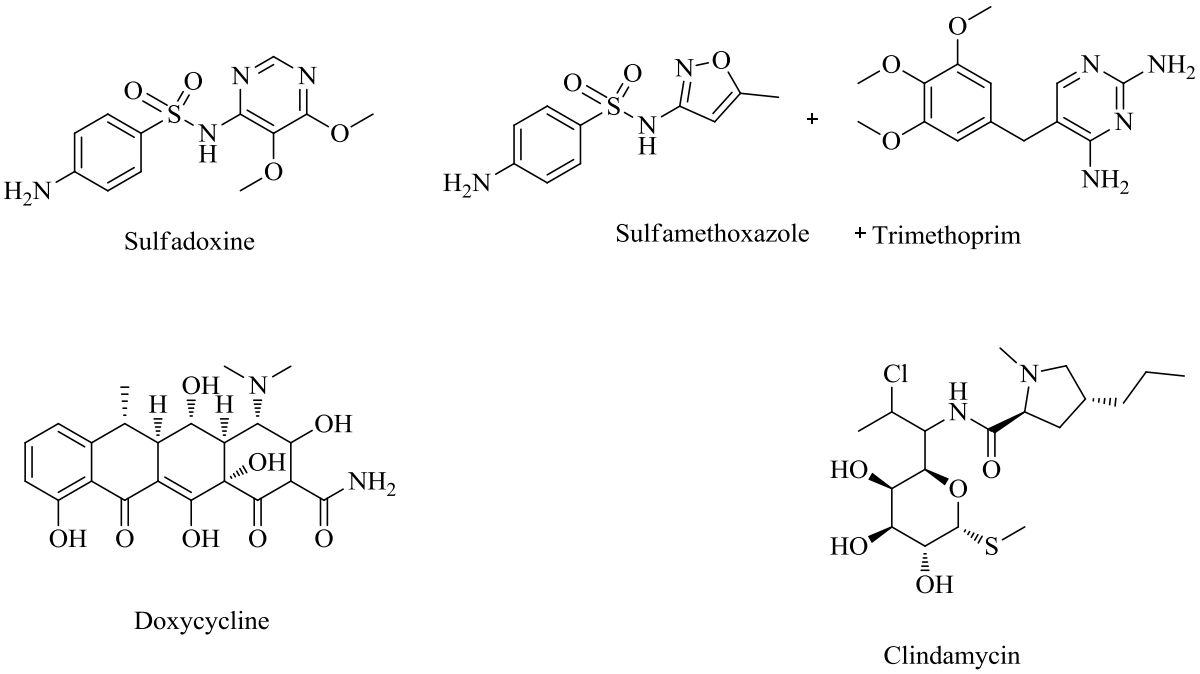

Figure 2.5: Chemical structures of repositioned antimalarial drugs

Since the successful repositioning of the above drugs, a number of FDA-approved drugs as well as those where clinical development has been discontinued before approval, have been screened for antiplasmodial activity. For example, screening of a library of 2,687 compounds containing 1,937 FDA-approved and 750 other compounds in clinical development identified the antiplasmodial activity of astemizole (a histamine H1 antagonist) with an IC_{50} value of 227 nM against the 3D7 *P. falciparum* strain[37]. Unfortunately, this drug could not be repositioned in malaria because of side effects linked to QT prolongation. Screening of another library of 1,037 existing drugs provided decoquinate (an antiprotozoal used in veterinary medicine) with potent activity against *Plasmodium* liver stages both *in vitro* and *in vivo*.[38] In addition to liver stage activity (IC_{50} 2.6 nM), the drug has also been shown to be potent against the blood (IC_{50} 10 nM) and sexual stages (IC_{50} 36 nM) of the parasite. The drug acts by selectively and specifically inhibiting the parasite's mitochondrial bc1 complex, with little cross-resistance with the antimalarial drug atovaquone, with a similar mechanism

of action. With such activity, decoquinate warrants further exploitation as a potent antimalarial compound.

Emetine dihydrochloride hydrate is another anti-protozoal drug with potent inhibitory properties against drug sensitive (IC_{50} 1 nM, 3D7 strain) and drug resistant (IC_{50} 47 nM, K1 strain) strains of *P. falciparum*. [39] Emetine dihydrochloride hydrate is a natural product which was developed for the treatment of intestinal and tissue amoebiasis but the use of this drug is restricted to severe cases because of its potential side effects such as nausea and vomiting following oral administration, and serious cardiotoxicity produced at high dose ranges.[40] The above-mentioned *in vitro* IC_{50} values of emetine against *P. falciparum* are much lower than those determined against various *Entamoeba* species (IC_{50} 26-60 μM)[41] which suggests that emetine may not produce potential toxicity at the doses required for malaria treatment. Further, the semisynthesis of a less toxic and equipotent anti-amoebic derivative of emetine dehydroemetine[42] indicates that emetine can be derivatized to reduce its toxic effects. All these studies suggest that emetine and its semisynthetic derivatives are worth investigating in malaria.

A phenotypic screening of 100 registered drugs has identified the *in vitro* antiplasmodial activity of the tricyclic antidepressants promazine, fluphenazine and nortriptyline. These drugs have shown potent *in vitro P. falciparum* activity against the K1 strain with an average IC_{50} value of 523 nM[43] and have previously been shown to reverse chloroquine resistance in *P. falciparum in vitro* and in monkey studies.[44] Additionally, a recent publication has described tricyclic antidepressant drugs as blocking agents for *Plasmodium* oocyst development and transmission.[45] With such activities, this class of antidepressants needs further investigation in malaria. In addition to tricyclic antidepressants, the same screening has also identified four antifungal azole derivatives, clotrimazole, econazole, miconazole and tioconazole (Figure 2.6), to be active against the K1 strain of *P. falciparum* with IC_{50} values of 110, 320, 490 and 630 nM respectively.[43]

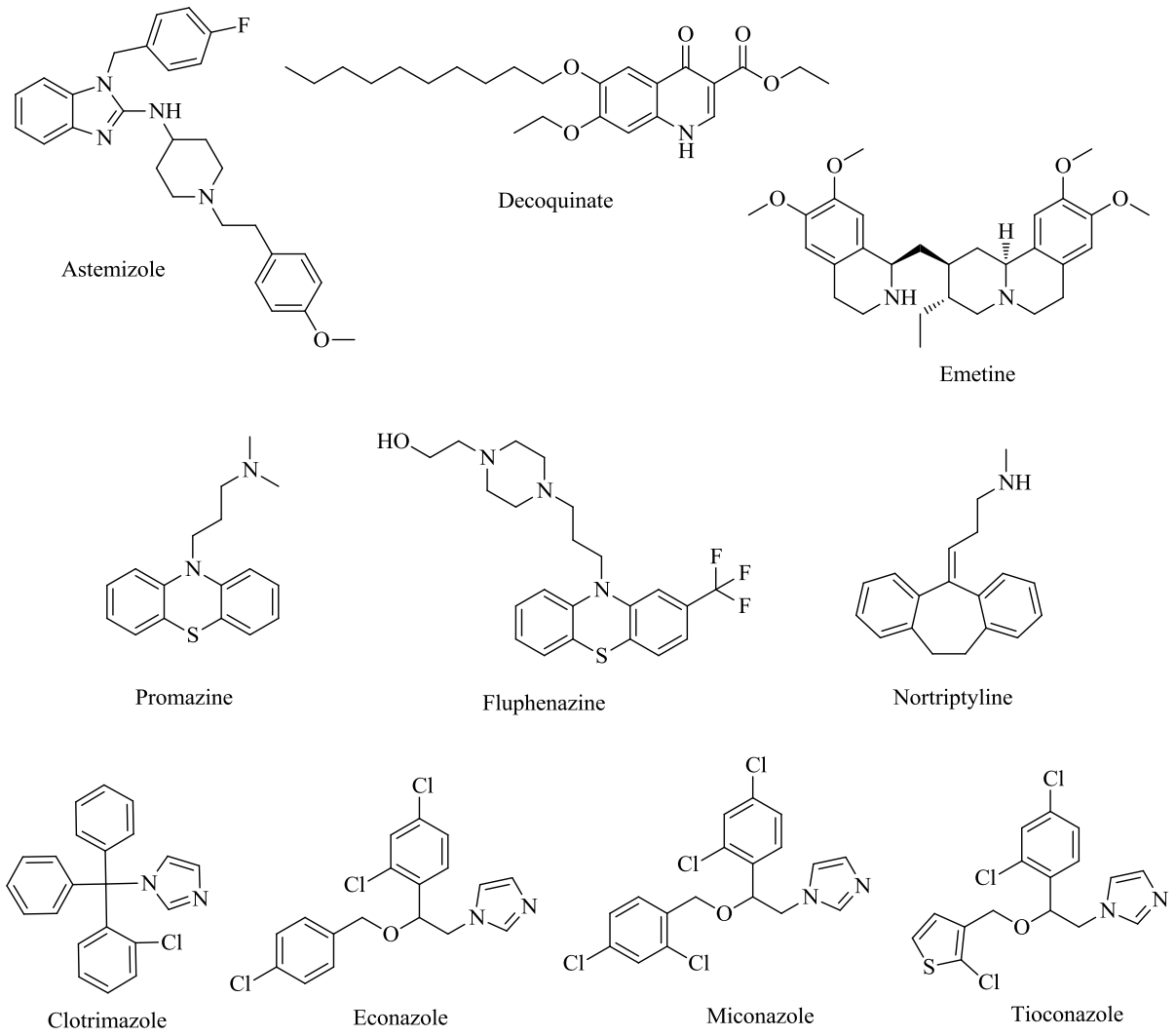

Figure 2.6: Chemical structures of drugs with potent *in vitro* activity in malaria

From the above discussion, it is clear that drug repositioning/repurposing can be adopted as a useful strategy to accelerate drug discovery in TB and malaria. Potential candidates for repositioning can be identified using high-throughput screening (HTS) platforms. Subsequent medicinal chemistry approaches can be applied to such candidates in order to have them suitably repositioned for the treatment of TB and/or malaria.

The present study focuses on two candidates for repositioning: fusidic acid (an antibiotic drug) and metergoline (an antipsychotic drug). The antimycobacterial activities of these candidates were identified from a HTS conducted by the Tuberculosis Antimicrobial Acquisition Coordinating Facility (TAACF). The respective antiplasmodial activities have also been reported. It was therefore envisioned that these compounds could be used as effective templates for the synthesis of more potent derivatives. A brief description of these drugs is given below.

2.4 Fusidic acid

Fusidic acid (Figure 2.7) is a naturally occurring steroid-based narrow spectrum antibiotic. It was first isolated from the fungus *Fusidium coccineum* by Godtfredsen in 1962[46] at Leo laboratories in Ballerup, Denmark and has since 1962 been used in the clinical treatment of both topical and systemic infections caused by staphylococci.[47–51] The drug is approved as its sodium salt, sodium fusidate, in many countries including South Korea, Japan, UK, Canada, Europe, Australia, New Zealand, Thailand, India and Taiwan, and is in clinical development in the Unites States.[52–54]The clinical value of fusidic acid is a result of its excellent distribution in various tissues, low degree of toxicity and allergic reactions, and the absence of cross-resistance with other clinically used antibiotics.

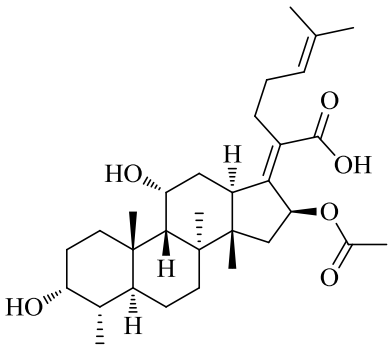

Figure 2.7: Structure of fusidic acid

Fusidic acid is most potent against *Staphylococcus aureus* and *Staphylococcus epidermidis*, including methicillin-resistant strains. It also shows activity against several other Gram-positive species and Gram-negative *Neisseria* species.[48,51,55–58] The antimicrobial spectrum of fusidic acid is given in Table 2.2.

Table 2.2: Antimicrobial spectrum of fusidic acid[59]

Microorganisms	***In vitro* MIC_{90} (µg/ml)**
Gram-positive	
Staphylococcus aureus (methicillin-susceptible)	0.06
Staphylococcus aureus (methicillin-resistant)	0.12
Staphylococcus epidermidis (methicillin-susceptible)	0.25
Staphylococcus epidermidis (methicillin-resistant)	0.50
Corynebacterium diptheriae	0.0044
Clostridium tetani	0.05
Clostridium perfringens	0.5
Propionibacterium acnes	1.0
Other Corynebacterium spp.	2.0
Clostridium difficile	2.0
Other Clostridium spp.	≤ 1.0
Staphylococcus saprophyticus	3.12
Streptococcus faecalis	6.25
Streptococcus pyogenes	12.5
Streptococcus pneumoniae	25.0
Gram-negative	
Neisseria meningitidis	0.12
Legionella pneumophila	≤ 0.25
Neisseria gonorrhoeae	1.0
Bacteroides fragilis	2.0
Other Bacteroides species	≤ 2.0

2.4.1 SAR studies on fusidic acid

Fusidic acid represents the fusidane class of antibiotics and is the most potent member of its familiy. Unlike regular tetracyclic triterpenes and sterols, the fusidanes possess an unusual stereochemistry of the tetracyclic ring system. Rings A, B and C are arranged in a trans-syn-trans manner in contrast to usual trans-anti-trans arrangement in tetracyclic triterpenes and sterols. This unusual trans-syn-trans arrangement forces ring B to have a boat conformation (Figure 2.8).[60] Fusidanes, therefore, do not possess any steroid like hormonal activity.

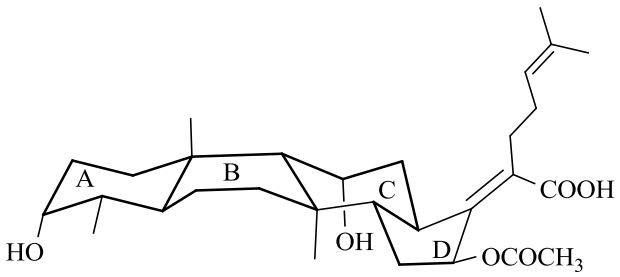

Figure 2.8: Trans-syn-trans arrangement of tetracyclic ring system of fusidic acid

The antibacterial structure-activity relationship (SAR) of fusidic acid has been extensively studied by Leo Pharma and a number of derivatives have been prepared (Figure 2.9). These structural modifications on fusidic acid include replacing the carboxylic acid group with esters and amides; hydrogenations of C-24,25 and C-17,20 double bonds; substitution reactions at C-24,25 double bond; ozonolysis of the C-24,25 and C-17,20 double bonds and introduction of other side chains; cyclopropanation of the C-17,20 double bond; C-3 ester and amine derivatives; as well as C-16 ester, ether and thioether derivatives. However, none of these derivatives displayed better antibacterial activity compared to fusidic acid.[60–66]

SAR studies of fusidic acid have shown that the tetracyclic skeleton, lipophilic side-chain and the carboxylic acid group at C-20 are essential for its biological activity. The orientation of the lipophilic side-chain, rather than the double bond at C-17, is crucial to the antibacterial activity.

In order to investigate whether or not the C17,20 double bond is required for activity, four stereoisomers (17*R,*20*S*), (17*R,*20*R*), (17*S,*20*S*) and (17*S,*20*R*) were prepared by reducing this double bond. One stereoisomer (17*S,*20*S*) was equipotent to fusidic acid, whereas others had low or no antibacterial activity in comparison to fusidic acid.[64] The 17*S*,20*S*-methanofusidic acid derivative of fusidic acid was obtained by replacing the C17,20 double bond with a cyclopropane ring and has activity comparable to fusidic acid.[63] A conformational analysis to obtain correlation between low energy conformations and antibacterial activity of these derivatives demonstrated that the double bond between C-17 and C-20 is not essential for antibacterial activity, but rather that the carboxyl group and the lipophilic side chain must be oriented in a constrained conformational space similar to that of fusidic acid.

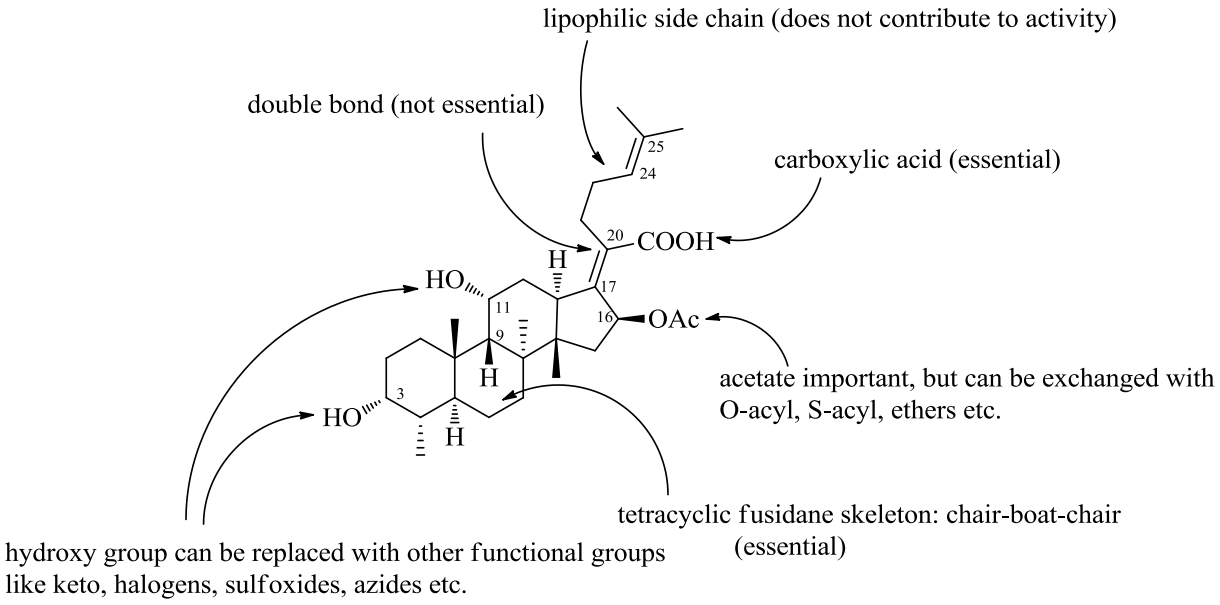

Figure 2.9: Structure-activity relationship of fusidic acid[64]

2.4.2 Mechanism of action of fusidic acid in bacteria

The synthesis of new proteins in living cells occurs in the ribosome. The elongation factor G (EF-G) plays an important role in the elongation phase of protein synthesis by catalysing the translocation of the peptidyl transfer RNA (tRNA) from the A-site to the P-site of the ribosome. EF-G binds to the ribosome in a complex with guanosine triphosphate (GTP). Hydrolysis of GTP to guanosine 5′-diphosphate (GDP) leads to the translocation step of protein synthesis, which is followed by dissociation of the EF-G–GDP complex from the ribosome. Fusidic acid binds with high affinity to the EF-G–GDP after the hydrolysis of GTP and prevents the release of the EF-G–GDP complex from the ribosome, thereby interfering with and obstructing protein synthesis (Figure 2.10).[67,68]

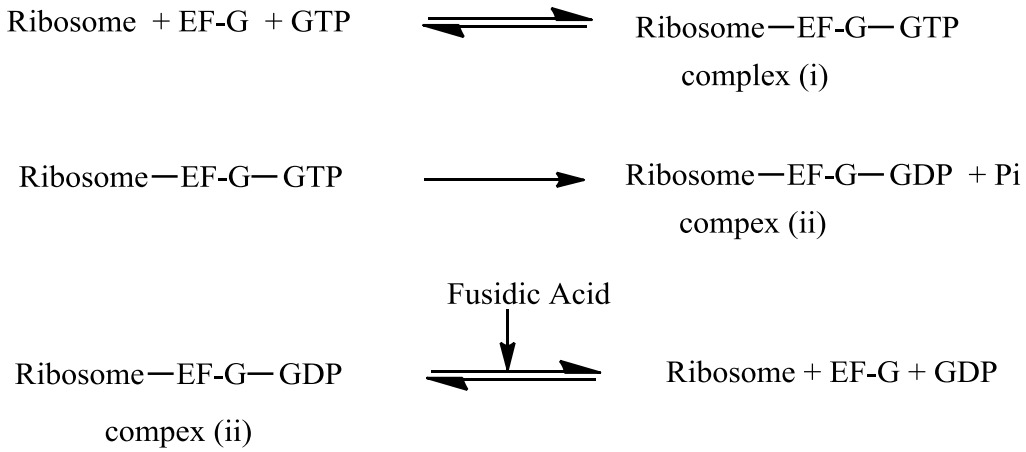

Figure 2.10: Inhibition of protein synthesis by fusidic acid[68]

2.5 Metergoline

Metergoline (Figure 2.11) is a semisynthetic ergoline alkaloid and was first described in 1965.[69] Metergoline has a number of applications as a serotonin antagonist and dopamine agonist, both in human and veterinary medicine. Metergoline is a nonspecific serotonin antagonist binding several 5-HT receptor subtypes ($5HT_1$, $5HT_2$, $5HT_7$) with high affinity (Ki < 10 nM).[70] Metergoline also has dopamine agonist properties, possibly due to serotonergic modulation of dopaminergic systems. It is marketed mostly in Europe and is used clinically for the management of disorders associated with hyperprolactinemia, and in the prophylaxis of migraine headaches.[71–73] Metergoline has also been investigated for the management of certain psychiatric disorders in which 5-HT has been implicated, including seasonal depression,[70] obsessive-compulsive disorder,[74] carbon dioxide-induced anxiety,[75] and premenstrual syndrome.[76] It has also been used in veterinary medicine as a pregnancy termination drug for dogs.[77]

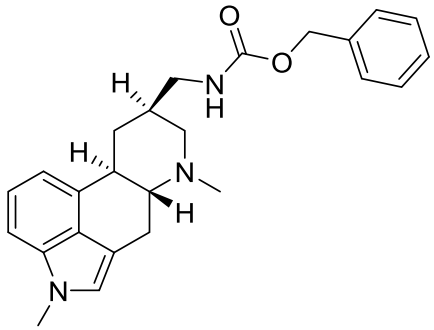

Figure 2.11: Structure of metergoline

Besides its antipsychiatric properties, metergoline has been documented to have *in vitro* antifungal activity (MIC_{80} 4 µg/ml) against clinical isolates of *Candida krusei*.[78] The proposed mechanism of action is the inhibition of extracellular phospholipase secretion, a well-known virulence factor in *Candida*, which degrades the cell membrane of host tissue. The same study has also shown the *in vitro* synergistic interaction of metergoline with other antifungal agents such as amphotericin B and fluconazole.

2.6 Research question

The research question that this study aims to answer is whether it will be possible to identify new analogues of fusidic acid and metergoline that display potent antimycobacterial/antiplasmodial activity and favourable pharmacokinetic properties.

2.7 Aim

To explore structure-activity relationship (SAR) studies of fusidic acid and metergoline as antimycobacterial/ antiplasmodial agents.

2.8 Specific objectives

I. To synthesize semisynthetic derivatives of fusidic acid and metergoline and evaluate these derivatives *in vitro* as antimycobacterial and/or antiplasmodial agents

II. To evaluate selected derivatives for *in vivo* pharmacokinetic (PK) studies

III. To apply *in silico* tools to build a pharmacophore model based on the antiplasmodial SAR of synthesized fusidic acid derivatives and use the model to design new fusidic acid derivatives

IV. To apply *in silico* similarity search tools to identify fusidic acid-like compounds that possess antimycobacterial and/or antiplasmodial activities from an in-house database

2.9 References

(1) Ashburn, T. T.; Thor, K. B. Drug Repositioning: Identifying and Developing New Uses for Existing Drugs. *Nat. Rev. Drug discov.* **2004**, *3*, 673–683.

(2) Novac, N. Challenges and Opportunities of Drug Repositioning. *Trends Pharmacol. Sci* **2013**, *34*, 267–272.

(3) Geetharamani, G.; Padma, M.; Pandian, J. A. A New Therapeutic Applications for Drug Repositioning on the Cloud Computing. *International Conference on Inter Disciplinary Research in Engineering and Technology* **2015**, 119–129.

(4) Palomino, J. C.; Martin, A. Is Repositioning of Drugs a Viable Alternative in the Treatment of Tuberculosis? *J. Antimicrob. Chemother.* **2013**, *68*, 275–283.

(5) Nzila, A.; Ma, Z.; Chibale, K. Drug Repositioning in the Treatment of Malaria and TB. *Future Med. Chem.* **2011**, *3*, 1413–1426.

(6) Lesher, G. Y.; Froelich, E. J.; Gruett, M. D.; Bailey, J. H.; Brundage, R. P. 1,8-Naphthyridine Derivatives. A New Class of Chemotherapeutic Agents. *J. Med. Chem.* **1962**, *5*, 1063–1065.

(7) Von Rosenstiel N; Adam, D. Quinolone Antibacterials. An Update of Their Pharmacology and Therapeutic Use. *Drugs* **1994**, *47*, 872–901.

(8) Bearden, D. T.; Danziger, L. H. Mechanism of Action of and Resistance to Quinolones. *Pharmacotherapy* **2001**, *21*, 224S – 232S.

(9) Diekema, D. J.; Jones, R. N. Oxazolidinone Antibiotics. *Lancet* **2001**, *358*, 1975–1982.

(10) Park, I. N.; Hong, S. B.; Oh, Y. M.; Kim, M. N.; Lim, C. M.; Lee, S. D.; Koh, Y.; Kim, W. S.; Kim, D. S.; Kim, W. D.; Shim, T. S. Efficacy and Tolerability of Daily-Half Dose Linezolid in Patients with Intractable Multidrug-Resistant Tuberculosis. *J. Antimicrob. Chemother.* **2006**, *58*, 701–704.

(11) Wallis, R. S.; Jakubiec, W. M.; Kumar, V.; Silvia, A. M.; Paige, D.; Dimitrova, D.; Li, X.; Ladutko, L.; Campbell, S.; Friedland, G.; Mitton-Fry, M.; Miller, P. F. Pharmacokinetics and Whole-Blood Bactericidal Activity against Mycobacterium Tuberculosis of Single Doses of PNU-100480 in Healthy Volunteers. *J. Infect. Dis.* **2010**, *202*, 745–751.

(12) Balasubramanian, V.; Solapure, S.; Iyer, H.; Ghosh, A.; Sharma, S.; Kaur, P.; Deepthi, R.; Subbulakshmi, V.; Ramya, V.; Ramachandran, V.; Balganesh, M.; Wright, L.; Melnick, D.; Butler, S. L.; Sambandamurthy, V. K. Bactericidal Activity and Mechanism of Action of azd5847, a Novel Oxazolidinone for Treatment of Tuberculosis. *Antimicrob. Agents Chemother.* **2014**, *58*, 495–502.

(13) Manjunatha, U.; Boshoff, H. I. M.; Barry, C. E. The Mechanism of Action of PA-824: Novel Insights from Transcriptional Profiling. *Commun. integr. biol* **2009**, *2*, 215–218.

(14) Mukherjee, T.; Boshoff, H. Nitroimidazoles for the Treatment of TB: Past, Present and Future. *Future Med. Chem.* **2011**, *3*, 1427–1454.

(15) Wayne, L. G.; Sramek, H. a. Metronidazole Is Bactericidal to Dormant Cells of Mycobacterium Tuberculosis. *Antimicrob. Agents Chemother.* **1994**, *38*, 2054–2058.

(16) Lin, P. L.; Dartois, V.; Johnston, P. J.; Janssen, C.; Via, L.; Goodwin, M. B.; Klein, E.; Barry, C. E.; Flynn, J. L. Metronidazole Prevents Reactivation of Latent Mycobacterium Tuberculosis Infection in Macaques. *Proc. Natl. Acad. Sci. U.S.A.* **2012**, *109*, 14188–14193.

(17) Yano, T.; Kassovska-Bratinova, S.; Shin Teh, J.; Winkler, J.; Sullivan, K.; Isaacs, A.; Schechter, N. M.; Rubin, H. Reduction of Clofazimine by Mycobacterial Type 2 NADH: Quinone Oxidoreductase: A Pathway for the Generation of Bactericidal Levels of Reactive Oxygen Species. *J. Biol.Chem.* **2011**, *286*, 10276–10287.

(18) Wadee, A. A.; Anderson, R.; Rabson, A. R. Clofazimine Reverses the Inhibitory Effect of Mycobacterium Tuberculosis Derived Factors on Phagocyte Intracellnlar Killing Mechanisms. *J. Antimicrob. Chemother.* **1988**, *21*, 65–74.

(19) Gopal, M.; Padayatchi, N.; Metcalfe, J. Z.; O'Donnell, M. R. Systematic Review of Clofazimine for the Treatment of Drug-Resistant Tuberculosis. *Int. J.Tuberc. Lung Dis.* **2013**, *17*, 1001–1007.

(20) Zhang, D.; Lu, Y.; Liu, K.; Liu, B.; Wang, J.; Zhang, G.; Zhang, H.; Liu, Y.; Wang, B.; Zheng, M.; Fu, L.; Hou, Y.; Gong, N.; Lv, Y.; Li, C.; Cooper, C. B.; Upton, A. M.; Yin, D.; Ma, Z.; Huang, H. Identification of Less Lipophilic Riminophenazine Derivatives for the Treatment of Drug-Resistant Tuberculosis. *J. Med. Chem.* **2012**, *55*, 8409–8417.

(21) Redd, V. M.; O'Sullivan, J. F.; Gangadharam, P. R. J. Antimycobacterial Activities of Riminophenazines. *J. Antimicrob. Chemother.* **1999**, *43*, 615–623.

(22) Drug pipeline. http://www.newtbdrugs.org/pipeline.php (accessed Jul 16, 2016).

(23) Van Soolingen, D.; Hernandez-Pando, R.; Orozco, H.; Aguilar, D.; Magis-Escurra, C.; Amaral, L.; Van Ingen, J.; Boeree, M. J. The Antipsychotic Thioridazine Shows Promising Therapeutic Activity in a Mouse Model of Multidrug-Resistant Tuberculosis. *PLoS ONE* **2010**, *5*, 1–6.

(24) Amaral, L.; Amaral, L.; Martins, A.; Spengler, G.; Hunyadi, A.; Molnar, J. The Mechanism by Which the Phenothiazine Thioridazine Contributes to Cure Problematic Drug-Resistant Forms of Pulmonary Tuberculosis : Recent Patents for " New Use " The Mechanism by Which the Phenothiazine Thioridazine Contributes to Cure Problematic Dru. *Recent Pat. Antiinfect. Drug Discov.* **2013**, *8*, 206–212.

(25) Lougheed, K. E. A.; Taylor, D. L.; Osborne, S. A.; Bryans, J. S.; Buxton, R. S. New Anti-Tuberculosis Agents amongst Known Drugs. *Tuberculosis* **2009**, *89*, 364–370.

(26) Horita, Y.; Takii, T.; Yagi, T.; Ogawa, K.; Fujiwara, N.; Inagaki, E.; Kremer, L.; Sato, Y.; Kuroishi, R.; Lee, Y.; Makino, T.; Mizukami, H.; Hasegawa, T.; Yamamoto, R.; Onozaki, K. Antitubercular Activity of Disulfiram, an Antialcoholism Drug, against Multidrug- and Extensively Drug-Resistant Mycobacterium Tuberculosis Isolates. *Antimicrob. Agents Chemother.* **2012**, *56*, 4140–4145.

(27) Forsman, L. D.; Sch??n, T.; Simonsson, U. S. H.; Bruchfeld, J.; Larsson, M.; Jur??en, P.; Stureg??rd, E.; Giske, C. G.; ??ngebyh, K. Intra- And Extracellular Activities of Trimethoprim-Sulfamethoxazole against Susceptible and Multidrug-Resistant Mycobacterium Tuberculosis. *Antimicrob. Agents Chemother.* **2014**, *58*, 7557–7559.

(28) De Carvalho, L. P. S.; Lin, G.; Jiang, X.; Nathan, C. Nitazoxanide Kills Replicating and Nonreplicating Mycobacterium Tuberculosis and Evades Resistance. *J. Med. Chem.* **2009**, *52*, 5789–5792.

(29) Krieger, D.; Vesenbeckh, S.; Schönfeld, N.; Bettermann, G.; Bauer, T. T.; Rüssmann, H.; Mauch, H. Mefloquine as a Potential Drug against Multidrug-Resistant Tuberculosis. *Eur. Respir J.* **2015**, *46*, 1503–1505.

(30) Bermudez, L. E.; Meek, L. Mefloquine and Its Enantiomers Are Active against Mycobacterium Tuberculosis In Vitro and in Macrophages. *Tuberc. Res. Treat.* **2014**, *2014*, 1–5.

(31) Pradel, G.; Schlitzer, M. Antibiotics in Malaria Therapy and Their Effect on the Parasite Apicoplast. *Curr. Mol. Med.* **2010**, *10*, 335–349.

(32) Andrews, K. T.; Fisher, G.; Skinner-Adams, T. S. Drug Repurposing and Human Parasitic Protozoan Diseases. *Int. J. Parasitol. Drugs Drug Resist.* 2014, pp 95–111.

(33) World Health Organization. *Guidelines For The Treatment of Malaria, 3rd Edition*; 2015.

(34) Libecco, J. A.; Powell, K. R. Trimethoprim/sulfamethoxazole: Clinical Update. *Pediatr. Rev.* **2004**, *25*, 375–380.

(35) Suthar, A. B.; Granich, R.; Mermin, J.; Van Rie, A. Effect of Cotrimoxazole on Mortality in HIV-Infected Adults on Antiretroviral Therapy: A Systematic Review and Meta-Analysis. *Bull. World Health Organ.* 2012, pp 128–138C.

(36) Kasirye, R.; Baisley, K.; Munderi, P.; Grosskurth, H. Effect of Cotrimoxazole Prophylaxis on Malaria Occurrence in HIV-Infected Patients on Antiretroviral Therapy in Sub-Saharan Africa. *Trop. Med. Int. Health* **2015**, *20*, 569–580.

(37) Chong, C. R.; Chen, X.; Shi, L.; Liu, J. O.; Sullivan, D. J. A Clinical Drug Library Screen Identifies Astemizole as an Antimalarial Agent. *Nat. Chem. Biol.* **2006**, *2*, 415–416.

(38) Da Cruz, F. P.; Martin, C.; Buchholz, K.; Lafuente-Monasterio, M. J.; Rodrigues, T.; Sönnichsen, B.; Moreira, R.; Gamo, F. J.; Marti, M.; Mota, M. M.; Hannus, M.; Prudêncio, M. Drug Screen Targeted at Plasmodium Liver Stages Identifies a Potent Multistage Antimalarial Drug. *J. Infect. Dis.* **2012**, *205*, 1278–1286.

(39) Matthews, H.; Usman-Idris, M.; Khan, F.; Read, M.; Nirmalan, N. Drug Repositioning as a Route to Anti-Malarial Drug Discovery: Preliminary Investigation of the in Vitro Anti-Malarial Efficacy of Emetine Dihydrochloride Hydrate. *Malaria journal* **2013**, *12*, 359.

(40) Combs, A. B.; Acosta, D. Toxic Mechanisms of the Heart: A Review. *Toxicol Pathol.* **1990**, *18*, 583–596.

(41) Bansal, D.; Sehgal, R.; Chawla, Y.; Mahajan, R. C.; Malla, N. In Vitro Activity of Antiamoebic Drugs against Clinical Isolates of Entamoeba Histolytica and Entamoeba Dispar. *Ann. Clin. Microbiol .Antimicrob.* **2004**, *3*, 27–31.

(42) Dempsey, J. J.; Salem, H. H. An Enzymatic Electrocardiographic Study on Toxicity of Dehydroemetine. *Br. Heart J.* **1966**, *28*, 505–511.

(43) Kaiser, M.; Mäser, P.; Tadoori, L. P.; Ioset, J. R.; Brun, R.; Sullivan, D. J. Antiprotozoal Activity Profiling of Approved Drugs: A Starting Point toward Drug Repositioning. *PLoS ONE* **2015**, *10*, 1–16.

(44) Bitonti, A. J.; Sjoerdsma, A.; McCann, P. P.; Kyle, D. E.; Oduola, a M.; Rossan, R. N.; Milhous, W. K.; Davidson, D. E. Reversal of Chloroquine Resistance in Malaria Parasite Plasmodium Falciparum by Desipramine. *Science* **1988**, *242*, 1301–1303.

(45) Eastman, R. T.; Pattaradilokrat, S.; Raj, D. K.; Dixit, S.; Deng, B.; Miura, K.; Yuan, J.; Tanaka, T. Q.; Johnson, R. L.; Jiang, H.; Huang, R.; Williamson, K. C.; Lambert, L. E.; Long, C.; Austin, C. P.; Wu, Y.; Su, X. Z. A Class of Tricyclic Compounds Blocking Malaria Parasite Oocyst Development and Transmission. *Antimicrob. Agents Chemother.* **2013**, *57*, 425–435.

(46) Godtfredsen, W. O.; Jahnsen, S.; Lorck, H.; Roholt, K.; Tybring, L. Fusidic Acid: A New Antibiotic. *Nature* **1962**, *193*, 987.

(47) Spelman, D. Fusidic Acid in Skin and Soft Tissue Infections. *Int. J. Antimicrob. Agents* **1999**, *12*, S59–S66.

(48) Verbist, L. The Antimicrobial Activity of Fusidic Acid. *J. Antimicrob. Chemother.* **1990**, *25*, 1–5.

(49) Godtfredsen, W.; Roholt, K.; Tybring, L. Fusidic Acid: A New Orally Active Antibiotic. *Lancet* **1962**, *1*, 928–931.

(50) O'Neill, a J.; McLaws, F.; Kahlmeter, G.; Henriksen, a S.; Chopra, I. Genetic Basis of Resistance to Fusidic Acid in Staphylococci. *Antimicrob. Agents Chemother.* **2007**, *51*, 1737–1740.

(51) Collignon, P.; Turnidge, J. Fusidic Acid in Vitro Activity. *Int. J. Antimicrobial . Agents* **1999**, *12 Suppl 2*, S45–S58.

(52) Taksta (CEM-102). https://newdrugapprovals.org/tag/fusidic-acid/ (accessed Jul 23, 2016).

(53) Kraus, C. N.; Burnstead, B. W. The Safety Record of Fusidic Acid in Non-US Markets: A Focus on Skin Infections. *Clin. Infect. Dis.* **2011**, *52*, S527–S537.

(54) Sahm, D. F.; Deane, J.; Pillar, C. M.; Fernandes, P. In Vitro Activity of CEM-102 (Fusidic Acid) against Prevalent Clones and Resistant Phenotypes of Staphylococcus Aureus. *Antimicrob. Agents Chemother.* **2013**, *57*, 4535–4536.

(55) Guenthner, S. H.; Wenzel, R. P. In Vitro Activities of Teichomycin , Fusidic Acid , Flucloxacillin , Fosfomycin , and Vancomycin Against Methicillin-Resistant Staphylococcus Aureus. *Antimicrob. Agents Chemother.* **1984**, *26*, 268–269.

(56) Toma, E.; Barriault, D. Antimicrobial Activity of Fusidic Acid and Disk Diffusion Susceptibility Testing Criteria for Gram-Positive Cocci. *J. Clin. Microbiol.* **1995**, *33*, 1712–1715.

(57) Mcghee, P.; Clark, C.; Credito, K.; Beachel, L.; Pankuch, G. A.; Appelbaum, P. C.; Kosowska-shick, K. In Vitro Activity of Fusidic Acid (CEM-102 , Sodium Fusidate) against Staphylococcus Aureus Isolates from Cystic Fibrosis Patients and Its Effect on the Activities of Tobramycin and Amikacin against Pseudomonas Aeruginosa and Burkholderia Cepacia. *Antimicrob. Agents Chemother.* **2011**, *55*, 2417–2419.

(58) Sahm, D. F.; Deane, J.; Pillar, C. M.; Fernandes, P. In Vitro Activity of CEM-102 (Fusidic Acid) against Prevalent Clones and Resistant Phenotypes of Staphylococcus Aureus. *Antimicrob. Agents Chemother.* **2013**, *57*, 4535–4536.

(59) Product Monograph: FUCITHALMIC ® Fusidic acid. www.leo-pharma.ca (accessed Jul 23, 2016).

(60) Godtfredsen, W. O.; Daehne, V. W.; Tybring, L.; Vangedal, S. Fusidic Acid Derivatives. I. Relationship between Structure and Antibacterial Activity. *J. Med. Chem.* **1966**, *9*, 15–22.

(61) Janssen, G.; Vanderhaeghe, H. Modification of the Side Chain of Fusidie Acid (Ramycin). *J. Med. Chem.* **1967**, *10*, 205–208.

(62) Von Daehne, W.; Rasmussen, P. R. l6-Ethers Of Fusidic Acid Derivatives. US4060606, 1977.

(63) Duvold, T.; Jørgensen, A.; Andersen, N. R.; Henriksen, A. S.; Sørensen, M. D.; Bjo, F. 17 S , 20 S -Methanofusidic Acid , a New Potent Semi-Synthetic Fusidane Antibiotic. *Bioorg. Med. Chem. Lett.* **2002**, *12*, 3569–3572.

(64) Duvold, T.; Sørensen, M. D.; Bjorkling, F.; Henriksen, A. S.; Rastrup-Andersen, N. Synthesis and Conformational Analysis of Fusidic Acid Side Chain Derivatives in Relation to Antibacterial Activity. *J. Med. Chem.* **2001**, *44*, 3125–3131.

(65) Duvold, T.; Bretting, C. A. S.; Rasmussen, P. A. ; Bouerat, L.; Thorhauge, J. Novel Fusidic Acid Derivatives. WO2005007669 A1, 2005.

(66) Duvold, T. Novel Polyaminated Fusidic Acid Derivatives. WO2002077007 A2, 2002.

(67) Besier, S.; Ludwig, A.; Brade, V.; Wichelhaus, T. a. Molecular Analysis of Fusidic Acid Resistance in Staphylococcus Aureus. *Mol. microbiol.* **2003**, *47*, 463–469.

(68) Bodley, J. W.; Zieve, F. J.; Lin, L. Studies on Translocation. IV. The Hydrolysis of a Single Round of Guanosine Triphosphate in the Presence of Fusidic Acid. *J. Biol .Chem.* **1970**, *45*, 5662–5667.

(69) Beretta, C.; Ferrini, R.; Glässer, A. H. 1-Methyl-8-Beta-Carbobenzyloxy-Aminomethyl-10-Alpha-Ergoline, a Potent and Long-Lasting 5-Hydroxytryptamine Antagonist. *Nature* **1965**, *207*, 421–422.

(70) Turner, E. H.; Schwartz, P. J.; Lowe, C. H.; Nawab, S. S.; Feldman-Naim, S.; Drake, C. L.; Myers, F. S.; Barnett, R. L.; Rosenthal, N. E. Double-Blind, Placebo-Controlled

Study of Single-Dose Metergoline in Depressed Patients with Seasonal Affective Disorder. *J. Clin. Psychopharmacol.* **2002**, *22*, 216–220.

(71) Caballero, A.; Mena, P.; Caballero-Díaz, J. L.; Caballero-Asensi, A. Metergoline as an Inhibitor of Prolactin Release. *J. reprod. med.* **1987**, *32*, 115–119.

(72) Lee, J.; Liu, J.; Shin, M.; Hong, M.; Nah, S.; Bae, H. Metergoline Inhibits the Neuronal Nav1.2 Voltage-Dependent Na+ Channels Expressed in Xenopus Oocytes. *Acta Pharmacol. Sin.* **2014**, *35*, 862–868.

(73) Watson, C. P. Antidepressant Drugs as Adjuvant Analgesics. *J. Pain Symptom manage.* **1994**, *9*, 392–405.

(74) Greenberg, B. D.; Benjamin, J.; Martin, J. D.; Keuler, D.; Huang, S. J.; Altemus, M.; Murphy, D. L. Delayed Obsessive-Compulsive Disorder Symptom Exacerbation after a Single Dose of a Serotonin Antagonist in Fluoxetine-Treated but Not Untreated Patients. *Psychopharmacology* **1998**, *140*, 434–444.

(75) Ben-Zion, I. Z.; Meiri, G.; Greenberg, B. D.; Murphy, D. L.; Benjamin, J. Enhancement of CO2-Induced Anxiety in Healthy Volunteers with the Serotonin Antagonist Metergoline. *Am. J. Psychiatry* **1999**, *156*, 1635–1637.

(76) Roca, C. a.; Schmidt, P. J.; Smith, M. J.; Danaceau, M. a.; Murphy, D. L.; Rubinow, D. R. Effects of Metergoline on Symptoms in Women with Premenstrual Dysphoric Disorder. *Am. J. Psychiatry* **2002**, *159*, 1876–1881.

(77) Nöthling, J. O.; Gerber, D.; Gerstenberg, C.; Kaiser, C.; Döbeli, M. Abortifacient and Endocrine Effects of Metergoline in Beagle Bitches during the Second Half of Gestation. *Theriogenology* **2003**, *59*, 1929–1940.

(78) Kang, K.; Wong, K. S.; Jayampath Seneviratne, C.; Samaranayake, L. P.; Fong, W. P.; Tsang, P. W. K. In Vitro Synergistic Effects of Metergoline and Antifungal Agents against Candida Krusei. *Mycoses* **2010**, *53*, 495–499.

Chapter 3

Synthesis, structure-activity relationship and biological evaluation of fusidic acid derivatives

3.1 Introduction

This chapter describes the synthesis of fusidic acid derivatives. It then reports and discusses the characterization of the target compounds followed by a discussion of their *in vitro* antimycobacterial, antiplasmodial and cytotoxic activity profile. The *in vivo* mouse pharmacokinetic data of some representative compounds are also reported.

3.2 Rationale

A High-Throughput Screen (HTS) conducted by the Tuberculosis Antimicrobial Acquisition Coordinating Facility (TAACF) revealed the antimycobacterial activity of fusidic acid with an IC_{90} of 0.6 μg/ml (1.2 μM) against the H37Rv strain of *Mtb*.[1] The antimycobacterial activity of fusidic acid against clinical isolates has also been revealed in the literature.[2] Fusidic acid was tested *in vitro* against 170 clinical *Mtb* isolates of which 151 were susceptible to first-line drugs (SM, INH, RIF and EMB) and 19 were resistant to one or more first-line drugs. Only 3 out of 170 isolates were found to be resistant to fusidic acid while the remaining 167 isolates displayed $MIC_{90} \leq 31$ μM. Moreover, fusidic acid did not show cross-resistance with first-line drugs.[2]

In summary, the *in vitro* effect of fusidic acid on *Mtb* is promising. Coupled with the excellent pharmacokinetic properties of fusidic acid in humans and the novelty in its mechanism of action, this makes fusidic acid a promising new antimycobacterial scaffold for repositioning via medicinal chemistry approaches.

Apart from its antimycobacterial activity, fusidic acid has also shown *in vitro* antiplasmodial activity with an IC_{50} value of 52.8 μM against the D10 strain of *P. falciparum*.[3] Although this IC_{50} value is high, fusidic acid also has the potential for repositioning in malaria through semisynthesis. Therefore, the synthesized derivatives of fusidic acid were also evaluated against *P. falciparum*.

3.3 Fusidic acid derivatives for structure-activity relationship (SAR) studies

The SAR studies performed by Leo pharma on fusidic acid as an antibacterial agent were described in Chapter 2. These studies have shown that the tetracyclic skeleton and the carboxylic acid group are essential for its antibacterial activity. The C-16 acetoxy, as well as the C-3 and C-11 hydroxyl groups are also important for activity but can be replaced with other functional groups such as esters, ethers, thioethers, keto, amines, oximes, halogen, and sulfoxide.[4] Based on this antibacterial SAR, three sites in fusidic acid were chosen for initial antimycobacterial SAR studies as shown in Figure 3.1.

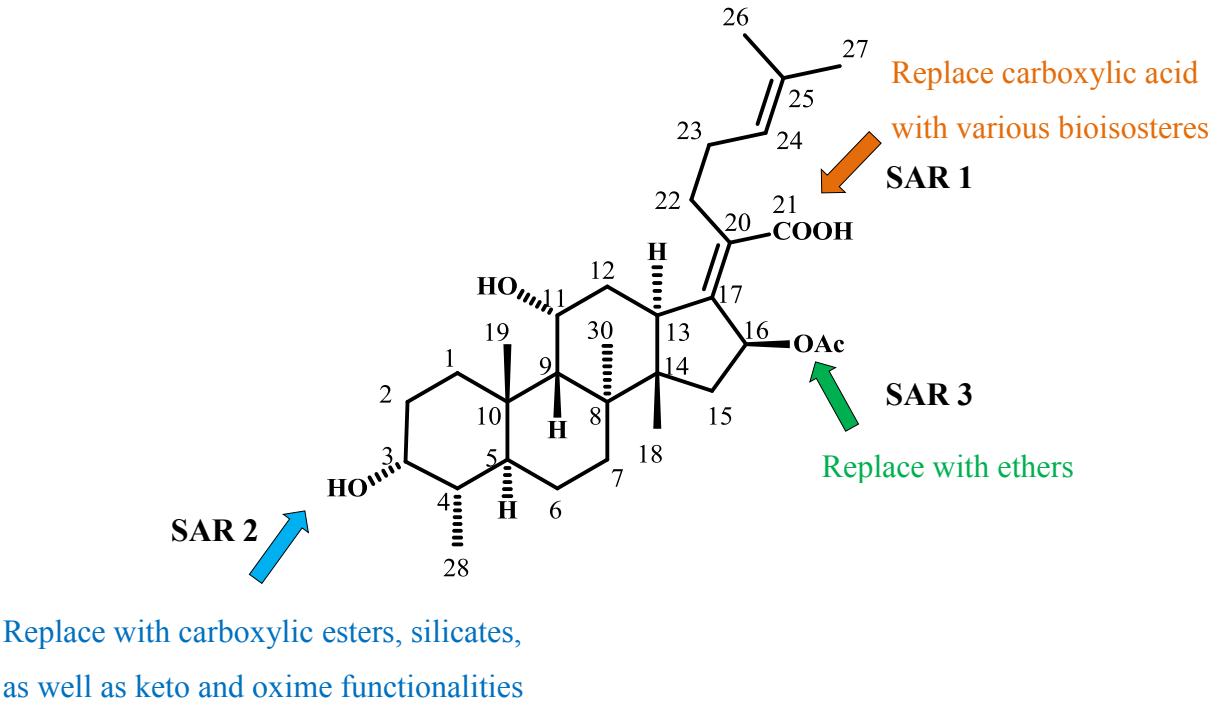

Figure 3.1: Proposed initial antimycobacterial SAR studies

SAR 1 includes replacement of the C-21 carboxylic acid with various bioisosteres such as esters, amides, sulfonamides, hydrazides, sulfonyl hydrazides and oxadiazoles. Bioisosteres are generally defined as those atoms or groups or molecules that exhibit similar volume, shape, and/or physicochemical properties, and whose replacement retains the biological activity of compounds.[5] Bioisosteric replacement of a carboxylic acid group is a widely used approach within medicinal chemistry in order to improve properties such as bioavailability, selectivity, and potency of a lead compound. In addition, ester, amide, and hydrazide derivatives may act as stable molecules or as prodrugs that can generate fusidic acid *in vivo*.

SAR 2 includes replacement of the C-3 OH group with other functional groups. The C-3 OH can be selectively derivatized as the C-11 OH is sterically hindered due to the chair-boat-chair arrangement of the tetracyclic ring system of fusidic acid (Figure 3.2).[6] Therefore, the C-3 OH is much more reactive than the C-11 OH. In this study, the C-3 OH group was replaced with various carboxylic and silicate esters as well as with keto and oxime functionalities.

SAR 3 includes replacement of the C-16 acetoxy group with ethers.

In addition to the above, fusidic acid derivatives with modifications at more than one site (termed as miscellaneous derivatives) were also synthesized.

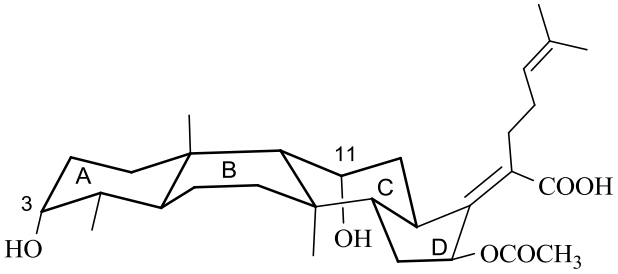

Figure 3.2: Chair-boat-chair arrangement of tetracyclic ring system of fusidic acid

3.4 Chemical synthesis

3.4.1 Synthesis of C-21 fusidic acid derivatives (SAR 1)

Synthetic routes used to synthesize C-21 derivatives of fusidic acid are outlined in Schemes 3.1-3.3.[7] Synthesis of various ester, amide and sulfonamide derivatives is shown in Scheme 3.1. Fusidic acid methyl ester **3.2** was obtained by heating commercially available fusidic acid (**3.1**, 4500USD/100g from Ava Chem Scientific) with methyl iodide in the presence of the inorganic base K_2CO_3 in DMF. Reaction of **3.1** with ammonium chloride using PyBOP-HOBt as a coupling reagent furnished fusidic acid amide **3.3**.[8] Likewise, EDCI-mediated coupling of **3.1** with cyanamide and 5-aminotetrazole furnished amide derivatives **3.4** and **3.5**, respectively. Amide derivatives **3.6-3.9** were obtained through the coupling of **3.1** with a corresponding amine in the presence of EDCI using DMAP as a catalyst. Likewise, an EDCI-DMAP mediated coupling of **3.1** with the respective sulfonamide furnished sulfonamide derivatives **3.10-3.12**.

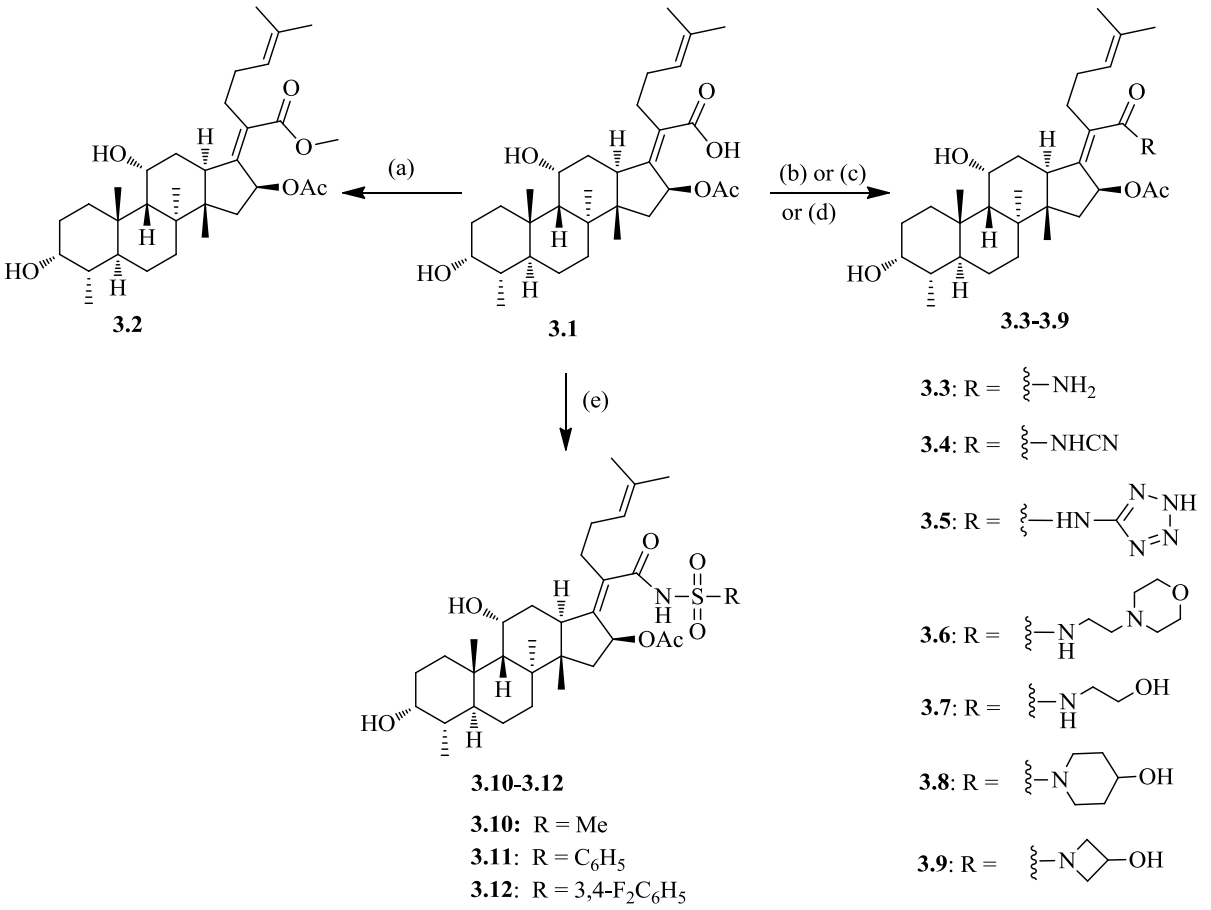

Scheme 3.1: *Reagents and conditions*: (a) K_2CO_3, CH_3I, DMF, 50 ^oC, 3 h; (b) PyBOP, HOBt, DIPEA, NH_4Cl, DMF, 25 ^oC, 16 h for compound **3.3**; (c) RNH_2, EDCI, HOBt, DIPEA, DCM, 25 ^oC, 24 h for compounds **3.4** and **3.5**; (d) RNH_2, EDCI, DMAP, DCM, 25 ^oC, 16 h, for compounds **3.6-3.9**; (e) RSO_2NH_2, EDCI, DMAP, DCM, 25 ^oC, 48 h

Various hydrazide and sulfonyl hydrazide derivatives of fusidic acid were synthesized as shown in Scheme 3.2. Fusidic acid hydrazide **3.13**[8] was synthesized by reacting **3.1** with hydrazine hydrate using EDCI-HOBt as a coupling agent. Hydrazide derivative **3.14** was obtained by the reaction of **3.1** with thiophene-2-carbohydrazide in the presence of the coupling reagent TBTU, while derivative **3.15** was obtained by the reaction of **3.1** with isoniazid in the presence of n-propanephosphonic acid anhydride (T3P) as the coupling agent. Synthesis of hydrazide derivatives **3.16** and **3.17** was accomplished by refluxing **3.13** with 3- or 4- pyridinecarboxaldehyde, respectively, in ethanol for 8 h. Sulfonylhydrazide derivatives (**3.18-3.23**) were obtained by reacting **3.13** with the respective sulfonyl chloride (aliphatic sulfonyl chlorides with varying carbon chain lengths for **3.18-3.21** and 4-substituted aromatic sulfonyl chlorides for **3.22-3.23**) using pyridine as a base and solvent.

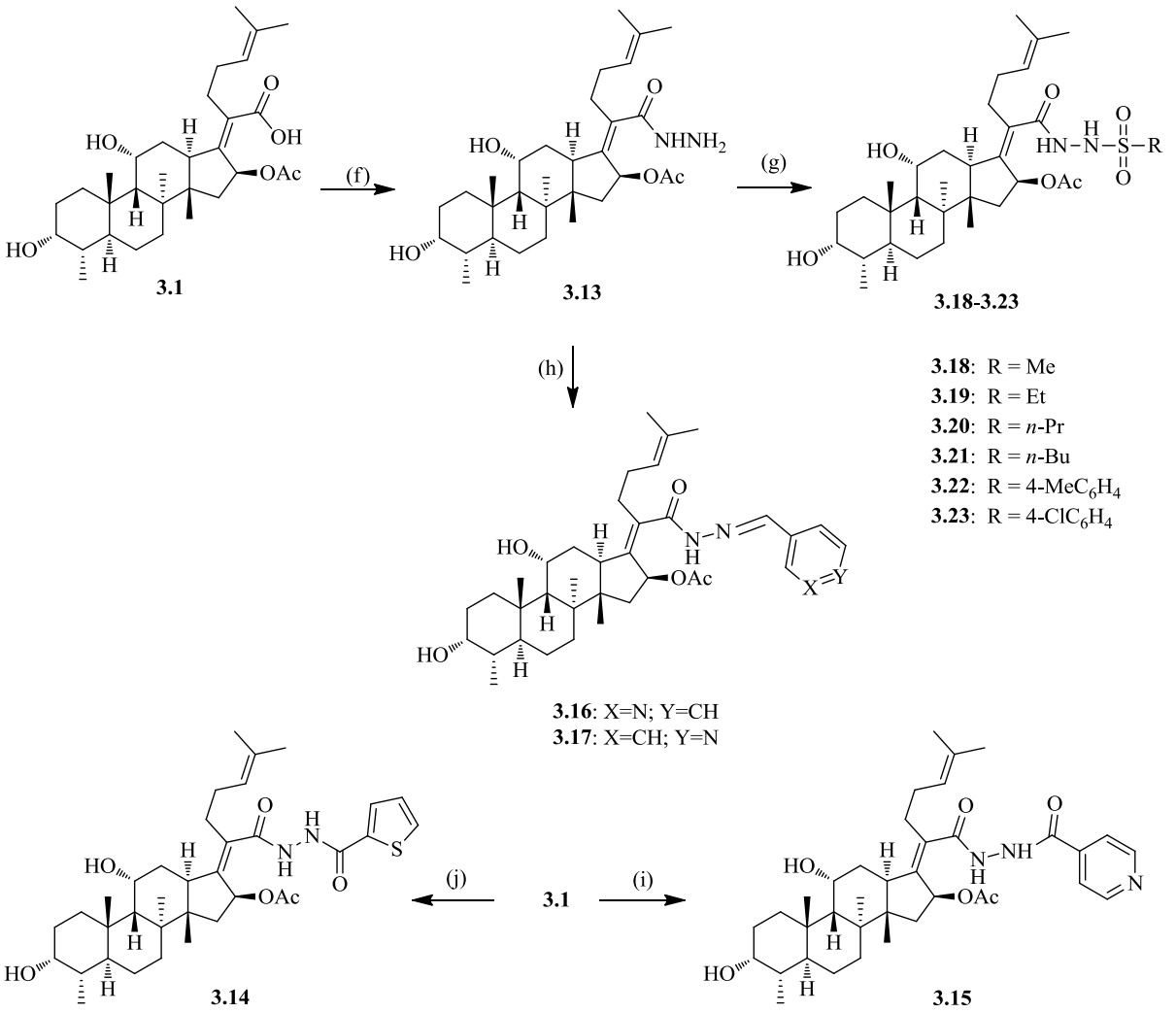

Scheme 3.2: *Reagents and conditions*: (f) EDCI, HOBt, acetonitrile, 25 ^{o}C, 3 h, $NH_2NH_2.H_2O$, 25 ^{o}C, 16 h; (g) RSO_2Cl, pyridine, 25 ^{o}C, 1-3 h; (h) 3-or 4-pyridinecarboxaldehyde, ethanol, 85 ^{o}C, 8 h; (i) Isoniazid, T3P (50% w/v solution in DMF), Et_3N, DCM, 0 ^{o}C - 25 ^{o}C, 5 h; (j) Thiophene-2-carbohydrazide, TBTU, DIPEA, DMF, 25 ^{o}C, 16 h

Various oxadiazole derivatives were synthesized as shown in Scheme 3.3. Reaction of **3.1** with the respective aliphatic and aromatic amidoximes in the presence of EDCI-HOBt in acetonitrile furnished intermediates, which upon reaction with sodium acetate in ethanol under microwave irradiation furnished 3-substituted-1,2,4-oxadiazole derivatives **3.24**-**3.27**. The synthesis of 2-oxo-1,3,4-oxodiazole **3.28** was accomplished by reacting compound **3.13** with CDI and Et_3N at 25 ^{o}C in THF (Scheme 3.3). On the other hand, the reaction of **3.13** with carbon disulphide and potassium hydroxide in refluxing ethanol furnished 2-thioxo-1,3,4-oxadiazole **3.29**.

All target compounds were purified using column chromatography and fully characterized by analytical and spectroscopic techniques. Table 3.1 reports the isolated yields and melting points of the target compounds. Some of these derivatives were obtained in relatively poor yields either due to formation of undesired side products (**3.5**, **3.7**-**3.8**, **3.20**, and **3.24**-**3.27**) or due to incomplete conversion of the starting material into product (**3.9**). Detailed synthetic procedures are described in Chapter 7.

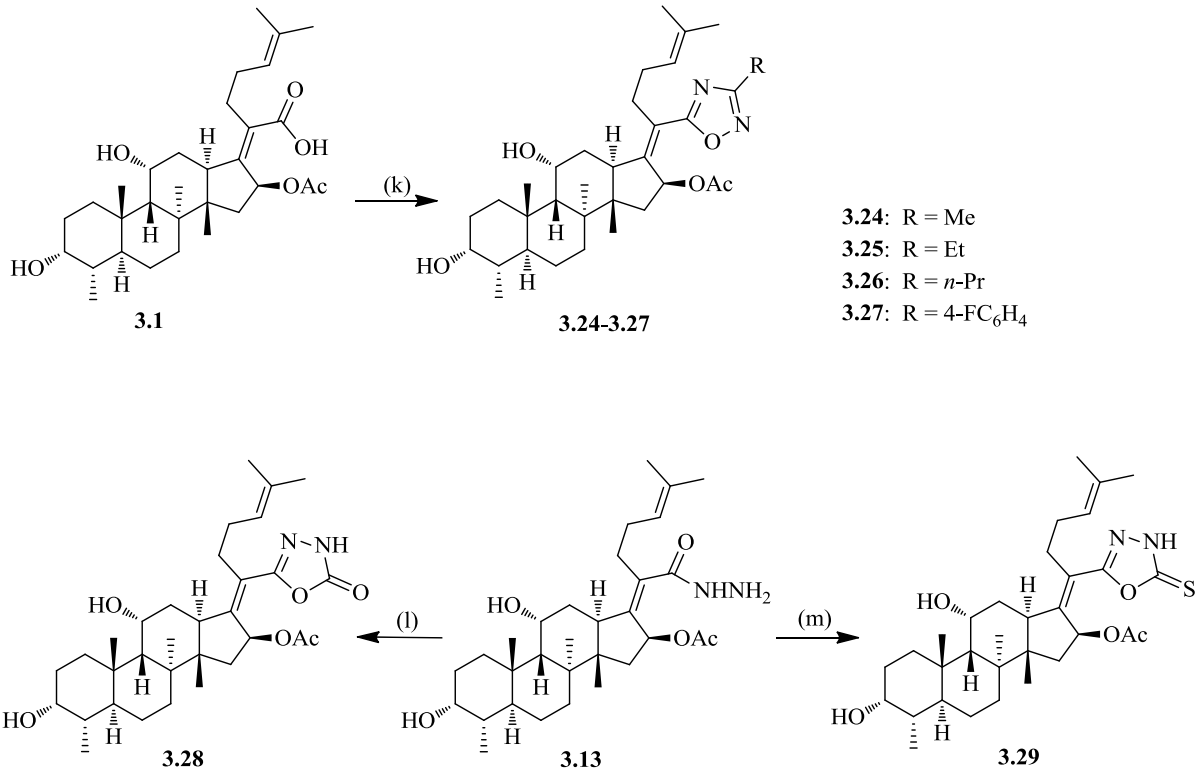

Scheme 3.3: *Reagents and conditions*: (k) (1) EDCI, HOBt, acetonitrile, 25 ^{o}C, 3 h, amidoxime, 80 ^{o}C, 12 h, (2) NaOAc, ethanol, MW, 100 ^{o}C, 2 h; (l) CDI, Et_3N, THF, 0 ^{o}C - 25 ^{o}C, 16 h; (m) CS_2, KOH, ethanol, reflux, 16 h

Table 3.1: Isolated yields and melting points of C-21 fusidic acid derivatives

Compound	Yield (%)	Mp (^{o}C)	Compound	Yield (%)	Mp (^{o}C)
3.1	-	203-205	**3.16**	63	230-232
3.2	92	166-168	**3.17**	63	159-161
3.3	31	223-225	**3.18**	44	125-127
3.4	53	142-144	**3.19**	45	127-129
3.5	29	> 280	**3.20**	25	125-127
3.6	67	216-218	**3.21**	71	121-123
3.7	25	162-164	**3.22**	46	220-222
3.8	18	195-197	**3.23**	65	230-232
3.9	18	178-180	**3.24**	24	152-154
3.10	31	214-216	**3.25**	23	126-128
3.11	38	229-231	**3.26**	14	110-112
3.12	30	232-234	**3.27**	20	86-88
3.13	98	128-130	**3.28**	24	137-139
3.14	50	144-146	**3.29**	56	130-132
3.15	46	189-191			

3.4.1.1 Mechanism of T3P-mediated coupling

n-Propanephosphonic acid anhydride is popularly known as T3P.[9] T3P is a phosphorus-based six-membered cyclic anhydride in which the P and O atoms are alternatively linked to each other, with each P atom bearing a n-propyl group (Figure 3.3). T3P is mainly employed as a coupling and dehydrating agent. However, due to the facile nature of the -P-O-P- bond, T3P shows exceptional reactivity towards a wide range of nucleophiles. As such, T3P has also found use in various other reactions such as functional group transformations, rearrangements, heterocycle synthesis and catalysis. It is mostly available as 50% (w/w) solution in ethyl acetate or DMF. Owing to increased sensitivity towards water, T3P can be easily removed from the reaction by extracting with water. The mechanism of peptide coupling of fusidic acid (R_1COOH) with various amines (R_2-NH_2) in the presence of T3P is shown in Figure 3.3. The reaction occurs by attack of the carboxylate ion on a P atom of T3P, thus opening the P-O-P ring and converting the O atom of the carboxylate ion into a good leaving group. Excess T3P and the un-cyclised by-product are removed by aqueous work-up.

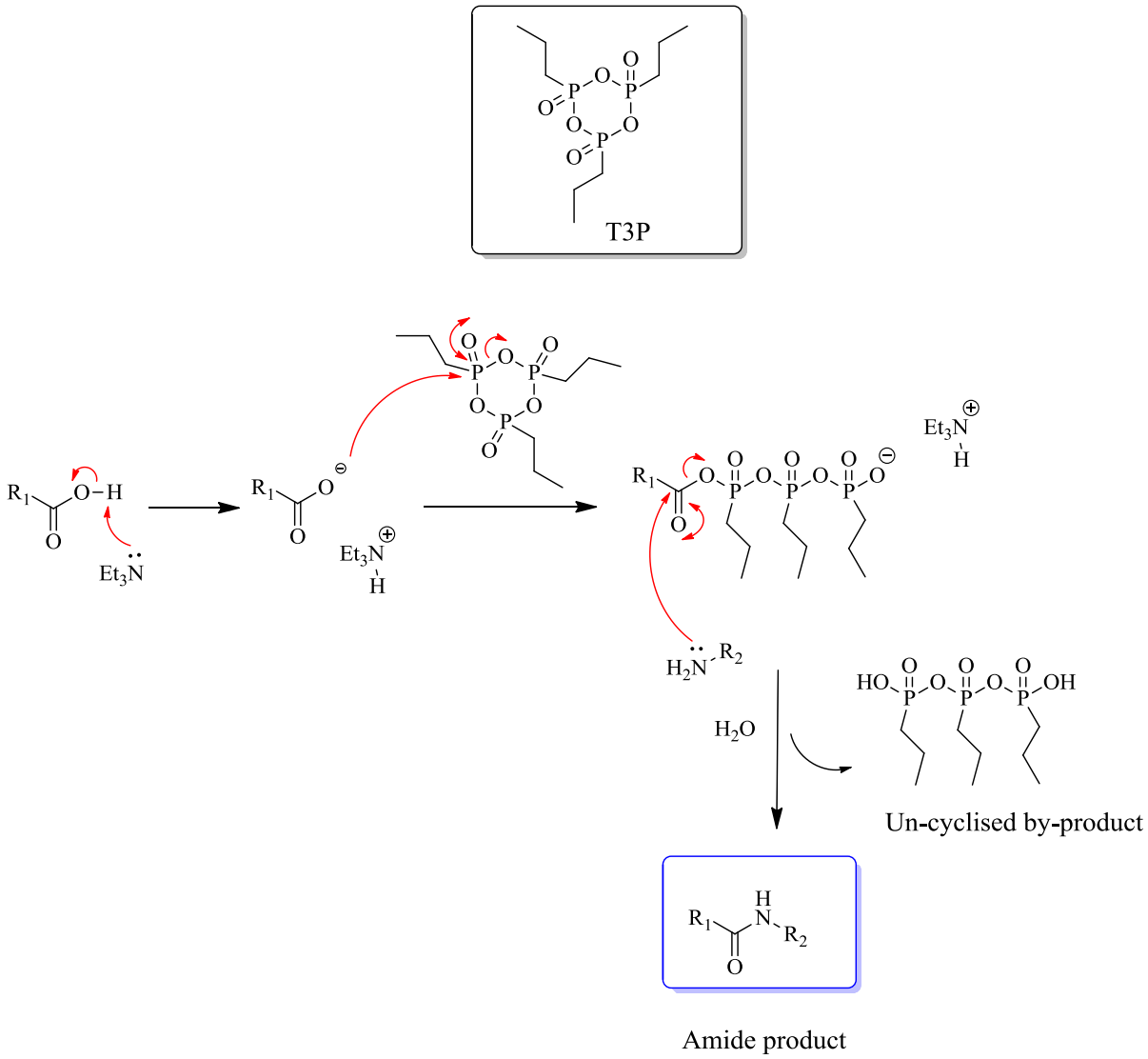

Figure 3.3: The mechanism for T3P coupling reaction[9]

3.4.1.2 Characterization of C-21 derivatives

All fusidic acid derivatives were characterized using ^{1}H NMR, ^{13}C NMR and mass spectroscopy (MS). Proton assignments were made with the help of ^{1}H-^{1}H COSY spectra.

The ^{1}H NMR spectrum of fusidic acid was recorded in $CDCl_3$ and is shown in Figure 3.4. The characteristic proton signals of fusidic acid appeared at δ 5.88 (d, J = 8.4 Hz, H-16), 5.10 (t, J = 7.2 Hz, H-24), 4.34 (m, H-11), 3.76 (m, H-3), 3.07-3.04 (m, H-13), 1.96 (s, OAc), 1.67 (s, CH_3-27), 1.60 (s, CH_3-26), 1.38 (s, CH_3-30), 0.98 (s, CH_3-19), 0.92 (d, J = 5.9 Hz, CH_3-28), and 0.91 (s, CH_3-18) ppm. Remaining protons of the tetracyclic ring system of fusidic acid, as well as the H-22 and H-23 protons appeared in the aliphatic region 2.52-1.02 ppm (Figure 3.4).

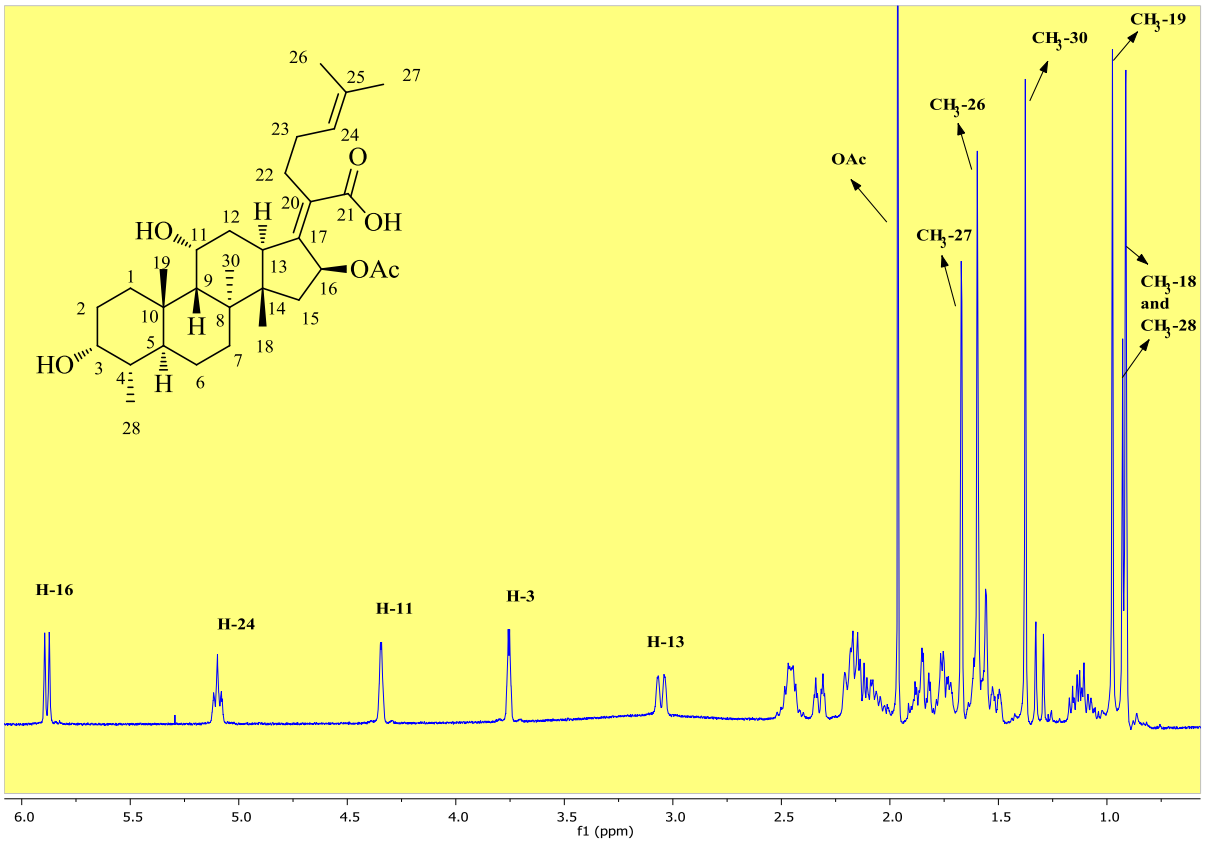

Figure 3.4: ^{1}H NMR spectrum ($CDCl_3$, 400MHz) of fusidic acid

The ^{13}C NMR spectrum of fusidic acid (Figure 3.5) depicted 31 distinct signals corresponding to 31 carbon atoms. Six signals appeared in the aromatic region 175-120 ppm. Signals at 174.0 and 170.5 ppm correspond to two carbonyl carbons of the -COOH and -OAc groups respectively, while signals at 150.9, 132.6, 129.5, 123.0 ppm correspond to C-17, C-25, C-20 and C-24 respectively. Twenty five signals appeared in the aliphatic region 75-15 ppm. The C-16, C-3 and C-11 carbons appeared at 74.4, 71.4, and 68.2 ppm respectively while C-13 appeared at 44.3 ppm. The remaining carbon atoms appeared in the aliphatic region 50-15 ppm. The ^{1}H and ^{13}C NMRs of fusidic acid were further verified in comparison with those reported in the literature.[10]

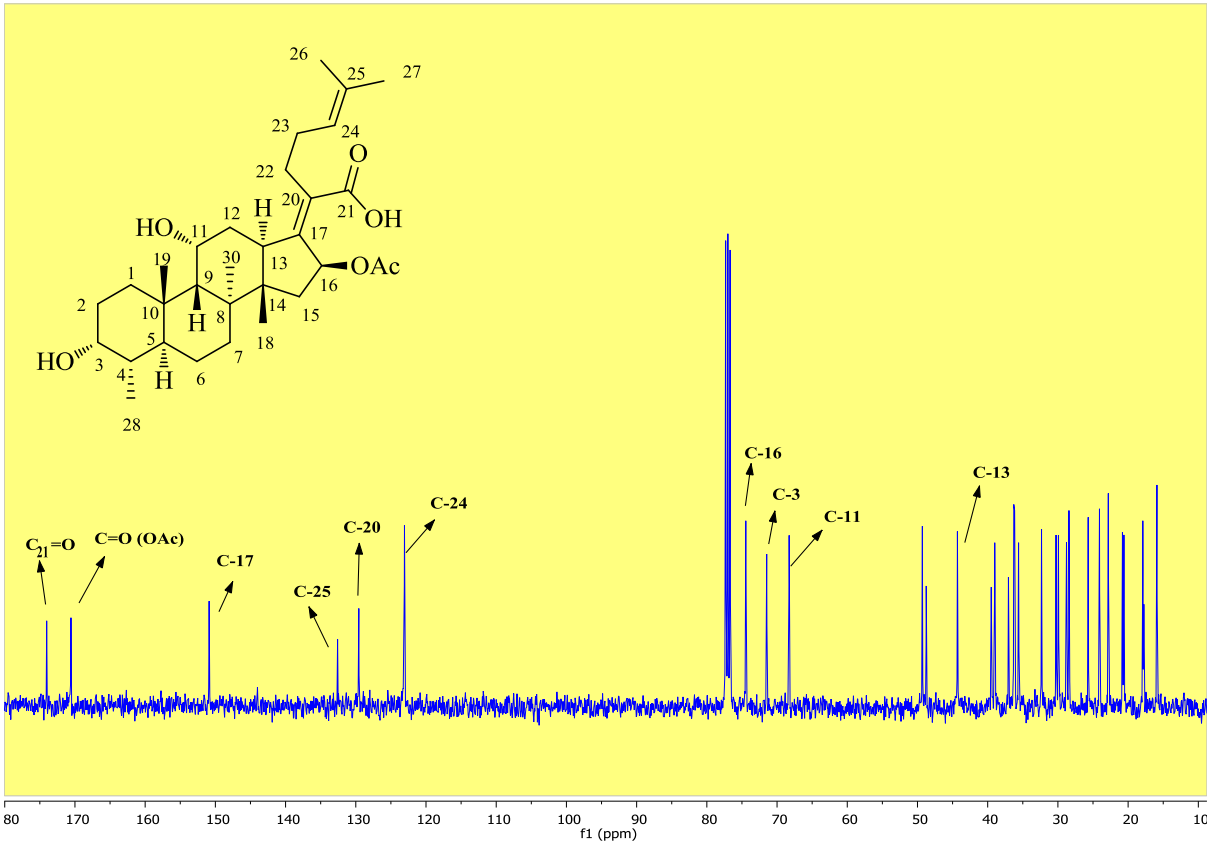

Figure 3.5: ^{13}C NMR spectrum ($CDCl_3$, 100 MHz) of fusidic acid

All C-21 derivatives depicted similar chemical shifts in their ^{1}H and ^{13}C NMR spectra along with additional proton signals representing the attached moiety. Both ^{1}H and ^{13}C NMR spectra of the C-21 derivatives can be described overall by considering representative examples (**3.14** and **3.16**) from the series of compounds.

The ^{1}H NMR spectrum of compound **3.14** was recorded in $CDCl_3$ at 400 MHz and is displayed in Figure 3.6. This compound was obtained by the coupling of fusidic acid with thiophene-2-carbohydrazide. Two broad singlets corresponding to two -CONH protons at 8.83 ppm and 8.48 ppm indicated the formation of the hydrazide carbonyl group. Further, two doublets at 7.64 ppm and 7.55 ppm, as well as a triplet at 7.10 ppm, corresponding to H-31, H-33 and H-32, respectively, indicated incorporation of the thiophene moiety into the fusidic acid structure. The remaining proton signals appeared in regions similar to fusidic acid.

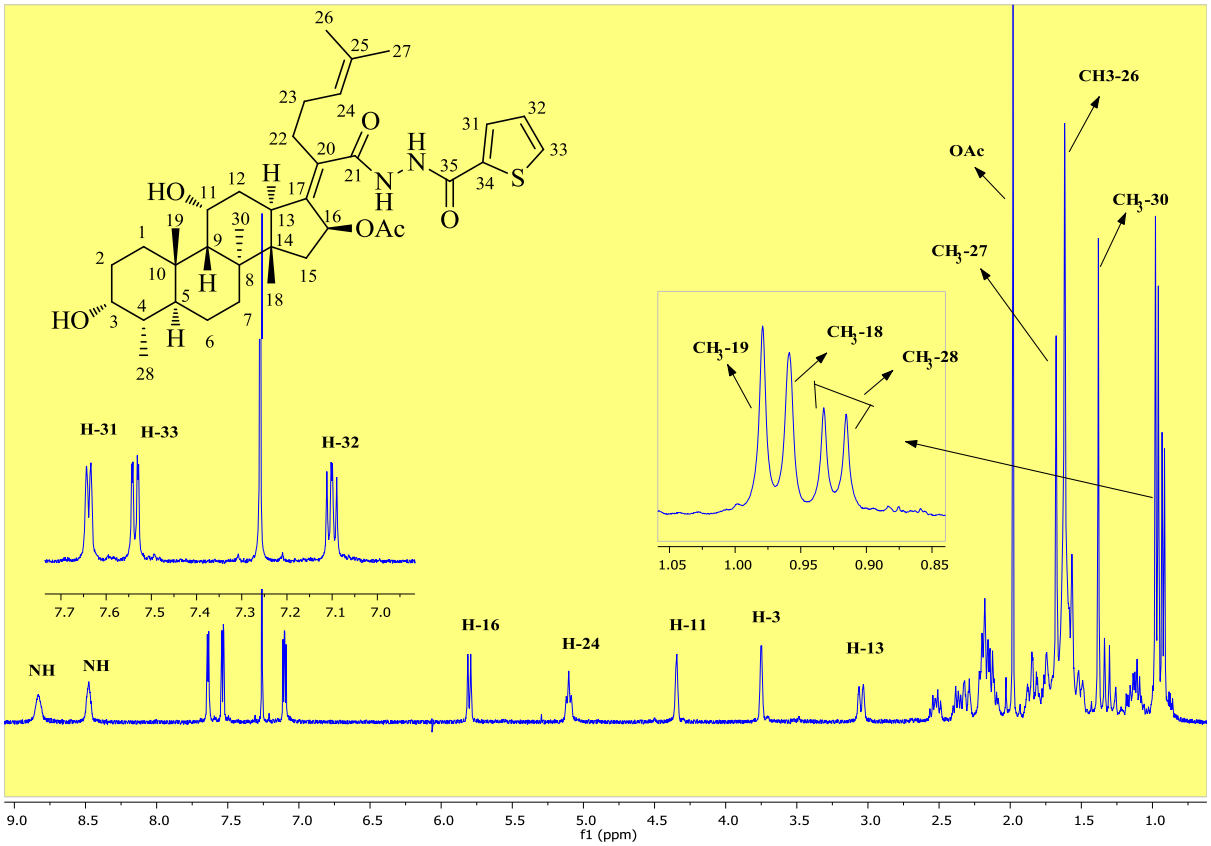

Figure 3.6: ^{1}H NMR spectrum ($CDCl_3$, 400 MHz) of compound **3.14**

Further, the ^{13}C NMR spectrum of **3.14** (Figure 3.7) depicted an additional carbon signal in the carbonyl region at 159.1 ppm, as well as 4 signals in the aromatic region at 135.4, 132.7, 131.0 and 127.8 ppm. These 5 additional signals indicated the presence of the thiophene-2-carbohydrazide moiety in the structure. Overall, the ^{13}C NMR of **3.14** depicted 36 distinct signals corresponding to 36 carbon atoms. Additionally, the MS displayed mass peaks at 641 [M+H] and 581 [M-OAc], as expected, which further supported the formation of the desired compound. Based on ^{1}H, ^{13}C and MS spectra, structure **3.14** was assigned to this compound.

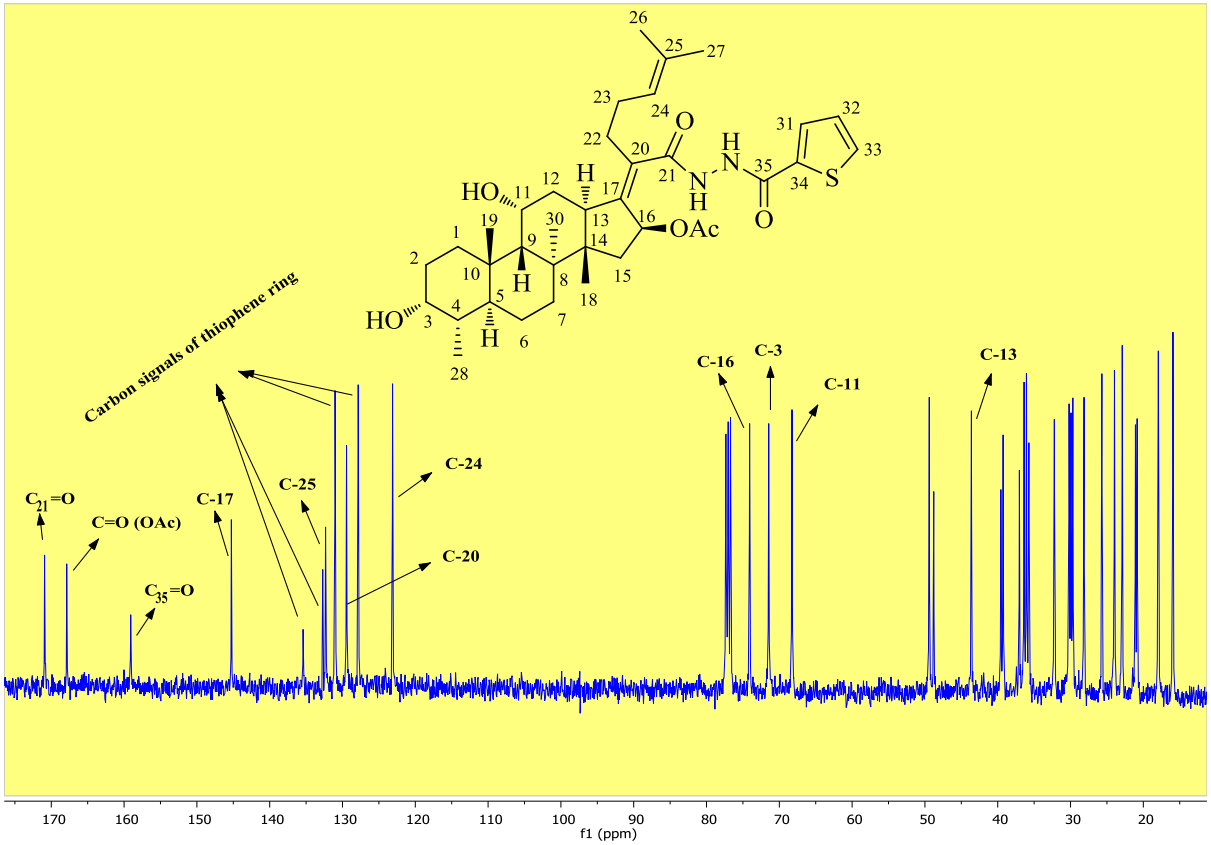

Figure 3.7: ^{13}C NMR spectrum ($CDCl_3$, 100 MHz) of compound **3.14**

Compound **3.16** was obtained by refluxing fusidic acid hydrazide **3.13** with 3-pyridinecarboxaldehyde in ethanol. The characteristic feature of the ^{1}H NMR spectrum (Figure 3.8) is the presence of additional peaks in the aromatic region at 8.84 (s, H-35), 8.56 (d, J = 5.2 Hz, H-34), 8.30 (d, J = 8.1 Hz, H-32), 8.13 (s, H-31) and 7.49 (dd, J = 8.0 and 4.9 Hz, H-33) ppm, which confirmed the coupling of compound **3.13** with 3-pyridinecarboxaldehyde. This type of coupling also delivered a mixture of E/Z isomers around the newly formed C=N double bond. This can be determined based on the splitting of some signals, as highlighted in Figure 3.8.

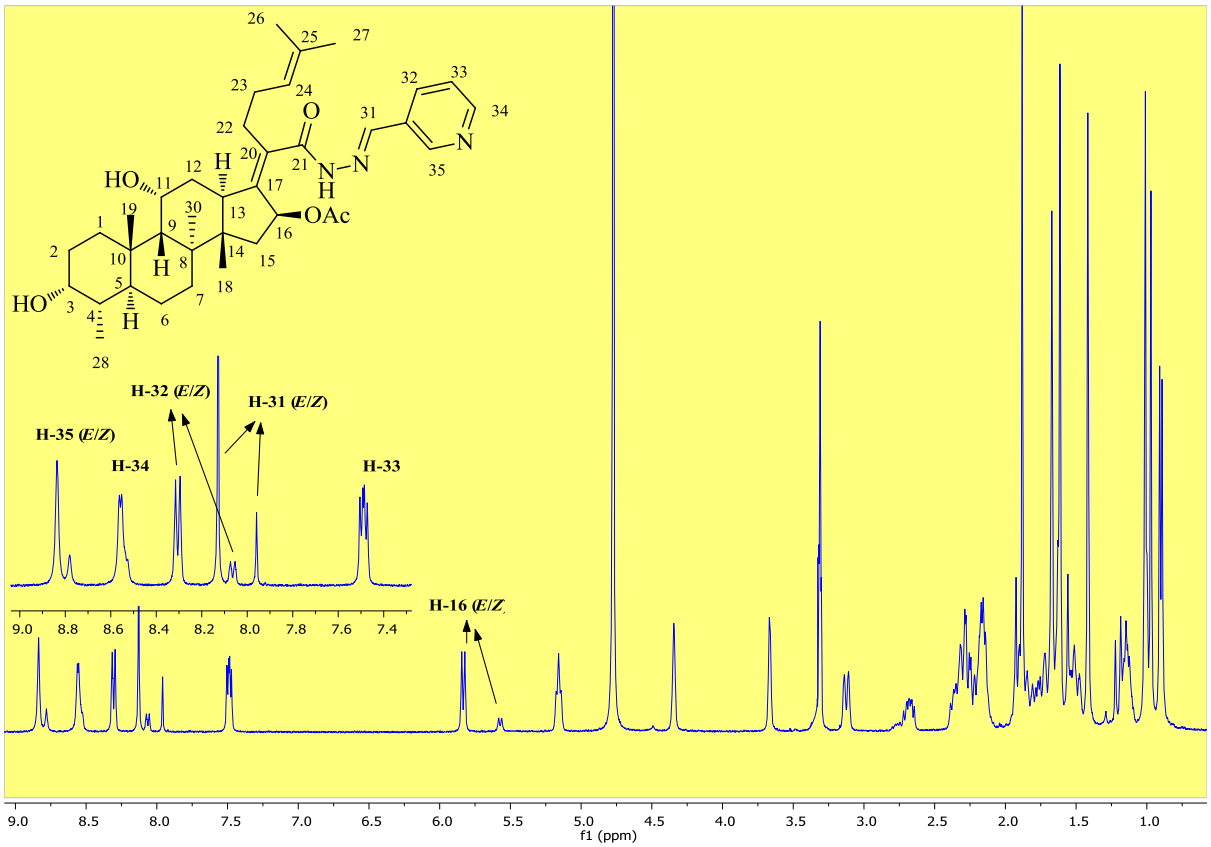

Figure 3.8: ^{1}H NMR spectrum (CD_3OD, 400 MHz) of compound **3.16**

Further, the ^{13}C NMR spectrum (Figure 3.9) displayed 6 signals in the aromatic region at 150.0, 148.3, 144.6, 134.5, 130.9 and 124.1 ppm, in addition to the expected signals for fusidic acid. These 6 additional signals indicated the presence of the 3-pyridyl moiety in the structure. Splitting of signals was also observed in the spectrum confirming the formation of E/Z isomers. Additionally, the MS displayed mass peaks at 620 [M+H] and 560 [M-OAc] as expected, which further confirmed the formation of the desired compound. Based on ^{1}H, ^{13}C and MS spectra, structure **3.16** was assigned to this compound.

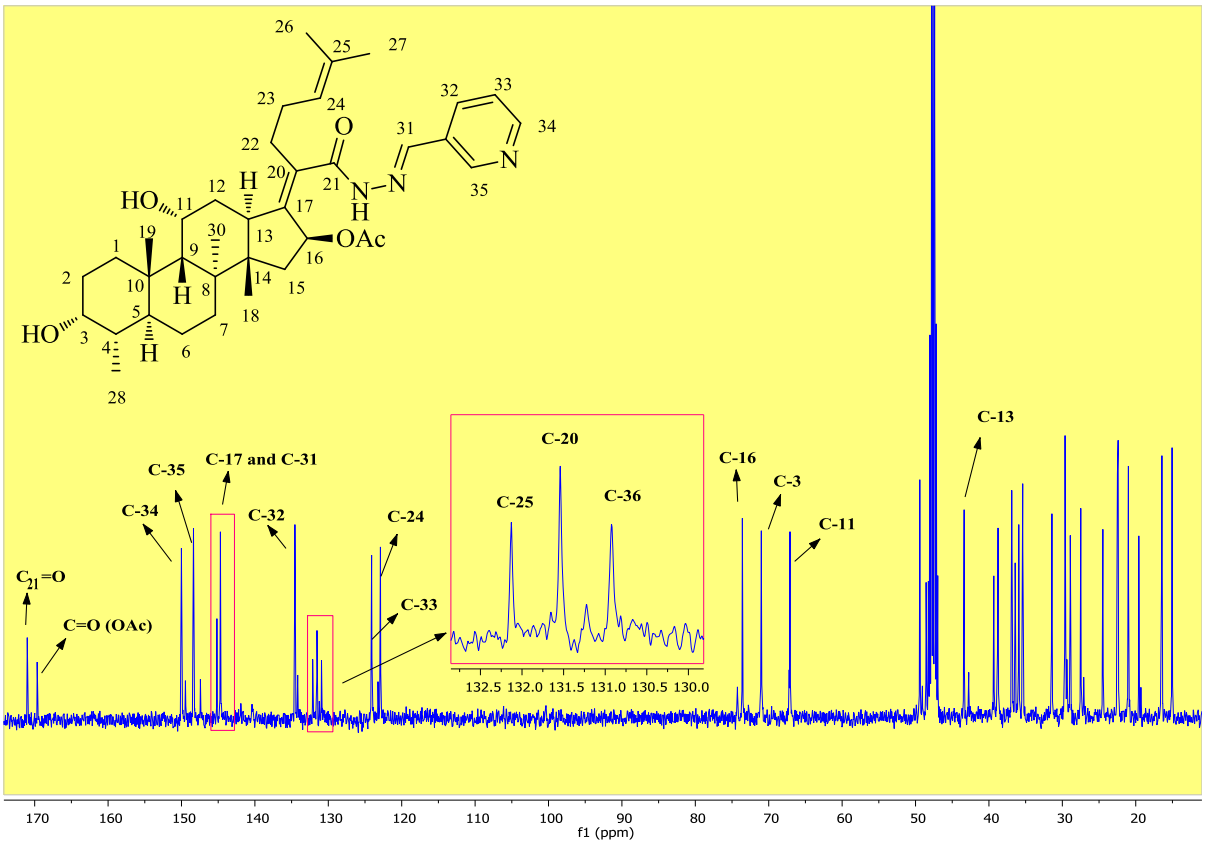

Figure 3.9: ^{13}C NMR spectrum (CD_3OD, 100 MHz) of compound **3.16**

3.4.2 Synthesis of C-3 fusidic acid derivatives (SAR 2)

Synthetic routes used to synthesize C-3 derivatives of fusidic acid are outlined in Scheme 3.4-3.5. Short, medium and long chain aliphatic C-3 carboxylic esters of fusidic acid were synthesized under two different conditions depending upon availability of the starting materials. Ester derivatives **3.30**[11] and **3.32** were synthesized by the reaction of fusidic acid (**3.1**) with the corresponding anhydride using pyridine as base and solvent, while **3.31** and **3.33-3.35** were synthesized by the reaction of fusidic acid with the corresponding carboxylic acid using the coupling reagent T3P in the presence of pyridine.

C-3 oximes **3.37-3.39** were synthesized by irradiating a mixture of 3-keto fusidic acid (**3.36**)[12] and the respective hydroxyl amine hydrochloride under microwave irradiation at 80 ^{o}C in the presence of NH_4OAc. Oximes were obtained as a mixture of *E*- and *Z*-isomers. 3-Keto fusidic acid was synthesized from fusidic acid using the Jones reagent as an oxidising agent. Oxidation of fusidic acid with the Jones reagent yielded both mono (3-keto, **3.36**) as well as disubstituted (3,11-diketo **3.54**) derivatives, which explains the low yield of 3-keto fusidic acid (**3.36**, 33%, Table 3.2). 3-Keto fusidic acid was also reduced to 3-epi fusidic acid (**3.40**)

using $NaBH_4$ in methanol. This reaction yielded both fusidic acid as well as its epimer **3.40**, which led to the poor yield of **3.40**.

Three silicate esters of fusidic acid (**3.41**-**3.43**) were synthesized by reacting the relevant trialkoxychlorosilane with fusidic acid at 0 ^{o}C for 1 h in the presence of imidazole as base and DMF as solvent (Scheme 3.5). Trialkoxychlorosilanes were prepared in house by dropwise addition of the respective alcohols to a solution of $SiCl_4$ in pentane at 25 ^{o}C for 1 h and used without purification.[13] Silicate ester **3.43** was obtained in relatively poor yield due to formation of undesired side products.

All target compounds were purified using column chromatography and fully characterized by analytical and spectroscopic techniques. Table 3.2 reports the isolated yields and melting points of target compounds. Detailed synthetic procedures are described in Chapter 7.

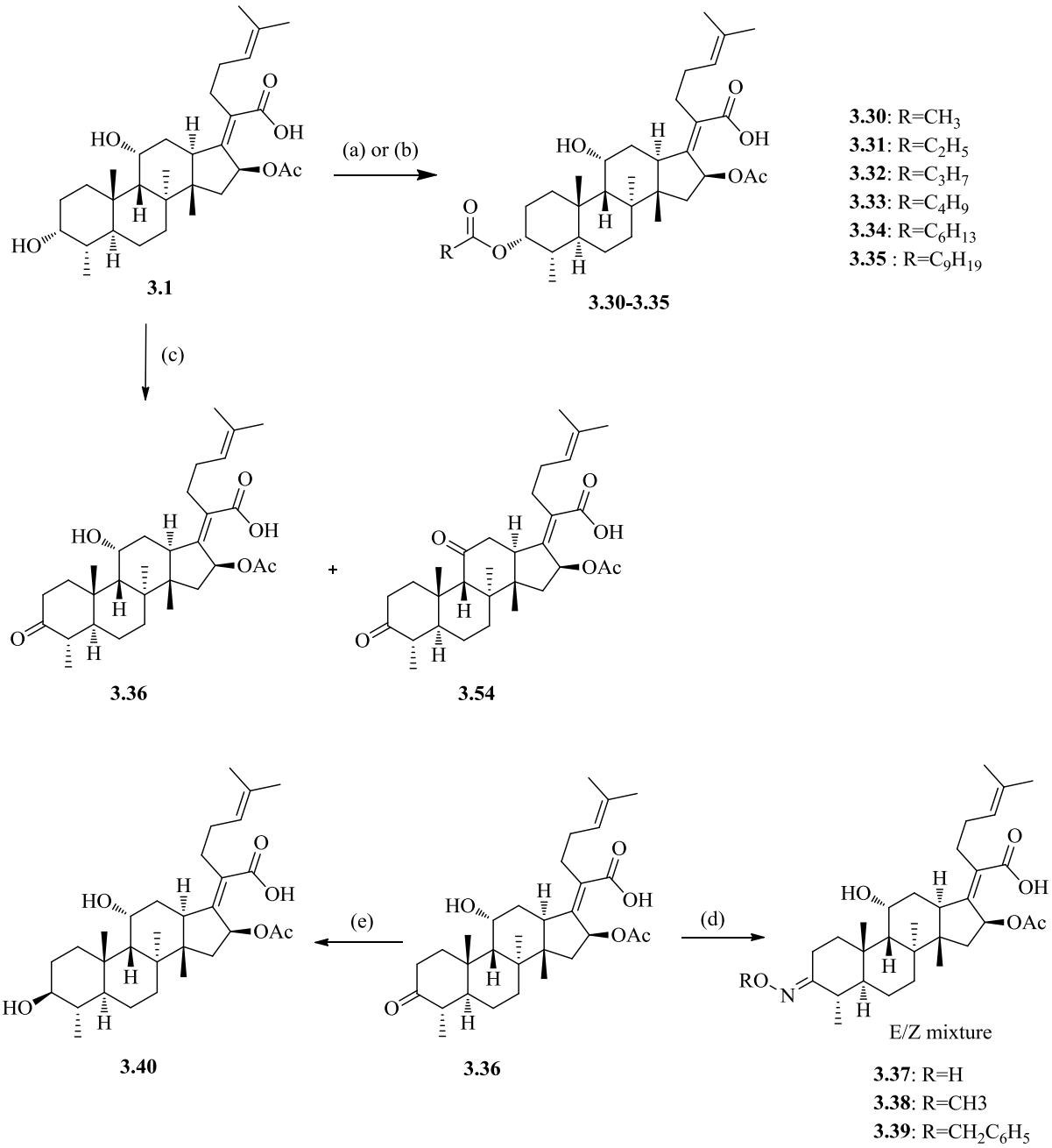

Scheme 3.4: *Reagents and conditions*: (a) $(RCO)_2O$, pyridine, 25 ^oC, 3 h for compounds **3.30** and **3.32**; (b) ROOH, T3P (50% w/v solution in DMF), pyridine, 0 ^oC – 25 ^oC, 16 h for compounds **3.31** and **3.33-3.35**; (c) Jones reagent, acetone, 0 ^oC, 40 min; (d) $RONH_2.HCl$, NH_4OAc, ethanol, MW, 80 ^oC, 20 min; (e) $NaBH_4$, methanol, 25 ^oC, 3 h

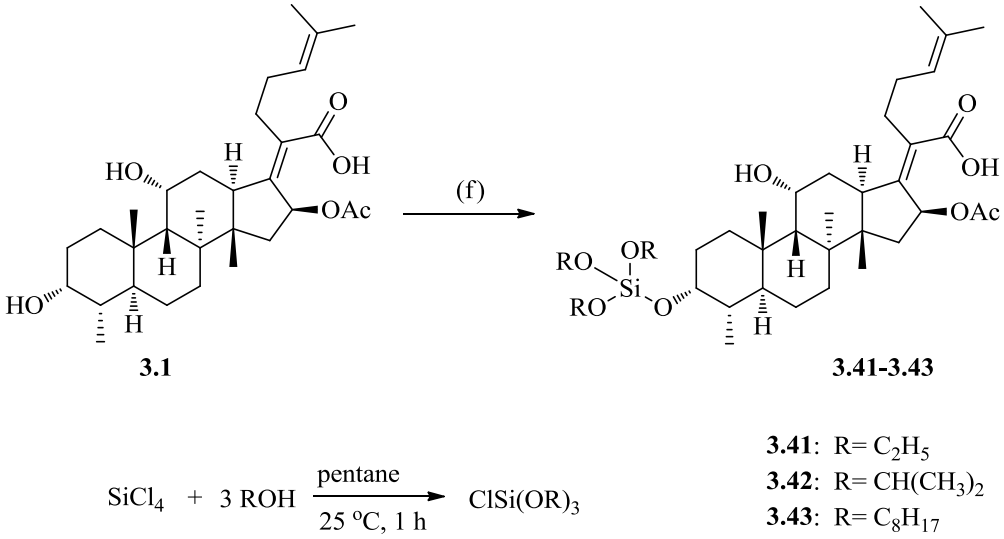

Scheme 3.5: *Reagents and conditions*: (f) $ClSi(OR)_3$, Imidazole, DMF, 0 ^oC, 1 h

Table 3.2: Isolated yields and melting points of C-3 derivatives

Compound	Yield (%)	Mp (^oC)
3.30	58	112-114
3.31	56	93-95
3.32	66	162-164
3.33	56	118-120
3.34	62	167-169
3.35	63	Oil
3.36	33	119-121
3.37	23	149-151
3.38	59	176-178
3.39	51	176-178
3.40	25	211-213
3.41	50	72-74
3.42	35	70-72
3.43	23	Oil

3.4.2.1 Characterization of C-3 derivatives

3.4.2.1.1 C-3 caboxylic esters

^{1}H and ^{13}C NMR spectra of C-3 carboxylic esters of fusidic acid can be described by using a representative compound **3.31** from this series. Compound **3.31** was prepared by reacting fusidic acid with propanoic acid in the presence of T3P and pyridine. The characteristic feature of the ^{1}H NMR spectrum is the downfield shift of the H-3 proton from 3.76 ppm (in fusidic acid) to 4.95 ppm (in **3.31**), indicating the successful coupling of propanoic acid to the C-3 OH of fusidic acid to form an ester bond. Additional peaks in the aliphatic region (highlighted in Figure 3.10) at 2.36 (q, J = 7.6 Hz, H-32) and 1.16 (t, J = 7.6 Hz, H-33) ppm indicated incorporation of an aliphatic chain in the structure of fusidic acid.

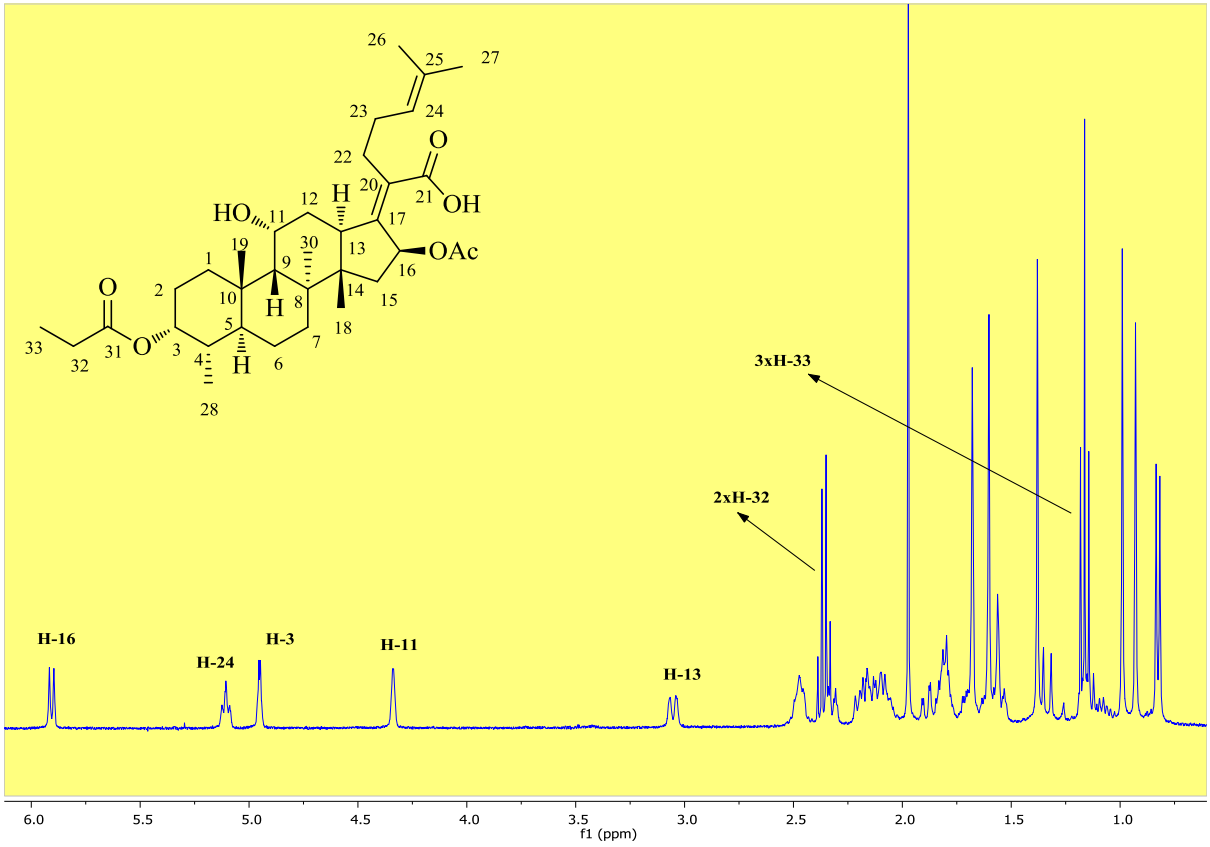

Figure 3.10: ^{1}H NMR spectrum ($CDCl_3$, 400 MHz) of compound **3.31**

Further, the appearance of an additional peak at 173.2 ppm in the ^{13}C NMR spectrum of **3.31** indicated the presence of an additional carbonyl group (C-31, Figure 3.11), while the appearance of two additional peaks in the aliphatic region at 27.4 ppm and 9.4 ppm indicated the presence of two additional aliphatic carbons (C-32 and C-33) in the structure. The spectral data was well supported by MS, which displayed mass peaks at 573 [M+1], 595 [M+23] and

513 [M-OAc]. On the basis of spectral data, structure **3.31** was assigned to this compound. All C-3 ester derivatives (**3.30-3.35**) displayed similar patterns in their ^{1}H, ^{13}C and MS spectra.

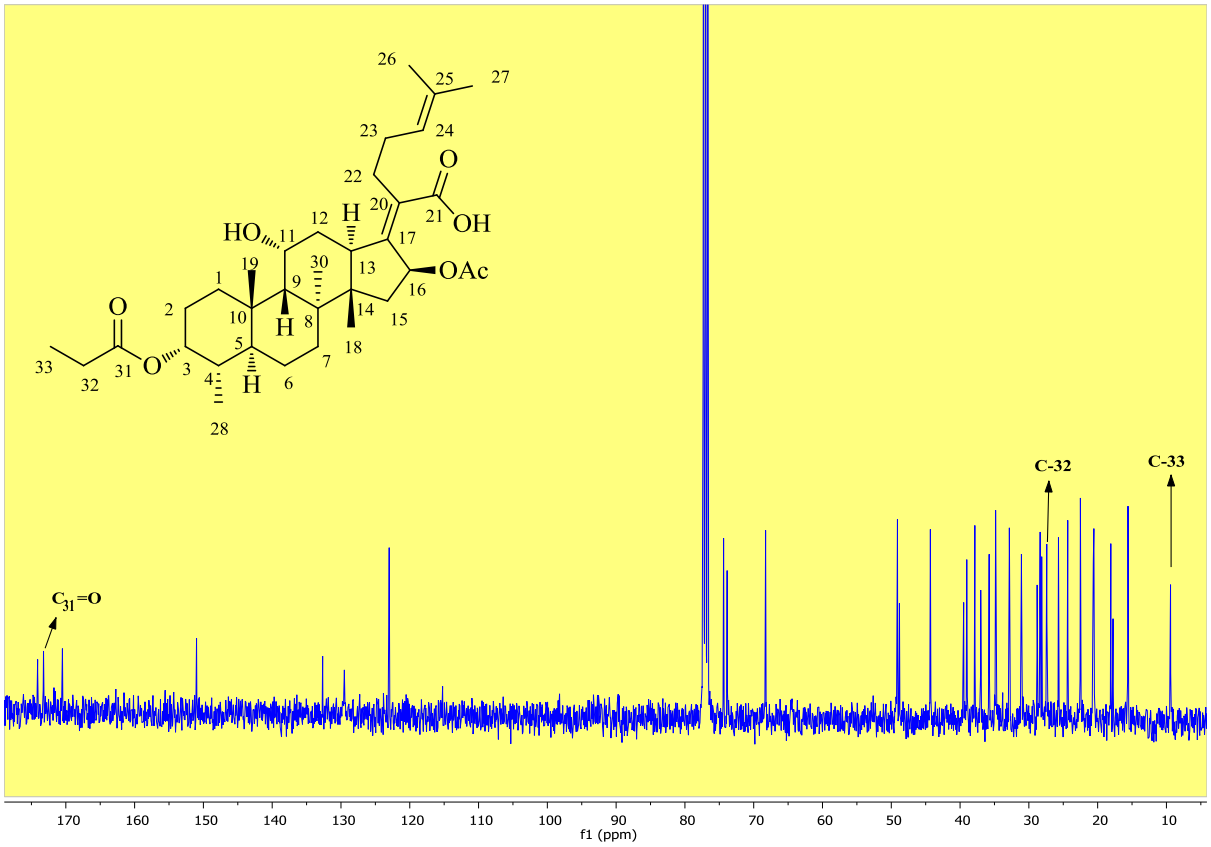

Figure 3.11: ^{13}C NMR spectrum ($CDCl_3$, 100 MHz) of compound **3.31**

3.4.2.1.2 C-3 oximes

C-3 oxime derivatives **3.37-3.39** were prepared by the coupling of 3-keto fusidic acid (**3.36**) with O-alkylhydroxylamines. The ^{1}H NMR spectrum of **3.38** (a member of this series) is described in Figure 3.12. The characteristic features of the ^{1}H spectrum are the disappearance of the H-3 proton of fusidic acid from 3.76 ppm and the appearance of a singlet at 3.82 ppm corresponding to =N-OCH_3, indicating the successful coupling of O-methylhydroxylamine with **3.36**. Formation of *E*/*Z* isomers is also observed in the ^{1}H spectrum as indicated by the splitting of singlet of =N-OCH_3.

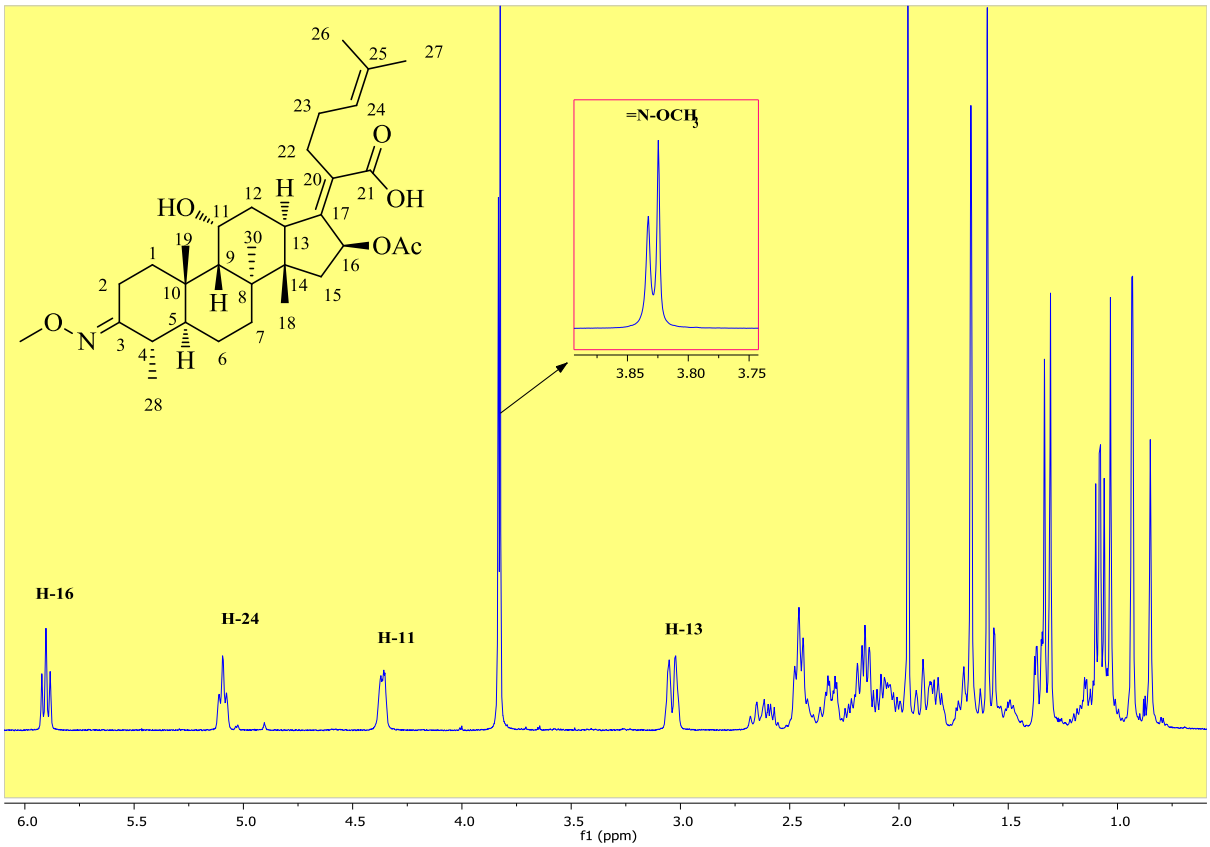

Figure 3.12: ^{1}H NMR spectrum ($CDCl_3$, 400 MHz) of compound **3.38**

The ^{1}H spectrum was well supported by the corresponding ^{13}C NMR spectrum (Figure 3.13). A shift in the C-3 signal from 71.4 ppm (in fusidic acid) to 161.9 (in **3.38)** and the appearance of an additional signal at 61.1 ppm, corresponding to the carbon of $=N\text{-}OCH_3$, was observed in the spectrum. Further, the MS of the compound displayed mass peaks at 544 [M+H], 566 [M+23] and 484 [M-OAc], as expected. On the basis of all spectral data obtained, the structure as depicted in **3.38** was assigned to this compound. Other members of the series (**3.37**, **3.39**) depicted similar patterns in their ^{1}H, ^{13}C and MS spectra.

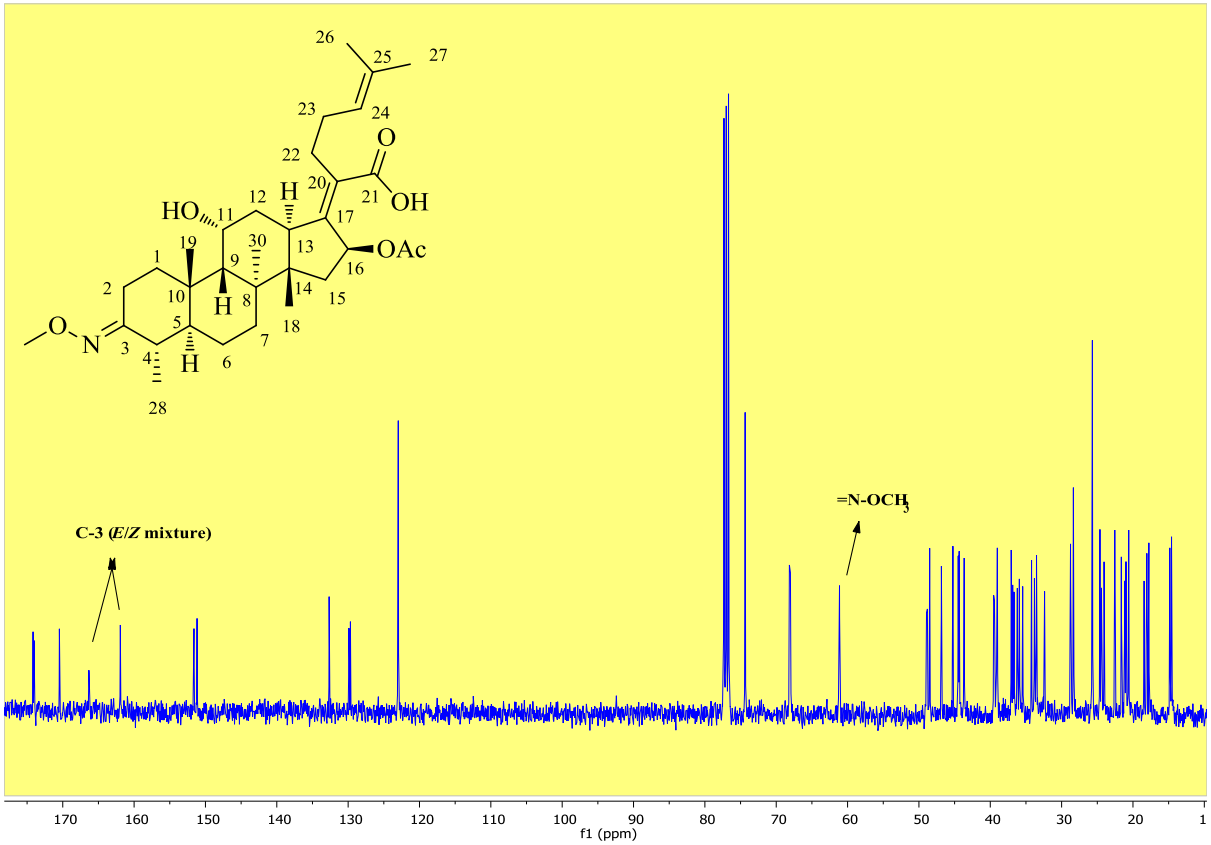

Figure 3.13: ^{13}C NMR spectrum ($CDCl_3$, 100 MHz) of compound **3.38**

3.4.2.1.3 C-3 silicates

The NMR spectra of C-3 silicates are described by using compound **3.42** as a representative from this series. The ^{1}H NMR spectrum of this compound was recorded in $CDCl_3$ at 400 MHz (Figure 3.14). The characteristic feature of the spectrum is the slight downfield shift of the H-3 proton from 3.76 ppm (in fusidic acid) to 3.99 ppm (in **3.42**), indicating the successful coupling of tripropoxychlorosilane with the C-3 OH of fusidic acid to form a silicate ester bond. The appearance of additional signals (highlighted in Figure 3.14) at 4.23 ppm (heptet of 3H due to the -CH of the isopropoxysilicate group, H-31) and 1.19 ppm (doublet of 18H due to the $-CH_3$ of the isopropoxysilicate group, H-32) indicated the successful incorporation of the triisopropoxysilicate moiety at the C-3 position of fusidic acid. All other protons showed a similar pattern to that observed for fusidic acid.

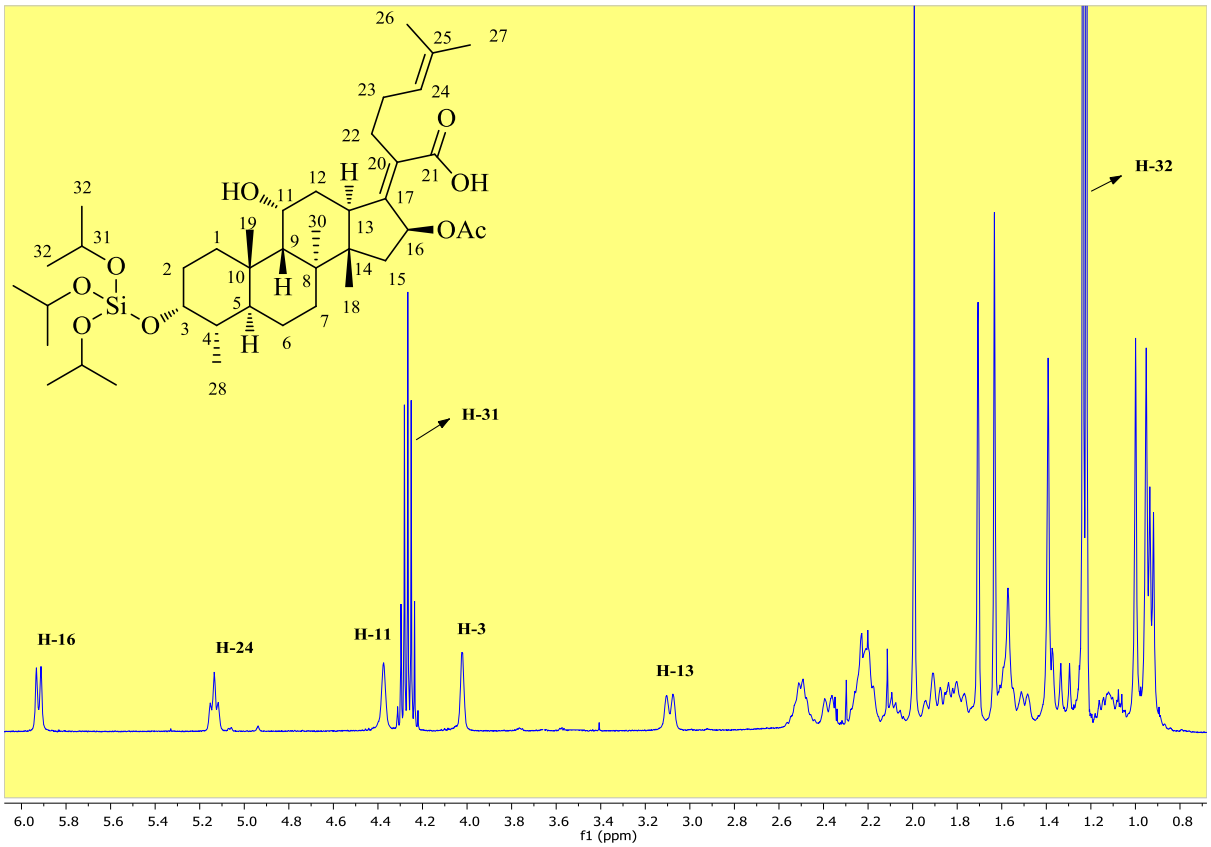

Figure 3.14: ^{1}H NMR spectrum ($CDCl_3$, 400 MHz) of compound **3.42**

The ^{1}H NMR spectrum was well supported by the corresponding ^{13}C NMR spectrum which depicted additional signals at 65.7 and 25.4 ppm, indicating three -CH carbons and six -CH_3 carbons of the isopropoxysilicate group (Figure 3.15). Further, the MS of the compound displayed mass peaks at 721 [M+1] and 661 [M-OAc], as expected. On the basis of spectral data obtained, structure **3.42** was assigned to this compound. Other silicate derivatives (**3.41**, **3.43**) depicted similar patterns in their ^{1}H, ^{13}C and MS spectra.

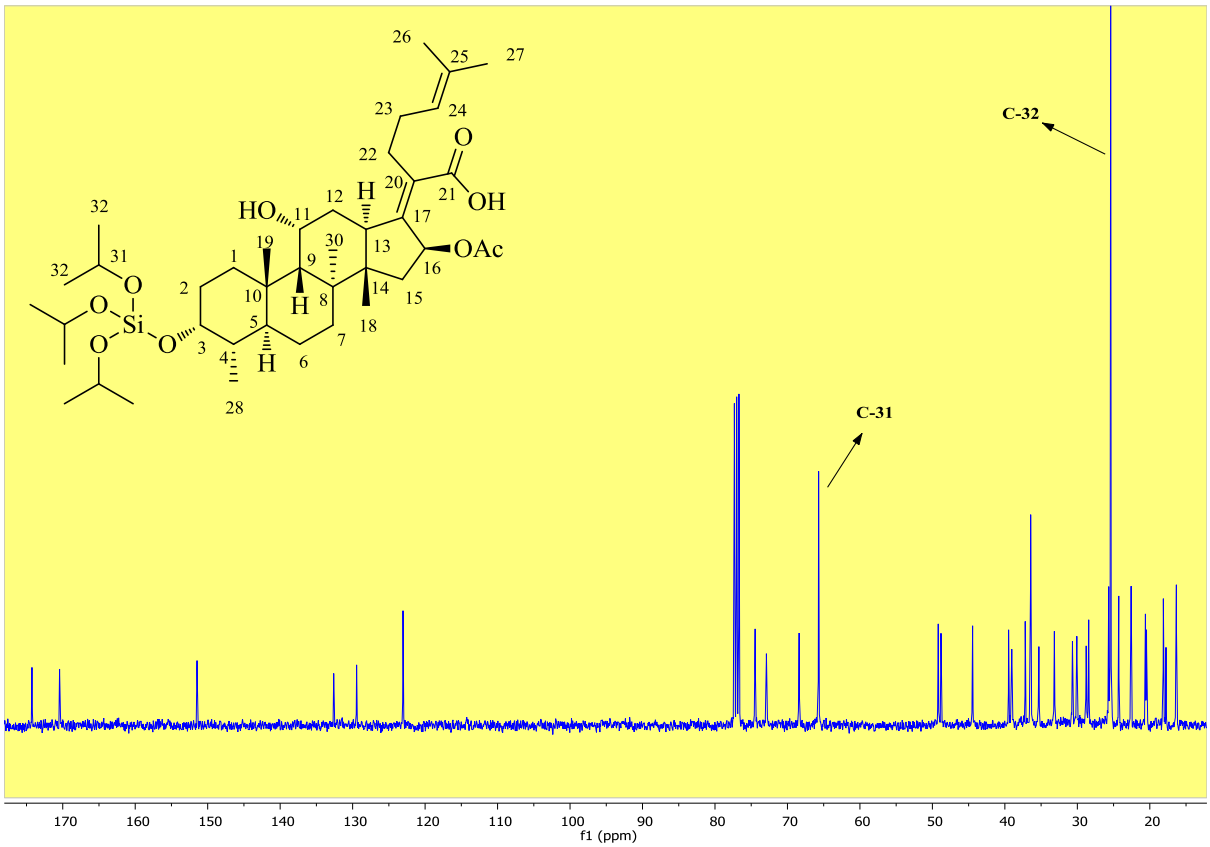

Figure 3.15: ^{13}C NMR spectrum ($CDCl_3$, 100 MHz) of compound **3.42**

3.4.3 Synthesis of C-16 fusidic acid derivatives (SAR 3)

C-16 derivatives of fusidic acid were synthesized as described in Scheme 3.6.[11,14] Synthesis commenced with protection of the C-3 OH group using acetic anhydride in pyridine to obtain the C-3 acetoxy derivative **3.30**. The C-16 acetoxy group was then selectively hydrolysed by heating **3.30** with saturated aq. $NaHCO_3$ under microwave irradiation at 100 ^oC to obtain intermediate **3.44** with inversion of configuration at C-16 (β-acetoxy to α-OH). The carboxylic group of **3.44** was then protected by reacting with chloromethyl pivalate to obtain pivaloyloxymethyl ester **3.45**, followed by bromination with CBr_4/PPh_3 to afford intermediate **3.46** with inversion of configuration (α-OH to β-bromo). The β-bromo intermediate **3.46** was converted to the α-bromo derivative **3.47** by stirring it with tetrabutylammonium bromide in acetonitrile at 25 ^oC for 65 h. Compound **3.47** was then reacted with the respective alcohols in the presence of Ag_2CO_3 to afford the C-16 ether derivatives which, upon hydrolysis with 5 N aq. NaOH, provided target compounds **3.48-3.49**. Intermediates as well as target compounds were purified using column chromatography and fully characterized by analytical and spectroscopic techniques. Table 3.3 reports the isolated yields and melting points of the intermediate and target compounds. Detailed synthetic procedures are described in Chapter 7.

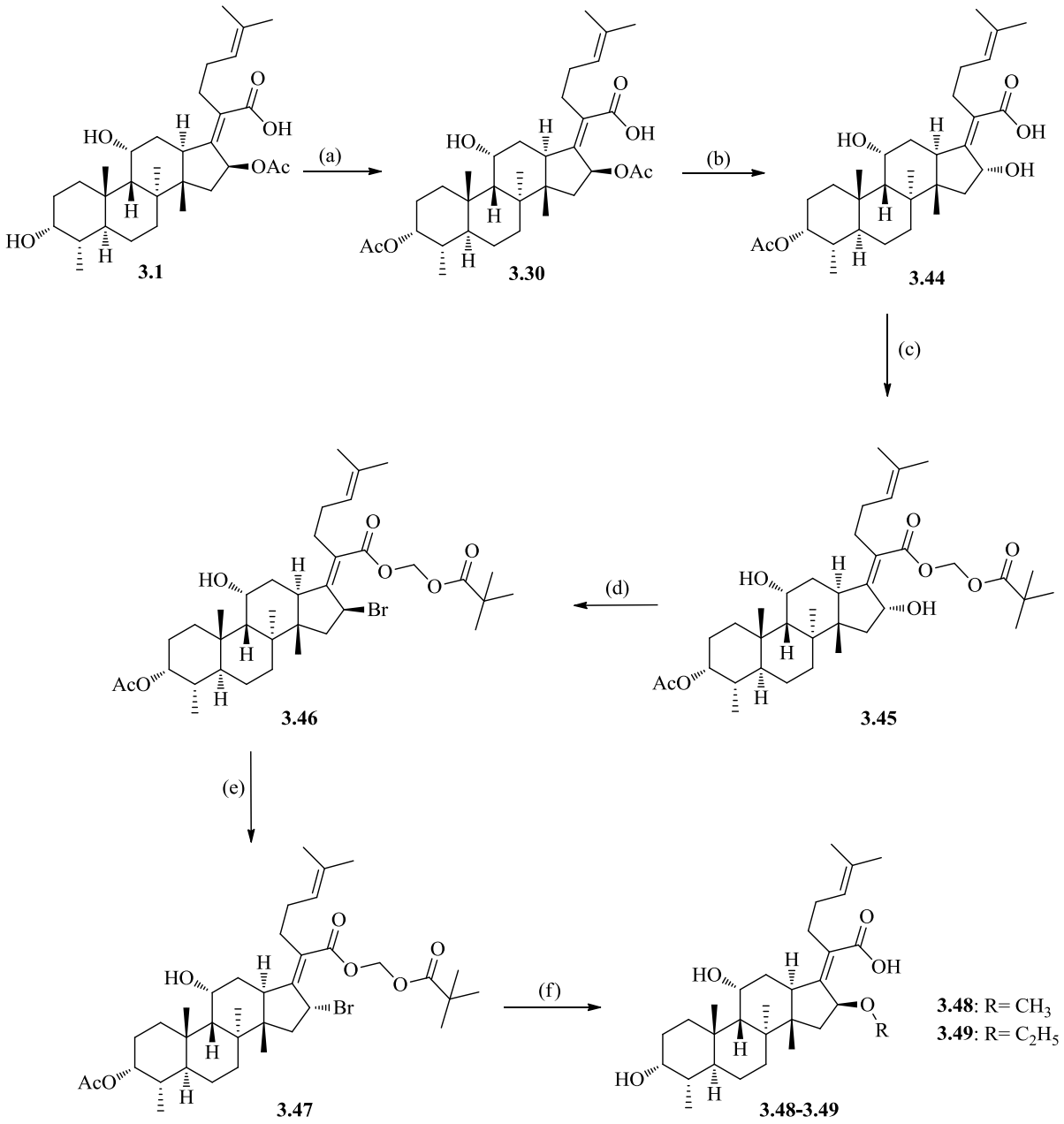

Scheme 3.6: *Reagents and conditions*: (a) $(Ac)_2O$, pyridine, 25 ^oC, 3 h; (b) Sat. aq.$NaHCO_3$, MW, 100 ^oC, 10 min; (c) $ClCH_2OCOC(CH_3)_3$, Et_3N, DMF, 25 ^oC, 16 h; (d) PPh_3, CBr_4, benzene, 25 ^oC, 1 h; (e) $Bu_4N^+Br^-$, acetonitrile, 25 ^oC, 65 h; (f) ROH, Ag_2CO_3, 25 ^oC, 16 h, 5 N aq. NaOH, 80 ^oC, 1 h

Table 3.3: Isolated yields and melting points of C-16 derivatives

Compound	Yield (%)	Mp (^{o}C)
3.44	37	ND
3.45	49	Oil
3.46	68	Oil
3.47	83	Oil
3.48	35	139-141
3.49	37	177-179

ND = Not determined

3.4.3.1 Characterisation of C-16 derivatives

The spectral data of C-16 derivatives can be explained by using the C-16 ethoxy derivative (**3.49**) as a representative example of the series. The characteristic feature of the ^{1}H NMR spectrum (Figure 3.16) is the upfield shift of H-16 from 5.88 ppm (in fusidic acid) to 4.45 ppm (in **3.49**) and the disappearance of the -OAc peak from 1.96 ppm. Further, the appearance of three additional peaks, two mutiplets of H-31 at 3.66-3.59 and 3.42-3.35 ppm and a triplet (J = 7.0 Hz) of H-32 at 1.20 ppm, confirmed the incorporation of the ethoxy group at the C-16 position.

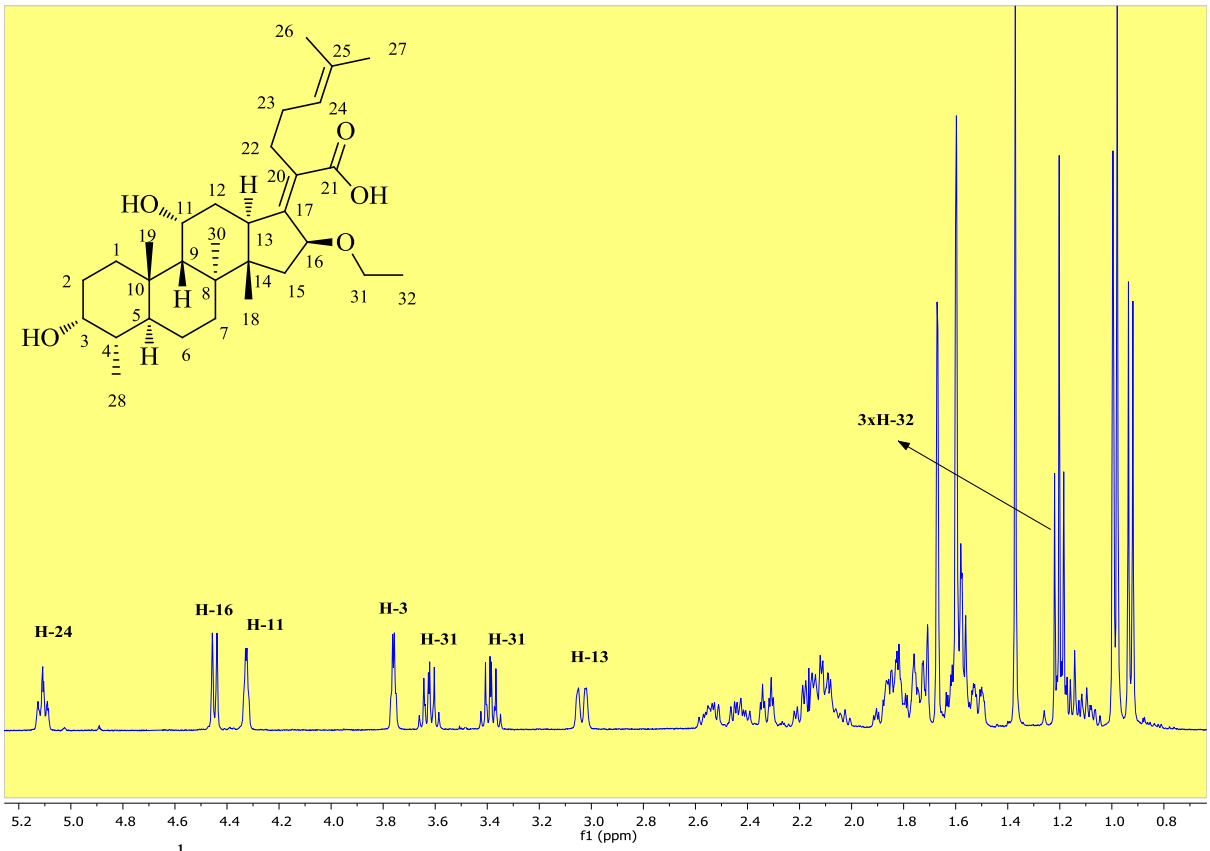

Figure 3.16: ^{1}H NMR spectrum ($CDCl_3$, 400 MHz) of compound **3.49**

The ^{1}H NMR spectrum was well supported by the corresponding ^{13}C NMR spectrum (Figure 3.17), which showed the disappearance of the C=O group of –OAc moiety from 170.6 ppm and the appearance of the C-31 of the ethoxy group at 80.6 ppm. Other carbon signals were found at their expected positions with minor shifts. Further, the MS of the compound displayed mass peaks at 503 [M+1] and 443 [M-OAc], as expected. On the basis of spectral data obtained, the structure **3.49** was assigned to this compound. The C-16 methoxy derivative **3.48** depicted a similar pattern in its ^{1}H, ^{13}C and MS spectra.

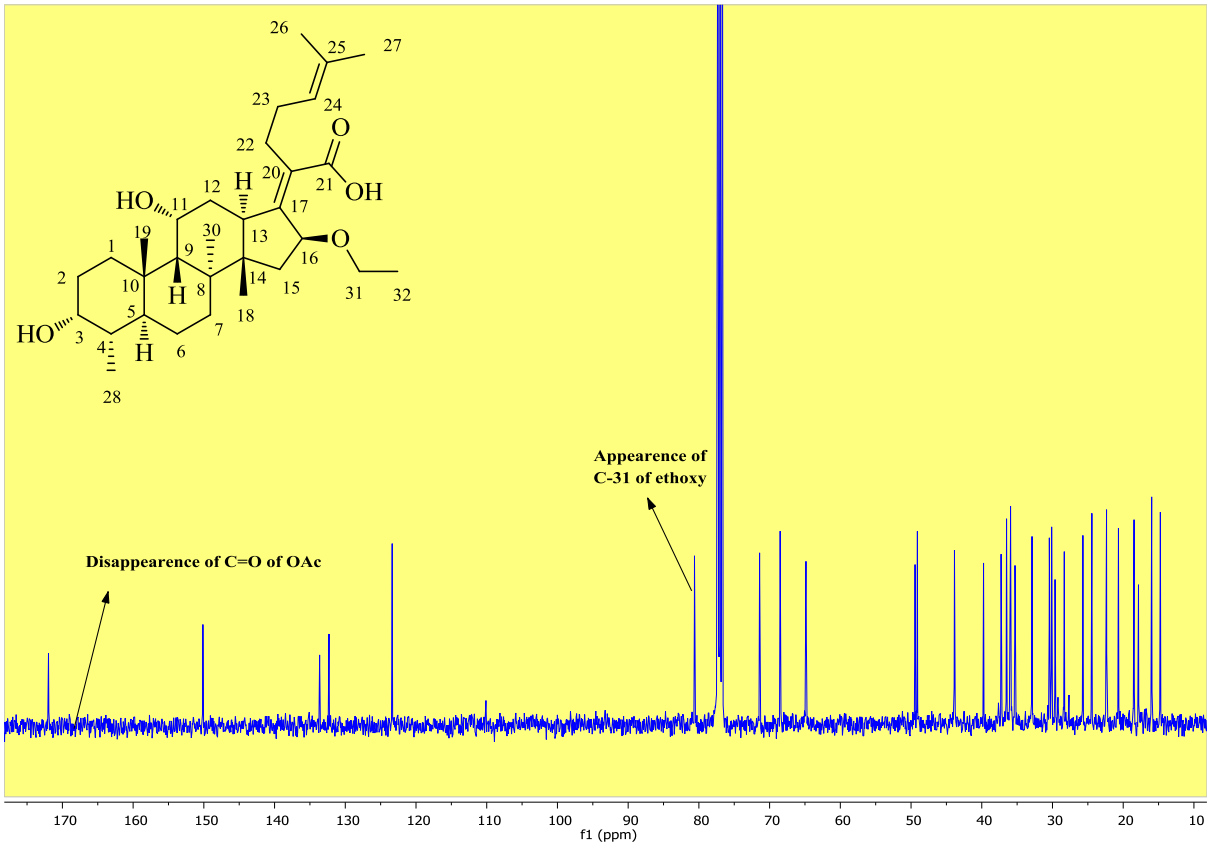

Figure 3.17: ^{13}C NMR spectrum ($CDCl_3$, 100 MHz) of compound **3.49**

3.4.4 Synthesis of miscellaneous derivatives

Some fusidic acid derivatives with modification at more than one site were also synthesized and included under the miscellaneous category (Scheme 3.7). Compound **3.50** was obtained by hydrogenation of the double bond between C-24 and C-25 of fusidic acid bioisostere **3.18** in the presence of H_2/Pd-C in ethanol. Compound **3.51** was obtained by hydrolysis of **3.18** in the presence of K_2CO_3 in methanol. Ozonolysis of fusidic acid (**3.1**) generated an aldehyde **3.52** and a ketone **3.53**.[15] C-3,C-11-diketo derivative **3.54**, which was obtained as a by-product during Jones oxidation of fusidic acid to generate 3-keto fusidic acid (Scheme 3.4), has also been included in the miscellaneous category. The derivative **3.55** was obtained by heating fusidic acid with acetic anhydride in the presence of pyridine under microwave irradiation at 80 ^oC. Further heating of **3.55** with methyl iodide at 50 ^oC in the presence of K_2CO_3 provided the methyl ester derivative **3.56**. Target compounds were purified using column chromatography and fully characterized by analytical and spectroscopic techniques. Table 3.4 reports the isolated yields and melting points of target compounds. Some of these derivatives were obtained in relatively poor yields either due to the formation of undesired

side products (**3.52** and **3.53**) or due to incomplete conversion of the starting material into product (**3.51**). Detailed synthetic procedures are described in Chapter 7.

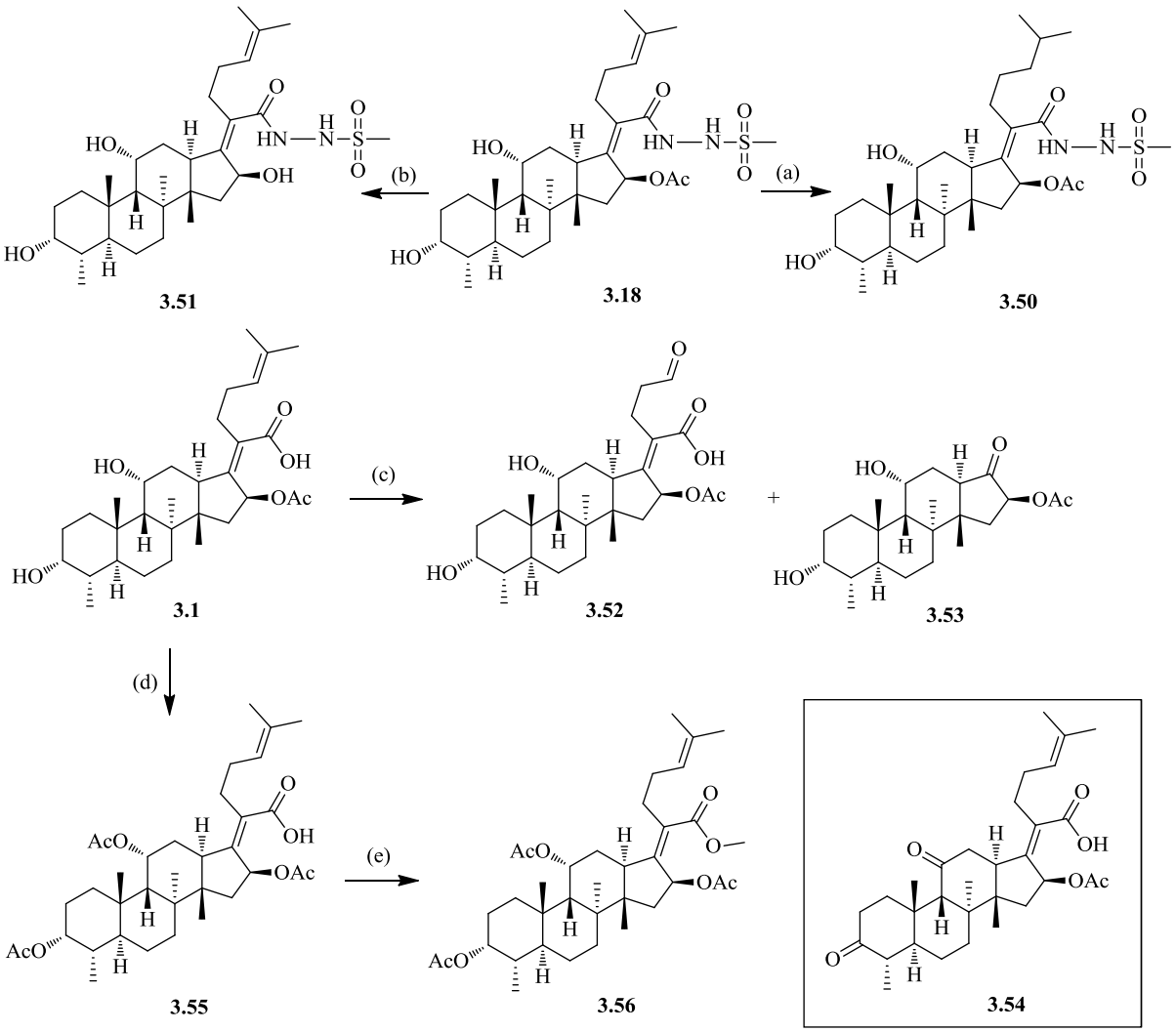

Scheme 3.7: *Reagents and conditions*: (a) H_2/Pd-C, ethanol, 25 ^oC, 16 h; (b) K_2CO_3, methanol, 25 ^oC, 24 h; (c) O_3/PPh_3, DCM, -78 ^oC to 25 ^oC, 2 h; (d) $(Ac)_2O$, pyridine, MW, 80 ^oC, 1.5 h; (e) K_2CO_3, CH_3I, DMF, 50 ^oC, 3 h

Table 3.4: Isolated yields and melting points of miscellaneous derivatives

Compound	Yield (%)	Mp (^{o}C)
3.50	58	198-200
3.51	22	169-171
3.52	27	237-239
3.53	26	92-94
3.54	45	192-194
3.55	35	305-307
3.56	72	259-261

3.4.4.1 Characterisation of miscellaneous derivatives

The ^{1}H and ^{13}C NMR spectra of one of the miscellaneous derivatives (compound **3.51)** are described below. The characteristic features of the ^{1}H NMR spectrum of **3.18** (Figure 3.18) are the appearance of two -NH protons at 7.79 ppm and 6.89 ppm, as well as the appearance of the -SO_2CH_3 signal at 3.00 ppm. These proton signals confirmed incorporation of the methyl sulfonyl hydrazide moiety into fusidic acid at the C-21 position.

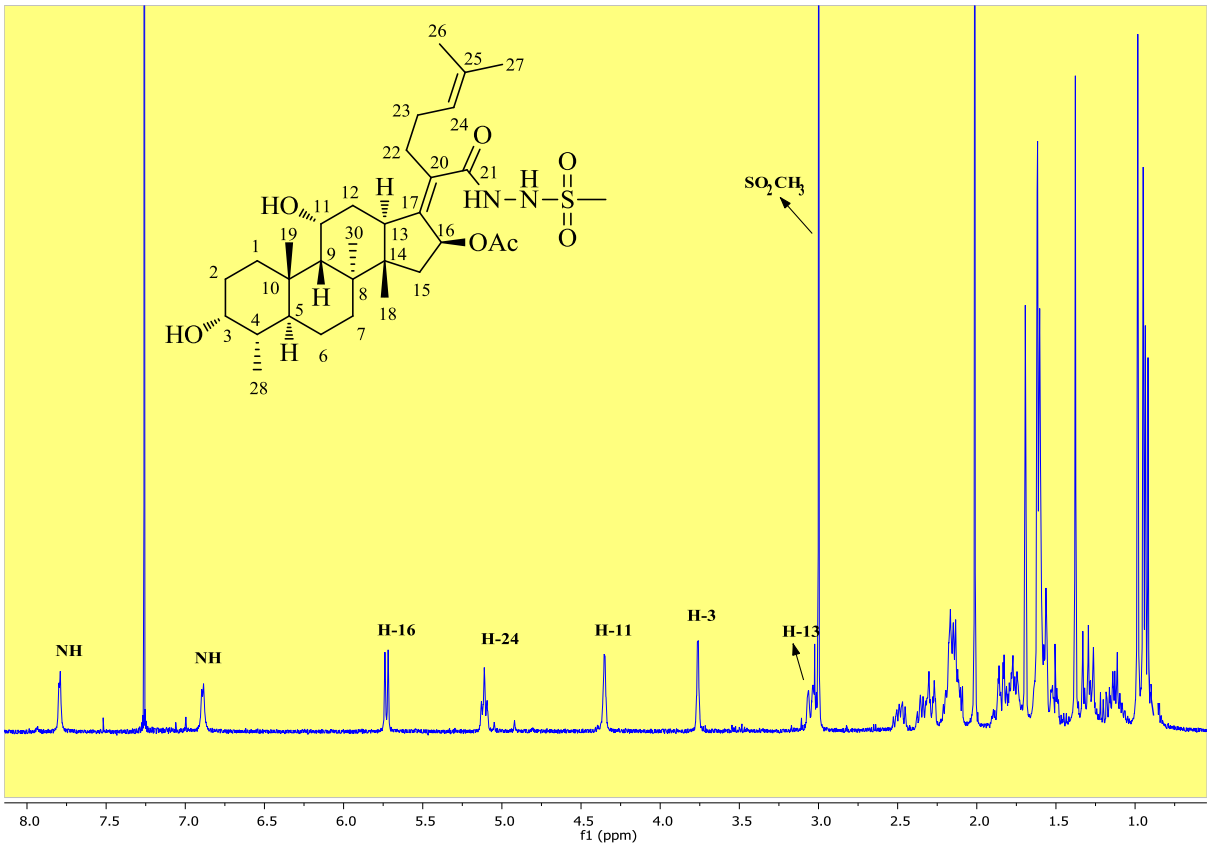

Figure 3.18: ^{1}H NMR spectrum ($CDCl_3$, 400 MHz) of compound **3.18**

The ^{1}H spectrum of **3.51** showed the disappearance of the -OAc signal from 2.01 ppm and an upfield shift of H-16 from 5.74 ppm (Figure 3.19).

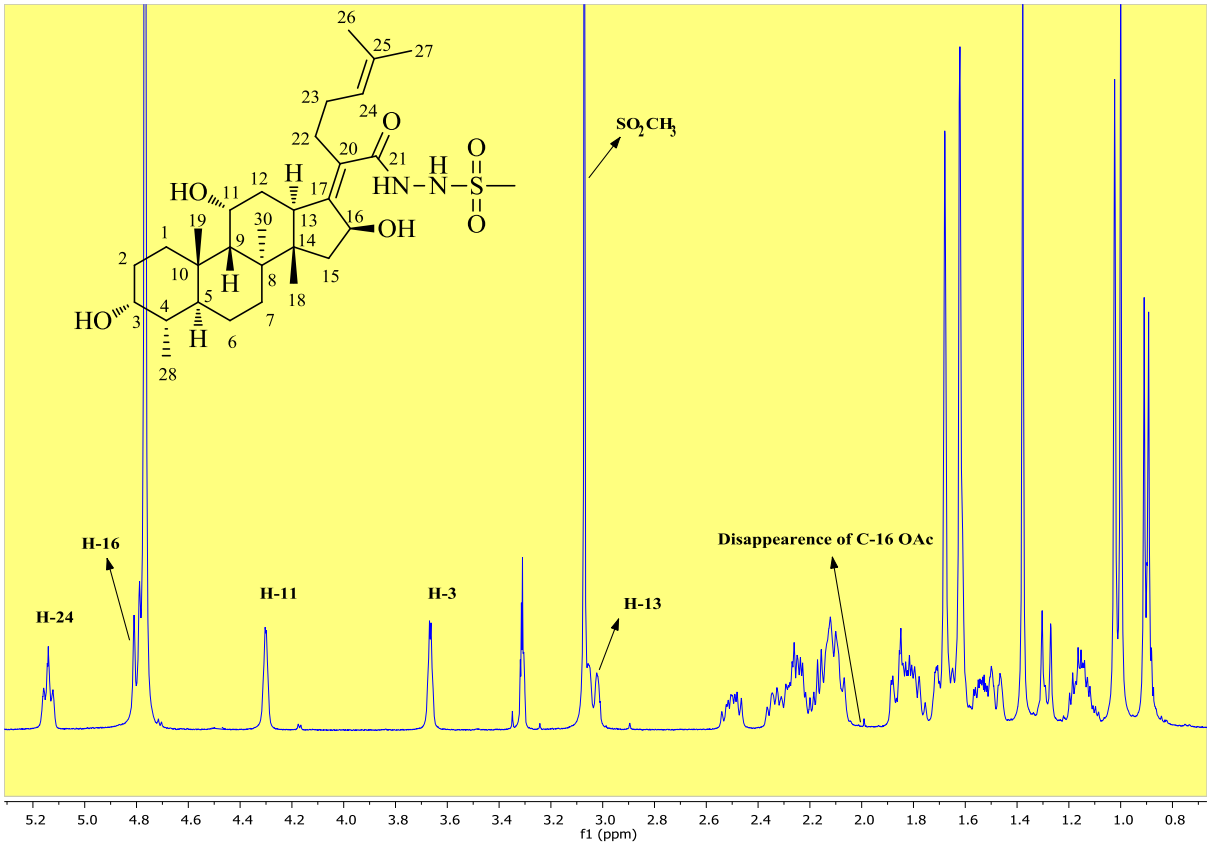

Figure 3.19: ^{1}H NMR spectrum (CD_3OD, 400 MHz) of compound **3.51**

The ^{1}H NMR spectrum was well supported by the corresponding ^{13}C NMR spectrum (Figure 3.20), which showed the disappearance of the C=O group of the -OAc moiety in the carbonyl region. Further, MS of the compound displayed mass peaks at 567 [M+1] and 507 [M-OAc], as expected. On the basis of the spectral data obtained, structure **3.51** was assigned to this compound.

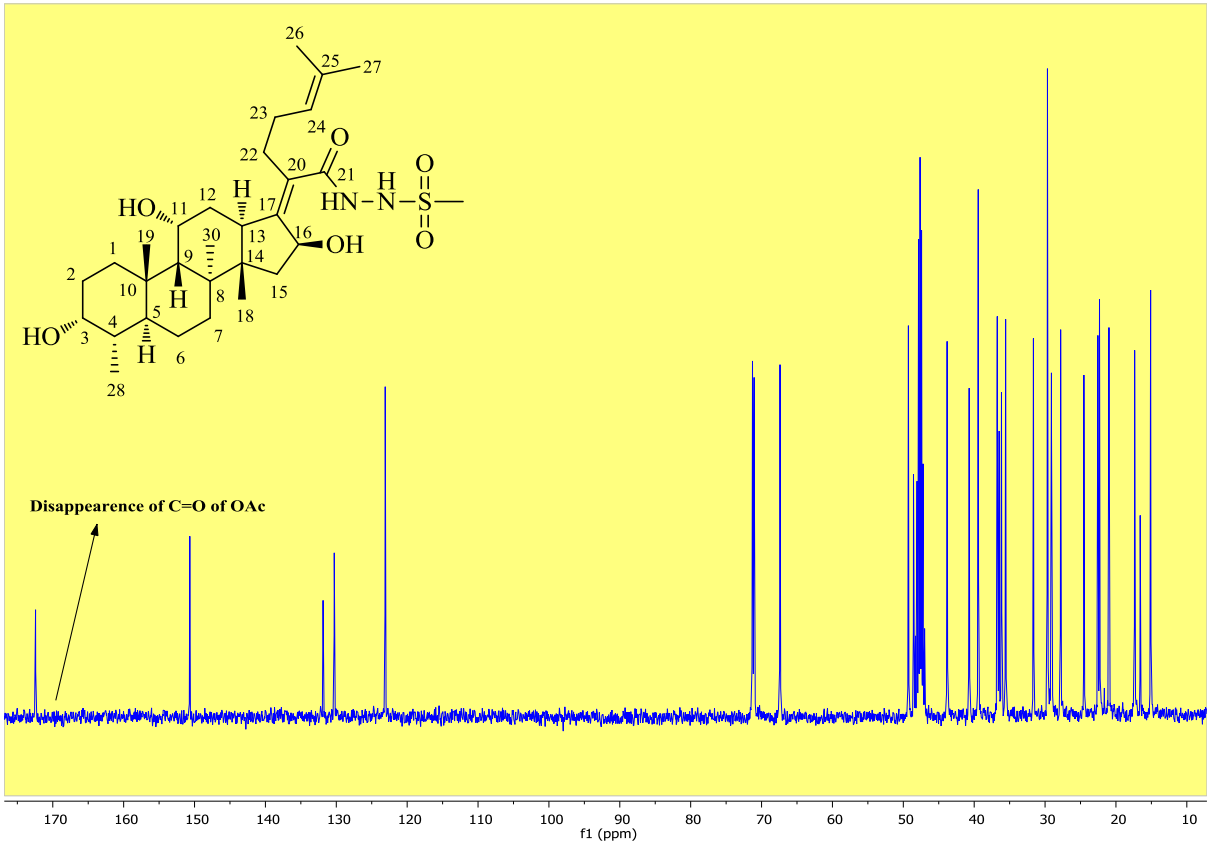

Figure 3.20: ^{13}C NMR spectrum (CD_3OD, 100 MHz) of compound **3.51**

3.5 Biological results and discussion

Synthesized derivatives were screened *in vitro* against the H37Rv strain of *Mtb* at the Institute of Infectious Diseases and Molecular Medicine (IDM), University of Cape Town, South Africa. The MIC_{99} (minimum concentration required to inhibit the growth of 99% of the bacterial population) was determined for each compound and a maximum concentration limit was set at 160 µM. Rifampicin and kanamycin, were used as reference drugs. These derivatives were also evaluated for cytotoxicity against the Chinese Hamster Ovarian (CHO) mammalian cell line, and their half minimal inhibitory concentration (IC_{50}) was determined. Emetine was used as reference drug in this assay.

In vitro antiplamodial activities (IC_{50}) were determined against the chloroquine (CQ)-sensitive NF54 strain of *P. falciparum* at the Swiss Tropical and Public Health Institute, Basel, Switzerland. CQ and artesunate were used as the reference drugs.

3.5.1 C-21 fusidic acid derivatives

3.5.1.1 Antimycobacterial activity

The antimycobacterial activity (MIC_{99}) of fusidic acid (**3.1**) was found to be 0.6 μM (Table 3.5). All fusidic acid bioisosteres exhibited poor antimycobacterial activity as compared to fusidic acid, with MIC_{99} values ranging from 10 to >160 μM (Table 3.5).

The effect of acyclic bioisosteric replacement of the carboxylic acid group was investigated through derivatives **3.2**-**3.23**. Replacing the -COOH group with $-COOCH_3$ and $-CONH_2$ groups (**3.2**-**3.3**, MIC_{99} >160 μM) diminished the activity. Most of the substituted amide derivatives (**3.4**-**3.9**, Table 3.5) showed improved activity as compared to the unsubstituted amide derivative **3.3** but were found to be far less active as compared to fusidic acid. Among sulfonamide derivatives (**3.10**-**3.12**), alkyl (**3.10**) and unsubstituted aromatic (**3.11**) derivatives were found to be either poorly active or inactive at the highest concentration tested. The substitution of the phenyl ring in **3.11** restored the activity and the resulting 3,4-difluorophenylsulfonamide derivative **3.12** was found to be the most active among amide and sulphonamide derivatives, displaying antimycobacterial activity with a MIC_{99} value of 20 μM. Among hydrazide derivatives (**3.13**-**3.17**), compound **3.15**, which is a conjugate of fusidic acid and the antituberculosis drug isoniazid, was found to be the most active, displaying a MIC_{99} value of 10 μM with encouraging cytotoxicity (IC_{50} CHO 88.3 μM). Two more hydrazide derivatives **3.16** and **3.17** containing N-pyridin-3-ylmethylene and N-pyridin-4-ylmethylene group, respectively, also showed an improvement in antimycobacterial activity (MIC_{99} of 20 μM). Among the sulfonylhydrazide derivatives (**3.18**-**3.23**), aromatic derivatives (**3.22**-**3.23**) were found to be inactive as compared to aliphatic derivatives (**3.18**-**3.21**). Further, among aliphatic derivatives, activity decreased with an increase in the carbon chain length from methyl (**3.18**, MIC_{99} 10 μM) to butyl (**3.21**, MIC_{99} 160 μM). The methane sulfonyl hydrazide derivative **3.18** was found to be the most active, displaying a MIC_{99} value of 10 μM with encouraging cytotoxicity at IC_{50} 92.2 μM.

Replacement of the carboxylic acid group of fusidic acid with less acidic and similar molecular-size cyclic bioisosteres, such as an oxadiazole, was also explored. Oxadiazole rings can exist in three regioisomeric forms; 1,2,4-oxadiazoles, 1,3,4-oxadiazoles and 1,2,5-oxadiazoles, the first two being the most common and recurrent motifs in drug-like molecules. However, these two isomeric forms offer different physiochemical profiles in terms of lipophilicity, aqueous solubility, metabolic stability and, hERG activity, thereby

resulting in diverse biological activities.[16] Five oxadiazole bioisosteres were synthesized and included the 1,2,4-oxadiazole derivatives **3.24-3.27**, the 5-oxo-1,3,4-oxadiazole derivative **3.28** and the 5-thioxo-1,3,4-oxadiazole derivative **3.29**. However, all of these derivatives were found to be either poorly active or inactive.

In summary, bioisosteric replacement of the carboxylic acid group of fusidic acid resulted in poor antimycobacterial activity as compared to fusidic acid. However, two compounds **3.15** and **3.18** showed moderate activity (MIC_{99} 10 µM) and reasonably low cytotoxicity (IC_{50} 88.3 µM and 92.2 µM, respectively).

Table 3.5: *In vitro* antimycobacterial activity (H37Rv strain), antiplasmodial activity (NF54 strain) and cytotoxicity (CHO cell line) of C-21 fusidic acid bioisosteres

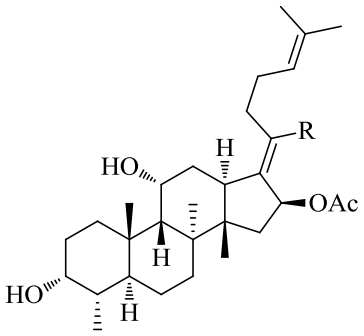

Compound	R	MIC_{99} H37Rv (µM)	IC_{50} NF54 (µM)	IC_{50} CHO (µM)
3.1		0.6	59.0	>194.0
3.2		>160	4.7	ND
3.3		>160	35.9	113.0
3.4		40	10.8	>185.0
3.5	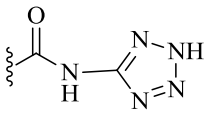	40	>15	>171.0
3.6	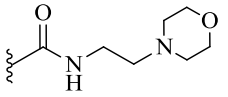	>160	11.9	ND
3.7	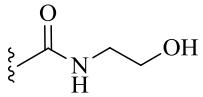	>160	>18	ND
3.8	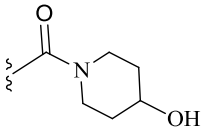	40	3.0	ND

3.9	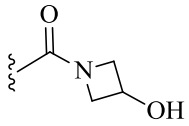	40	10.5	ND
3.10	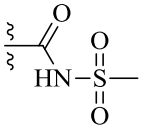	80	>15	>169.0
3.11	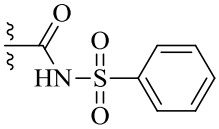	>160	>15	96.1
3.12	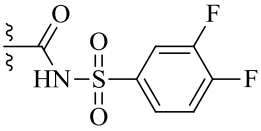	20	7.3	81.4
3.13		40	21.3	112.0
3.14	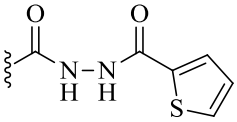	40	8.4	78.8
3.15	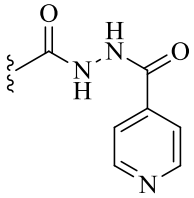	10	3.2	88.3
3.16	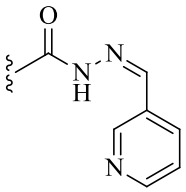	20	8.4	ND
3.17	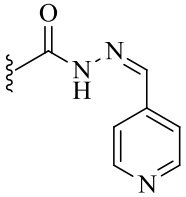	20	2.0	ND
3.18	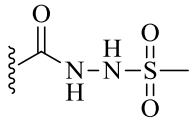	10	14.7	92.2
3.19	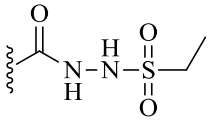	40	12.4	77.3
3.20	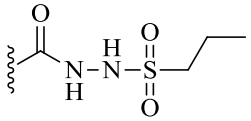	40	5.7	79.7
3.21	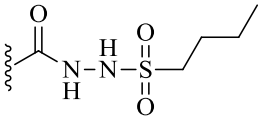	160	8.0	49.9

3.22	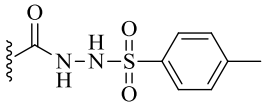	>160	13.4	48.2
3.23	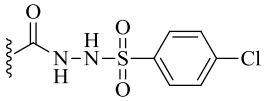	>160	31.3	53.2
3.24	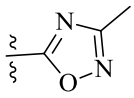	>160	3.8	47.8
3.25	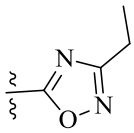	>160	1.9	71.7
3.26	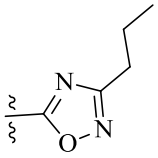	80	2.1	68.2
3.27	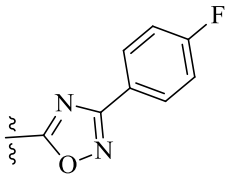	>160	1.7	77.4
3.28	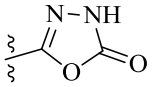	80	9.2	82.0
3.29	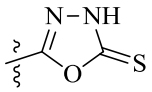	80	7.0	70.0
	Rifampicin	0.005		
	Kanamycin	3.2		
	CQ		16 nM	
	Artesunate		4 nM	
	Emetine			0.4

CQ = chloroquine; ND = Not determined

3.5.1.2 Antiplasmodial activity

The IC_{50} value of fusidic acid (**3.1**) against the NF54 strain of *P. falciparum* was found to be 59 µM, which is comparable to that reported for the D10 strain (52.8 µM). Most of the fusidic acid bioisosteres exhibited micromolar potencies, with 24 out of the 28 compounds displaying IC_{50} values between 1.7-35.9 µM.[7] Additionally, these derivatives were found to have low cytotoxicity against the CHO cell line.

Replacing the carboxylic acid group with a methyl ester augmented the antiplasmodial activity by 12-fold (**3.2**, IC_{50} 4.7 µM). Among amide derivatives, unsubstituted amide

derivative **3.3** exhibited a 2-fold increase in activity (IC_{50} 35.9 μM) compared to fusidic acid (Table 3.5). Substitution with an amide group brought improvement in antiplasmodial activity in most of the derivatives with 4-hydroxy piperidine amide (**3.8**, IC_{50} 3.0 μM) being the most active. Among the sulfonamide derivatives (**3.10**-**3.12**), alkyl (**3.10**) and unsubstituted aromatic (**3.11**) derivatives were found to be inactive at the highest concentration tested (>15 μM). On the other hand, substitution of the phenyl ring restored the activity as demonstrated by the 3,4-difluorophenylsulfonamide derivative **3.12** (IC_{50} 7.3 μM), displaying an 8-fold increase in activity compared to fusidic acid.

Among the hydrazide and sulfonyl hydrazide derivatives (**3.13**-**3.23**), substituted derivatives (**3.14**-**3.23**) demonstrated superior activity compared to the unsubstituted derivative **3.13**, with the exception of compound **3.23**, which displayed inferior antimycobacterial activity to **3.13**. Further, among sulfonylhydrazides, the antiplasmodial activity of the aliphatic derivatives (**3.14**-**3.21**) increased from 14.7 μM to 5.7 μM, which coincided with an increase in carbon chain length from methyl to propyl. This activity then decreased with insertion of one more -CH_2- spacer or due to substitution with an aromatic ring. The N-pyridin-4-ylmethylene fusidic acid hydrazide **3.17** was found to be the most active (IC_{50} 2.0 μM) among all the hydrazide derivatives and demonstrated a 29-fold increase in activity compared to fusidic acid.

Among cyclic bioisosteres, 1,2,4-oxadiazole derivatives **3.24**-**3.27** substituted at the 3-position with aliphatic and aromatic substituents displayed superior antiplasmodial activity (15-35 fold higher) relative to fusidic acid. Introduction of a 4-fluorophenyl group at the 3-position of the 1,2,4-oxadiazole ring (**3.19**, IC_{50} 1.7 μM) conferred a 35-fold increase in activity. Two other cyclic bioisosteres, the 5-oxo-1,3,4-oxadiazole derivative **3.20** (IC_{50} 9.2 μM) and its thio analogue **3.21** (IC_{50} 7.0 μM), also showed improvement in antiplasmodial activity by 6- and 8-fold, respectively, but were found to be less active than 1,2,4-oxadiazole derivatives.

In summary, bioisosteric replacement of the carboxylic acid group of fusidic acid led to a 2-35 fold increase in antiplasmodial activity, and the best activity was observed with 1,2,4-oxadiazoles.

Overall, the decreased *in vitro* antimycobacterial activity of C-21 derivatives on replacement of the carboxylic acid group of fusidic acid with other moieties suggests that the free carboxylic group is essential for antimycobacterial activity. This is consistent with its antibacterial activity where a free carboxylic acid is reported to be essential.[4] On the other hand, the improved antiplasmodial activity suggests that the free carboxylic acid is not essential for antiplasmodial activity.

3.5.2 C-3 fusidic acid derivatives

3.5.2.1 Antimycobacterial activity

A total of fourteen C-3 derivatives of fusidic acid were evaluated against the H37Rv strain of *Mtb* (Table 3.6). Most of the derivatives displayed antimycobacterial activity at concentrations ≤ 20 μM. Nine out of 14 derivatives displayed activity at concentrations ≤ 5 μM.

C-3 carboxylic esters were synthesized by reacting fusidic acid with aliphatic carboxylic acids with short, medium and long alkyl carbon chains (**3.30-3.35**). C-3 acetoxy fusidic acid (**3.30**), the shortest carbon chain ester derivative, exhibited moderate activity (MIC_{99} 20 μM). As the carbon chain length was increased beyond this, the antimycobacterial activity was found to improve up to a certain chain length (**3.30-3.32**) and then decreased with further increase in chain length (**3.33-3.35**). The C-3 butyrate derivative **3.32** was found to be the most active and non-cytotoxic, displaying antimycobacterial activity with a MIC_{99} value of 1.25 μM and cytotoxicity with an IC_{50} value of 170 μM. C-3 propionate (**3.31**), pentanoate (**3.33**) and heptanoate (**3.34**) derivatives also displayed good activities with MIC_{99} values of 2.5 μM, 2.5 μM and 5 μM, respectively. Derivatives **3.33** and **3.34** were also evaluated for cytotoxicity and were found to have low cytotoxicity (Table 3.6). The long carbon chain ester, the decanoate derivative **3.35**, was found to be inactive suggesting that a long carbon chain is not tolerated.

C-3 oximes were synthesized by reacting 3-keto fusidic acid (**3.36**) with various hydroxyl amines. Among these derivatives, 3-keto fusidic acid was found to be the most active with a MIC_{99} value of 1.25 μM (Table 3.6). The unsubstituted 3-oxime derivative **3.37** also exhibited good antimycobacterial activity with a MIC_{99} value of 2.5 μM. However, substituted oximes: 3-O-methyl oxime **3.38** (MIC_{99} 20 μM) and 3-O-benzyl oxime **3.39** (MIC_{99} 40 μM), showed inferior activity. The active derivatives, **3.36** and **3.37**, were also

evaluated for cytotoxicity against the CHO cell line and were found to be non-cytotoxic. 3-Epifusidic acid (**3.40**, with inversion of configuration at C-3 OH group) was also investigated and was found to be far less active (MIC_{99} 11.4 μM) as compared to fusidic acid (MIC_{99} 0.6 μM), suggesting that inversion of stereochemistry at the C-3 position of fusidic acid reduces the antimycobacterial activity significantly. However, the presence of a double bond at the C-3 position is well tolerated, as demonstrated by the antimycobacterial activities of 3- keto (**3.36**) and unsubstituted 3-oxime derivatives (**3.37**).

Silicate esters of fusidic acid were synthesized based on the prodrug approach. It was hypothesized that these derivatives would revert back to fusidic acid through hydrolysis. Moreover, orthosilicic acid [$Si(OH)_4$], the eventual stoichiometric by-product of silicate ester cleavage, is not associated with any significant toxicity as indicated by a number of studies.[17–19] Two out of three silicate esters, triethoxy silicate ester **3.41** and trioctyloxy silicate ester **3.43**, exhibited antimycobacterial activity comparable to fusidic acid, displaying MIC_{99} values of 0.2 and 0.3 μM, respectively. Triisopropoxy silicate ester **3.42** exhibited relatively lower activity (MIC_{99} 2.5 μM) compared to the above silicate derivatives. An increase in *in vitro* antimycobacterial activity of silicate esters may also be attributed to the hydrophobic nature of these compounds, which facilitates penetration through *Mtb* cell wall. Further, all these silicate esters were found to be relatively non-cytotoxic against the CHO cell line (Table 3.6).

3.5.2.2 Antiplasmodial activity

Most of the C-3 derivatives exhibited better antiplasmodial activity than fusidic acid (Table 3.6). C-3 carboxylic esters exhibited variable antiplasmodial activity ranging from 6.6-56 μM. The activity was found to increase with an increase in the carbon chain length and the decanoate derivative (**3.35**, MIC_{99} 6.6 μM) was found to be the most active showing a 9-fold increase in antiplasmodial activity compared to fusidic acid (MIC_{99} 59 μM).

A similar trend was observed with C-3 oxime derivatives where antiplasmodial activity improved with increase in lipophilicity from unsubstituted oxime (**3.37**, IC_{50} > 19 μM) to 3-O-benzyl oxime (**3.39**, IC_{50} 3.4 μM). Conversion of the C-3 OH group of fusidic acid to the corresponding C-3 keto derivative (**3.36**, IC_{50} 8.2 μM) resulted in a 7-fold increase in activity. 3-Epi fusidic acid (**3.40**) also resulted in a 1.8-fold improvement in activity. This suggests that the orientation of C-3 OH group has little effect on antiplasmodial activity. This is in

contrast to antimycobacterial activity, which was found to decrease with inversion of the C-3 OH configuration.

Among silicates, triisopropoxy silicate **3.42** displayed better antiplasmodial activity compared to the other two silicate derivatives (Table 3.6).

In summary, C-3 derivatives were obtained by substitution of the C-3 OH group with various moieties such as esters, oximes and silicates. These C-3 derivatives exhibited better antimycobacterial activity as compared to C-21 derivatives, with 9 out of 14 derivatives displaying $MIC_{99} \leq 5$ μM. Further, these derivatives also showed improved antiplasmodial activity which, as with C-21 derivatives, was found to increase with lipophilicity. The *in vitro* antimycobacterial and antiplasmodial results obtained for 3-epifusidic acid (**3.40**) suggest that inversion of configuration at the C-3 position may significantly reduce the antimycobacterial activity, but this has little effect on antiplasmodial activity. However, a double bond at the C-3 position is well tolerated.

Table 3.6: *In vitro* antimycobacterial activity (H37Rv strain), antiplasmodial activity (NF54 strain) and cytotoxicity (CHO cell line) of C-3 fusidic acid derivatives

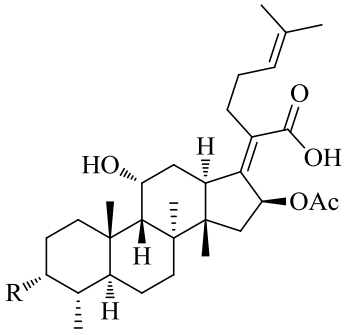

Compound	R	MIC_{99} H37Rv (µM)	IC_{50} NF54 (µM)	IC_{50} CHO (µM)
3.1	—OH	0.6	59.0	>194.0
3.30	—$OCOCH_3$	20	56	ND
3.31	—$OCOC_2H_5$	2.5	19	ND
3.32	—$OCOC_3H_7$	1.25	14.9	170
3.33	—$OCOC_4H_9$	2.5	7.5	74.4
3.34	—$OCOC_6H_{13}$	5.0	7.9	36.2
3.35	—$OCOC_9H_{19}$	>160	6.6	ND
3.36	=O	1.25	8.2	>194
3.37	=N-OH	2.5	>19	164
3.38	=N-OCH_3	20	4.6	ND
3.39	=N-$OCH_2C_6H_5$	40	3.4	ND
3.40	—OH (epi)	11.4	31.6	>194.0
3.41	—O-Si(OC_2H_5)(OC_2H_5)(OC_2H_5)	0.2	10	79.5
3.42	—O-Si($OCH(CH_3)_2$)($OCH(CH_3)_2$)($OCH(CH_3)_2$)	2.5	4.6	115
3.43	—O-Si(OC_8H_{17})(OC_8H_{17})(OC_8H_{17})	0.3	>11	>107
	Rifampicin	0.005		
	Kanamycin	3.2		
	CQ		16 nM	
	Artesunate		4 nM	
	Emetine			0.4

CQ = chloroquine; ND = Not determined

3.5.3 C-16 fusidic acid derivatives

Two C-16 ether derivatives (**3.48** and **3.49**) were also evaluated for antimycobacterial and antiplasmodial activity (Table 3.7). Antimycobacterial activity of the C-16-ethoxy derivative (**3.49**, MIC_{99} 0.8 μM) was found to be comparable to fusidic acid, while the C-16-methoxy derivative (**3.48**, MIC_{99} 18.7 μM) displayed inferior activity. The antiplasmodial activity of these two derivatives, however, did not show much improvement.

Table 3.7: *In vitro* antimycobacterial activity (H37Rv strain), antiplasmodial activity (NF54 strain) of C-16 fusidic acid derivatives

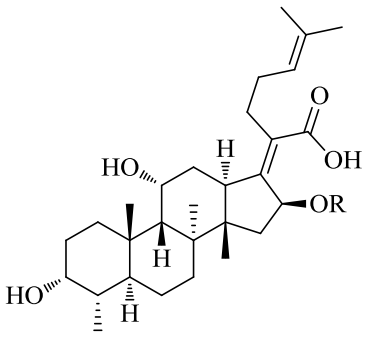

Compound	R	MIC_{99} H37Rv (μM)	IC_{50} NF54 (μM)
3.1	$COCH_3$	0.6	59.0
3.48	CH_3	18.7	29.0
3.49	C_2H_5	0.8	48.1
	Rifampicin	0.005	
	Kanamycin	3.2	
	CQ		16 nM
	Artesunate		4 nM

CQ = chloroquine

3.5.4 Miscellaneous derivatives

Derivatives with modifications at more than one site of fusidic acid have been included under the miscellaneous category. The biological results of these miscellaneous derivatives are reported in Table 3.8. Compound **3.50**, which was obtained by hydrogenation of the double bond at the C-24,25 position of fusidic acid bioisostere **3.18** showed antimycobacterial activity, antiplasmodial activity and cytotoxicity similar to **3.18**. This suggests that saturation of the C-24,25 double bond does not affect the antimycobacterial/antiplasmodial activity.

Another derivative **3.51**, which was obtained by hydrolysis of the C-16 acetoxy group of **3.18**, resulted in reduced antimycobacterial activity and cytotoxicity, indicating the importance of the C-16 acetoxy group. The ketone derivative **3.53**, obtained during ozonolysis of fusidic acid, did not show antimycobacterial activity at the highest concentrations tested. This complete loss of the side chain and the carboxylic acid group resulting in complete loss of activity indicates the importance of the side chain and the carboxylic acid group for antimycobacterial activity. C-3,C-11-diketo fusidic acid (**3.54**, MIC_{99} 11.9 μM) displayed lower antimycobacterial activity as compared to C-3 keto fusidic acid (**3.36**, MIC_{99} 1.25 μM). Likewise, C-3,C-11-diacetoxy fusidic acid (**3.55**, MIC_{99} 52.5 μM) also displayed lower antimycobacterial activity as compared to C-3 acetoxy fusidic acid (**3.30**, MIC_{99} 20 μM). These results indicate that C-3,C-11 disubstitution is not tolerated for antimycobacterial activity. A methyl ester of **3.55** further reduced the antimycobacterial activity resulting in an inactive compound **3.56**.

Similar to C-21 and C-3 fusidic acid derivatives, the antiplasmodial activity of these miscellaneous derivatives was also found to increase with increase in lipophilicity. The most lipophilic derivative **3.56** was found to be the most active, displaying an IC_{50} of 0.4 μM. Further, the antiplasmodial activity of **3.53** (IC_{50} 90.8 μM), though found to be lower than fusidic acid, was, however, retained in the absence of the side chain and -COOH group. This suggests that fusidic acid derivatives with different functionalities at this site can be explored as potential antiplasmodial agents.

Table 3.8: *In vitro* antimycobacterial activity (H37Rv strain), antiplasmodial activity (NF54 strain) and cytotoxicity (CHO cell line) of miscellaneous fusidic acid derivatives

Compound	Structure	MIC_{99}H37Rv (µM)	IC_{50} NF54 (µM)	IC_{50} CHO (µM)
3.1	Fusidic acid	0.6	59.0	>194.0
3.50	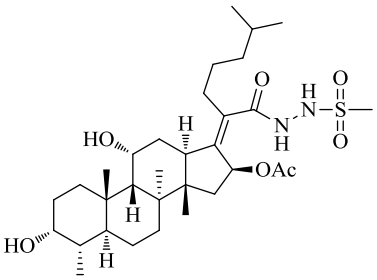	10	> 16	97.8
3.51	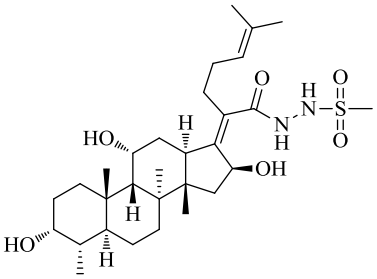	40	> 16	32.0
3.52	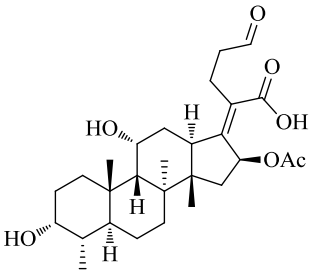	40	43.4	ND
3.53	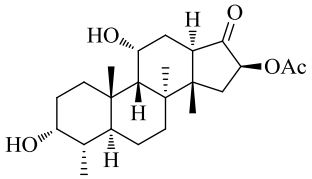	>160	90.8	ND
3.54	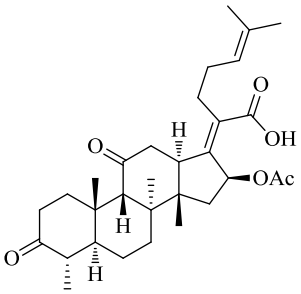	11.9	10.3	ND

3.55	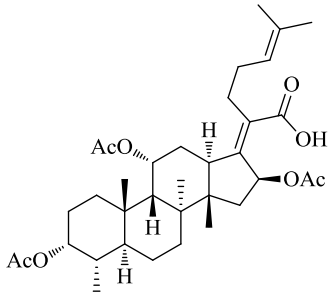	52.5	2.9	ND
3.56	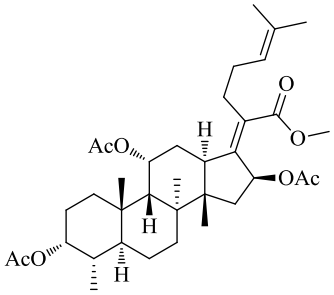	>125	0.4	>163
	Rifampicin	0.005		
	Kanamycin	3.2		
	CQ		16 nM	
	Artesunate		4 nM	
	Emetine			0.4

CQ = chloroquine; ND = Not determined

3.5.5 *In vivo* pharmokinetics study of some representative fusidic acid derivatives

Based on the *in vitro* data, the *in vivo* pharmacokinetic properties of some of the derivatives were evaluated in mice in order to determine the suitability of these compounds as potential candidates to be evaluated for efficacy in a mouse model of tuberculosis. The pharmacokinetic parameters of these compounds are described in Table 3.9 and Figure 3.21 shows a concentration-time curve plotted for these derivatives.

Fusidic acid has a short half-life (0.42 h) in mice as reported in a recent study,[20] which can also be seen from its pharmacokinetic parameters in Table 3.9. Among all tested compounds, the triisopropoxy silicate **3.42** showed a better pharmacokinetic profile than fusidic acid, with higher concentrations achieved in blood, a longer half-life, and lower clearance rate after oral as well as intravenous administration (Table 3.9, Figure 3.21). This derivative was found to be relatively stable *in vivo* and did not act as a prodrug, as hypothesized initially. However, the silicate derivative **3.41** acted as a prodrug as it was completely converted into fusidic acid within 30 min after intravenous administration. All other derivatives showed similar or poorer pharmacokinetic profiles when compared to fusidic acid.

Table 3.9: Pharmacokinetic parameters of fusidic acid derivatives in mice

	Oral administration: 20 mg/kg				**Intravenous administration: 5 mg/kg**				
Compound	**$AUC_{0\text{-}inf}$ (min.µmol/L)**	**t_{max} (h)**	**C_{max} (µg/L)**	**$t_{1/2}$ (h)**	**$AUC_{0\text{-}inf}$ (min.µmol/L)**	**Vd (L/kg)**	**Cl (ml/min/kg)**	**$t_{1/2}$ (h)**	**F (%)**
3.1 Fusidic acid	351.6	0.5	745.3	1.00	238.4	3.6	37.3	0.21	37
3.37	1064.3	0.5	5 496.7	0.58	748.4	0.8	12.7	0.75	38
3.18	349.3	0.7	1206.7	1.57	275.4	0.9	24.4	0.41	23
3.50	178.6	0.7	412.7	1.82	571.9	1.2	38.9	0.36	6
3.41	248.7	0.5	1450.0	1.34	ND	ND	ND	ND	ND
3.42	2171.5	2.3	2496.7	5.05	1312.5	3.7	4.9	4.7	41

$AUC_{0\text{-}inf}$ = Area under the concentration-time curve extrapolated to infinity; C_{max} = Maximum concentration of a drug in the body; t_{max} = Time taken to reach the maximum concentration; $t_{1/2}$ (h) = Half-life in hours; Vd = Volume of distribution; Cl = Rate of clearance of a drug from the body; F = Bioavailbility

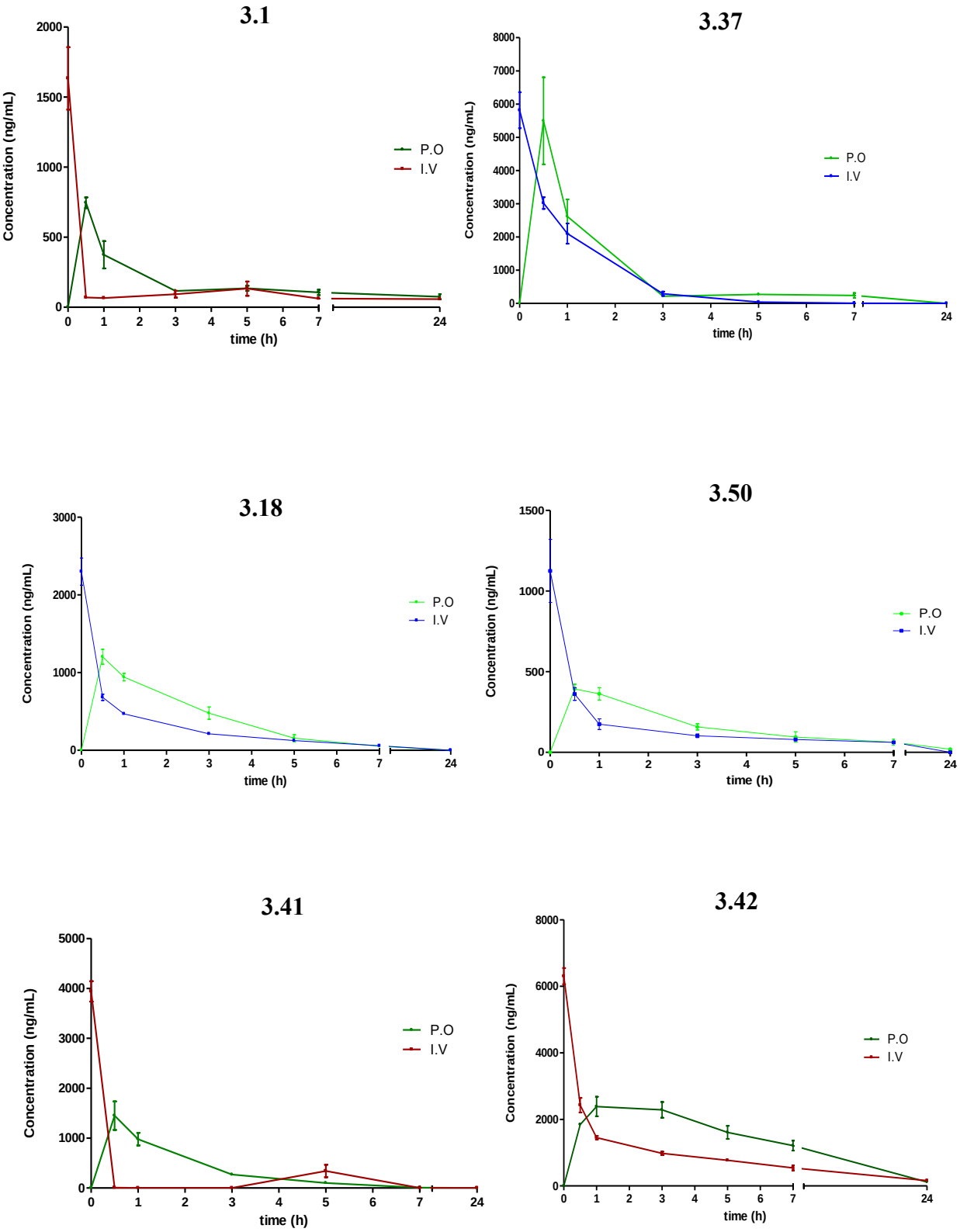

Figure 3.21: Concentration-time curves of fusidic acid derivatives; per oral (P.O) and intravenous (I.V)

3.6 Conclusion

Although fusidic acid has shown potent *in vitro* antimycobacterial activity this has not translated into activity *in vivo* in *Mtb* infected mice. It was hypothesized that subjecting fusidic acid to semisynthesis may generate derivatives with *in vivo* efficacy. In an attempt to achieve this objective, fusidic acid derivatives were synthesized by structural modifications at the C-21, C-3 and C-16 positions. C-21 derivatives were obtained by replacing the C-21 carboxyl group of fusidic acid with various bioisosteres. This approach led to derivatives with far lower antimycobacterial activity compared to fusidic acid, with most of the derivatives displaying MIC_{99} values $\geq$ 20 µM. However, two derivatives, a fusidic acid-isoniazid conjugate **3.15**, and methane sulfonyl hydrazide bioisostere **3.18** showed respectable activity each with MIC_{99} values of 10 µM. The decreased *in vitro* antimycobacterial activity of C-21 derivatives on replacement of the carboxyl group of fusidic acid with other moieties suggests that the free carboxyl group is essential for antimycobacterial activity. C-3 derivatives were obtained by replacing the C-3 OH group with its epimer (as epifusidic acid), various carboxylic and silicate esters as well as oxime and keto functionalities. C-3 derivatives exhibited better antimycobacterial activity compared to the C-21 derivatives, with 9 out of 14 derivatives displaying antimycobacterial (MIC_{99}) activity $\leq$ 5 µM. Further, the *in vitro* antimycobacterial activity of 3-epifusidic acid (**3.40**) suggests that the inversion of configuration at the C-3 position may significantly reduce the antimycobacterial activity of fusidic acid derivatives. The C-16 ether derivatives **3.48** and **3.49** were obtained by replacing the C-16 acetoxy group with methoxy and ethoxy groups, respectively. The ethoxy derivative **3.48** showed antimycobacterial activity comparable to fusidic acid. Seven miscellaneous derivatives with modifications at more than one site of fusidic acid were also obtained. Antimycobacterial evaluation of these compounds indicated that the lipophilic side chain, carboxylic acid, and the C-16 substitution are essential for antimycobacterial activity.

Some of the fusidic acid derivatives (**3.18**, **3.37**, **3.41**, **3.42** and **3.50**) were evaluated for *in vivo* pharmacokinetic properties in mice. Among these, the triisopropoxy silicate **3.42** showed a better pharmacokinetic profile than that of fusidic acid, with higher concentrations achieved in blood, a longer half-life (5 h versus 1 h after oral administration), and a lower clearance rate. The derivative was found to be stable *in vivo* and did not act as a prodrug. All other derivatives showed similar or poorer pharmacokinetic profiles when compared to fusidic acid.

In addition, the reported *in vitro* antiplasmodial activity of fusidic acid prompted antiplasmodial evaluation of the synthesized derivatives. The derivatives were tested against the NF54 strain of *P. falciparum*, and most of them displayed better IC_{50} values compared to fusidic acid. The antiplasmodial activity was found to increase with an increase in lipophilicity and the C-3, C-11-dicaetyl fusidic acid methyl ester **3.56 (**IC_{50} 0.4 μM) was found to be the most active. Further, antiplasmodial data for fusidic acid derivatives suggest that, unlike antimycobacterial activity, a free carboxyl group is not required for antiplasmodial activity.

3.7 References

(1) National Center for Biotechnology Information. PubChem BioAssay Database; AID=1332, https://pubchem.ncbi.nlm.nih.gov/bioassay/1332 (accessed May 10, 2016).

(2) Cicek-Saydam, C.; Cavusoglu, C.; Burhanoglu, D.; Hilmioglu, S.; Ozkalay, N.; Bilgic, A. In Vitro Susceptibility of Mycobacterium Tuberculosis to Fusidic Acid. *Clin. Microbiol . Infect.* **2001**, *7*, 700–702.

(3) Johnson, R. A.; McFadden, G. I.; Goodman, C. D. Characterization of Two Malaria Parasite Organelle Translation Elongation Factor G Proteins: The Likely Targets of the Anti-Malarial Fusidic Acid. *PLoS ONE* **2011**, *6*, e20633.

(4) Duvold, T.; Sørensen, M. D.; Bjorkling, F.; Henriksen, A. S.; Rastrup-Andersen, N. Synthesis and Conformational Analysis of Fusidic Acid Side Chain Derivatives in Relation to Antibacterial Activity. *J. Med. Chem.* **2001**, *44*, 3125–3131.

(5) Meanwell, N. A. Synopsis of Some Recent Tactical Application of Bioisosteres in Drug Design. *J. Med. Chem.* **2011**, *54*, 2529–2591.

(6) Godtfredsen, W. O.; Daehne, V. W.; Tybring, L.; Vangedal, S. Fusidic Acid Derivatives. I. Relationship between Structure and Antibacterial Activity. *J. Med. Chem.* **1966**, *9*, 15–22.

(7) Kaur, G.; Singh, K.; Pavadai, E.; Njoroge, M.; Espinoza-moraga, M.; Kock, C. De; Smith, P. J.; De, S. W.; Chibale, K. Synthesis of Fusidic Acid Bioisosteres as Antiplasmodial Agents and Molecular Docking Studies in the Binding Site of Elongation Factor-G. *Med.Chem.Commun.* **2015**, *6*, 2023–2028.

(8) Acornley, J. E.; Bessell, C. J.; Bynoe, M. L.; Godtfredsen, W.; Knoyle, J. M. Antiviral Activity of Sodium Fusidate and Related Compounds. *Br. J. Pharmac. Chemother.* **1967**, *31*, 210–220.

(9) Basavaprabhu, Vishwanatha, T. M.; Panguluri, N. R.; Sureshbabu, V. V. Propanephosphonic Acid Anhydride (T3P ®) - A Benign Reagent for Diverse Applications Inclusive of Large-Scale Synthesis. *Synthesis* **2013**, *45*, 1569–1601.

(10) Rastrup-andersen, N.; Duvold, T. Spectral Assignments and Reference Data Reassignment of the 1 H NMR Spectrum of Fusidic Acid and Total Assignment of 1 H and 13 C NMR Spectra of Some Selected Fusidane Derivatives. *Magn. Reson. Chem.* **2002**, *40*, 471–473.

(11) Duvold, T.; Bretting, C. A. S.; Rasmussen, P. A. ; Bouerat, L.; Thorhauge, J. Novel Fusidic Acid Derivatives. WO2005007669 A1, 2005.

(12) Duvold, T. Novel Polyaminated Fusidic Acid Derivatives. WO2002077007 A2, 2002.

(13) Wohl, A. R.; Michel, A. R.; Kalscheuer, S.; Macosko, C. W.; Panyam, J.; Hoye, T. R. Silicate Esters of Paclitaxel and Docetaxel: Synthesis, Hydrophobicity, Hydrolytic Stability, Cytotoxicity, and Prodrug Potential. *J. Med. Chem.* **2014**, *57*, 2368–2379.

(14) Von Daehne, W.; Rasmussen, P. R. l6-Ethers Of Fusidic Acid Derivatives. US4060606, 1977.

(15) Janssen, G.; Vanderhaeghe, H. Modification of the Side Chain of Fusidie Acid (Ramycin). *J. Med. Chem.* **1967**, *10*, 205–208.

(16) Bostro, J.; Hogner, A.; Llina, A.; Wellner, E.; Plowright, A. T. Oxadiazoles in Medicinal Chemistry. *J. Med. Chem.* **2012**, *55*, 1817–1830.

(17) Anglin, E. J.; Cheng, L.; Freeman, W. R.; Sailor, M. J. Porous Silicon in Drug Delivery Devices and Materials. *Adv. Drug Deliv. Rev.* **2008**, pp 1266–1277.

(18) Marcofranco, J. E.; Torres, V. E.; Nixon, D. E.; Wilson, D. M.; James, E. M.; Bergstralh, E. J.; Mccarthy, J. T. Oxalate, Silicon and Vanadium in Acquired Cystic Kidney-Disease. *Clin. Nephrol.* **1991**, *35*, 52–58.

(19) Gitelman, H. J.; Alderman, F.; Perry, S. J. Renal Handling of Silicon in Normals and Patients with Renal Insufficiency. *Kidney int.* **1992**, *42*, 957–959.

(20) Murphy, T.M.; Little, S.; Wu, R.; Slee, A.; Fernandes, P. Assessment of In Vivo Activity of CEM-102 (Fusidic Acid) in Murine Infection Models (Poster Presentation). http://www.cempra.com/common/pdf/Posters/Assessment of In Vivo Activity of CEM-102 in Murine.pdf (accessed Jun 20, 2016).

Chapter 4

Use of *in silico* tools to design fusidic acid derivatives and to identify new fusidic acid-like compounds

4.1 Introduction

This chapter introduces the use of *in silico* tools to design new fusidic acid derivatives and fusidic acid-like compounds. It is divided into two sections. The first section describes the building of a pharmacophore model based on the antiplasmodial activities of previously synthesized fusidic acid derivatives. This model was used to design new fusidic acid derivatives, which were then synthesized and subjected to *in vitro* biological evaluation. In the second section, the application of 2D and 3D similarity search methods to identify fusidic acid-like compounds from an in-house database is described.

4.2 Rationale

Ligand-based (LBVS) and structure-based (SBVS) virtual screening (VS) techniques are well-established computational tools used in the modern drug discovery process to identify new hit compounds, as well as facilitate hit-to-lead and lead optimization efforts for a particular molecular target.[1–4] SBVS, such as structure-based 3D pharmacophore modelling and molecular docking, uses the 3D structure of a biological target. On the other hand, LBVS, such as ligand-based 3D pharmacophore modelling and 2D/3D similarity search methods, become the approach of choice when the biological target is not known or its 3D structure is not available. Since the biological targets of fusidic acid in *Mtb* and *P. falciparum* are not known, LBVS was the focus.

The ligand-based 3D pharmacophore modelling superimposes a set of active compounds and extracts the common chemical features that are essential for their biological activity. By deriving a 3D pharmacophore model from a set of known active compounds and validating it on various active and inactive compound data sets, the model can then be used for virtual screening of a library of compounds in a database to identify new hit compounds. Application of such a technique prior to synthesis not only reduces the number of compounds for synthesis but also increases the % hit rate. The ligand-based 3D pharmacophore approach has been widely reported in literature for its use in identifying new hit compounds for a particular target. In this study, a 3D-QSAR pharmacophore model was derived based on the

antiplasmodial activities of fusidic acid derivatives synthesized in our lab and has been utilized to design new potent fusidic acid derivatives.

Similarity searching is another commonly used LBVS that does not require the 3D structure of a biological target. It is based on searching a database for compounds that most closely (structurally) resemble a given query compound. This query compound can represent a natural product or a known inhibitor of a target protein, or even a patented compound. The fundamental assumption is that the compounds that are structurally similar to the active query compound are likely to have similar properties, especially in terms of biological activity, as defined by the Similarity Property Principle.[5] Different types of 2D fingerprint methods and 3D shape similarity search methods are available in various drug discovery software packages. 2D similarity methods account for structural and/or topological features and the overlap between fingerprints of the query and the database compounds is quantified as a measure of molecular similarity.[6] 3D shape similarity methods measure overlapping volumes by comparing molecular conformations of the query and database compounds.[7] These 2D and 3D similarity search methods can use fusidic acid as a query compound to identify more fusidic acid-like compounds from a database. Since these compounds have a similar structure to fusidic acid, they may possess similar biological activities with a possibility of sharing the same biological target.

4.3 3D-QSAR Pharmacophore model

The purpose of this study was to derive a 3D-QSAR pharmacophore model based on the antiplasmodial activities of some previously synthesized fusidic acid derivatives and then use the model to design new fusidic acid derivatives.

4.3.1 Materials and methods

Data set: Sixty one compounds with available IC_{50} values, determined against the NF54 strain of *P. falciparum*, were used to build the 3D-QSAR model. In order to build and validate the pharamacophore model, the data was divided into two sets: a training set of 29 compounds and a test set of 32 compounds. The training set compounds were selected in such a way that they contained information in terms of both their structural features and biological activity ranges. Structures of the training set and test set compounds are shown in Table 4.1 and Table 4.2 respectively.

Table 4.1: Chemical structures of the training set compounds with IC_{50} values

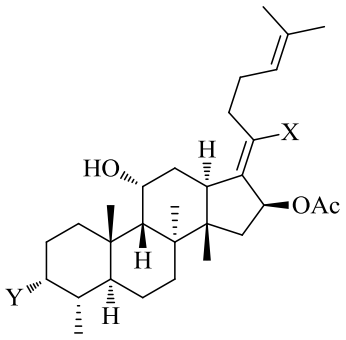

S. No.	X	Y	IC_{50} NF54 (nM)	S. No.	X	Y	IC_{50} NF54 (nM)
1	COOH	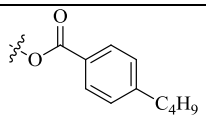	390	**12**	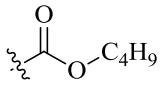	OH	2900
2	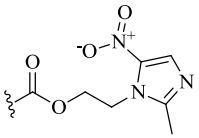	OH	500	**13**	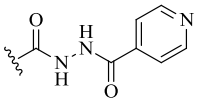	OH	3240
3	COOH	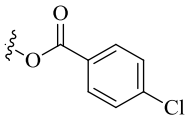	1060	**14**	COOH	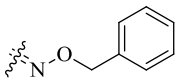	3430
4	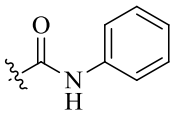	OH	1200	**15**	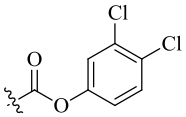	OH	3600
5	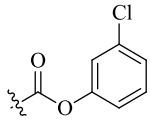	OH	1400	**16**	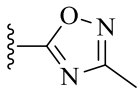	OH	3800
6	COOH	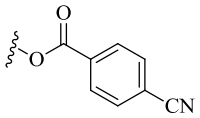	1520	**17**	COOH	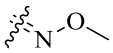	4650
7	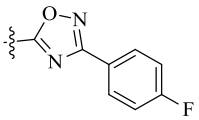	OH	1730	**18**	COOH	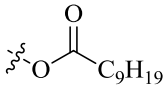	6630
8	COOH	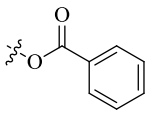	1960	**19**	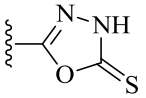	OH	7040
9	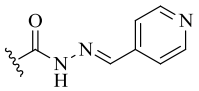	OH	2000	**20**	COOH		8220
10	COOH	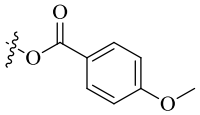	2600	**21**	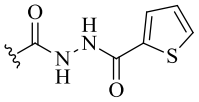	OH	8420
11	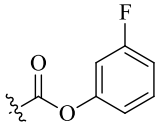	OH	2600	**22**	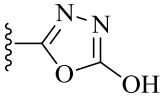	OH	9230

Table 4.1: Continued…

S. No.	X	Y	IC_{50} NF54 (nM)	S. No.	X	Y	IC_{50} NF54 (nM)
23	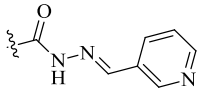	OH	13584	**27**	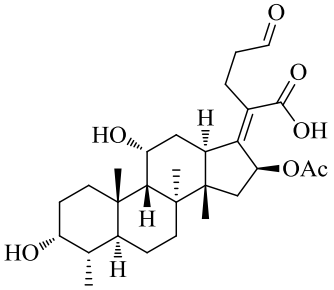		43400
24	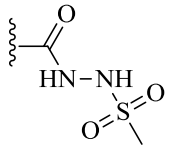	OH	14700	**28**	COOH	OH	59000
25	-$CONHNH_2$	OH	21300	**29**	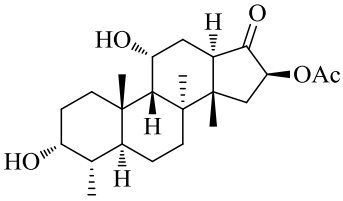		91000
26	-$CONH_2$	OH	35900				

Table 4.2: Chemical structures of the test set compounds with IC_{50} values

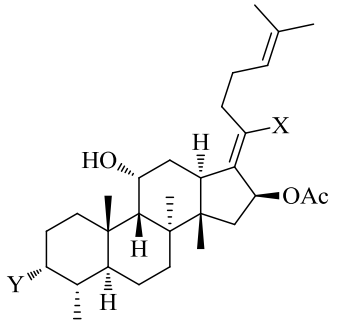

S. No.	X	Y	IC_{50} NF54 (nM)	S. No.	X	Y	IC_{50} NF54 (nM)
30	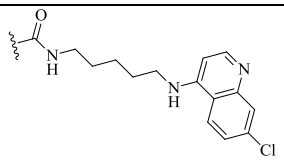	OH	59	**39**	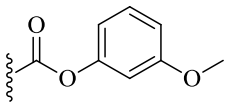	OH	1800
31	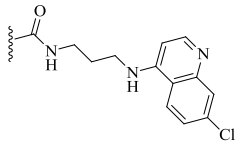	OH	120	**40**	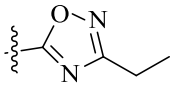	OH	1890
32	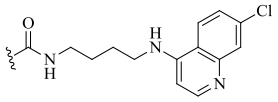	OH	121	**41**	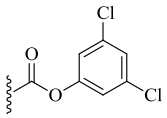	OH	2000
33	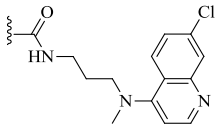	OH	136	**42**	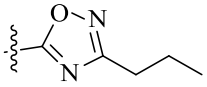	OH	2090
34	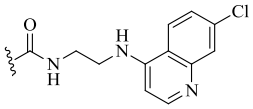	OH	340	**43**	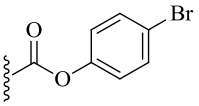	OH	2100
35	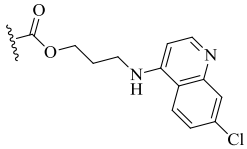	OH	708	**44**	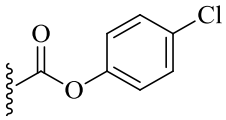	OH	2300
36	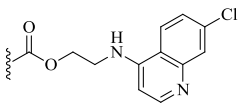	OH	1074	**45**	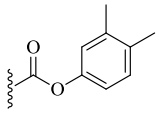	OH	2400
37	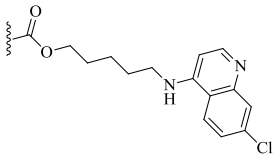	OH	1225	**46**	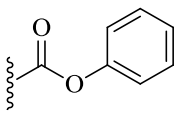	OH	2400
38	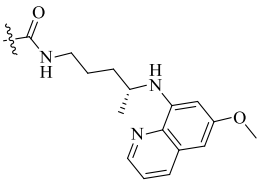	OH	1464	**47**	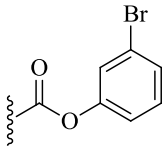	OH	2600

Table 4.2: Continued…

S. No.	X	Y	IC_{50} NF54 (nM)	S. No.	X	Y	IC_{50} NF54 (nM)
48	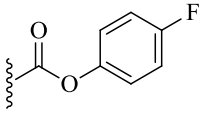	OH	2900	**55**	COOH	$-OCOC_4H_9$	7450
49	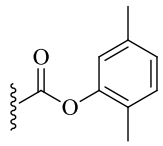	OH	3000	**56**	COOH	$-OCOC_6H_{13}$	7920
50	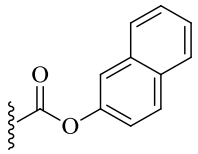	OH	3200	**57**	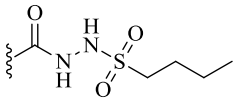	OH	8040
51	$-COOC_2H_5$	OH	3400	**58**	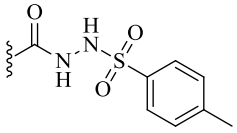	OH	13370
52	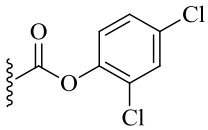	OH	3500	**59**	COOH	$-OCOC_3H_7$	14880
53	$-COOC_8H_{17}$	OH	4600	**60**	COOH	$-OCOC_2H_5$	19030
54	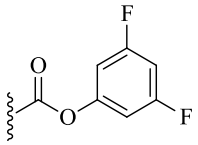	OH	4700	**61**	COOH	$-OCOCH_3$	56020

3D-QSAR pharmacophore generation: The 'HypoGen' algorithm of Discovery Studio 4.0 was employed to build a 3D-QSAR pharmacophore model with a set of selected 29 training set compounds (Table 4.1). Different possible conformations for each training set compound were generated using the 'Best' conformation method with the maximum number of conformations set to 255. These conformations were created within a relative energy threshold of 10 kcal/mol. The 'Feature Mapping' protocol was used to identify the common features present in active compounds and, accordingly, HB_acceptor, HB_donor, Hydrophobic and Ring aromatic were selected as key input pharmacophore features for the generation of the pharmacophore model. All other parameters were used at their default values except the uncertainty value which was set at 1.5. The 'HypoGen' algorithm generated a set of 10 pharmacophore hypotheses with corresponding statistical parameters such as cost values, root mean square deviation (RMSD), correlation coefficient and fit values. The best quality hypothesis was selected based on these parameters.

Validation of the pharmacophore model: In addition to having good statistical data, a good pharmacophore model should also be able to accurately predict the activity of compounds and retrieve active compounds from the database. Therefore, to check the reliability of the selected model, the model was validated using various techniques, such as Fischer's randomization method, test set validation, and inactive set validation.

Combinatorial library design: In order to identify hit compounds, the best pharmacophore model after validation was used as the 3D structural search query to screen a combinatorial library. The library was generated using the 'Enumerate Library from Ligands' protocol of Discovery Studio 4.0. A conformational ensemble of each library compound was then generated in the 'Generate Conformation' program, setting the confirmation method to 'Best', the maximum number of conformations to 255, and the relative energy threshold to 10kcal/mol. All these conformations were used in the virtual screening, which was performed using the 'Ligand Pharmacophore Mapping' program with the 'Flexible' fit method. The selection of compounds for synthesis was based on their fit value computed by the pharmacophore model in the virtual screening. Selected hit compounds were synthesized and evaluated for biological activity.

4.3.2 Results and discussion

4.3.2.1 Pharmacophore modelling

As mentioned in materials and methods (Section 4.3.1), the 'HypoGen' algorithm of Discovery Studio 4.0 generated a set of 10 pharmacophore hypotheses with corresponding statistical parameters such as cost values, root mean square deviation (RMSD), correlation coefficient and fit values. The best quality hypothesis was selected based on these parameters using Debnath's analysis.[8] The statistical parameters of these 10 pharmacophore are shown in Table 4.3.

Table 4.3: Statistical results of the 10 pharmacophore hypotheses generated by 'HypoGen' algorithm

Hypothesis	Total Cost	[a]Cost Difference	[b]RMSD	Correlation Training Set	[c]Features	Correlation Test Set
Hypo 1	115.806	111.46	1.30259	0.919356	HY, HY, HY, RA	0.619677
Hypo 2	118.772	108.49	1.34949	0.913164	HY, HY, HY, RA	0.832466
Hypo 3	127.014	100.25	1.63088	0.870076	HY, HY, HY, RA	0.433590
Hypo 4	127.593	99.668	1.64589	0.86748	HY, HY, HY, RA	0.574456
Hypo 5	127.798	99.463	1.52039	0.888284	HY, HY, HY, RA	0.629285
Hypo 6	131.349	95.912	1.73001	0.852355	HY, HY, HY, RA	0.366060
Hypo 7	132.382	94.879	1.74801	0.849004	HY, HY, HY, RA	0.273861
Hypo 8	136.537	90.724	1.81551	0.836014	HBA, HY, HY, RA	0.583952
Hypo 9	137.504	89.757	1.80439	0.838285	HBA, HY, HY, RA	0.594138
Hypo 10	138.409	88.852	1.81525	0.836151	HBA, HY, HY, RA	0.465832

[a]Cost difference between the null and the total cost; The null cost, the fixed cost and the configuration cost are 227.261, 87.4891 and 17.7258, respectively; [b]RMSD = root mean square deviation; [c]Abbreviation used for features: HBA = hydrogen bond acceptor, HY = hydrophobic, and RA = ring aromatic

According to Debnath's analysis, the best pharmacophore model should have the highest cost difference, a good correlation coefficient, the least RMSD, and the lowest total cost values. Cost difference represents the difference between the null and total cost of hypothesis. The cost values of 10 pharmacophore models ranged from 115.806 to 138.409 (Table 4.3). Out of these 10 hypotheses, Hypo 1 and Hypo 2 showed lower cost values (115.806 - Hypo 1, 118.772 - Hypo 2) compared to the other hypothesis. The correlation coefficient is based on linear regression derived from the geometric fit index. A higher correlation coefficient stands for better predictive ability of the model. The correlation coefficients for Hypo 1 and Hypo 2 were 0.919356 and 0.913164, respectively, which were prominently higher than other hypotheses. The RMSD factor represents the deviation of the predicted activity value from the experimental value; therefore, a lower RMSD value further supports the predictive ability of the model. The RMSD values of Hypo 1 (1.30259) and Hypo 2 (1.34949) were found to be

lower than other models. Both of the hypotheses also showed the same pharmacophore features: 3 hydrophobic regions and one aromatic ring feature. The selection of the best model for virtual screening was performed after checking the reliability of these two models on the test set. The highest correlation coefficient in the test set was obtained for Hypo 2 (0.832466) while Hypo 1 showed a correlation coefficient of 0.619677. However, none of the other 8 pharmacophore models showed a correlation coefficient close to Hypo 2. The correlation coefficient values for all the 10 pharmacophore models in the test set are also shown in Table 4.3. Consequently, Hypo 2 was selected for virtual screening. Figure 4.1 represents the best HypoGen model-Hypo 2, and mapping of Hypo 2 with one of the most active (**1**, IC_{50} = 390 nM) and the least active (**29**, IC_{50} = 91000 nM) compounds from the training set. The most active compound (**1**) overlapped with all four pharmacophore features of Hypo 2 and showed the highest fit value of 3.69. On the other hand, the least active compound (**29**) missed one ring aromatic and one hydrophobic feature of Hypo 2 and thus showed the lowest fit value of 1.53. The fit values and the predicted IC_{50} values of all the training set compounds, as computed by Hypo 2, are shown in Table 4.4. Figure 4.2 shows the plot of the correlation between the experimental and predicted activity of these compounds.

A. B.

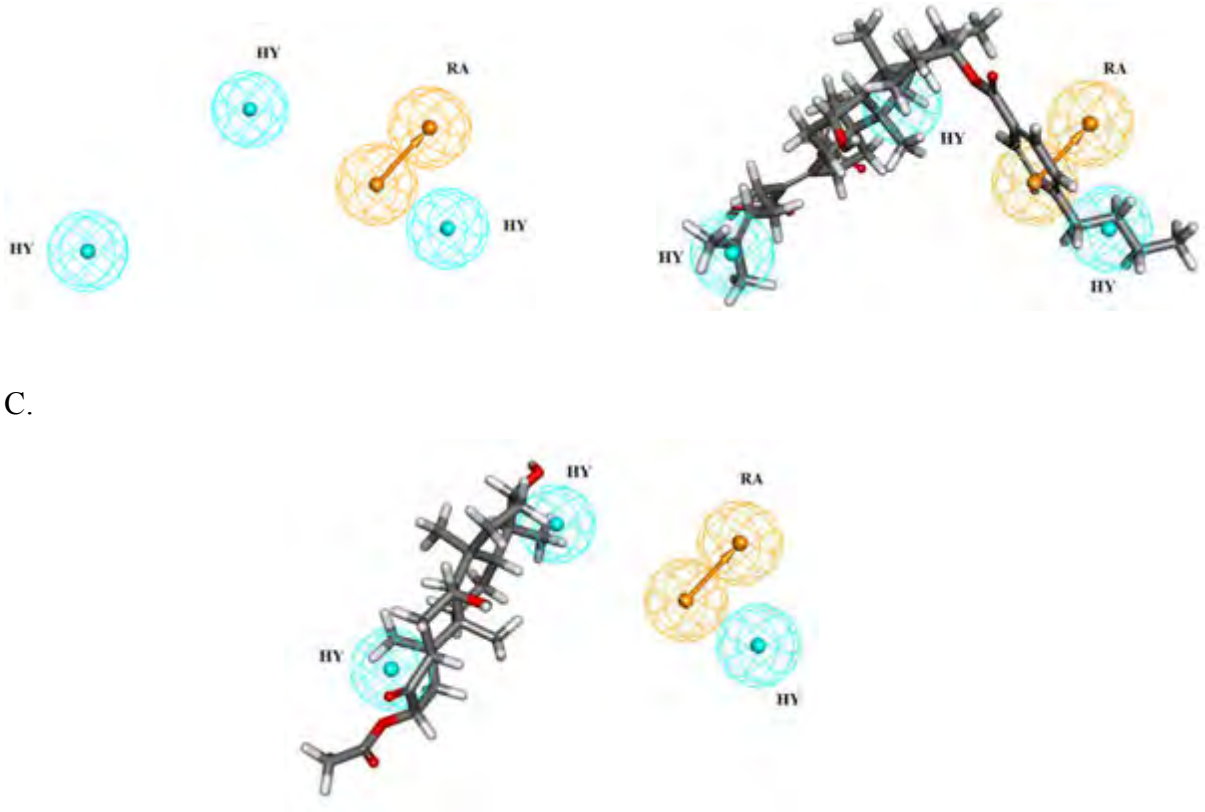

C.

Figure 4.1: Pharmacophore models based on fusidic acid derivatives generated by HypoGen; **A.** The best HypoGen model, Hypo 2; **B.** Mapping of Hypo 2 with one of the most active compounds (IC_{50} = 390 nM) from the training set; **C.** Mapping of Hypo 2 with one of the least active compounds (IC_{50} = 91000 nM) from the training set; Pharmacophore features are color-coded: orange for ring aromatic (RA) and cyan for hydrophobic (HY)

Table 4.4: Experimental (Exp IC_{50}) and predicted (Pred IC_{50}) IC_{50} values of the training set compounds based on best pharmacophore hypothesis Hypo 2

S. No.	[d] Fit Value	Exp IC_{50} (nM)	Pred IC_{50} (nM)	[e] Error	S. No.	[d] Fit Value	Exp IC_{50} (nM)	Pred IC_{50} (nM)	[e] Error
1	3.69	390	500	+1.3	**16**	3.04	3800	2200	-1.7
2	3.14	500	1800	+3.6	**17**	2.98	4700	2600	-1.8
3	3.52	1100	750	-1.4	**18**	2.53	6600	7300	+1.1
4	3.05	1200	2200	+1.8	**19**	2.18	7000	16000	+2.3
5	3.14	1400	1800	+1.3	**20**	2.11	8200	19000	+2.3
6	3.13	1500	1800	+1.2	**21**	2.85	8400	3500	-2.4
7	3.13	1700	1800	+1.1	**22**	2.11	9200	19000	+2.1
8	3.01	2000	2400	+1.2	**23**	2.38	14000	10000	-1.3
9	3.03	2000	2300	+1.2	**24**	2.11	15000	19000	+1.3
10	3.13	2600	1800	-1.4	**25**	2.11	21000	19000	-1.1
11	2.75	2600	4400	+1.7	**26**	2.11	36000	19000	-1.9
12	2.96	2900	2700	-1.1	**27**	1.63	43000	57000	+1.3
13	3.03	3200	2300	-1.4	**28**	2.11	59000	19000	-3.1
14	3.06	3400	2100	-1.6	**29**	1.53	91000	73000	-1.2
15	3.06	3600	2100	-1.7					

[d] Fit value indicates how well the features in the pharmacophore overlap the chemical features in the molecule;
[e]Division of higher value of experimental/predicted IC_{50} by lower predicted/experimental IC_{50} value; '+' indicates that the predicted IC_{50} is higher than the experimental IC_{50}, '–' indicates that the predicted IC_{50} is lower than the experimental IC_{50}, a value of 1 indicates that the predicted IC_{50} is equal to the experimental IC_{50}

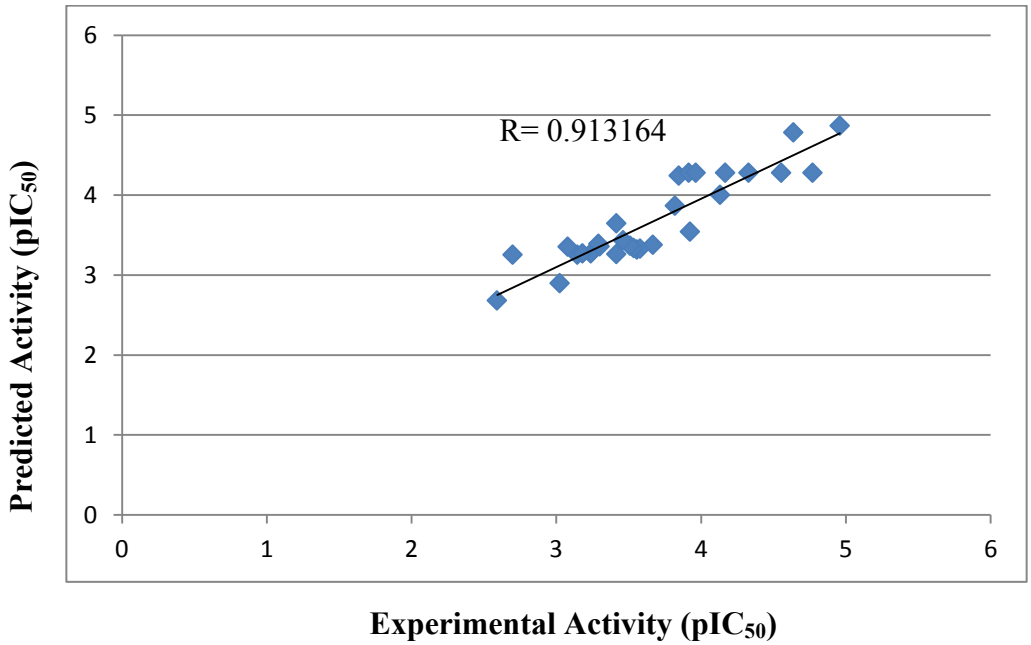

Figure 4.2: Plot of the correlation (R) between the experimental activity and the activity predicted by Hypo 2 for the training set compound

The selected model 'Hypo 2' was subjected to a reliability check using three techniques- Fischer's randomization test, test set validation, and inactive set validation. Fischer's randomization test validates the correlation between the chemical structures and the biological activity of the compounds. In this technique, the activity data is randomised among the training set compounds and new pharmacophore hypotheses are generated under the same features and parameters as used in the original hypothesis generation. If these random pharmacophores show similar or better statistics, such as cost values and correlation coefficients, than the original hypothesis, then the original hypothesis is considered as generated by chance. Fischer's randomization test was performed simultaneously during the original hypothesis generation. A confidence level of 95% was selected, which generated 19 random pharmacophore hypotheses. The lower correlation coefficients and the higher total cost values of these 19 hypotheses as compared to Hypo2 indicated that the Hypo 2 has not been generated by chance (Figure 4.3).

Hypo	total cost	random 1	random 2	random 3	random 4	random 5	random 6	random 7	random 8	random 9	random 10	random 11	random 12	random 13	random 14	random 15	random 16	random 17	random 18	random 19
Hypo1	115.81	163.3	163.53	126.19	159.92	152.66	127.35	151.08	142.45	179.81	153.6	160.33	159.64	150.27	143.94	124.26	133.94	178.64	160.53	155.54
Hypo2	118.77	182.32	178.17	167.61	184.05	166.83	168.79	193.18	146.77	185.28	169.59	169.09	179.01	166.72	167.95	160.23	147.25	179.82	172.28	175.83
Hypo3	127.01	184.95	178.88	168.26	204.51	166.84	174.69	202.37	175.83	211.68	195.75	170.69	182.8	166.83	191.65	171.76	153.31	209.83	173.82	176.72
Hypo4	127.59	185.83	183.79	171.98	204.88	170.36	175.85	205.11	178.48	213.45	198.57	179.81	182.83	171.81	198.6	181.27	156.91	212.58	177.45	179.13
Hypo5	127.8	186.04	184.12	172.89	206.64	167.29	175.85	205.12	185.4	217.02	201.43	182.98	184.5	176.07	199.69	185.66	158.88	212.62	179.19	182.56
Hypo6	131.35	187.38	184.5	173.06	208.13	171.26	176.56	205.96	190.1	217.24	209.63	185.6	185.86	182.05	200.13	188.77	159.58	213.21	179.71	186.26
Hypo7	132.38	188.75	190.8	174.94	210	175.64	176.79	206.38	192.44	218.31	209.85	188.18	186.4	182.56	200.81	190.19	159.77	213.52	180.08	187.85
Hypo8	136.54	188.82	192.91	175.69	212.75	175.91	177.02	206.16	193.66	218.69	209.95	190.57	193.56	183.21	201.03	190.26	161.56	214.41	181.07	189.23
Hypo9	137.5	189.49	193.56	175.73	212.88	177.45	178.93	207.84	194.45	218.7	213.59	195.14	193.75	185.34	201.39	190.7	164.46	214.68	181.54	190.18
Hypo10	138.41	190.42	193.91	177.33	214.58	179.1	180.44	210.18	197.64	219.52	214.27	199.31	194.7	187.64	201.76	190.88	167.07	214.83	184.1	190.39

Hypo	Correlation	Random 1	Random 2	Random 3	Random 4	Random 5	Random 6	Random 7	Random 8	Random 9	Random 10	Random 11	Random 12	Random 13	Random 14	Random 15	Random 16	Random 17	Random 18	Random 19
Hypo 1	0.919356	0.71528	0.73123	0.86894	0.7497	0.77185	0.8655	0.77196	0.8083	0.64836	0.77379	No data	0.74594	0.7813	0.8016	0.87526	0.8412	0.65124	0.7386	0.7556
Hypo 2	0.913164	0.63279	0.66196	0.71992	0.6563	0.70818	0.7113	0.57287	0.7896	0.62162	0.70597	0.6965	0.66394	0.7114	0.7039	0.73723	0.7899	0.63866	0.6857	0.6749
Hypo 3	0.870076	0.61198	0.67045	0.70121	0.5089	0.71166	0.6899	0.52074	0.6698	0.48622	0.56819	0.6988	0.64413	0.7125	0.5833	0.69905	0.7664	0.48058	0.675	0.6685
Hypo 4	0.86748	0.63272	0.65487	0.68292	0.5182	0.70413	0.6893	0.50268	0.6531	0.48716	0.57353	0.6585	0.65923	0.693	0.5663	0.63855	0.752	0.46403	0.6668	0.6595
Hypo 5	0.888284	0.63378	0.64515	0.69381	0.4978	0.70638	0.6894	0.54165	0.6343	0.45039	0.56585	0.6417	0.63376	0.675	0.5502	0.62156	0.7459	0.47047	0.6531	0.6485
Hypo 6	0.852355	0.63359	0.64063	0.69709	0.5056	0.70282	0.6892	0.54237	0.6039	0.46027	0.51207	0.6262	0.62788	0.6449	0.544	0.61854	0.741	0.4564	0.6507	0.64
Hypo 7	0.849004	0.60469	0.61121	0.68755	0.4909	0.68422	0.6878	0.52519	0.5822	0.47508	0.47955	0.6232	0.63481	0.6486	0.5523	0.61061	0.7408	0.46543	0.6523	0.6103
Hypo 8	0.836014	0.60973	0.60323	0.66642	0.499	0.68683	0.6829	0.54054	0.5721	0.45294	0.49222	0.6112	0.6013	0.6459	0.5546	0.60446	0.7317	0.43755	0.6427	0.6262
Hypo 9	0.838285	0.61924	0.60774	0.68662	0.4537	0.67097	0.6799	0.52724	0.5972	0.46192	0.47725	0.5984	0.59975	0.6261	0.5477	0.6042	0.7224	0.43553	0.638	0.6146
Hypo 10	0.836151	0.5993	0.59014	0.67162	0.4827	0.65833	0.66	0.50991	0.5564	0.41496	0.46608	0.5624	0.5886	0.6271	0.5453	0.59976	0.7143	0.44228	0.6329	0.602

Figure 4.3: Total cost (above) and correlation (below) values of all pharmacophore models at 95% confidence level

A validation process using a test set of 32 fusidic acid derivatives (not included in the training set) was performed on the entire 10 hypotheses. A conformational space for 32 test set compounds was prepared in the same manner as in the pharmacophore generation process. The 'Ligand pharmacophore mapping' protocol was used for predicting the activity of all test set compounds. The highest correlation between the experimental and the predicted activity for the test set compounds was obtained in the case of Hypo 2 (Table 4.3) showing that Hypo 2 fits, not only for training set compounds, but also for other fusidic acid derivatives. Table 4.5 shows experimental and predicted IC_{50} values of the test set compounds. Figure 4.4 represents the plot of the correlation between the experimental and predicted activity by Hypo 2 for the test set compounds.

Table 4.5: Experimental (Exp IC_{50}) and predicted (Pred IC_{50}) IC_{50} values of the test set compounds against Hypo 2

S. No.	[d] Fit Value	Exp IC_{50} (nM)	Pred IC_{50} (nM)	[e] Error	S. No.	[d] Fit Value	Exp IC_{50} (nM)	Pred IC_{50} (nM)	[e] Error
30	3.55	59	694	+11.76	**46**	2.94	2400	2852	+1.19
31	3.53	120	720	+6.00	**47**	3.08	2600	2026	-1.28
32	3.63	121	580	+4.79	**48**	2.92	2900	2964	+1.02
33	4.04	136	222	+1.63	**49**	3.11	3000	1912	-1.57
34	3.49	340	785	+2.31	**50**	3.13	3200	1822	-1.76
35	3.18	708	1792	+2.53	**51**	3.09	3400	2010	-1.69
36	3.13	1074	1833	+1.71	**52**	2.95	3500	2741	-1.28
37	3.18	1225	1639	+1.34	**53**	2.94	4600	2805	-1.64
38	3.12	1464	1860	+1.27	**54**	2.75	4700	4350	-1.1
39	3.07	1800	2090	+1.16	**55**	3.07	7450	2079	-3.58
40	3.11	1890	1924	+1.02	**56**	2.96	7920	2668	-2.97
41	3.53	2000	724	-2.76	**57**	3.01	8040	2398	-3.35
42	3.04	2090	2220	+1.06	**58**	2.99	13370	2490	-5.37
43	3.01	2100	2426	+1.16	**59**	3.03	14880	2275	-6.54
44	3.15	2300	1742	-1.32	**60**	2.99	19030	2586	-7.36
45	3.09	2400	1988	-1.21	**61**	2.28	56020	12871	-4.35

[d] *Fit value indicates how well the features in the pharmacophore overlap the chemical features in the molecule;* [e] *Division of higher value of experimental/predicted IC_{50} by lower predicted/experimental IC_{50} value; '+' indicates that the predicted IC_{50} is higher than the experimental IC_{50}, '–' indicates that the predicted IC_{50} is lower than the experimental IC_{50}, a value of 1 indicates that the predicted IC_{50} is equal to the experimental IC_{50}*

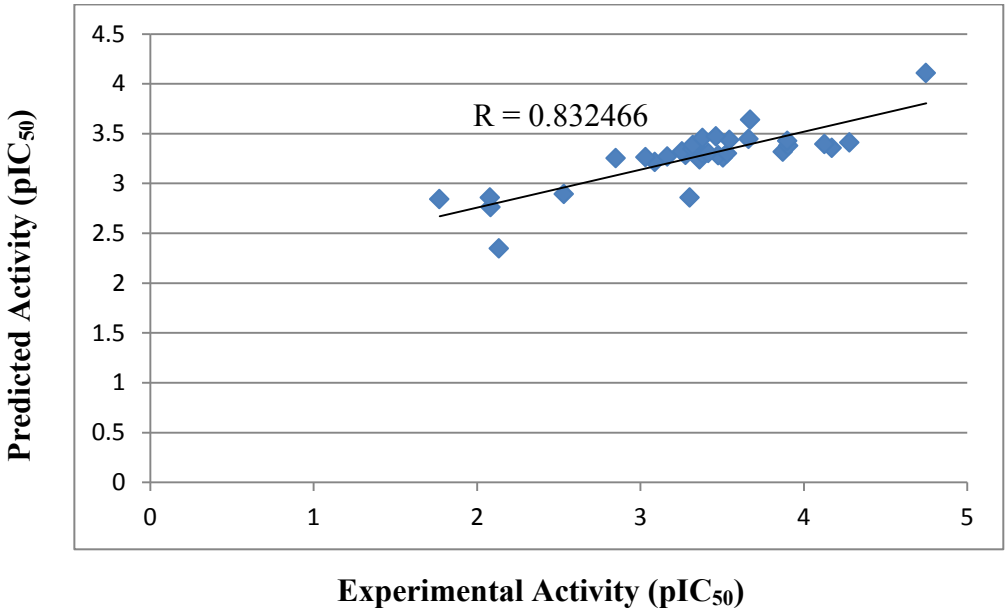

Figure 4.4: Plot of the correlation (R) between the experimental activity and the activity predicted by Hypo 2 for the test set molecules

The ability of Hypo 2 to reject inactive compounds was also validated by screening a set of four inactive fusidic acid derivatives (IC_{50} > 100 μM) which were predicted to be inactive by Hypo 2. Hypo 2, after validation, was used to screen a fusidic acid-based combinatorial library.

A general structure representing the library design is shown in Figure 4.5.

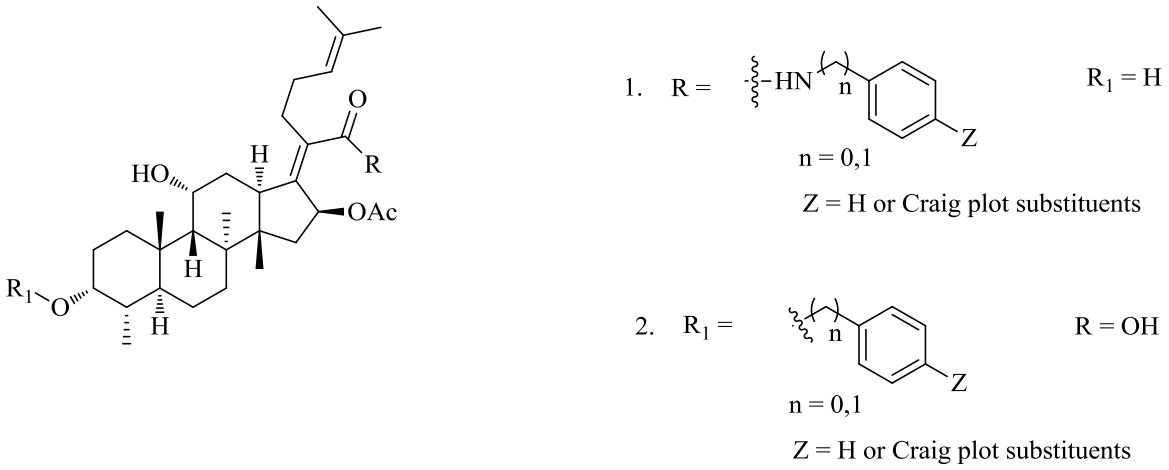

Figure 4.5: A combinatorial library design for fusidic acid derivatives.

A total of 120 compounds were screened through Hypo 2 using the 'Ligand Pharmacophore Mapping' protocol, which computed a fit value for each library compound. The selection of

hit compounds was based on these fit values. The threshold for the fit value was decided from the fit values of the two most active compounds (compounds **1** and **2**, Table 4.4) used in 3D-QSAR pharmacophore model generation. Accordingly, compounds with fit values > 3 were prioritized and 8 compounds were selected for synthesis. These 8 hits include derivatization either at the C-21 carboxylic acid to make C-21 amide derivatives of fusidic acid or at the C-3 position to make C-3 ethers. The chemical structures of the compounds with their fit value and predicted value of activity are shown in Figure 4.6.

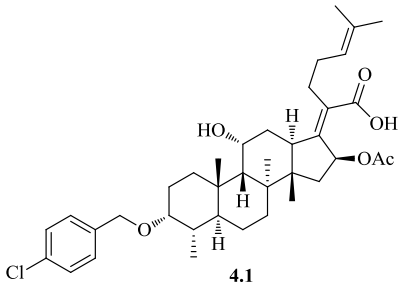

4.1

Fit value: 4.00
Predicted activity: 242 nM

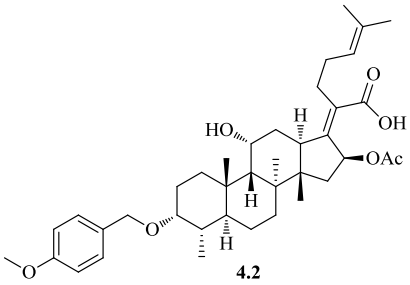

4.2

Fit value: 3.98
Predicted activity: 256 nM

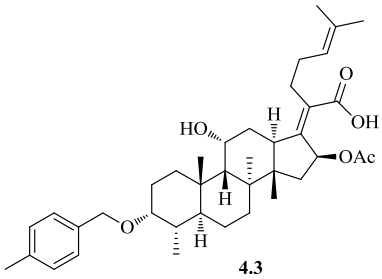

4.3

Fit value: 3.87
Predicted activity: 334 nM

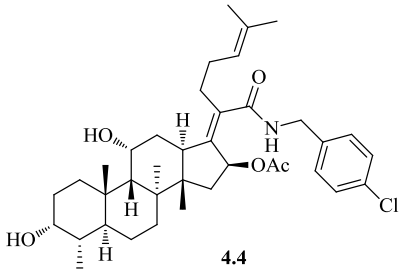

4.4

Fit value: 3.77
Predicted activity: 420 nM

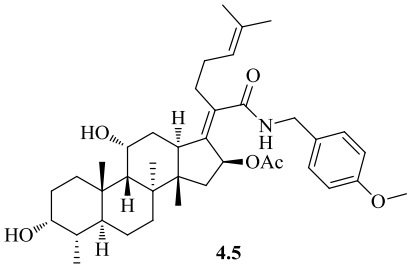

4.5

Fit value: 3.53
Predicted activity: 728 nM

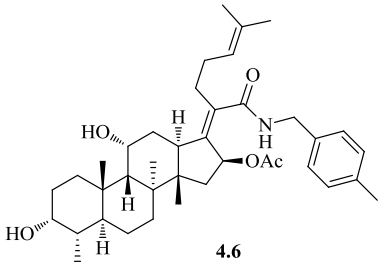

4.6

Fit value: 3.89
Predicted activity: 315 nM

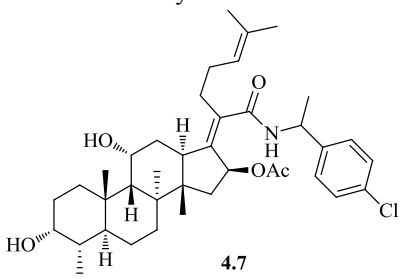

4.7

Fit value: 3.90
Predicted activity: 307 nM

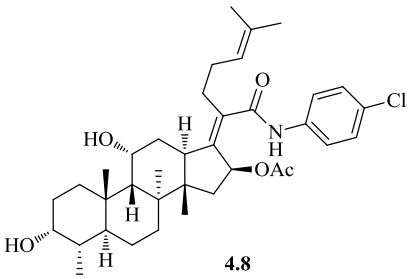

4.8

Fit value: 3.40
Predicted activity: 966 nM

Figure 4.6: Structures of hit compounds selected for synthesis with fit values and predicted activity

4.3.2.2 Synthesis of hit compounds (4.1-4.8)

Two different synthetic routes (Scheme 4.1) were adopted for synthesis. Compounds **4.4-4.8** were synthesized by the reaction of fusidic acid (**3.1**) with the corresponding amine using T3P (50% w/v in DMF) as a coupling reagent. All these compounds were obtained in good to very

good yields (70-89%). However, compounds **4.7** (20%) and **4.8** (25%) were obtained in poor yields as reactions did not proceed to completion and fusidic acid was recovered in these reactions. Synthesis of compounds **4.1**-**4.3** was achieved in 3 steps. Fusidic acid was first protected as pivaloyloxymethyl ester to yield **4.0**. This intermediate was then heated with the corresponding benzyl halides at 130 ^{o}C using DIPEA as a base. This reaction yielded both C-3-mono substituted (**4.1a**-**4.3a)** as well as C-3,C-11-disubstituted products, which were separated by silica gel column chromatography. Finally, the pivaloyloxymethyl group of **4.1a**-**4.3a** was removed using K_2CO_3 in methanol, yielding target compounds **4.1**-**4.3**. Detailed synthetic procedures are described in the experimental section (Chapter 7). All compounds were well characterised by ^{1}H NMR, ^{13}C NMR and mass spectroscopy. Purities were checked by LCMS and found to be greater than 95%. Table 4.6 reports the yields of isolated intermediates while Table 4.7 reports the isolated yields and melting points of the target compounds.

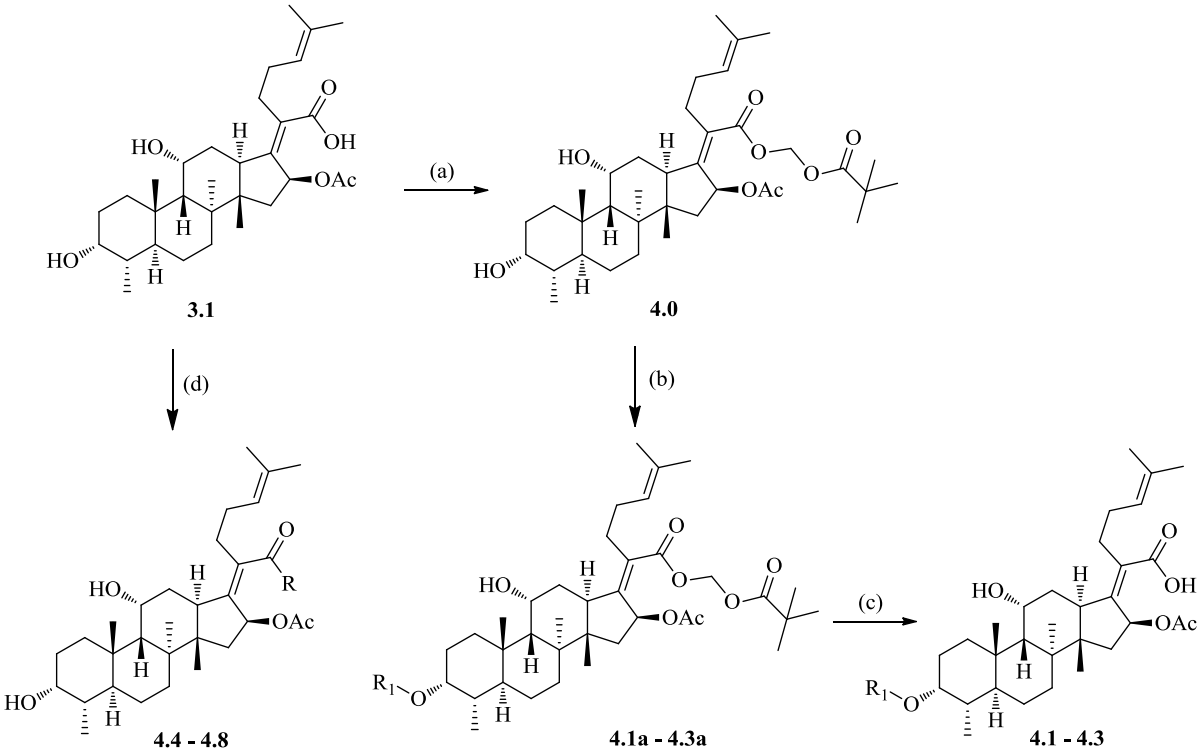

Scheme 4.1: (a) $ClCH_2OCOC(CH_3)_3$, Et_3N, DMF, 25 ^{o}C, 36 h; (b) R_1-Cl or R_1-Br, DIPEA, 16 h, 130 ^{o}C; (c) K_2CO_3, Methanol, 25 ^{o}C, 2.5 h; (d) R-NH_2, Et_3N, DCM, T3P (50% w/v solution in DMF), 0 ^{o}C - 25 ^{o}C, 5 h

Table 4.6: Yields of isolated intermediates

Compound	R_1	Yield (%)
4.0	H	93
4.1a	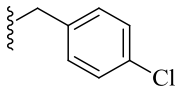	45
4.2a	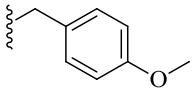	31
4.3a	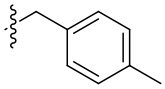	62

Table 4.7: Isolated yields and melting points of synthesized fusidic acid derivatives

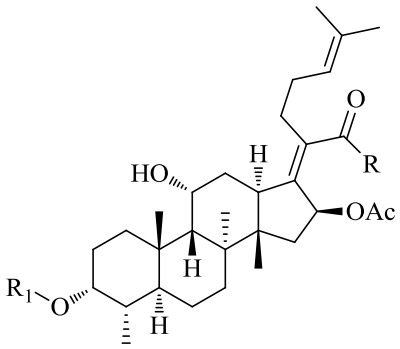

Compound	R	R_1	Yield* (%)	Mp (^oC)
4.1	OH	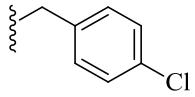	89	301-303
4.2	OH	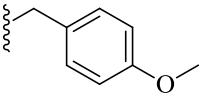	78	271-273
4.3	OH	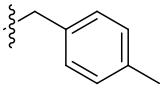	82	206-208
4.4	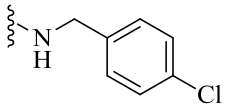	H	74	195-197
4.5	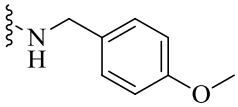	H	70	106-108
4.6	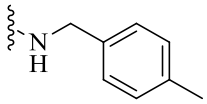	H	70	110-112
4.7	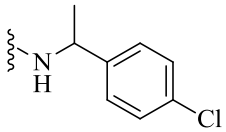	H	20	127-129
4.8	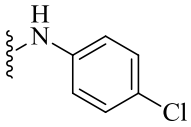	H	25	250-252

**Yields are reported for the final step of synthesis*

4.3.2.3 Antiplasmodial activity

Synthesized hit compounds were screened for *in vitro* antiplasmodial activity against the CQ-sensitive NF54 strain of *P. falciparum*. CQ and artesunate were used as the reference drugs. The most active compounds were screened for cytotoxicity against the Chinese Hamster Ovarian (CHO) mammalian cell line.

The antiplasmodial activity (IC_{50} value) of fusidic acid was found to be 59 μM. All synthesized compounds were found to be more active than fusidic acid with IC_{50} values ranging from 0.3 to 9.2 μM (Table 4.8). C-21 amide derivatives **4.4**-**4.8** displayed better activities than C-3 ether derivatives **4.1**-**4.3**. Among C-21 derivatives, the antiplasmodial activity of the compounds improved significantly when the $-CH_2$ of benzyl was removed (compound **4.8**) or substituted for a hydrogen atom (compound **4.7**). The IC_{50} values for these two compounds were also found to be close to those predicted by the pharmacophore model (Figure 4.6). However, IC_{50} values for other compounds were found to be higher than those predicted by the pharmacophore model. This suggests that a new series of hits with C-21 phenyl amide derivatives in place of the benzyl amide derivatives may be useful. However, a substituent at the 4-position of the benzyl group had no effect on antiplasmodial activity. Compounds **4.7** (IC_{50} 0.3 μM) and **4.8** (IC_{50} 0.7 μM) were found to be the most active. These two compounds also showed potent *in vitro* activity against the CQ-resistant K1 strain with IC_{50} values of 0.2 μM each and were also found to be non-cytotoxic on CHO cell line (Table 4.9).

4.3.2.4 Antimycobacterial activity

As mentioned in chapter 3, fusidic acid possesses potent *in vitro* antimycobacterial activity. Therefore, the compounds were additionally screened against the H37Rv strain of *Mtb* to determine their MIC_{99} values (Table 4.8). However, none of the compounds displayed antimycobacterial activity even at the highest concentrations tested (125 μM).

Table 4.8: *In vitro* antiplasmodial (NF54 strain) and antimycobacterial activity (H37Rv strain) of fusidic acid derivatives

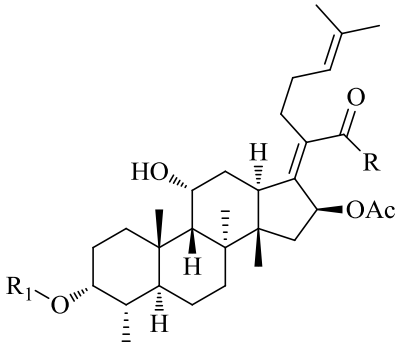

Compound	R	R_1	IC_{50} NF54 (µM)	MIC_{99} H37Rv (µM)
Fusidic acid 3.1	OH	H	59	0.6
4.1	OH	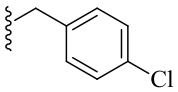	6.4	>125
4.2	OH	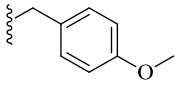	7.6	>125
4.3	OH	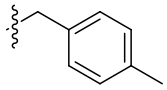	9.2	>125
4.4	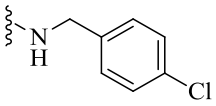	H	2.7	>125
4.5	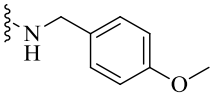	H	5.9	>125
4.6	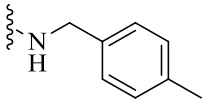	H	3.6	>125
4.7	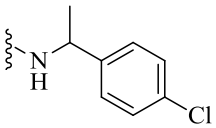	H	0.3	>125
4.8	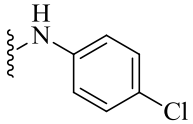	H	0.7	>125
	CQ		16 nM	
	Artesunate		4 nM	
	Rifampicin			0.005
	Kanamycin			3.2

Table 4.9: *In vitro* antiplasmodial activity and cytotoxicity of the most active hit compounds

Compound	IC_{50} NF54 (µM)	IC_{50} K1 (µM)	IC_{50} CHO (µM)
4.7	0.3	0.2	>153
4.8	0.7	0.2	134
CQ	16 nM	215 nM	
Artesunate	4 nM	2.6 nM	
Emetine			0.05

CQ = Chloroquine

4.4 2D and 3D similarity searches for the identification of fusidic acid-like compounds as antiplasmodial agents

The purpose of this study was to search for new fusidic acid-like compounds using 2D and 3D similarity search methods using an in-house database. For this, fusidic acid was used as the 'query compound' in order to search for similar compounds from the database. These compounds, according to the Similarity Property Principle, may show similar biological activity.

4.4.1 Materials and Methods

Database: The database used was built in-house. It consisted of 708 steroid-type natural products or their semisynthetic derivatives with defined chemical structures and stereochemistry.

2D fingerprints: Thirteen fingerprint methods are available in Discovery Studio 4.0: one MDL PublicKeys and 12 extended-connectivity fingerprints. Extended-connectivity fingerprints are circular topological fingerprints and their generation process systematically records the neighbourhood of each non-hydrogen atom into multiple circular layers up to a given bond diameter.[6] The extended connectivity fingerprints are further subgrouped into three ECFPs (ECFP_2, ECFP_4, ECFP_6), three FCFPs (FCFP_2, FCFP_4, FCFP_6), three ECFCs (ECFC_2, ECFC_4, ECFC_6) and three FCFCs (FCFC_2, FCFC_4, FCFC_6). ECFPs (atom-types) and FCFPs (functional class) consider only the presence or absence of a feature while ECFCs and FCFCs also consider as many times a feature appears, the numeric 2, 4 and 6 represent bond diameter length or maximum number of bonds considered. In this experiment, three fingerprints were generated using FCFP_2, ECFC_4 and FCFC_4 methods.

Ligand preparation: Ligands were prepared in order to remove any duplicates from the database using the method 'Prepare Ligands' in Discovery Studio 4.0. Ligands were prepared in 2D coordinates and ionisation/tautomerisation/isomerisation options were switched off.

Similarity coefficient: The Tanimoto coefficient (Tc) was calculated to measure similarity between the query and the database compounds. Tc is generally defined as the fraction of features common between two compounds to the total number of features present in two compounds. The value of Tc lies between 0 and 1 where 0 stands for 'not similar' and 1 stands for 'highly similar'.

3D shape: Besides structural/topological features, molecular shapes/conformations were also compared between the database molecules and the query molecule (Fusidic Acid). A 'Phase-Shape' screening was performed by Maestro 8.0, Schrodinger. According to the author[4], Phase-Shape considers volume overlapping of all the conformations of a molecule with the query molecule and returns an aligned structure, which shows the best overlap with the query. Four different Phase-Shape methods are available in this software: Shape_none, Shape_mmod., Shape_ele, Shape_pharm. Shape_none computes volume overlaps only and does not discriminate between the different atoms. Shape_mmod computes volume overlaps only between atoms that have the same macromodel atom type. Shape_ele and Shape_pharm also consider atom-related information in their calculations. Shape_ele computes volume overlaps only between atoms of the same element. Shape_pharm computes volume overlaps between atoms that have the same pharmacophore type such as acceptor and donor. Out of these four Phase-Shape screening methods, we chose Shape_ele and Shape_pharm methods.

Ligand preparation: The query compound, as well as all the database compounds, were prepared by 'LigPrep' in Maestro. OPLS_2005 was selected as force field. Epik was chosen to generate all possible protonation states of the compounds at a pH from 5.0 to 9.0. The remaining parameters were used at their default values. A conformational search was then performed using 'ConfGen' in the fast search mode and different energy conformations of the query and the database compounds were generated. Only the lowest energy conformation of the query was allowed to screen the database.

Similarity coefficient: Like Tanimoto, the value of 'shape similarity coefficient' also lies between 0 and 1 where 0 stands for 'not similar' and 1 stands for 'highly similar'.

4.4.2 Results and discussion

4.4.2.1 Similarity searching

A similarity search of an in-house database containing 708 steroid-type natural products or their semisynthetic derivatives with defined chemical structures and stereochemistry was performed using fusidic acid as a query compound. 2D as well as 3D similarity search methods were applied to find compounds with a similar structure or shape as that of fusidic acid. Instead of focussing on one single 2D or 3D method, a combination of these was preferred. Furthermore, instead of opting for one fingerprint method from 2D methods, a combination of FCFP_2, ECFC_4 and FCFC_4 was preferred. Similarly, a combination of Shape_ele and Shape_pharm was applied from 3D methods. A work flow leading to the selection of hit compounds from the database using the two similarity search protocols is shown in Figure 4.7. Twenty five top ranked compounds from each 2D fingerprint method were selected which makes Tc threshold values of 0.66, 0.60 and 0.92 for FCFP_2, ECFC_4 and FCFC_4, respectively. Similarly, 20 top ranked compounds from each 3D method were selected which makes a cut-off value of 0.69 for Shape_ele and 0.39 for Shape_pharm.

After combining all the top ranked compounds resulting from 2D/3D similarity searches and removing any duplicates found, Log P filter was applied to the compounds. Log P values were computed using StarDrop 5.5 and any compound having Log P > 5.5 owing to undesired lipophilicity was eliminated. Finally, 27 hit compounds were selected and screened for antiplasmodial activity.

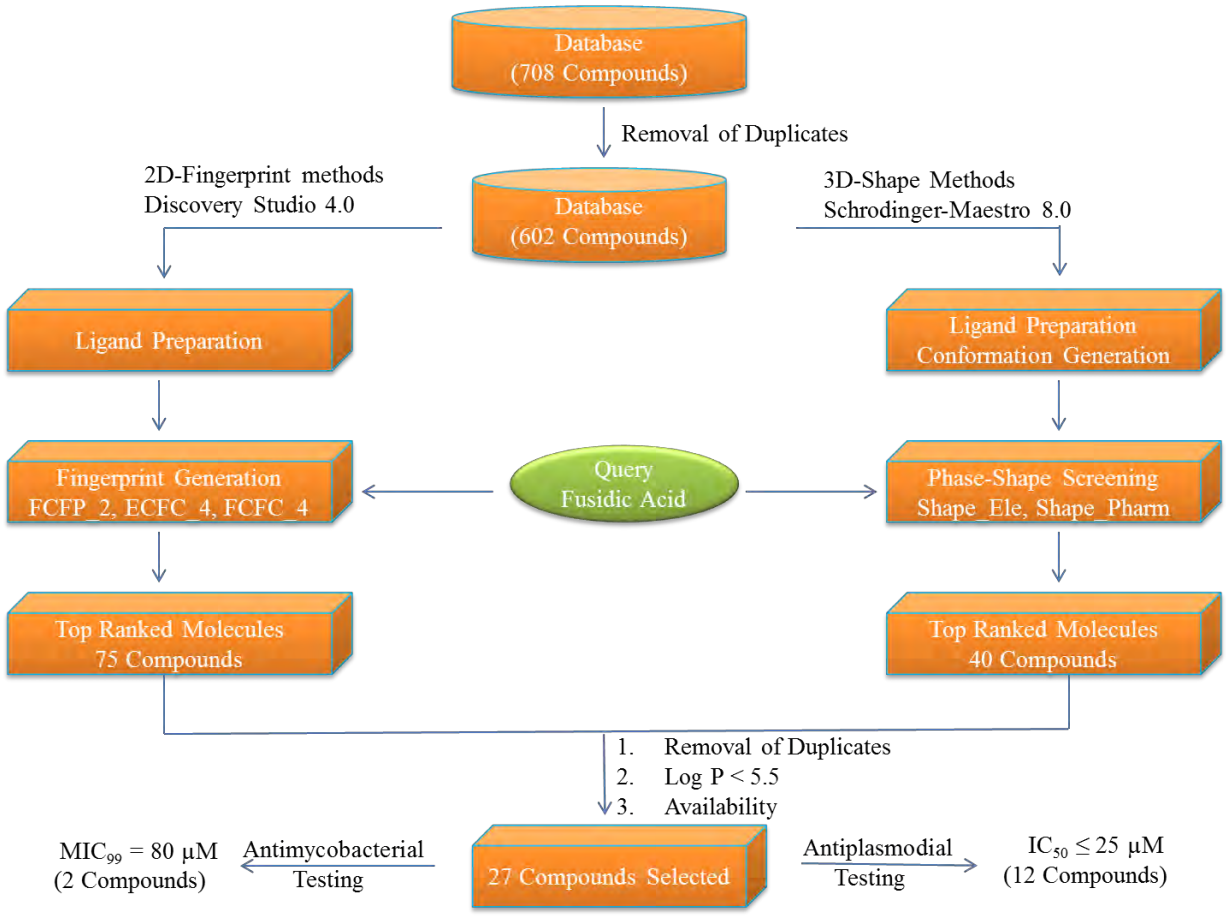

Figure 4.7: Flow diagram for *in silico* selection process

4.4.2.2 Antiplasmodial activity

Antiplasmodial activities (IC_{50} values) for all the compounds were determined against the NF54 strain of *P. falciparum*. IC_{50} value of fusidic acid (**3.1)** was found to be 59 µM (Table 4.10). Twelve out of 27 compounds were found to be active with IC_{50} < 25 µM. However, none of the compounds except fusidic acid was tested beyond this concentration. Compound **4.13** (Cucurbitacin B) was found to be the most active with an IC_{50} value of 1.4 µM. Five compounds, **4.9**, **4.11**, **4.21**, **4.30** and **4.32** exhibited activity below 10 µM with IC_{50} values of 2.9 µM**,** 1.8 µM, 3.4 µM**,** 7.0 µM and 6.0 µM, respectively. Six compounds (**4.12**, **4.23**, **4.24**, **4.25**, **4.27** and **4.35**) were found to have activity between 10-25 µM (Table 4.10). Similarity search methods provided 12 compounds, with superior antiplasmodial activity than fusidic acid. The most active compounds **4.9**, **4.11**, **4.13** and **4.21** were further screened for *in vitro* cytotoxicity against the CHO cell line and found to have IC_{50} values of 55.2 µM, 8.5 µM, 2.0 µM and 141 µM respectively (Table 4.10). An increase in cytotoxicity with increasing activities was observed in the three cucurbitacin derivatives **4.9 (**Cucurbitacin A), **4.11**

(Cucurbitacin C) and **4.13** (Cucurbitacin B) which indicate that an increasing activity from **4.9** to **4.11** to **4.13** may be due to increased cytotoxicity of these compounds.

4.4.2.3 Antimycobacterial activity

Since fusidic acid displays potent *in vitro* activity against *Mtb*, the compounds were also screened for antimycobacterial activity. MIC_{99} values of all the compounds were determined against the H37Rv strain of *Mtb* (Table 4.10). A maximum concentration limit was set at 160 μM. MIC_{99} of fusidic acid was found to be 0.6 μM. Only two compounds (**4.16** and **4.26)** were found to possess some antimycobacterial activity (80 μM each). Although none of the compounds showed promising antimycobacterial activity, **4.16** and **4.26** could be good candidates for chemical modifications to achieve derivatives with improved activities.

Table 4.10: Chemical structures and biological activities of the hit compounds

Compound	Structure	MIC_{99}H37Rv (µM)	IC_{50}NF54 (µM)	IC_{50}CHO (µM)
3.1	Fusidic Acid	0.6	59	194
4.9	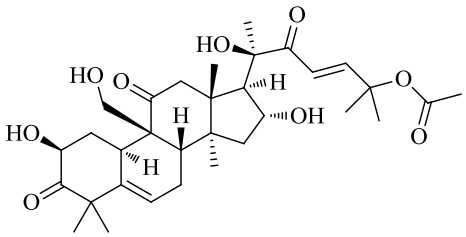	>160	2.9	55.2
4.10	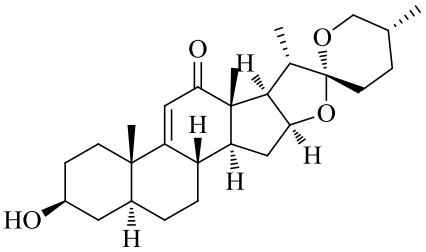	>160	>25	ND
4.11	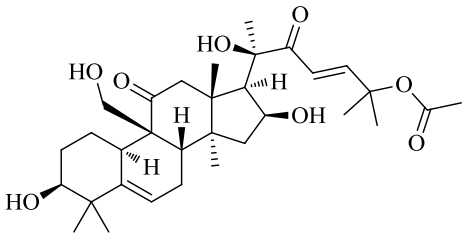	>160	1.8	8.5
4.12	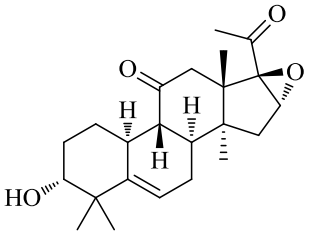	>160	24	ND
4.13	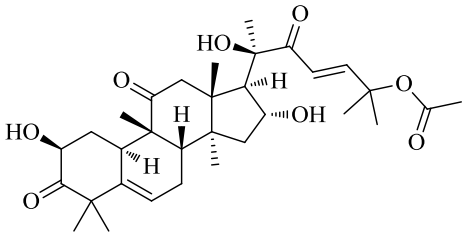	>160	1.4	2.0
4.14	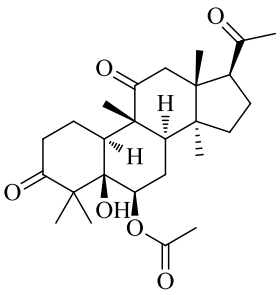	>160	>25	ND

Table 4.10: Continued…

Compound	Structure	MIC_{99}H37Rv (µM)	IC_{50}NF54 (µM)	IC_{50}CHO (µM)
4.15	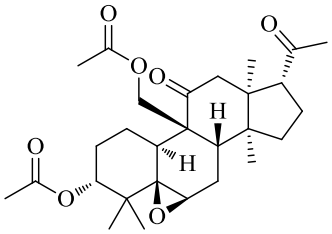	>160	>25	ND
4.16	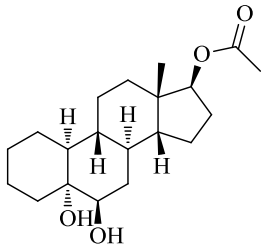	80	>25	ND
4.17	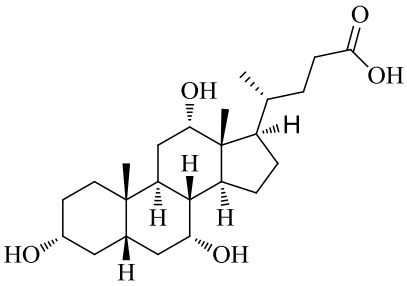	>160	>25	ND
4.18	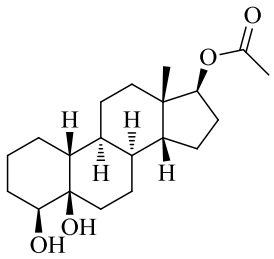	>160	>25	ND
4.19	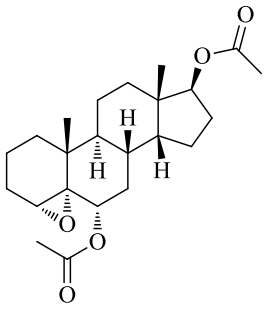	>160	>25	ND
4.20	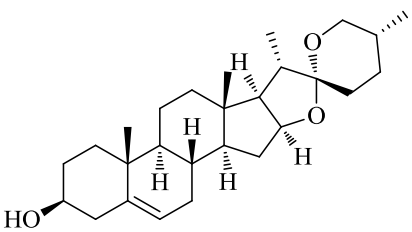	>160	>25	ND

Table 4.10: Continued…

Compound	Structure	MIC_{99}H37Rv (µM)	IC_{50}NF54 (µM)	IC_{50}CHO (µM)
4.21	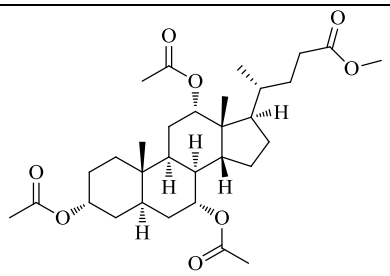	>160	3.4	141
4.22	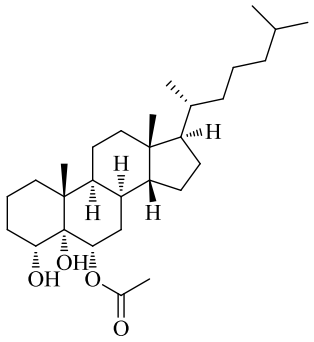	>160	>25	ND
4.23	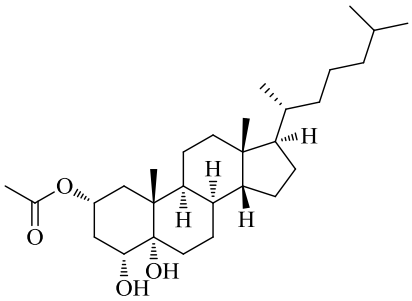	>160	13.0	ND
4.24	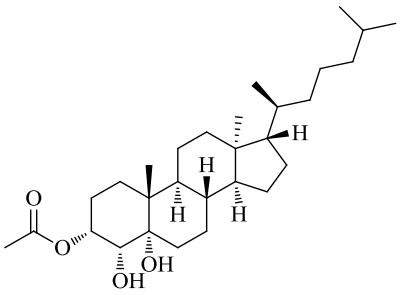	>160	21.4	ND
4.25	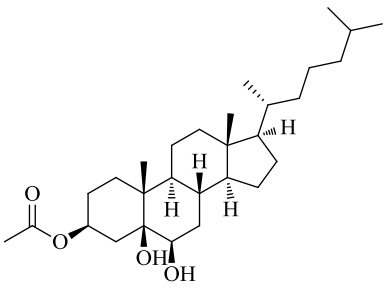	>160	18.6	ND
4.26	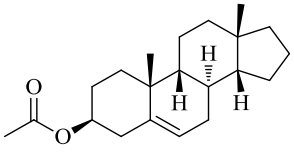	80	>25	ND

Table 4.10: Continued…

Compound	Structure	MIC_{99}H37Rv (µM)	IC_{50}NF54 (µM)	IC_{50}CHO (µM)
4.27	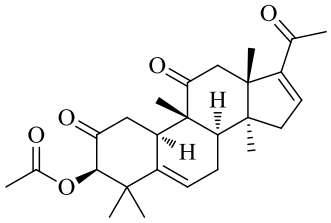	>160	19.8	ND
4.28	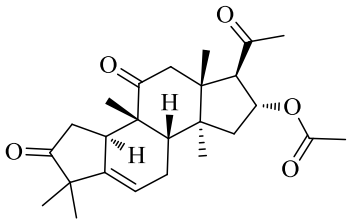	>160	>25	ND
4.29	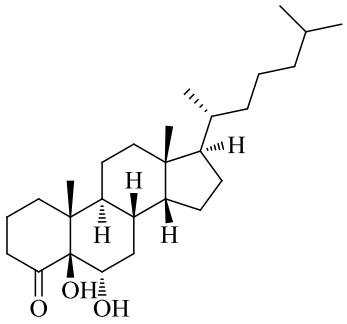	>160	>25	ND
4.30	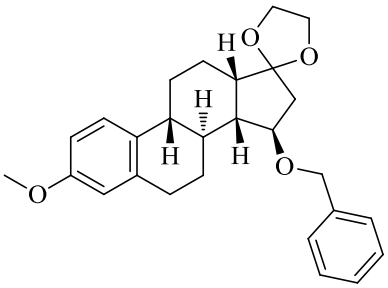	>160	7.0	ND
4.31	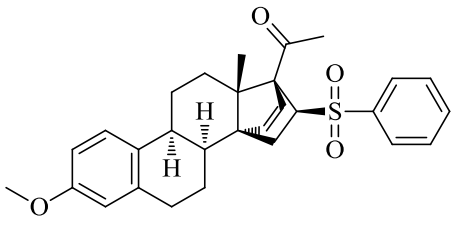	>160	>25	ND
4.32	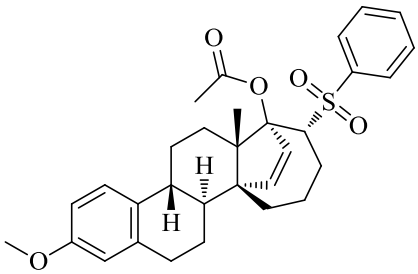	>160	6.0	ND

Table 4.10: Continued…

Compound	Structure	MIC_{99}H37Rv (µM)	IC_{50}NF54 (µM)	IC_{50}CHO (µM)
4.33	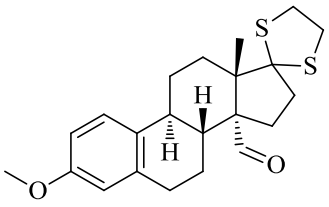	>160	>25	ND
4.34	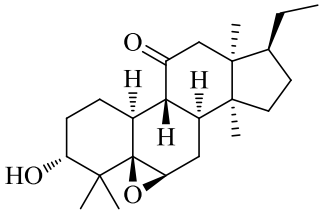	>160	>25	ND
4.35	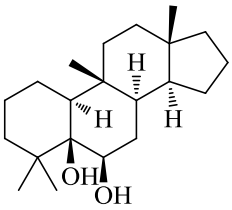	>160	15.80	ND
	CQ		16 nM	
	Artesunate		4 nM	
	Rifampicin	0.005		
	Kanamycin	3.2		
	Emetine			0.05

CQ = Chloroquine; ND = Not determined

4.5 Conclusion

Two different *in silico* approaches were used to design new fusidic acid derivatives. In one approach, a 3D-QSAR pharmacophore model based on the antiplasmodial activities of 61 fusidic acid derivatives was developed using the 'Hypogen' program of Discovery Studio 4.0. After validating the reliability of the pharmacophore model using different methods, it was then used as 3D-query for virtual screening to search for potential hits from a fusidic acid-based combinatorial library. Eight hit compounds were synthesized and evaluated for their antiplasmodial activity against the NF54 strain of *P. falciparum*. All compounds were found to be more active than fusidic acid. Compounds **4.7** and **4.8** displayed high activity with IC_{50} values of 0.3 µM and 0.7 µM, respectively. Compounds **4.7** and **4.8** were non-cytotoxic and

also displayed potent *in vitro* activity against the resistant strain (K1) with IC_{50} values of 0.2 μM each.

In another approach, 2D fingerprint and 3D shape similarity searches were performed on an in-house database using fusidic acid as the query compound. The aim of the study was to find structurally similar compounds with similar biological activities as that of fusidic acid. Selected hit compounds were tested for antiplasmodial as well as antimycobacterial activities. Twelve out of the 27 compounds were found to possess antiplasmodial activities (IC_{50} < 25 μM) superior to fusidic acid (IC_{50} 59 μM). Only two compounds (**4.16** and **4.26**) were found to possess some antimycobacterial activity (80 μM each). Although none of the compounds showed promising antimycobacterial activity, it may be beneficial to consider compounds **4.16** and **4.26** for chemical modification in an effort to generate derivatives with improved activities. Furthermore, the high structural similarity of these compounds indicates that they may have the same biological target as fusidic acid.

4.6 References

(1) Braga, R. C.; Alves, V. M.; Silva, A. C.; Nascimento, M. N.; Silva, F. C.; Liao, L. M.; Andrade, C. H. Virtual Screening Strategies in Medicinal Chemistry: The State of the Art and Current Challenges. *Curr. Top. Med. Chem.* **2014**, *14*, 1899–1912.

(2) Ghoneim, O. M.; Ibrahim, D. A.; El-deeb, I. M.; Ha, S.; Booth, R. G. A Novel Potential Therapeutic Avenue for Autism : Design , Synthesis and Pharmacophore Generation of SSRIs with Dual Action. *Bioorg. Med. Chem. Lett.* **2011**, *21*, 6714–6723.

(3) Lionta, E.; Spyrou, G.; Vassilatis, D. K.; Cournia, Z. Structure-Based Virtual Screening for Drug Discovery : Principles , Applications and Recent Advances. *Curr. Top. Med. Chem.* **2014**, *14*, 1923–1938.

(4) Hu, G.; Kuang, G.; Xiao, W.; Li, W.; Liu, G.; Tang, Y. Performance Evaluation of 2D Fingerprint and 3D Shape Similarity Methods in Virtual Screening. *J. Chem. Inf. Model.* **2012**, *52*, 1103–1113.

(5) *Concepts and Applications of Molecular Similarity*; Mark A. Johnson (Editor), G. M. M. (Editor), Ed.; **1990**.

(6) Rogers, D.; Hahn, M. Extended-Connectivity Fingerprints. *J. Chem. Inf. Model.* **2010**, *50*, 742–754.

(7) Good, A. C.; Richards, W. G. Excplicit Calculation of 3{D} Molecular Similarity. *Perspect. Drug Discovery Des.* **1998**, *9-11*, 321–338.

(8) Debnath, A. K. Generation of Predictive Pharmacophore Models for CCR5 Antagonists: Study with Piperidine- and Piperazine-Based Compounds as a New Class of HIV-1 Entry Inhibitors. *J. Med. Chem.* **2003**, *46*, 4501–4515.

(9) Maggiora, G.; Vogt, M.; Stumpfe, D.; Bajorath, J. Molecular Similarity in Medicinal Chemistry. *J. Med. Chem.* **2014**, *57*, 3186–3204.

Chapter 5

Synthesis, characterization and biological evaluation of metergoline derivatives

5.1 Introduction

This chapter describes the design and synthesis of new metergoline derivatives. It then reports and discusses the characterization of the target compounds by ^{1}H and ^{13}C NMR. It further discusses the antimycobacterial, antiplasmodial and cytotoxicity profiles of metergoline derivatives.

5.2 Rationale

As mentioned earlier in Chapter 2, metergoline is an antipsychotic drug belonging to the ergoline family of compounds. It is used in a variety of medical applications as a serotonin antagonist and dopamine agonist, both in human and veterinary medicine. A High-Throughput Screen (HTS) conducted by the Tuberculosis Antimicrobial Acquisition Coordinating Facility (TAACF) revealed that metergoline displays antimycobacterial activity with an IC_{90} = 6.0 μg/ml (15 μM) against the H37Rv strain of *Mtb*.[1] In addition, a quantitative HTS on a National Institute of Health (NIH) molecular library to obtain delayed death inhibitors of the apicoplast of *P. falciparum* showed that metergoline also displays antiplasmodial activity with an IC_{50} of 7.4 μM.[2]

The above-mentioned data was the basis for the hypothesis that structural modifications of metergoline might result in derivatives with improved antimycobacterial and/or antiplasmodial activity. Metergoline is attractive template for repositioning because it has previously not been explored within the context of TB or malaria. Optimised derivatives of this compound might reveal a novel mode of action that circumvents drug resistance which is one of the main focus areas of current antituberculosis and antimalarial drug development efforts.

5.3 Synthesis of metergoline derivatives

Metergoline can be chemically viewed as benzyl carbamate (CBz) protected amine with an ergoline backbone in which the benzyl carbamate group can be easily deprotected and replaced with a number of other functionalised aliphatic, aromatic and heteroaromatic moieties. In the present study, the ergoline backbone of metergoline was retained and the benzyl carbamate group was replaced with various aliphatic, aromatic and heteroaromatic amides.[3]

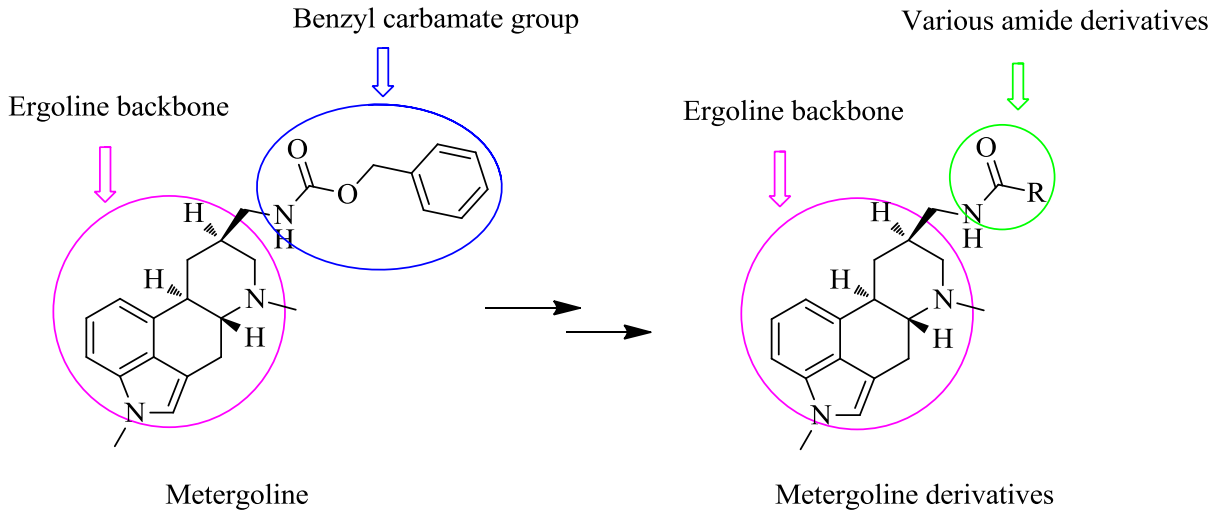

Figure 5.1: Synthetic strategy to obtain new metergoline derivatives[3]

Structural modification of metergoline (**5.1**) commenced with the removal of the benzyl carbamate group using Pd/C as a catalyst in methanol at 25 ^{o}C to afford the key amine intermediate **5.2** (Scheme 5.1). The intermediate **5.2** was then used as a scaffold for various amide derivatives, which were synthesized either through EDCI-HOBt coupling of the amine **5.2** with various carboxylic acids or by reacting it directly with respective acid chlorides (**5.6**, **5.7**, **5.15**, **5.20** and **5.22**) in the presence of an appropriate base. Substituted aromatic, heteroaromatic and aliphatic (acyclic and cyclic) carboxylic acids were used in these reactions to obtain the corresponding amide derivatives of metergoline and, subsequently, to study the effect of the amide moiety on the antimycobacterial and antiplasmodial activities. Table 5.1 shows isolated yields and melting points of synthesized metergoline derivatives.

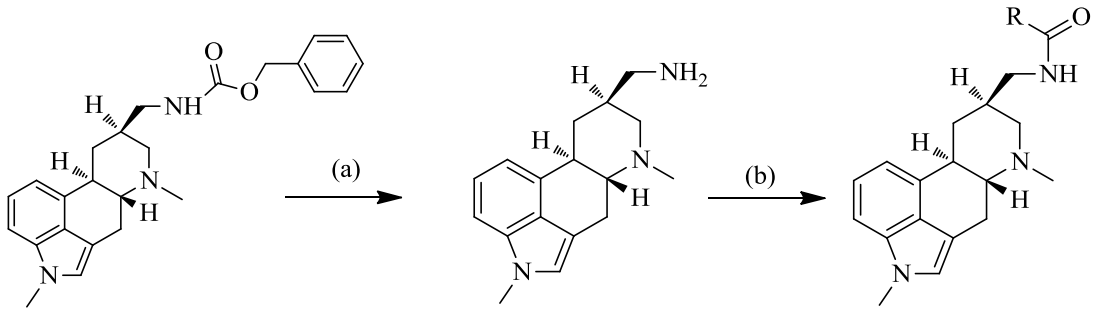

Scheme 5.1: (a) Methanol, H_2, 10% Pd/C (50% moisture), 25 ^oC, 16 h; (b) RCOOH, EDCI, HOBt, DIPEA, DCM, 25 ^oC, 24 h or RCOCl, DCM, 25 ^oC, 3 h

Table 5.1: Isolated yields and melting points of synthesized metergoline derivatives

Compound	R	Yield* (%)	Mp (^oC)	Compound	R	Yield* (%)	Mp (^oC)
5.1	Metergoline	-	148-150	**5.8**	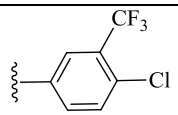	72	192-194
5.2[4]	Amine	95	151-153	**5.9**	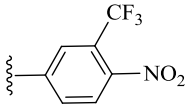	26	195-197
5.3	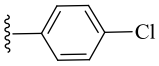	35	224-226	**5.10**[5]	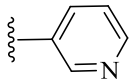	45	178-180
5.4	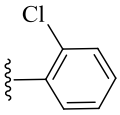	66	180-182	**5.11**[5]	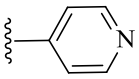	23	218-220
5.5	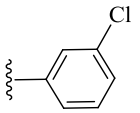	63	183-185	**5.12**[5]	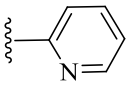	50	168-170
5.6	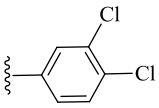	53	139-141	**5.13**	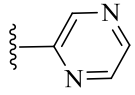	51	202-204
5.7	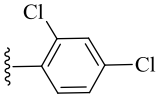	41	160-162	**5.14**	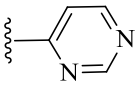	35	168-170

Table 5.1: Continued…

Compound	R	Yield* (%)	Mp (°C)	Compound	R	Yield* (%)	Mp (°C)
5.15[5]	CH_3	43	191-193	**5.21**	$(CH_2)_5CH_3$	49	146-148
5.16[5]	CH_2CH_3	67	185-187	**5.22**	$(CH_2)_6CH_3$	53	141-143
5.17	$(CH_2)_2CH_3$	71	169-171	**5.23**	$(CH_2)_8CH_3$	64	138-140
5.18	$C(CH_3)_3$	50	102-104	**5.24**	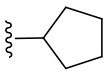	63	145-147
5.19	$(CH_2)_3CH_3$	91	166-168	**5.25**	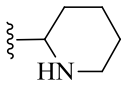	41	124-126
5.20	$(CH_2)_4CH_3$	52	133-135				

** Yields are reported for the final step of synthesis*

5.4 Mechanism of EDCI-HOBt mediated amide coupling

EDCI [1-Ethyl-3-(3-dimethylaminopropyl)carbodiimide] is a water soluble carbodiimide which is commercially available as an HCl salt. It is commonly used as coupling reagent for amide bond formation between a carboxylic acid and an amine. HOBt (1-Hydroxybenzotrizole) is commercially available as monohydrate and is the most usual combination with EDCI. The mechanism of coupling through EDCI-HOBt is well-known and widely reported in the literature.[6] Reaction of a carboxylic acid (RCOOH) with an EDCI is believed to involve a labile O-acylisourea, which reacts with 1 eq. of HOBt to form an active ester of carboxylic acid. EDCI is converted into a urea by-product. The active ester then reacts with 1 eq. of an amine (amine intermediate **5.2** in this case) to form the corresponding amide derivative. HOBt is recovered in the end. This mechanism is described in Figure 5.2.

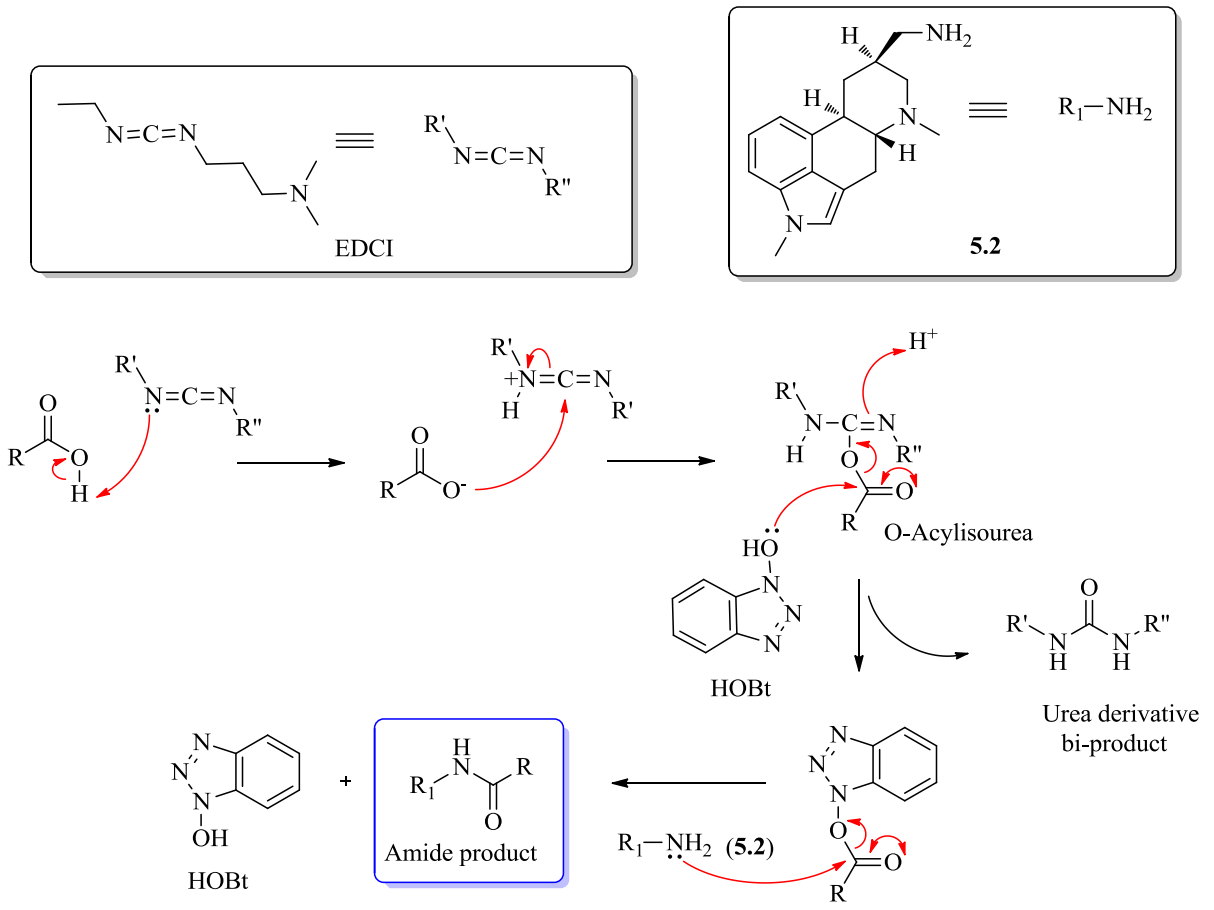

Figure 5.2: Known mechanism for an EDCI-HOBt coupling reaction[7]

5.5 Characterization of the synthesized metergoline derivatives

All synthesized metergoline derivatives were characterized using ^{1}H NMR, ^{13}C NMR and mass spectroscopy (MS). Proton assignments were made with the help of ^{1}H-^{1}H COSY spectrum.

All synthesized metergoline derivatives were obtained from a common amine intermediate **5.2**. ^{1}H NMR of the intermediate was recorded in $CDCl_3$ at 400 MHz and is displayed in Figure 5.3. The spectrum shows 4 characteristic signals corresponding to the indole region: a triplet at 7.18 ppm, two doublets at 7.10 and 6.92, and a singlet at 6.72 ppm. Two singlets at 3.74 and 2.52 ppm correspond to two methyl groups attached to N1 and N6 nitrogen atoms, respectively, with the methyl group at N1 being more downfield as it is attached to an aromatic nitrogen. A broad singlet at 2.37 ppm corresponds to NH_2 protons while protons of $-CH_2$ (H-17) attached to NH_2 appear in the region between 2.80-2.69 ppm. Other aliphatic protons displayed signals in the region 1.00-3.50 ppm. This NMR spectral data was confirmed by comparing with that reported in the literature.[4] Additionally, the mass spectrum

of **5.2** displayed a base peak at 270 [M+H], which further supported the formation of this intermediate.

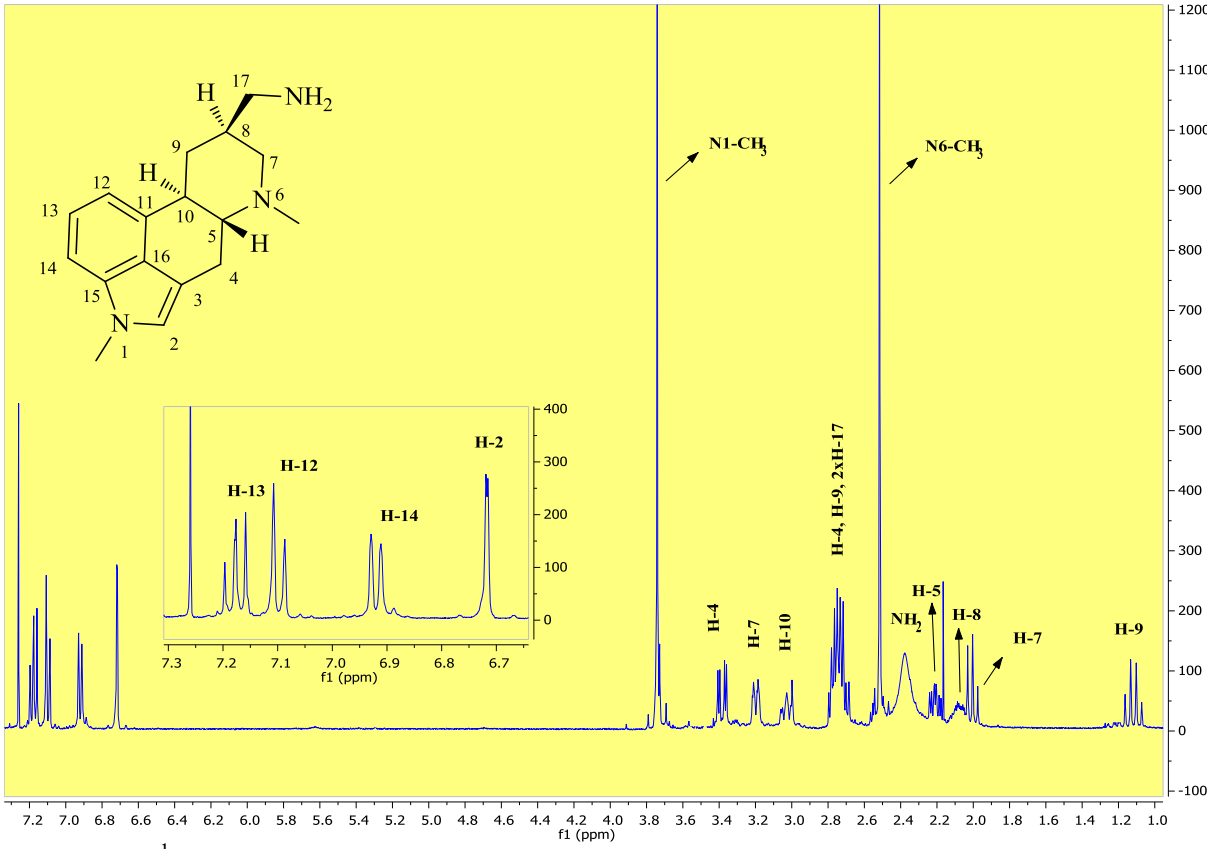

Figure 5.3: ^{1}H NMR spectrum ($CDCl_3$, 400 MHz) of the intermediate **5.2**

The intermediate **5.2** was reacted with various carboxylic acids or acid chlorides to obtain the target compounds. The ^{1}H NMR of one of the target compounds (**5.5**) is shown in Figure 5.4. Disappearance of NH_2 protons at 2.37 ppm (Figure 5.3) and appearance of a broad triplet at 6.48 ppm indicated the formation of an amide bond. The formation of this amide bond was also accompanied by a downfield shift of H-17 protons from 2.80-2.69 ppm (in **5.2**) to 3.50-3.46 ppm (in **5.5**). The appearance of four additional signals in the aromatic region of **5.5** indicated incorporation of the 3-chlorophenyl moiety. The protons of the 3-chlorophenyl moiety also showed *meta* coupling in addition to *ortho* coupling. Instead of appearing as a singlet, H-18 appeared as a triplet with J = 1.8 Hz due to *meta* coupling with H-19 and H-21. Similarly, H-19 appeared as doublet of doublet of doublets (ddd) with J = 8.0, 2.1, 1.1 Hz due to one *ortho* coupling with H-20 and two *meta* couplings with H-18 and H-21. H-21also appeared as ddd with J = 7.7, 1.7, 1.1 Hz due to one *ortho* coupling with H-20 and two *meta* couplings with H-18 and H-19. H-20 appeared as triplet with J = 7.8 Hz due to two *ortho* protons H-19 and H-21. All other proton signals showed a chemical shift similar to those observed in the intermediate **5.2**.

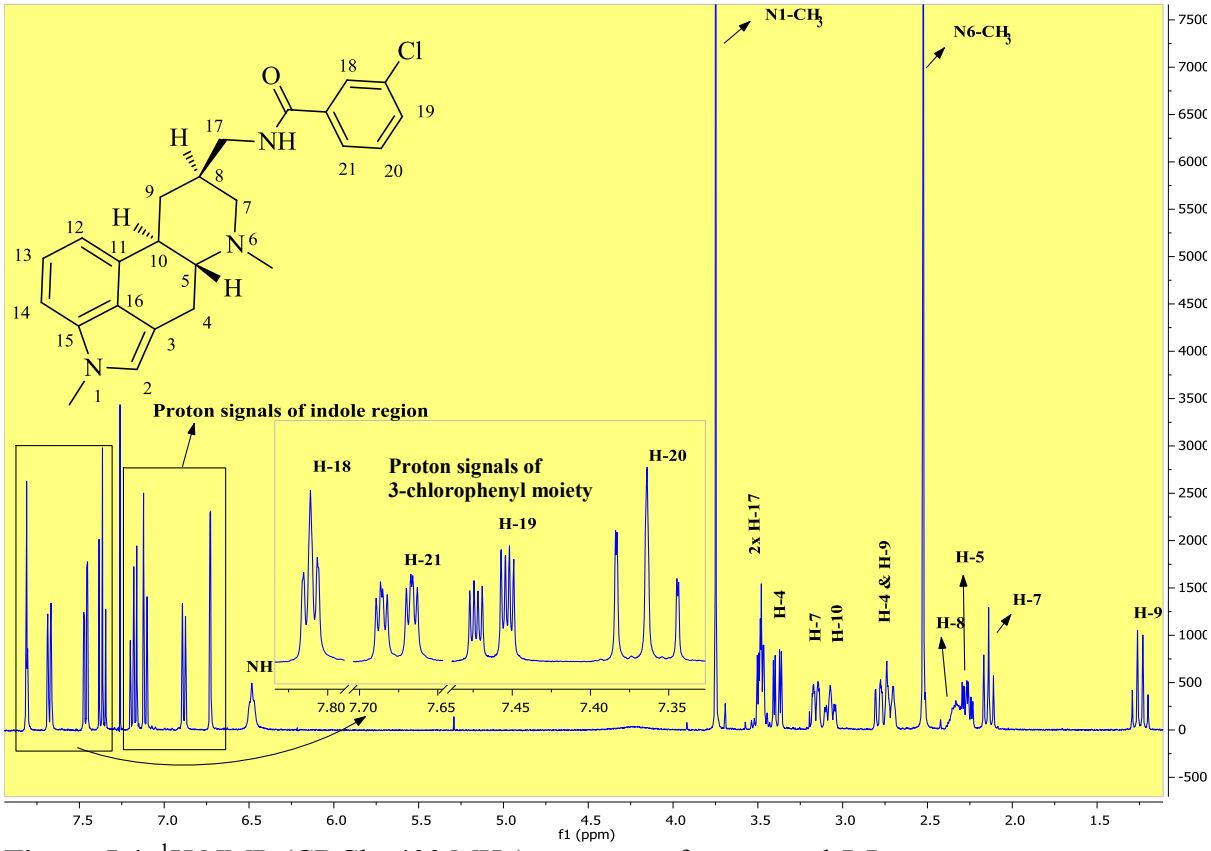

Figure 5.4: ^{1}H NMR ($CDCl_3$, 400 MHz) spectrum of compound **5.5**

Furthermore, the ^{13}C NMR spectrum showed a signal at δ 166.3 ppm indicating the presence of a carbonyl carbon in the structure (Figure 5.5). The appearance of six additional signals in the aromatic region at 136.5, 133.1, 131.5, 129.9, 127.3 and 124.9 ppm supported the incorporation of the 3-chlorophenyl moiety. Overall, the ^{13}C NMR of **5.5** depicted 24 distinct signals corresponding to 24 carbon atoms. Additionally, the mass spectrum displayed a mass peak at 408 [M+H], as expected, which further supported the formation of **5.5**.

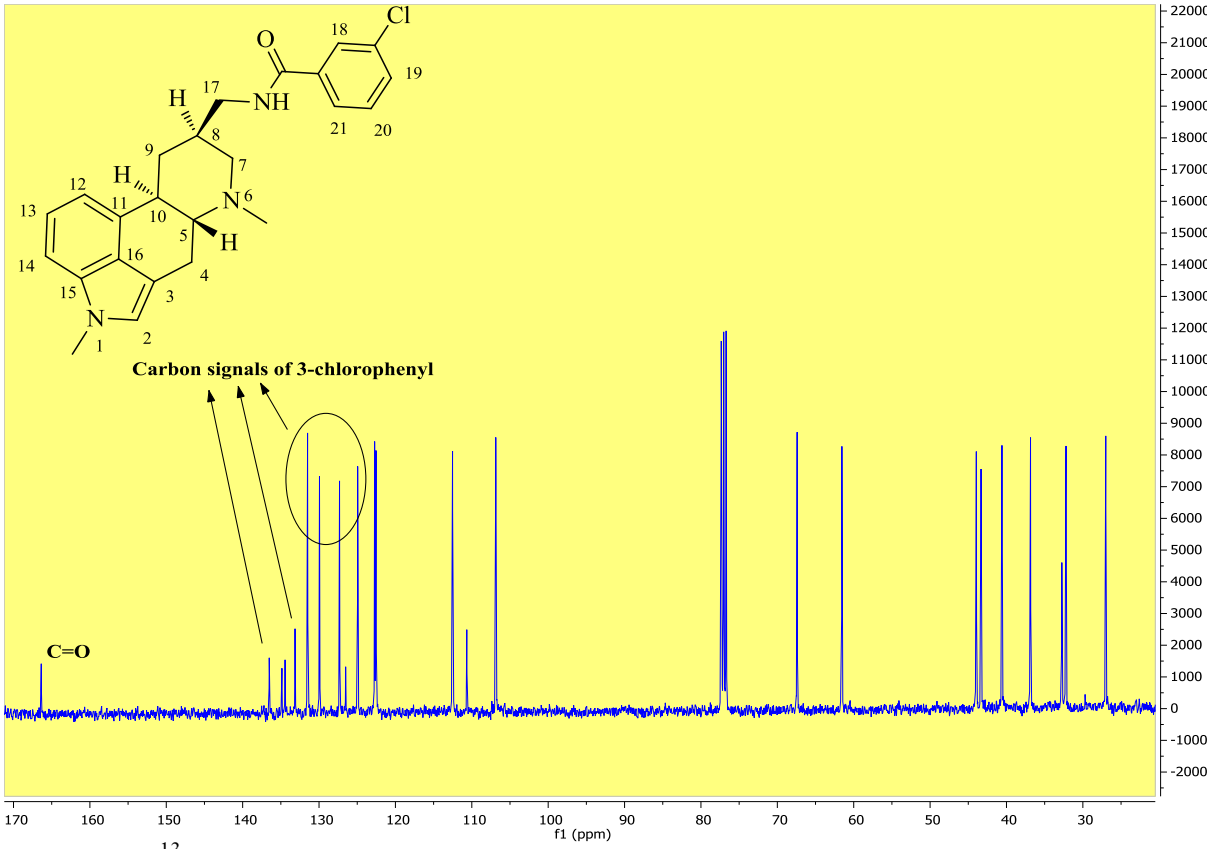

Figure 5.5: ^{13}C NMR ($CDCl_3$, 100 MHz) spectrum of compound **5.5**

Target compounds **5.3**-**5.14** depicted a similar pattern to **5.5** in their respective ^{1}H and ^{13}C NMR spectra. In compounds **5.15**-**5.25**, an aliphatic moiety was incorporated in place of the aromatic moiety and therefore, their ^{1}H NMR spectra displayed additional signals in the aliphatic region. Similar changes were also observed in the respective ^{13}C NMR spectra. However, the fragmentation pattern in the mass spectra remained unchanged for all target compounds.

The ^{1}H NMR data for one of the aliphatic amides (**5.22**) is shown in Figure 5.6. The disappearance of NH_2 protons at 2.37 ppm (Figure 5.3) and appearance of a broad triplet at 5.60 ppm in **5.22** indicated the formation of an amide bond, which was also accompanied by a downfield shift of H-17 protons from 2.80-2.69 ppm (in **5.2**) to 3.30-3.26 ppm (in **5.22**). Furthermore, the appearance of two triplets at 2.21 (J = 7.4 Hz, 2H, 2×H-18) and 0.88 (J = 6.9 Hz, 3×H-24), and two multiplets at 1.70-1.62 (m, 2H, 2×H-19) and 1.36-1.25 (m, 8H, 2×H-20, 2×H-21, 2×H-22, 2×H-23), indicated incorporation of the n-octyl group. All other proton signals showed a chemical shift similar to those observed in the intermediate **5.2**.

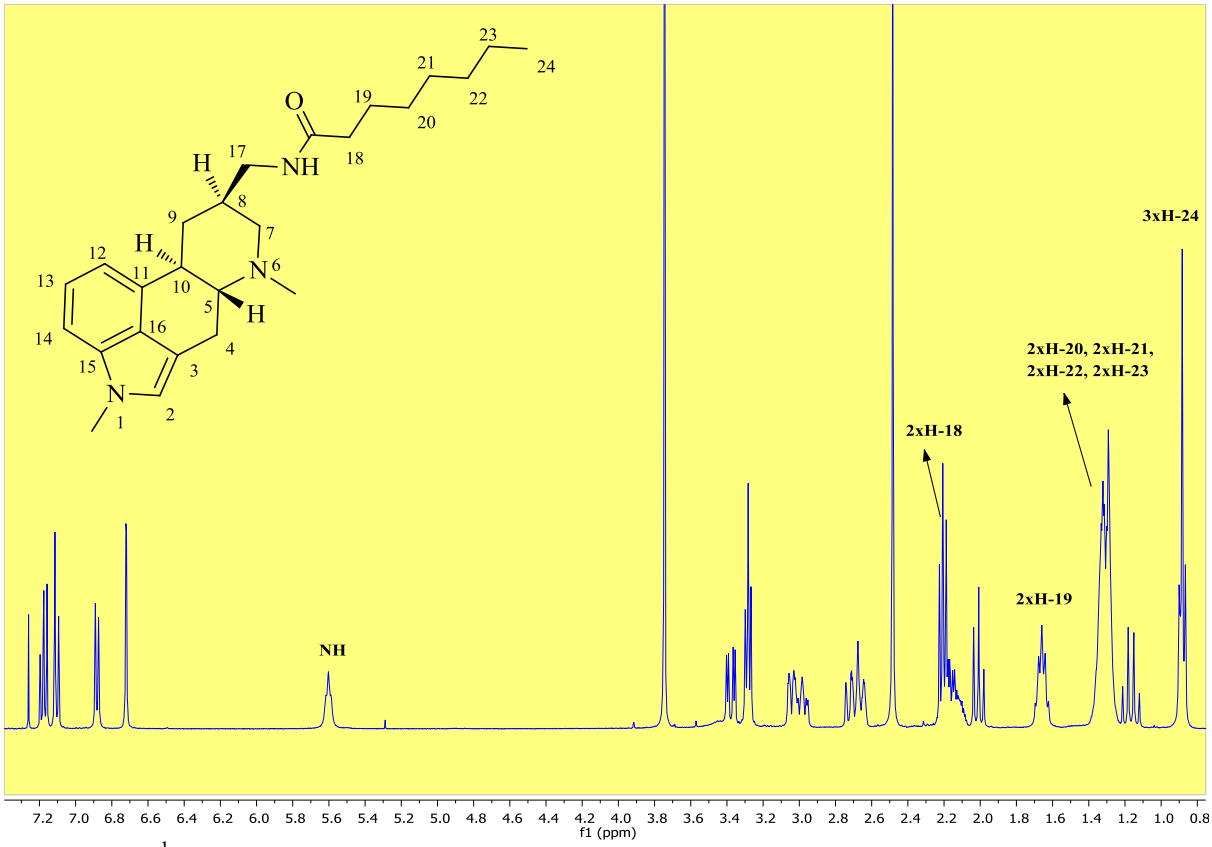

Figure 5.6: ^{1}H NMR ($CDCl_3$, 400 MHz) spectrum of compound **5.22**

The ^{1}H NMR spectrum was further supported by the ^{13}C NMR spectrum, which depicted a signal at 173.2 ppm indicating the presence of carbonyl carbon in the structure (Figure 5.7). Appearance of seven additional signals in the aliphatic region at 36.9, 31.7, 29.3, 29.0, 25.8, 22.6 and 14.0 ppm supported the incorporation of an n-octyl group. Overall, the ^{13}C NMR of **5.22** depicted 25 distinct signals corresponding to 25 carbon atoms. Additionally, the mass spectrum showed a mass peak at 396 [M+H], as expected, which further supported the formation of **5.22**.

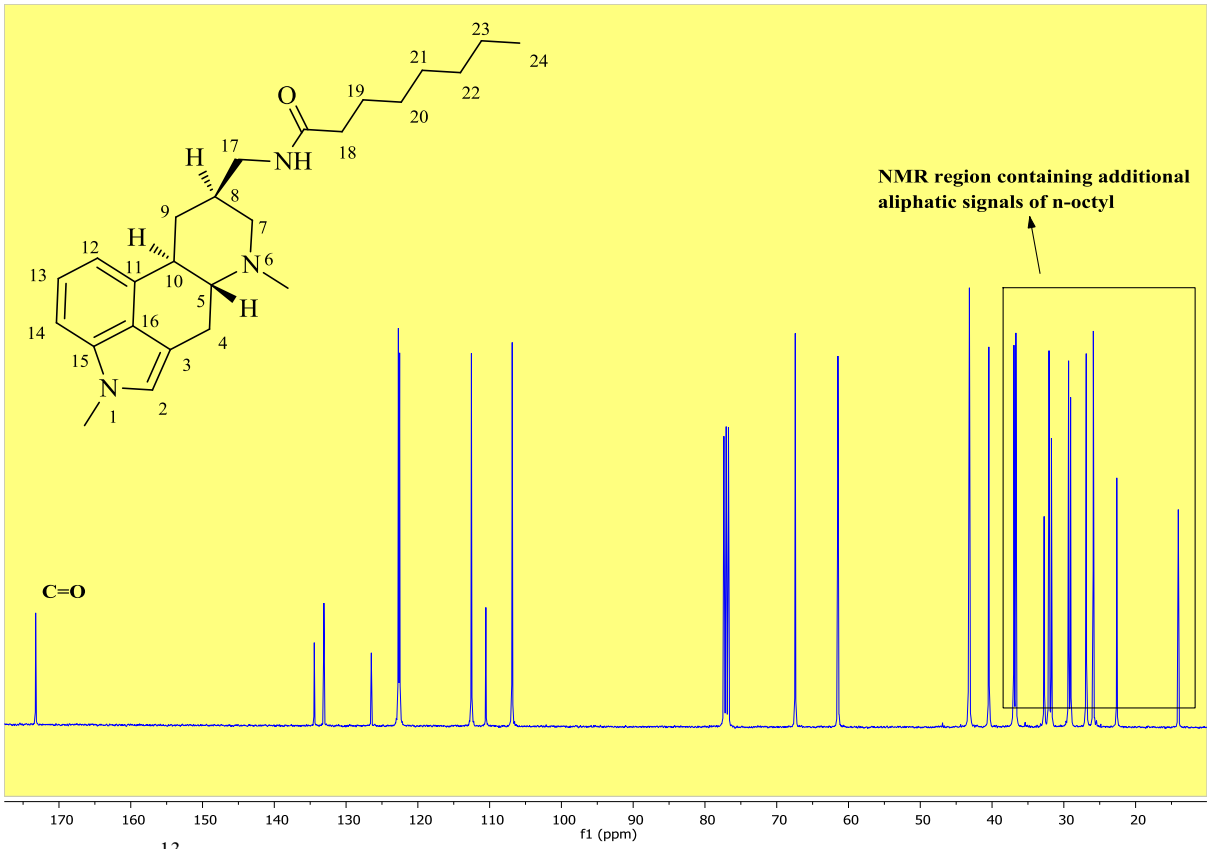

Figure 5.7: ^{13}C NMR ($CDCl_3$, 100 MHz) spectrum of compound **5.22**

5.6 Biological results and discussion

All synthesized compounds were evaluated for their antimycobacterial and antiplasmodial activity, as well as for cytotoxicity.

5.6.1 Antimycobacterial activity

Compounds were screened *in vitro* against the H37Rv strain of *Mtb* at the National Institute of Allergy and Infectious Diseases (NIAID) of the National Institute of Health (NIH). The MIC_{99} was determined for each compound. A maximum concentration limit was set at 50 µM. Rifampicin and kanamycin, were used as reference drugs.

Nine out of 23 amide derivatives exhibited MIC_{99} values ranging from 9.4 to 37 µM (Table 5.2). The MIC_{99} of metergoline (**5.1**) was found to be 25 µM in the same assay. Intermediate **5.2**, obtained after the removal of benzyl carbamate group from metergoline (Scheme 5.1), was also tested and found to be inactive, suggesting the importance of the benzyl carbamate group of metergoline for activity. Among mono-substituted amide derivatives (**5.3**-**5.9**), 3- and 4-chloro derivatives displayed superior activity (MIC_{99} 37 µM) relative to the 2-chloro derivative, which was found to be inactive at 50 µM. These results indicated a preference for *meta*- and *para*-substitutions over *ortho* substitution. Among di-substituted derivatives,

compound **5.8** (3-CF_3,4-Cl) was found to be the most active with a MIC_{99} of 19 μM. With the exception of **5.8**, all other aromatic amide derivatives displayed inferior activity relative to metergoline. Heteroaromatic amides (**5.10**-**5.14**) displayed no activity at the highest concentration tested.

Aliphatic amide derivatives with varying carbon chain lengths (**5.15**-**5.23**, Table 5.2) showed varying activity. Derivatives with short (from acetamide **5.15** to butanamide **5.17**), branched (*tertiary* butanamide **5.18**) and medium (pentanamide **5.19** and hexanamide **5.20**) carbon chain lengths were found to be inactive. However, as the carbon chain length was increased further (**5.21**-**5.23**), activity also improved. Octanamide **5.22** (MIC_{99} 19 μM) and decanamide **5.23** (MIC_{99} 9.4 μM) derivatives were found to have superior activity relative to metergoline. Compound **5.23** was the least cytotoxic as indicated by a high IC_{50} value of 86.6 μM against the CHO cell line as compared to metergoline (IC_{50} 16.6 μM). Cyclopentyl amide (**5.24**) and heterocyclic alkyl amide (**5.25**) derivatives were in active at the highest concentration tested (MIC_{99} > 50 μM).

To summarise, decanamide **5.23** with an MIC_{99} 9.4 μM was found to be the most active among all amide derivatives of metergoline and also displayed less cytotoxicity (IC_{50} CHO 86.6 μM) as compared to metergoline. Two more compounds, octanamide **5.22** and 3-CF_3,4-Cl-disustituted phenyl amide **5.8** with MIC_{99} of 19 μM each, also displayed better activity than metergoline but were found to be cytotoxic (IC_{50} CHO 4.6 and 4.4 μM, respectively). Data concerning the antimycobacterial activity of metergoline derivatives suggest that the benzyl carbamate group of metergoline is not necessary for activity.

Table 5.2: *In vitro* antimycobacterial activity (H37Rv strain), antiplasmodial activity (NF54 strain) and cytotoxicity (CHO cell lines) of metergoline derivatives

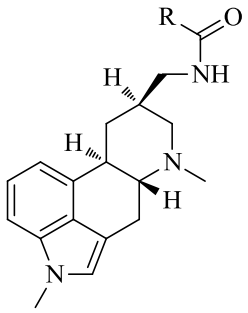

Compound	R	MIC_{99} H37Rv (µM)	IC_{50} NF54 (µM)	IC_{50} CHO (µM)	SI*
5.1	Metergoline	25	3.7	16.6	4.5
5.2	Amine	>50	3.6	26.1	7.0
5.3	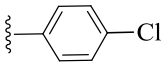	37	1.3	4.3	3.0
5.4	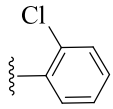	>50	14.6	25.0	2.0
5.5	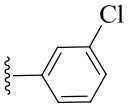	37	4.9	4.7	1.0
5.6	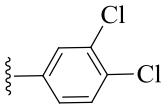	25	4.8	3.8	1.0
5.7	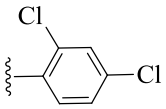	37	8.3	7.5	1.0
5.8	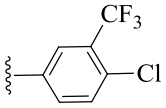	19	5.3	4.4	0.8
5.9	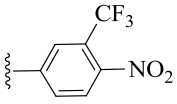	25	2.5	11.2	4.5
5.10	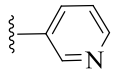	>50	17.4	162	9.0

Table 5.2: Continued…

Compound	R	MIC_{99} H37Rv (µM)	IC_{50} NF54 (µM)	IC_{50} CHO (µM)	SI*
5.11	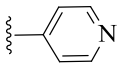	>50	17.5	161	9.0
5.12	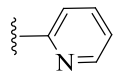	>50	11.4	112	10
5.13	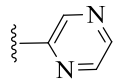	>50	8.4	163.5	20
5.14	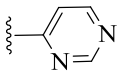	>50	27.4	ND	ND
5.15	CH_3	>50	199	ND	ND
5.16	CH_2CH_3	>50	40.3	ND	ND
5.17	$(CH_2)_2CH_3$	>50	32.1	ND	ND
5.18	$C(CH_3)_3$	>50	89.1	ND	ND
5.19	$(CH_2)_3CH_3$	>50	18.7	105.0	6.0
5.20	$(CH_2)_4CH_3$	>50	28.6	ND	ND
5.21	$(CH_2)_5CH_3$	37	9.1	8.9	1.0
5.22	$(CH_2)_6CH_3$	19	3.9	4.6	1.0
5.23	$(CH_2)_8CH_3$	9.4	5.2	86.6	17
5.24		>50	4.3	143.6	33
5.25	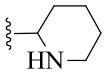	>50	1.2	16.6	13
	Rifampicin	0.005			
	Kanamycin	3.2			
	CQ		16 nM		
	Artesunate		4 nM		
	Emetine			0.05	

**SI = (selectivity index) = IC_{50}CHO/IC_{50}NF54; ND = Not determined; CQ = Chloroquine*

5.6.2 Antiplasmodial activity

As mentioned earlier, metergoline showed antiplasmodial activity (IC_{50} 7.4 μM) in a quantitative HTS conducted by the NIH. This prompted the evaluation of all synthesized metergoline derivatives for *in vitro* antiplasmodial activity against the CQ-sensitive NF54 strain of *P. falciparum*. CQ and artesunate were used as the reference drugs (Table 5.2).

The IC_{50} of metergoline was found to be 3.7 μM with a selectivity index (SI) value of 4.5. The amine intermediate **5.2**, obtained after the removal of benzyl carbamate group from metergoline, showed activity (IC_{50} 3.6 μM) comparable to that of metergoline (IC_{50} 3.7 μM), suggesting that the benzyl carbamate group of metergoline may not contribute to the observed antiplasmodial activity. Most of the amide derivatives exhibited micromolar potencies, with 17 of the 23 compounds displaying IC_{50} values between 1.2 μM and 20 μM (Table 5.2). Introduction of the 4-chlorophenyl group as in compound **5.3** resulted in improved antiplasmodial activity (IC_{50} 1.3 μM) relative to metergoline. The activity of this derivative was compared to that of its regioisomers [2-chloro **5.4** (IC_{50} 14.6 μM) and 3-chloro **5.5** (IC_{50} 4.9 μM)], as well as with dichloro-substituted amide derivatives [3,4-dichloro **5.6** (IC_{50} 4.8 μM) and 2,4-dichloro **5.7** (IC_{50} 8.3 μM)]. Compound **5.3** was found to be the most active among them. These results indicated a preference for the *para*-substituted phenyl ring over the *ortho*-, *meta*- and di-substituted phenyl rings. Further, among di-substituted aromatic amides, 3-CF_3,4-NO_2 substituted derivative **5.9** (IC_{50} 2.5 μM) displayed a slightly improved activity and comparable cytotoxicity to metergoline. Heteroaromatic amides (**5.10**-**5.14**) showed relatively higher IC_{50} values ranging from 8.4 to 27.4 μM (Table 5.2). These results indicated that heteroaromatic amides are not tolerated.

Short to medium chain aliphatic amide derivatives, **5.15**-**5.20**, showed much lower antiplasmodial activity as compared to metergoline (Table 5.2). However, as the chain length was increased further, **5.21**-**5.23**, the activity also increased and octanamide derivative **5.22** was found to be the most active with an IC_{50} value of 3.9 μM, which is comparable to metergoline. The cyclopentyl amide derivative **5.24** also showed activity similar to metergoline (IC_{50}, 4.3 μM) and had a much better SI value of 33. Heterocyclic alkyl amide **5.25** showed the best activity (IC_{50} 1.2 μM) when compared to metergoline and all other derivatives, with a SI of 13.

In summary, removal of the benzyl carbamate group from metergoline did not alter its antiplasmodial activity, suggesting that the benzyl carbamate group is not required for

antiplasmodial activity. Most of the amide moieties substituted for the benzyl carbamate group resulted in either comparable or reduced activities. However, three derivatives **5.3**, **5.9** and **5.25** resulted in improved activities. The derivative **5.25** was found to be the most active of all with an IC_{50} of 1.2 μM with a SI value of 13.

5.7 Conclusion

A series of new metergoline derivatives was synthesized to establish the potential of metergoline to act as a template for new antimycobacterial and/or antiplasmodial derivatives. In these semisynthetic derivatives, the ergoline part of metergoline was retained and the benzyl carbamate group was replaced with various aromatic, heteroaromatic and aliphatic amides. All synthesized compounds were evaluated for antimycobacterial activity against the H37Rv strain of *Mtb*, antiplasmodial activity against the NF54 strain of *P. falciparum*, as well as cytotoxicity against the CHO cell line.

Nine out of 23 amide derivatives exhibited antimycobacterial activity (MIC_{99} < 50 μM). 3-CF_3,4-Cl-disustituted aromatic amide **5.8** (MIC_{99} 19 μM), octanamide **5.22** (MIC_{99} 19 μM), and decanamide **5.23** (MIC_{99} 9.4 μM) showed higher antimycobacterial activity than metergoline (MIC_{99} 25 μM). Decanamide derivative **5.23** was found to have superior antimycobacterial activity with an improved cytotoxicity profile as compared to metergoline and all other derivatives. Most of these amide derivatives also exhibited micromolar potencies against the NF54 strain of *P. falciparum*, with 17 of the 23 compounds having IC_{50} values between 1.2 μM and 20 μM. Three derivatives **5.3**, **5.9** and **5.25** displayed improved antiplasmodial activities as compared to metergoline. Compound **5.25** was found to be the most active of all with an IC_{50} 1.2 μM. This compound also had an encouraging SI value of 13.

The antimycobacterial and antiplasmodial data suggests that the benzyl carbamate group of metergoline is not required for activity and its substitution with other moieties may result in compounds with improved antimycobacterial and/or antiplasmodial activity. Over all, this work shows the potential of metergoline for repositioning in TB and /or malaria via medicinal chemistry approaches.

5.8 References

(1) National Center for Biotechnology Information. PubChem BioAssay Database; AID=1332, https://pubchem.ncbi.nlm.nih.gov/bioassay/1332 (accessed May 10, 2016).

(2) National Center for Biotechnology Information. PubChem BioAssay Database; AID=488752, https://pubchem.ncbi.nlm.nih.gov/bioassay/488752 (accessed May 10, 2016).

(3) Singh, K.; Kaur, G.; Mjambili, F.; Smith, P. J.; Chibale, K. Synthesis of Metergoline Analogues and Their Evaluation as Antiplasmodial Agents. *Med.Chem.Commun.* **2014**, *5*, 165–170.

(4) Dosa, P. I.; Ward, T.; Walters, M. A.; Kim, S. W. Synthesis of Novel Analogs of Cabergoline: Improving Cardiovascular Safety by Removing 5-HT2B Receptor Agonism. *ACS Med. Chem. Lett.* **2013**, *4*, 254–258.

(5) Camerino, B.; Patelli, B.; Glaesser, A. Derivatives of 6-Methyl and 1,6-Dimethyl Ergoline. U.S. Patent 3238211, **1966**.

(6) Montalbetti, C. A. G. N.; Falque, V. Amide Bond Formation and Peptide Coupling. *Tetrahedron* **2005**, *61*, 10827–10852.

(7) Amine to Amide (HOBt/EDC) http://www.commonorganicchemistry.com/Rxn_Pages/Amine_to_Amide_Coupling/Amine_to_Amide_Coupling_HOBt_EDC_Mech.htm (accessed May 10,2016).

Chapter 6

Summary, conclusion and recommendations for future work

6.1 General

Drug resistance and other challenges associated with existing TB and malaria treatments have necessitated the development of novel agents. The process of new drug development can potentially be accelerated by applying drug repositioning approaches. This study focussed on the repositioning of two drugs, an antibacterial agent fusidic acid and an antipsychotic agent metergoline, in TB and/or malaria. New semisynthetic derivatives of fusidic acid and metergoline were synthesized and biologically evaluated for antimycobacterial and antiplasmodial activities. In addition, *in silico* tools were applied to fusidic acid with the aim of identifying new fusidic acid-like compounds, which possess antimycobacterial and/or antiplasmodial activity.

6.2 Fusidic acid derivatives

Fusidic acid is a naturally-occurring antibiotic and is mainly used in the treatment of staphylococcal bacterial infections. Fusidic acid was identified with potent *in vitro* antimycobacterial activity (IC_{90} 1.2 μM, H37Rv strain of *Mtb*) in a High-Throughput Screen (HTS) conducted by the Tuberculosis Antimicrobial Acquisition Coordinating Facility (TAACF). It is also reported to have activity against a range of sensitive and resistant clinical isolates of *Mtb*. The aforementioned data prompted the synthesis of fusidic acid derivatives and their evaluation as antimycobacterial agents. Apart from its antimycobacterial activity, fusidic acid has also shown antiplasmodial activity (IC_{50} 52.8 μM, D10 strain of *P. falciparum*) as reported in the literature. Although this IC_{50} value is high, fusidic acid also has the potential for repositioning in malaria through semisynthesis. Therefore, the synthesized derivatives of fusidic acid were also evaluated against *P. falciparum*.

Fusidic acid derivatives were synthesized by performing various structural modifications at C-21, C-3 and C-16 positions as reflected in SAR 1, SAR 2, and SAR 3 studies in Chapter 3. The chemistry involved various types of reactions, mainly including amide coupling, esterification, cyclization, substitution, condensation, and oxidation. All the synthesized target compounds were characterized by ^{1}H, ^{13}C NMR and MS. Purities of these compounds were determined by HPLC or LCMS and found to be more than 95%.

C-21 derivatives were obtained by replacing the C-21 carboxyl group of fusidic acid with various bioisosteres. In total, twenty eight compounds were evaluated for antimycobacterial activity against the H37Rv strain of *Mtb* and antiplasmodial activity against the NF54 strain of *P. falciparum*. These replacements led to lower antimycobacterial activity ($MIC_{99} \geq 20$ μM) as compared to fusidic acid (MIC_{99} 0.6 μM). However, two compounds, fusidic acid-isoniazid conjugate **3.15** and methane sulfonyl hydrazide derivative **3.18**, displayed moderate activity (MIC_{99} 10 μM) and reasonably low cytotoxicity (IC_{50} CHO 88.3 and 92.2 μM, respectively). Further, most of these derivatives showed a 2-35 fold increase in antiplasmodial activity compared to fusidic acid (IC_{50} 59 μM) and were also found to have low cytotoxicity. The antimycobacterial and antiplasmodial data of C-21 fusidic acid derivatives suggest that the carboxylic acid group is essential for its antimycobacterial activity but not for antiplasmodial activity.

C-3 derivatives were obtained by replacing the C-3 hydroxyl group of fusidic acid with various carboxylic and silicate esters, as well as with keto and oxime functionalities. C-3 derivatives exhibited much potent antimycobacterial activity as compared to C-21 derivatives, with 9 out of 14 derivatives displaying $MIC_{99} \leq 5$ μM. Similar to C-21 derivatives, structural modifications at the C-3 position also resulted in improved antiplasmodial activity as compared to fusidic acid. Further, the *in vitro* antimycobacterial (MIC_{99} 11.4 μM) and antiplasmodial (IC_{50} 31.6 μM) results of 3-epifusidic acid (**3.40**) suggests that inversion of configuration at the C-3 position significantly reduces the antimycobacterial activity of fusidic acid, but has little effect on the antiplasmodial activity. The antimycobacterial and antiplasmodial activities of keto (**3.36**) and oxime derivatives (**3.37**-**3.39**) suggest that these functionalities are tolerated at the C-3 position.

C-16 derivatives were obtained by replacing the C-16 acetoxy group of fusidic acid with methoxy and ethoxy groups. The antimycobacterial activity of the ethoxy derivative (**3.49**, MIC_{99} 0.8 μM) was found to be comparable to fusidic acid (MIC_{99} 0.6 μM).

Seven miscellaneous derivatives with modifications at more than one site of fusidic acid were also obtained. Antimycobacterial evaluation of these compounds indicated that the lipophilic side chain, the carboxylic acid group, and C-16 substitution are essential for antimycobacterial activity. Antiplasmodial evaluation revealed that C-3, C-11-diacetoxy fusidic acid methyl ester (**3.56**, IC_{50} 0.4 μM) has superior antiplasmodial activity with no cytotoxicity.

Some of the fusidic acid derivatives (**3.18**, **3.37**, **3.41**, **3.42** and **3.50**) were also evaluated for *in vivo* pharmacokinetics in mice. Among these, the C-3 triisopropoxy silicate derivative (**3.42**) showed an improved pharmacokinetic profile relative to fusidic acid, with higher concentrations achieved in blood, a longer half-life (5 h vs 1 h after oral administration), and a lower clearance rate. All other derivatives showed similar or poorer pharmacokinetic profiles when compared to fusidic acid.

6.3 *In silico* tools

Two separate *in silico* approaches were applied to fusidic acid. In one approach, a 3D-QSAR pharmacophore model was developed based on the antiplasmodial activity of 61 previously synthesized fusidic acid derivatives. This model was used as the 3D-structural search query to screen a fusidic acid based combinatorial library. Eight hit compounds were synthesized, including C-21 amide and C-3 ether fusidic acid derivatives. Chemistry mainly involved O-alkylation and amide coupling reactions. These compounds were evaluated for antiplasmodial activity against the NF54 strain of *P. falciparum*. All hit compounds showed superior antiplasmodial activity relative to fusidic acid. Two C-21 amide derivatives (**4.7** and **4.8**) displayed significant activity against the CQ-sensitive NF54 strain (IC_{50} values of 0.3 μM and 0.7 μM, respectively) and the CQ-resistant K1 strain (IC_{50} 0.2 μM), and were also found to be non-cytotoxic against the CHO cell line.

In another approach, 2D fingerprint and 3D shape similarity searches were performed on an in-house database using fusidic acid as the query compound. The database included 708 steroid-type natural products or their semisynthetic derivatives with defined chemical structures and stereochemistry. This study was conducted with the aim of finding structurally similar compounds with similar biological activities to fusidic acid. Selected hit compounds were evaluated for *in vitro* biological activity. Twelve out of 27 hit compounds displayed superior antiplasmodial activity (IC_{50} < 25 μM) as compared to fusidic acid. However, these compounds did not show any antimycobacterial activity except **4.16** and **4.26** (MIC_{99} 80 μM).

6.4 Metergoline derivatives

Metergoline is an antipsychotic drug belonging to ergoline family and is used in a variety of medical applications as serotonin antagonist and dopamine agonist, both in human and veterinary health. A HTS conducted by the TAACF revealed the antimycobacterial activity of metergoline (IC_{90} 15 μM, H37Rv strain of *Mtb*). In addition, a quantitative HTS on a NIH molecular library to obtain delayed death inhibitors of the malaria parasite plastid found

metergoline to have antiplasmodial activity with an IC_{50} of 7.4 μM. The above data prompted the synthesis of metergoline derivatives and their evaluation as antimycobacterial/antiplasmodial agents.

Metergoline was subjected to semisynthesis, in which its benzyl carbamate (CBz) group was removed to obtain an amine intermediate. This amine intermediate was then used to synthesize various aromatic, heteroaromatic and aliphatic amide derivatives. Chemistry mainly involved amide coupling using EDCI-HOBt as the coupling reagent. Synthesized derivatives were characterized by ^{1}H, ^{13}C NMR and MS, and evaluated for antimycobacterial activity against the H37Rv strain of *Mtb*, antiplasmodial activity against the NF54 strain of *P. falciparum* and cytotoxicity against the CHO cell line. Nine out of 23 compounds exhibited antimycobacterial activity with MIC_{99} < 50 μM. The decanamide derivative (**5.23**, MIC_{99} 9.4 μM, IC_{50} CHO 86.6 μM) was found to have a superior antimycobacterial activity and cytotoxicity profile relative to metergoline (MIC_{99} 25 μM, IC_{50} CHO 16.6 μM). Further, most of these amide derivatives also exhibited micromolar potencies against the NF54 strain of *P. falciparum*, with 17 of the 23 compounds having IC_{50} values between 1.2 μM and 20 μM. Three derivatives, **5.3** (IC_{50} 1.3 μM), **5.9** (IC_{50} 2.5 μM) and **5.25** (IC_{50} 1.2 μM) were found to have superior antiplasmodial activity as compared to metergoline (IC_{50} 3.7 μM). Compound **5.25** was found to be the most active derivative with an encouraging selectivity index value of 13. The antimycobacterial and antiplasmodial data of metergoline and its derivatives suggest that the benzyl carbamate group of metergoline is not required for activity and its substitution with other moieties may result in compounds with improved antimycobacterial and/or antiplasmodial activity.

Overall, this study demonstrates the potential of fusidic acid and metergoline as a promising novel antimycobacterial and antimalarial templates for repositioning purposes.

6.5 Recommendations for future work

In case of fusidic acid, three C-3 silicate ester derivatives were synthesized based on the hypothesis that these derivatives would revert back to fusidic acid through hydrolysis. Two silicate derivatives, triethoxy silicate ester **3.41** and trioctyloxy silicate ester **3.43** exhibited comparable antimycobacterial activity to fusidic acid, with MIC_{99} values of 0.2 and 0.3 μM, respectively. This *in vitro* activity data suggests that these derivatives may be hydrolysed to fusidic acid either in the culture medium or inside the cell. LC-MS analysis of the culture

medium and *Mtb* lysate incubated with the silicate esters needed to be performed in order to generate data to confirm or disprove this hypothesis.

The antimycobacterial activity of a fusidic acid bioisostere **3.11** increased sharply from MIC_{99} > 160 µM to MIC_{99} 20 µM, by adding fluorine atoms at the 3 and 4-positions of the phenyl group (**3.12**, Figure 6.1). Further structural modification around the phenyl group of **3.11** can be performed, either by adding substituents (for example Cl, OCF_3, Me, and OMe) at 3- and/or 4- positions of the phenyl group, or by replacing the phenyl group with various heterocyclic moieties.

Two C-16 ether derivatives of fusidic acid were obtained by replacing the acetoxy group with methoxy and ethoxy groups. The C-16 ethoxy derivative (**3.49**) was found to be equipotent to fusidic acid. This suggests that this site needs to be explored with various aliphatic or aromatic ether, thioether, ester and oxime moieties (Figure 6.1).

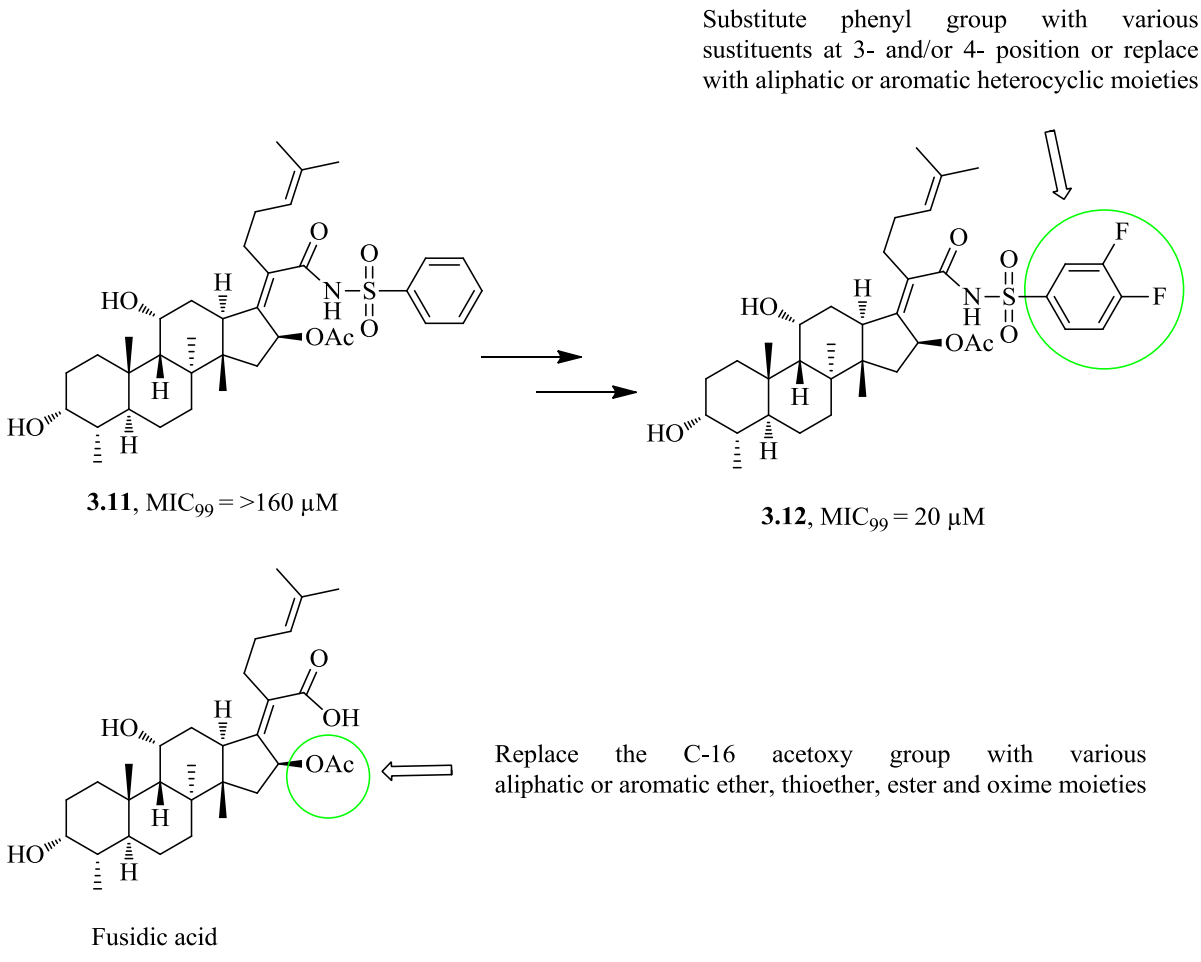

Figure 6.1: Future recommendations to obtain new fusidic acid derivatives

Removal of the carboxylic acid bearing lipophilic side chain (ketone derivative **3.53)** did not significantly diminish the antiplasmodial activity when compared to fusidic acid (IC_{50} 90.8 vs 59 µM). This suggests that further exploration of this site of fusidic acid by structural modification is warranted. The ketone derivative **3.53** can be condensed with various amines to obtain oxime derivatives or can also undergo reductive amination to produce amine derivatives (Figure 6.2). Likewise, 3-keto fusidic acid (**3.36**) can also be subjected to reductive amination to obtain various aliphatic, aromatic and heteroaromatic amine derivatives (Figure 6.2).

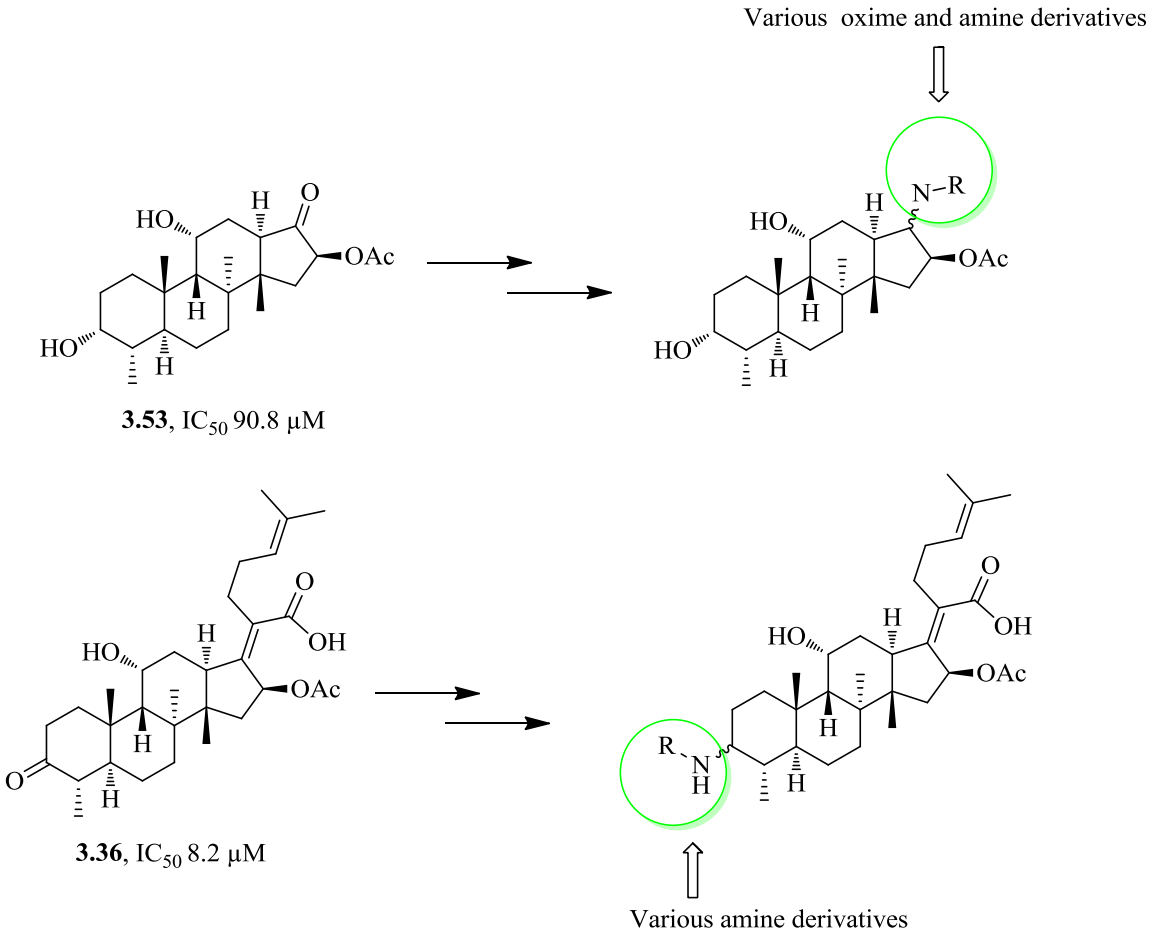

Figure 6.2: Future recommendations to obtain new fusidic acid derivatives

In case of metergoline, replacement of the CBz group of metergoline with various amide moieties generated some derivatives with improved antimycobacterial or antiplasmodial activity. However, further improvement in antimycobacterial or antiplasmodial activity is needed. From a SAR point of view, the amide group of active derivatives can be replaced with other functional groups such as sulphonamide or amino groups, in an effort to improve the antimycobacterial or antiplasmodial activity of these derivatives (Figure 6.3).

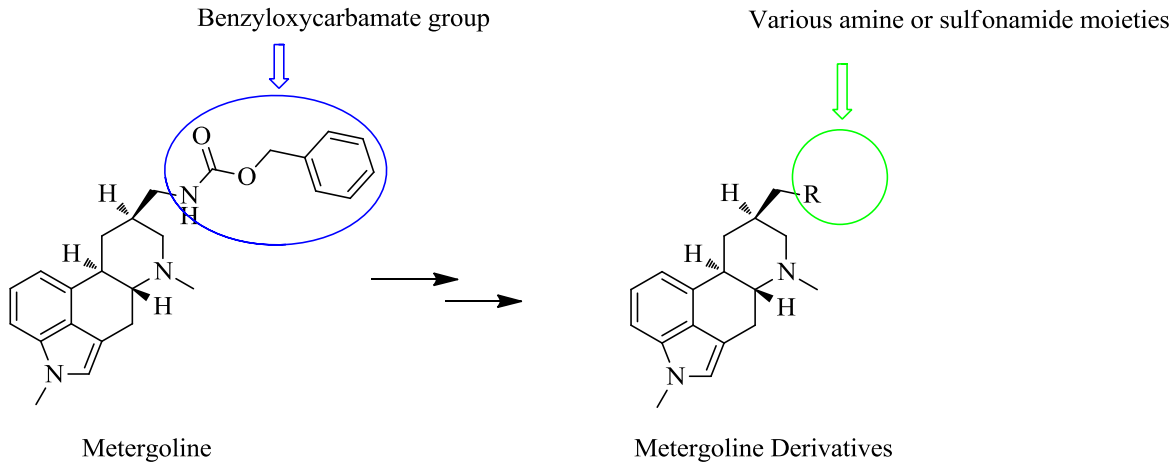

Figure 6.3: Future recommendations to obtain new metergoline derivatives

Chapter 7

Experimental

7.1 General

Fusidic acid was purchased from Ava Chem Scientific while metergoline and all other reagents were purchased from Sigma Aldrich. All solvents used for reactions, such as DMF, methanol, ethanol, acetonitrile and pyridine, were purchased from Sigma Aldrich and were anhydrous. Solvents like ethyl acetate (EtOAc), hexane, dichloromethane (DCM) and methanol, used for extraction and column chromatography purification purposes, were purchased from Kimix Chemicals and were of AR grade. Solvents and ammonium acetate used for HPLC and LC-MS purposes were bought from Sigma Aldrich (ammonium acetate and DMSO), Merck (glacial acetic acid) and Microsep (acetonitrile and methonol), and were of HPLC grade.

7.2 Synthetic procedure, physical and spectroscopic characterization of target compounds

All target compounds and intermediates were characterised by ^{1}H NMR, ^{13}C NMR and MS. ^{1}H and ^{13}C NMR spectra were recorded on a Bruker 400 spectrometer. The ^{1}H NMR data are reported as follows: chemical shift in parts per million (δ) downfield of tetramethylsilane (TMS), multiplicity (s = singlet, br s = broad singlet, d = doublet, t = triplet, q = quartet, dd = doublet of doublets, ddd doublet of doublet of doublets, dt =doublet of triplets, h = heptet, and m = multiplet), coupling constant (Hz), and integrated value. The ^{13}C NMR spectra were measured with complete proton decoupling.

Purities were determined either by high performance liquid chromatography (HPLC) or liquid chromatography - mass spectrometery (LC-MS) as described below. The purities of all compounds were found to be ≥ 95%.

HPLC: Compound purity was determined by Waters HPLC system using X-bridge C18 5µm column (4.6 x 150 mm) as stationary phase. Mobile phase consisted of 10 mM ammonium acetate in HPLC grade water (A) and acetonitrile (B). This mobile phase was delivered at a flow rate of 1.20 mL/min in gradient mode set to initially run at 75% A, then linearly increased to 100% B over 9 min and held constant for another 5 min and then decreased to

25% B over next 6 min to give total run time of 20 min. A photodiode array (PDA) detector was used and set to monitor wavelength at 254 nm.

LC-MS: LC-MS analysis was performed using an Agilent® 1260 Infinity Binary Pump, Agilent® 1260 Infinity Diode Array Detector (DAD), Agilent® 1290 Infinity Column Compartment, Agilent® 1260 Infinity Standard Autosampler, and a Agilent® 6120 Quadrupole (single) mass spectrometer, equipped with APCI and ESI multimode ionisation source. Stationary phase: Agilent Poroshell 120 C18 reversed phase column (3.0×50 mm) containing 2.7 µm particles. Mobile phase: 10 mM ammonium acetate in water (A) and 10 mM ammonium acetate in methanol (B); flow rate: 1.0 mL/min in gradient mode set to initially run at 10% B for 0.5 min, then linearly increased to 90% B over 2 min and held constant for another 3.5 min. The column was subsequently re-equilibrated to starting mobile phase composition for 2 min to give total run time of 8 min. Column temperature was maintained at 40 ^{o}C. The diode array detector was programmed to monitor absorption over the wavelength range of 190-600 nm.

Masses of some of the compounds were also determined by JEOL JMS–GCMS–GCMAT II GCMS mass spectrometer.

Melting points were obtained from a Reichert-Jung Thermovar hot-stage microscope apparatus and are uncorrected.

Thin layer chromatographic (TLC) was performed on aluminium-backed pre-coated silica gel 60 plates purchased from Merck. Spots were visualised using UV (254/366 nm) light as well as anisaldehyde stain.

7.2.1 Chapter 3

7.2.1.1 C-21 Fusidic acid derivatives

Fusidic acid methyl ester (3.2)[1]

K_2CO_3 (1.06 g, 7.67 mmol) was added to a solution of fusidic acid (**3.1**) (2.0 g, 3.87 mmol) in DMF (10 ml), followed by addition of methyl iodide (0.36 ml, 5.80 mmol). Resulting reaction mixture was then heated at 50 ^{o}C for 3 h. After completion of reaction (TLC), reaction

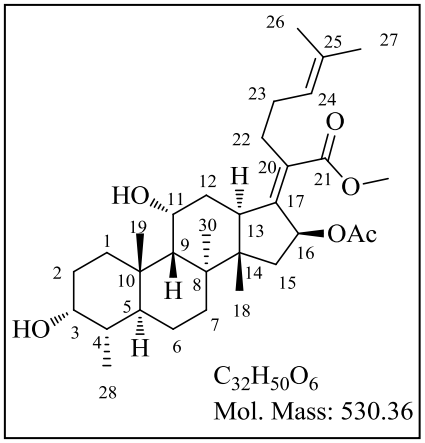

mixture was diluted with EtOAc (100 ml) and washed with water (3×100 ml). The organic layer was dried over anhydrous sodium sulfate, filtered and concentrated *in vacuo*. The yellowish product was stirred in n-pentane for 30 min to obtain **3.2** as a white solid (1.9 g, 92%); R_f 0.5 (60% EtOAc:hexane); Mp. 166-168 ^oC; ^1H NMR (400 MHz, $CDCl_3$) δ 5.83 (d, *J* = 8.4 Hz, 1H, H-16), 5.07 (t, *J* = 7.2 Hz, 1H, H-24), 4.33 (m, 1H, H-11), 3.73 (m, 1H, H-3), 3.63 (s, 3H, OCH_3), 3.04-3.01 (m, 1H, H-13), 2.51-2.36 (m, 2H, 2×H-22), 2.32-2.27 (m, 1H, H-12), 2.19-2.02 (m, 5H, H-1, H-5, H-15 and 2×H-23), 1.95 (s, 3H, OAc), 1.88-1.70 (m, 4H, 2×H-2, H-7 and H-12), 1.66 (s, 3H, CH_3-27), 1.58 (s, 3H, CH_3-26), 1.58-1.47 (m, 4H, H-1, H-4, H-6 and H-9), 1.37 (s, 3H, CH_3-30), 1.27-1.24 (m, 1H, H-15), 1.16-1.05 (m, 2H, H-6 and H-7), 0.96 (s, 3H, CH_3-19), 0.91-0.90 (m, 6H, CH_3-18 and CH_3-28); ^{13}C NMR (100 MHz, $CDCl_3$) δ 170.7, 170.3, 148.1, 132.5, 130.4, 123.1, 74.4, 71.4, 68.2, 51.3, 49.3, 48.7, 43.9, 39.4, 39.0, 37.0, 36.3, 36.0, 35.6, 32.3, 30.2, 29.9, 28.9, 28.3, 25.7, 23.9, 22.9, 20.9, 20.8, 17.7 (2C) and 15.9; LC-MS (ESI): *m/z* 553 $[M+23]^+$, 471 $[M-OAc]^+$; purity (LC-MS): 97% (t_r = 3.62 min).

Fusidic acid amide (3.3)[2]

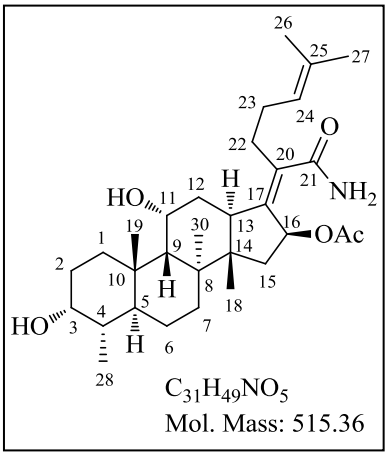

NH_4Cl (1.9 g, 35 mmol), DIPEA (6 ml, 35 mmol) and HOBt (1.2 g, 8.7 mmol) were added to a solution of fusidic acid (**3.1**) (3 g, 5.8 mmol) in DMF (10 ml), and the reaction mixture stirred at 25 ^oC for 15 min. This was followed by addition of benzotriazol-1-yl-oxytripyrrolidinophosphonium hexafluorophosphate (PyBOP) (4.53 g, 8.7 mmol) and the resulting reaction mixture was further stirred at 25 ^oC for 16 h. After completion of reaction (TLC), reaction mixture was diluted with EtOAc (150 ml) and washed with water (3×150 ml). The organic layer was dried over anhydrous magnesium sulfate, filtered and concentrated *in vacuo*. Purification by flash chromatography on 100-200 silica gel using EtOAc:hexane as eluent afforded product **3.3** as a white solid (0.93 g, 31%); R_f 0.5 (90% EtOAc:hexane); Mp. 223-225 ^oC; ^1H NMR (400 MHz, $CDCl_3$) δ 5.74 (d, *J* = 8.4 Hz, 1H, H-16), 5.42 (br s, 2H, NH_2), 5.09 (t, *J* = 6.8 Hz, 1H, H-24), 4.34 (m, 1H, H-11), 3.75 (m, 1H, H-3), 3.01-2.98 (m, 1H, H-13), 2.55-2.47 (m, 1H, H-22), 2.38-2.33 (m, 1H, H-22), 2.31-2.26 (m, 1H, H-12), 2.20-2.08 (m, 5H, H-1, H-5, H-15 and 2×H-23), 2.02 (s, 3H, OAc), 1.89-1.73 (m, 4H, 2×H-2, H-7 and H-12), 1.68 (s, 3H, CH_3-27), 1.61 (s, 3H, CH_3-26), 1.58-1.49 (m, 4H, H-1, H-4, H-6 and H-9), 1.37 (s, 3H, CH_3-30), 1.30-1.27 (m, 1H, H-15), 1.17-1.08 (m, 2H, H-6

and H-7), 0.97 (s, 3H, CH_3-19), 0.94 (s, 3H, CH_3-18), 0.92 (d, J = 6.8 Hz, CH_3-28); ^{13}C NMR (100 MHz, $CDCl_3$) δ 173.6, 171.0, 142.5, 133.9, 132.6, 123.2, 73.7, 71.3, 68.3, 60.3, 49.3, 48.7, 43.2, 39.5, 39.2, 37.1, 36.2, 35.6, 32.4, 30.3, 29.9, 29.3, 27.9, 25.6, 24.1, 22.7, 20.7 (2C), 17.8, 17.7 and 15.9; LC-MS (ESI): *m/z* 516 $[M+H]^+$, 456 $[M\text{-}OAc]^+$; purity (HPLC): 96% (t_r = 18.53 min).

General synthetic procedure for compounds 3.4 and 3.5

Cyanamide (in case of **3.4**) and 5-aminotetrazole (in case of **3.5**) (2.0 eq.), EDCI (1.20 eq.), HOBt (1.20 eq.) and DIPEA (3.0 eq.) were added to a solution of fusidic acid (**3.1**) (1.0 eq.) in DCM (20 ml), and the resulting reaction mixture was stirred at 25 ^oC for 24 h. After completion of reaction (TLC), reaction mixture was diluted with DCM (15 ml) and washed with water (3×15 ml), dried over anhydrous magnesium sulfate, filtered and concentrated *in vacuo*. Purification by flash chromatography on 100-200 silica gel using methanol:DCM as eluent afforded respective products.

***N*-cyanofusidic acid amide (3.4)**

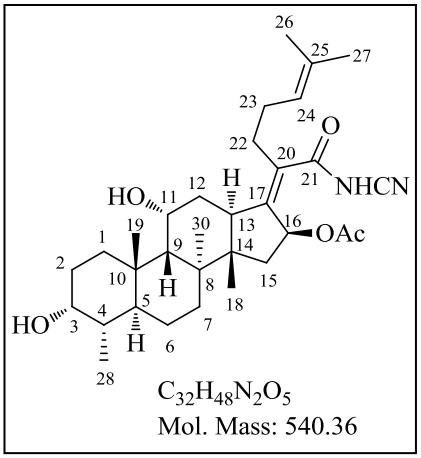

$C_{32}H_{48}N_2O_5$
Mol. Mass: 540.36

White solid (0.10 g obtained from 0.18 g of **3.1**, 53%); R_f 0.3 (8% Methanol:DCM); Mp. 142-144 ^oC; ^{1}H NMR (400 MHz, $CDCl_3$) δ 5.71 (d, J = 8.4 Hz, 1H, H-16), 5.09 (t, J = 6.8 Hz, 1H, H-24), 4.36 (m, 1H, H-11), 3.76 (m, 1H, H-3), 3.04-3.01 (m, 1H, H-13), 2.55-2.47 (m, 1H, H-22), 2.27-2.24 (m, 2H, H-12 and H-22), 2.17-2.12 (m, 5H, H-1, H-5, H-15 and 2×H-23), 2.06 (s, 3H, OAc), 1.85-1.82 (m, 4H, 2×H-2, H-7 and H-12), 1.70 (s, 3H, CH_3-27), 1.62 (s, 3H, CH_3-26), 1.58-1.48 (m, 4H, H-1, H-4, H-6 and H-9), 1.39 (s, 3H, CH_3-30), 1.27-1.23 (m, 1H, H-15), 1.13-1.11 (m, 2H, H-6 and H-7), 0.98 (s, 3H, CH_3-19), 0.93-0.92 (m, 6H, CH_3-18 and CH_3-28); ^{13}C NMR (100 MHz, $CDCl_3$) δ 170.8 (2C), 147.4, 133.5, 129.8, 122.5, 106.7, 73.8, 71.5, 68.3, 49.5, 48.7, 43.6, 39.5, 39.0, 36.8, 36.5, 35.8, 35.1, 31.9, 30.1, 29.7, 29.1, 28.1, 25.7, 23.8, 23.2, 20.8, 20.7, 17.8, 17.7 and 15.8; LC-MS (ESI): *m/z* 563 $[M+23]^+$, 481 $[M\text{-}OAc]^+$; purity (LC-MS): 96% (t_r = 3.85 min).

***N*-(2H-tetrazol-5-yl)fusidic acid amide (3.5)**

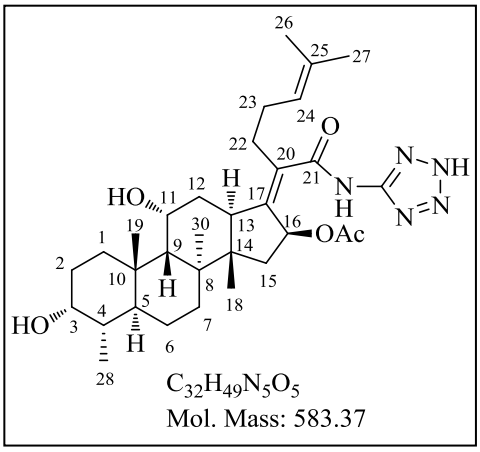

White solid (0.10 g obtained from 0.3 g of **3.1**, 29%); R_f 0.2 (8% Methanol:DCM); Mp. >280 ^oC; ^1H NMR (400 MHz, DMSO-d_6) δ 10.96 (br s, 1H, CONH), 5.63 (d, J = 8.8 Hz, 1H, H-16), 5.07 (t, J = 6.8 Hz, 1H, H-24), 4.13 (m, 1H, H-11), 4.05 (d, J = 3.5 Hz, 1H, OH), 3.95 (d, J = 3.1 Hz, 1H, OH), 3.48 (m, 1H, H-3), 2.92-2.89 (m, 1H, H-13), 2.49-2.42 (m, 1H, H-22), 2.29-2.20 (m, 2H, H-12 and H-22), 2.13-1.95 (m, 5H, H-1, H-5, H-15 and 2×H-23), 1.72-1.60 (m, 5H, H-2, H-12 and OAc), 1.58 (s, 3H, CH_3-27), 1.51 (s, 3H, CH_3-26), 1.49-1.28 (m, 6H, H-1, H-2, H-4, H-6, H-7 and H-9), 1.26 (s, 3H, CH_3-30), 1.08-1.04 (m, 1H, H-15), 1.00-0.97 (m, 2H, H-6 and H-7), 0.86 (s, 3H, CH_3-19), 0.82 (s, 3H, CH_3-18), 0.76 (d, J = 6.6 Hz, 3H, CH_3-28); ^{13}C NMR (100 MHz, CD_3OD) δ 170.6 (2C), 152.0, 145.0, 132.4, 132.2, 122.8, 73.9, 71.0, 67.1, 54.1, 49.4, 48.5, 43.3, 39.3, 38.8, 36.8, 36.4, 35.8, 35.4, 31.4, 29.6, 28.9, 27.4, 24.4, 22.4 (2C), 20.9, 19.1, 16.5 (2C) and 15.0; LC-MS (ESI): *m/z* 606 $[M+23]^+$, 524 $[M-OAc]^+$; purity (LC-MS): 99% (t_r = 3.92 min).

General synthetic procedure for compounds 3.6-3.9

Respective amine (1.5 eq.), EDCI (1.5 eq.) and 4-(dimethylamino)pyridine (DMAP) (0.4 eq.) were added to a solution of fusidic acid (**3.1**) (1.0 eq.) in DCM (5 ml). The reaction mixture was stirred at 25 ^oC for 16 h. After completion of reaction (TLC), reaction mixture was diluted with DCM (20 ml) and washed with water (3×15 ml). Organic layer was then dried over anhydrous magnesium sulfate, filtered and concentrated *in vacuo*. Purification by flash chromatography on 100-200 silica gel using methanol:DCM as eluent afforded products **3.6-3.9**.

***N*-(2-morpholinoethyl)fusidic acid amide (3.6)**

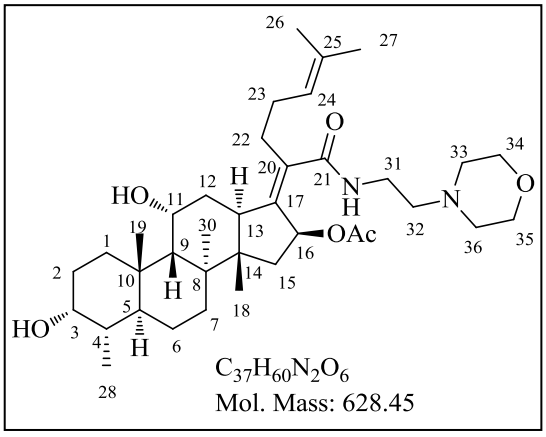

White solid (0.163 g obtained from 0.2 g of **3.1**, 67%); R_f 0.1 (100% EtOAc); Mp. 216-218 ^oC; ^1H NMR (400 MHz, $CDCl_3$) δ 5.73 (d, J = 7.3 Hz, 1H, H-16), 5.08 (t, J = 7.0 Hz, 1H, H-24), 4.33 (m, 1H, H-11), 3.76 (m, 5H, H-3, 2×H-34 and 2×H-35), 3.45-3.37 (m, 1H, H-31), 3.27-3.16 (m, 1H, H-31), 3.01-2.97 (m, 1H, H-13), 2.61-2.42

(m, 7H, H-22, 2×H-32, 2×H-33 and 2×H-36), 2.38-2.25 (m, 2H, H-12 and H-22), 2.20-2.05 (m, 5H, H-1, H-5, H-15 and 2×H-23), 1.98 (s, 3H, OAc), 1.88-1.71 (m, 4H, 2×H-2, H-7 and H-12), 1.67 (s, 3H, CH_3-27), 1.59 (s, 3H, CH_3-26), 1.59-1.47 (m, 4H, H-1, H-4, H-6 and H-9), 1.38 (s, 3H, CH_3-30), 1.25-1.21 (m, 1H, H-15), 1.15-1.05 (m, 2H, H-6 and H-7), 0.96 (s, 3H, CH_3-19), 0.93 (s, 3H, CH_3-18), 0.91 (d, J = 6.8 Hz, 3H, CH_3-28); ^{13}C NMR (100 MHz, $CDCl_3$) δ 171.2, 170.8, 141.3, 135.5, 132.2, 123.4, 73.6, 71.3, 68.3, 66.4, 56.8, 53.3, 53.1 (2C), 49.3, 48.6, 43.2, 39.5, 39.3, 37.0, 36.2, 36.1, 35.6, 35.1, 32.4, 30.3, 30.0, 29.3, 27.9, 25.7, 24.1, 22.7, 21.1, 20.8, 17.8, 17.7 and 15.9; LC-MS (ESI): *m/z* 629 $[M+1]^+$, 569 $[M-OAc]^+$, 651 $[M+23]^+$; purity (LC-MS): 97% (t_r = 4.12 min).

_N_-(2-hydroxyethyl)fusidic acid amide (3.7)

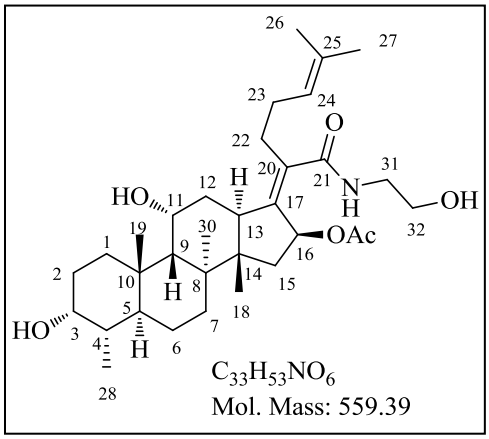

White solid (0.080 g obtained from 0.3 g of **3.1**, 25%); R_f 0.3 (100% EtOAc); Mp. 162-164 °C; ^{1}H NMR (400 MHz, CD_3OD) δ 5.79 (d, J = 8.5 Hz, 1H, H-16), 5.16 (t, J = 7.1 Hz, 1H, H-24), 4.33 (m, 1H, H-11), 3.68 (m, 1H, H-3), 3.59 (t, J = 6.2 Hz, 2H, H-32), 3.38-3.32 (m, 1H, H-31), 3.20-3.14 (m, 1H, H-31), 3.08-3.05 (m, 1H, H-13), 2.63-2.55 (m, 1H, H-22), 2.31-2.09 (m, 7H, H-1, H-5, H-12, H-15, H-22 and 2×H-23), 1.99 (s, 3H, OAc), 1.89-1.72 (m, 4H, 2×H-2, H-7, H-12), 1.70 (s, 3H, CH_3-27), 1.64 (s, 3H, CH_3-26), 1.62-1.48 (m, 4H, H-1, H-4, H-6 and H-9), 1.41 (s, 3H, CH_3-30), 1.25-1.10 (m, 3H, H-6, H-7, H-15), 1.02 (s, 3H, CH_3-19), 0.97 (s, 3H, CH_3-18), 0.92 (d, J = 6.8 Hz, 3H, CH_3-28); ^{13}C NMR (100 MHz, CD_3OD) δ 173.2, 171.0, 141.9, 134.3, 131.8, 123.1, 73.8, 71.0, 67.2, 60.1, 49.3, 48.4, 43.1, 41.6, 39.3, 38.9, 36.8, 36.4, 35.9, 35.4, 31.5, 29.6 (2C), 29.0, 27.3, 24.4, 22.4, 22.3, 20.9, 19.7, 16.4 (2C) and 15.0; LC-MS (ESI): *m/z* 500 $[M-OAc]^+$, 582 $[M+23]^+$; purity (LC-MS): 96% (t_r = 4.03 min).

_N_-(4-hydroxypiperidin-1-yl)fusidic acid amide (3.8)

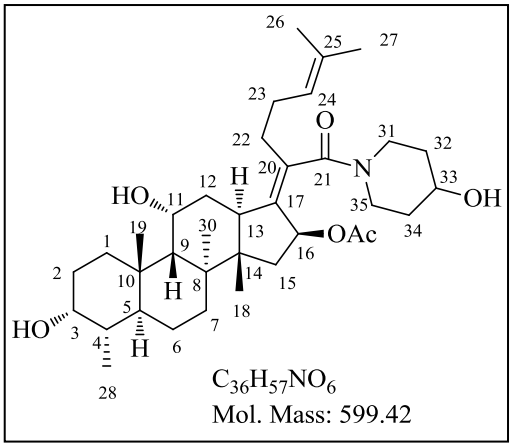

White solid (0.105 g obtained from 0.5 g of **3.1**, 18%); R_f 0.3 (100% EtOAc); Mp. 195-197 °C; ^{1}H NMR (400 MHz, $CDCl_3$) δ 5.47 (dd, J = 8.6, 4.7 Hz 1H, H-16), 5.05 (t, J = 7.1 Hz, 1H, H-24), 4.41-4.24 (m, 2H, H-11 and H-33), 3.86-3.70 (m, 3H, H-3, H-

31 and H-35), 3.40-3.15 (m, 2H, H-31 and H-35), 3.00-2.96 (m, 1H, H-13), 2.40-2.34 (m, 2H, 2×H-22), 2.31-2.25 (m, 1H, H-12), 2.20-2.03 (m, 9H, H-1, H-5, H-15, 2×H-23, 2×H-32 and 2×H-34), 1.96 (s, 3H, OAc), 1.89-1.69 (m, 4H, 2×H-2, H-7 and H-12), 1.65 (s, 3H, CH_3-27), 1.58 (s, 3H, CH_3-26), 1.57-1.45 (m, 4H, H-1, H-4, H-6 and H-9), 1.36 (s, 3H, CH_3-30), 1.20-1.15 (m, 1H, H-15), 1.13-1.03 (m, 2H, H-6 and H-7), 0.96 (s, 3H, CH_3-19), 0.94 (s, 3H, CH_3-18), 0.89 (d, J = 6.9 Hz, 3H, CH_3-28); ^{13}C NMR (100 MHz, $CDCl_3$) δ 170.9, 170.2, 139.9, 133.6, 132.4, 123.3, 72.9, 71.3, 68.3, 67.7, 49.3, 49.0, 43.7, 42.9 (2C), 39.5, 39.4, 38.6, 36.9, 36.3, 36.0, 35.5, 35.0, 33.9, 32.1, 30.2, 29.9, 27.7, 25.6, 23.9, 22.9, 21.1, 20.8, 17.9, 17.6 and 15.9; LC-MS (ESI): *m/z* 540 $[M\text{-}OAc]^+$, purity (LC-MS): 98% (t_r = 4.56 min).

_N_-(3-hydroxyazetidin-1-yl)fusidic acid amide (3.9)

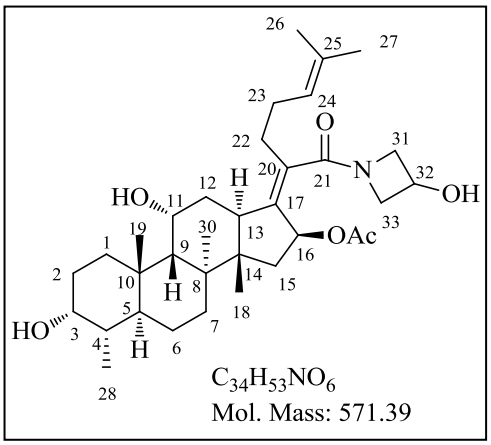

White solid (0.060 g obtained from 0.3 g of **3.1**, 18%); R_f 0.1 (80% EtOAc:hexane); Mp. 178-180 °C; ^{1}H NMR (400 MHz, $CDCl_3$) δ 5.79 (d, J = 8.7 Hz, 1H, H-16), 5.06 (t, J = 7.1 Hz, 1H, H-24), 4.42 (m, 1H, H-32), 4.34 (m, 1H, H-11), 4.27-4.15 (m, 2H, H-31 and H-33), 4.02-3.81 (m, 2H, H-31 and H-33), 3.75 (m, 1H, H-3), 3.00-2.96 (m, 1H, H-13), 2.51-2.40 (m, 1H, H-22), 2.35-2.25 (m, 2H, H-12 and H-22), 2.21-2.07 (m, 5H, H-1, H-5, H-15 and 2×H-23), 2.05 (s, 3H, OAc), 1.89-1.72 (m, 4H, 2×H-2, H-7 and H-12), 1.67 (s, 3H, CH_3-27), 1.60 (s, 3H, CH_3-26), 1.62-1.48 (m, 4H, H-1, H-4, H-6 and H-9), 1.38 (s, 3H, CH_3-30), 1.24-1.20 (m, 1H, H-15), 1.16-1.07 (m, 2H, H-6 and H-7), 0.97 (s, 3H, CH_3-19), 0.96 (s, 3H, CH_3-18), 0.92 (d, J = 6.8 Hz, 3H, CH_3-28); ^{13}C NMR (100 MHz, $CDCl_3$) δ 172.0, 171.8, 141.6, 132.4, 131.7, 123.3, 73.1, 71.4, 68.3, 62.2, 60.7, 58.1, 49.4, 48.8, 43.3, 39.5, 39.3, 37.0, 36.3, 36.1, 35.5, 32.3, 30.3, 29.9, 29.4, 27.7, 25.7, 24.0, 22.8, 21.3, 20.8, 17.9, 17.5 and 15.9; LC-MS (ESI): *m/z* 512 $[M\text{-}OAc]^+$, purity (LC-MS): 94% (t_r = 4.55 min).

General synthetic procedure for compounds 3.10-3.12

Respective sulphonamide (1.50 eq.), EDCI (1.50 eq.) and DMAP (0.4 eq.) were added to a solution of fusidic acid (**3.1**) (1.0 eq.) in DCM (10 ml) and reaction mixture was stirred at 25 °C for 48 h. After completion of reaction (TLC), solvent was removed *in vacuo* and the residue was taken in EtOAc (25 ml). The organic phase was washed with water (3×15 ml), dried over anhydrous magnesium sulfate, filtered and concentrated *in vacuo*. Purification by

flash chromatography on 100-200 silica gel using methanol:DCM as eluent afforded products **3.10-3.12**.

***N*-(methylsulfonyl)fusidic acid amide (3.10)**

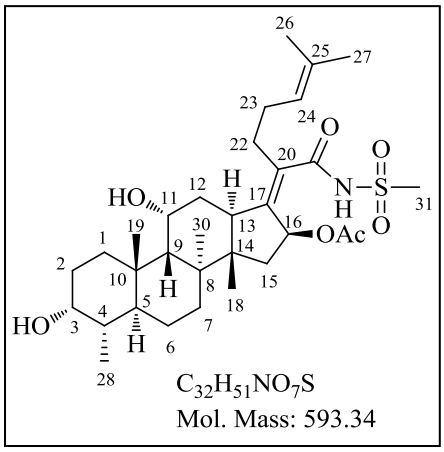

White solid (0.108 g obtained from 0.3 g of **3.1**, 31%); R_f 0.4 (5% Methanol:DCM); Mp. 214-216 ^oC; ^1H NMR (400 MHz, $CDCl_3$) δ 5.79 (d, *J* = 8.4 Hz, 1H, H-16), 5.10 (t, *J* = 6.7 Hz, 1H, H-24), 4.34 (m, 1H, H-11), 3.76 (m, 1H, H-3), 3.08-3.05 (m, 1H, H-13), 2.75 (s, 3H, H-31), 2.42-2.40 (m, 2H, H-12 and H-22), 2.34-2.30 (m, 1H, H-22), 2.21-2.09 (m, 5H, H-1, H-5, H-15 and 2×H-23), 2.02 (s, 3H, OAc), 1.93-1.73 (m, 4H, 2×H-2, H-7 and H-12), 1.68 (s, 3H, CH_3-27), 1.62 (s, 3H, CH_3-26), 1.58-1.50 (m, 4H, H-1, H-4, H-6 and H-9), 1.38 (s, 3H, CH_3-30), 1.34-1.30 (m, 1H, H-15), 1.17-1.07 (m, 2H, H-6 and H-7), 0.98 (s, 3H, CH_3-19), 0.93-0.91 (m, 6H, CH_3-28 and CH_3-18); ^{13}C NMR (100 MHz, $CDCl_3$) δ 170.9, 164.7, 153.1, 132.5, 129.1, 123.0, 74.1, 71.3, 68.2, 49.2, 48.8, 44.6, 43.3, 39.5, 39.1, 37.1, 36.3, 36.1, 35.4, 32.5, 30.3, 30.0, 29.0, 28.8, 25.7, 24.2, 22.6, 21.1, 20.7, 18.0, 17.8 and 15.9; LC-MS (ESI): *m/z* 594 $[M+H]^+$, 534 $[M-OAc]^+$; purity (LC-MS): 98% (t_r = 4.11 min).

***N*-(phenylsulfonyl)fusidic acid amide (3.11)**

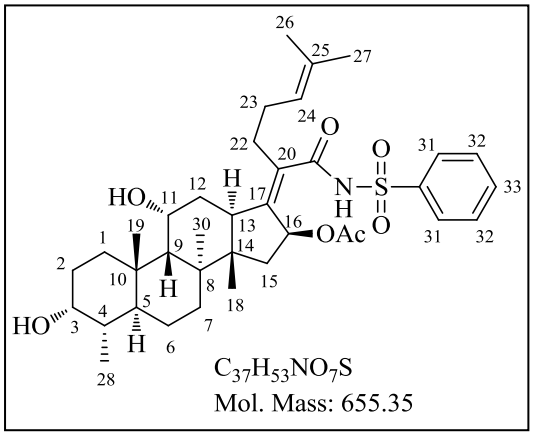

White solid (0.10 g obtained from 0.2 g of **3.1**, 38%); R_f 0.4 (5% Methanol:DCM); Mp. 229-231 ^oC; ^1H NMR (400 MHz, $CDCl_3$) δ 8.49 (br s, 1H, NH), 8.08 (d, *J* = 7.5 Hz, 2H, H-31), 7.62 (t, *J* = 7.3 Hz, 1H, H-33), 7.53 (t, *J* = 7.3 Hz, 2H, H-32), 5.65 (d, *J* = 8.4 Hz, 1H, H-16), 4.98 (t, *J* = 6.8 Hz, 1H, H-24), 4.33 (m, 1H, H-11), 3.76 (m, 1H, H-3), 2.99-2.97 (m, 1H, H-13), 2.41-2.34 (m, 1H, H-22), 2.23-2.08 (m, 5H, H-1, H-5, H-12, H-22 and H-23), 1.92-1.88 (m, 2H, H-15 and H-23), 1.85 (s, 3H, OAc), 1.76-1.72 (m, 4H, 2×H-2, H-7 and H-12), 1.65 (s, 3H, CH_3-27), 1.60-1.53 (m, 4H, H-1, H-4, H-6 and H-9), 1.47 (s, 3H, CH_3-26), 1.36 (s, 3H, CH_3-30), 1.30-1.26 (m, 1H, H-15), 1.12-1.09 (m, 2H, H-6 and H-7), 0.96 (s, 3H, CH_3-19), 0.92 (d, *J* = 6.8 Hz, 3H, CH_3-28), 0.89 (s, 3H, CH_3-18); ^{13}C NMR (100 MHz, $CDCl_3$) δ 170.7, 167.7, 146.7, 138.8, 133.8, 133.6, 132.0, 128.8 (2C), 128.5 (2C), 122.6, 73.7, 71.4, 68.2, 49.2, 48.6, 43.7, 39.5, 39.1,

37.0, 36.2, 36.0, 35.5, 32.3, 30.2, 29.9, 29.1, 27.9, 25.6, 24.0, 22.8, 20.7 (2C), 17.9, 17.7 and 15.9; LC-MS (ESI): *m/z* 678 $[M+23]^+$, 596 $[M\text{-}OAc]^+$; purity (LC-MS): 99% (t_r = 4.32 min).

_N_-(3,4-difluorophenylsulfonyl)fusidic acid amide (3.12)

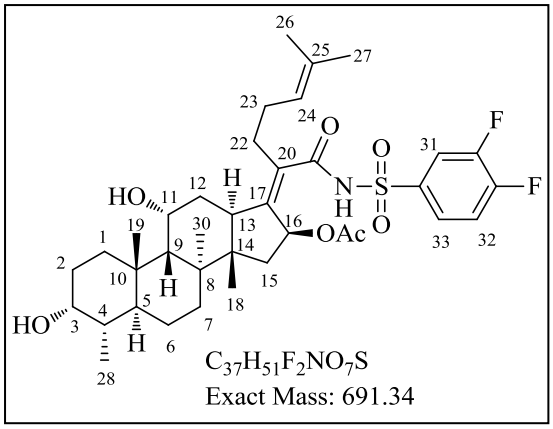

White solid (0.12 g obtained from 0.3 g of **3.1**, 30%); R_f 0.3 (4% Methanol:DCM); Mp. 232-234 ^oC; ^1H NMR (400 MHz, $CDCl_3$) δ 8.55 (br s, 1H, NH), 7.97-7.92 (m, 1H, H-31), 7.89-7.87 (m, 1H, H-33), 7.35-7.29 (m, 1H, H-32), 5.65 (d, *J* = 8.1 Hz, 1H, H-16), 4.99 (t, *J* = 6.8 Hz, 1H, H-24), 4.34 (m, 1H, H-11), 3.76 (m, 1H, H-3), 3.01-2.98 (m, 1H, H-13), 2.42-2.34 (m, 1H, H-22), 2.23-2.09 (m, 7H, H-1, H-5, H-12, H-15, H-22 and 2×H-23), 1.95 (s, 3H, OAc), 1.75-1.69 (m, 4H, 2×H-2, H-7 and H-12), 1.66 (s, 3H, CH_3-27), 1.61-1.54 (m, 4H, H-1, H-4, H-6 and H-9), 1.50 (s, 3H, CH_3-26), 1.36 (s, 3H, CH_3-30), 1.32-1.28 (m, 1H, H-15), 1.16-1.07 (m, 2H, H-6 and H-7), 0.97 (s, 3H, CH_3-19), 0.92 (d, *J* = 7.0 Hz, 3H, CH_3-28), 0.90 (s, 3H, CH_3-18); ^{13}C NMR (100 MHz, $CDCl_3$) δ 170.6, 167.8, 167.7, 152.6, 147.4, 131.8, 126.0, 122.5, 118.8, 118.6, 118.0, 117.8, 73.7, 71.4, 68.2, 49.3, 48.7, 43.8, 39.5, 39.2, 37.0, 36.2, 36.1, 35.5, 32.3, 30.3, 29.9, 29.1, 28.0, 25.6, 24.0, 22.8, 20.8, 20.7, 17.9, 17.6 and 15.8; LC-MS (ESI): *m/z* 714 $[M+23]^+$, 632 $[M\text{-}OAc]^+$; purity (LC-MS): 94% (t_r = 4.36 min).

Fusidic acid hydrazide (3.13)[2]

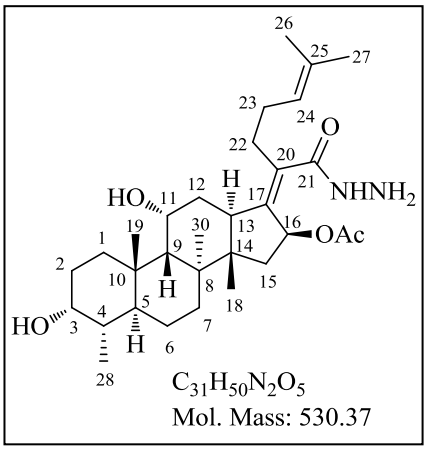

HOBt (0.062 g, 0.44 mmol) and EDCI (0.085 g, 0.44 mmol) were added to a solution of fusidic acid (**3.1**) (0.2 g, 0.38 mmol) in acetonitrile (10 ml) and the reaction mixture was stirred at 25 ^oC for 3 h. Hydrazine hydrate (0.07 ml, 1.52 mmol) was then added and the resulting reaction mixture was further stirred at 25 ^oC for 16 h. After completion of reaction (TLC), solvent was removed *in vacuo* and the residue was taken in EtOAc (25 ml). The organic phase was washed with water (3×15 ml), dried over anhydrous magnesium sulfate and concentrated *in vacuo*. Purification by flash chromatography on 100-200 silica gel using EtOAc:hexane mixture as eluent afforded product **3.13** as a white solid (0.2 g, 98%); R_f 0.2 (90% EtOAc:hexane); Mp. 128-130 ^oC; ^1H NMR (400 MHz, $CDCl_3$) δ 8.26 (br s, 1H, NH),

7.75 (br s, 2H, NH_2), 5.88 (d, *J* = 8.2 Hz, 1H, H-16), 5.10 (t, *J* = 6.8 Hz, 1H, H-24), 4.34 (m, 1H, H-11), 3.76 (m, 1H, H-3), 3.07-3.04 (m, 1H, H-13), 2.48-2.43 (m, 2H, 2×H-22), 2.34-2.31 (m, 1H, H-12), 2.21-2.02 (m, 5H, H-1, H-5, H-15 and 2×H-23), 1.96 (s, 3H, OAc), 1.88-1.73 (m, 4H, 2×H-2, H-7 and H-12), 1.67 (s, 3H, CH_3-27), 1.60 (s, 3H, CH_3-26), 1.56-1.49 (m, 4H, H-1, H-4, H-6 and H-9), 1.37 (s, 3H, CH_3-30), 1.32-1.29 (m, 1H, H-15), 1.17-1.06 (m, 2H, H-6 and H-7), 0.97 (s, 3H, CH_3-19), 0.93-0.91 (m, 6H, CH_3-18 and CH_3-28); ^{13}C NMR (100 MHz, $CDCl_3$) δ 174.0, 170.5, 150.9, 132.6, 129.5, 123.0, 74.4 (2C), 71.4, 68.2, 49.3, 48.7, 44.3, 39.5, 39.0, 37.0, 36.2, 36.1, 35.6, 32.3, 30.2, 29.9, 28.7, 28.4, 25.6, 22.8, 20.8, 20.6, 17.9, 17.7 and 15.9; LC-MS (ESI): *m/z* 531 $[M+H]^+$, 471 $[M-OAc]^+$; purity (HPLC): 97% (t_r = 18.44 min).

_N_-(thiophene-2-carbonyl)fusidic acid hydrazide (3.14)

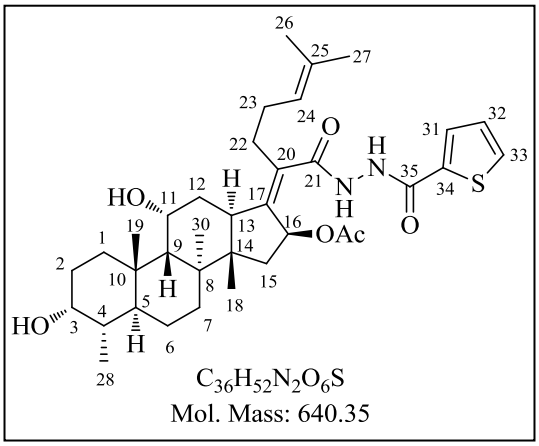

Thiophene-2-carbohydrazide (0.03 g, 0.23 mmol), TBTU (0.07 g, 0.23 mmol) and DIPEA (0.1 ml, 0.57 mmol) were added to a solution of fusidic acid (**3.1**) (0.1 g, 0.19 mmol) in DMF (3 ml) and the resulting reaction mixture was stirred at 25 °C for 16 h. After completion of reaction (TLC), reaction mixture was diluted with EtOAc (15 ml) and washed with water (3×15 ml), dried over anhydrous magnesium sulfate and concentrated *in vacuo*. Purification by flash chromatography on 100-200 silica gel using EtOAc:hexane as eluent afforded product **3.14** as a white solid (0.062 g, 50%); R_f 0.5 (60% EtOAc:hexane); Mp. 144-146 °C; ^{1}H NMR (400 MHz, $CDCl_3$) δ 8.83 (br s, 1H, NH), 8.48 (br s, 1H, NH), 7.64 (d, *J* = 4.0 Hz, 1H, H-31), 7.55 (d, *J* = 4.9 Hz, 1H, H-33), 7.10 (t, *J* = 4.7 Hz, 1H, H-32), 5.80 (d, *J* = 8.1 Hz, 1H, H-16), 5.10 (t, *J* = 6.8 Hz, 1H, H-24), 4.34 (m, 1H, H-11), 3.75 (m, 1H, H-3), 3.06-3.03 (m, 1H, H-13), 2.54-2.49 (m, 1H, H-22), 2.38-2.35 (m, 1H, H-22), 2.32-2.29 (m, 1H, H-12), 2.20-2.10 (m, 5H, H-1, H-5, H-15 and 2×H-23), 1.98 (s, 3H, OAc), 1.88-1.74 (m, 4H, H-2, H-12, H-2 and H-7), 1.68 (s, 3H, CH_3-27), 1.62 (s, 3H, CH_3-26), 1.62-1.49 (m, 4H, H-1, H-4, H-6 and H-9), 1.38 (s, 3H, CH_3-30), 1.34-1.30 (m, 1H, H-15), 1.18-1.09 (m, 2H, H-6 and H-7), 0.98 (s, 3H, CH_3-19), 0.96 (s, 3H, CH_3-18), 0.92 (d, *J* = 6.9 Hz, 3H, CH_3-28); ^{13}C NMR (100 MHz, $CDCl_3$) δ 170.9, 167.8, 159.1, 145.2, 135.4, 132.7, 132.3, 131.0, 129.4, 127.8, 123.1, 74.0, 71.4, 68.2, 49.4, 48.7, 43.6, 39.5, 39.2, 37.0, 36.3, 36.0, 35.7, 32.2, 30.1, 29.9, 29.6, 28.1,

25.6, 23.9, 22.9, 21.0, 20.8, 17.9, 17.8 and 15.9; LC-MS (ESI): *m/z* 641 $[M+H]^+$, 581 $[M-OAc]^+$; purity (HPLC): 98% (t_r = 11.39 min).

N-isonicotinoylfusidic acid hydrazide (3.15)

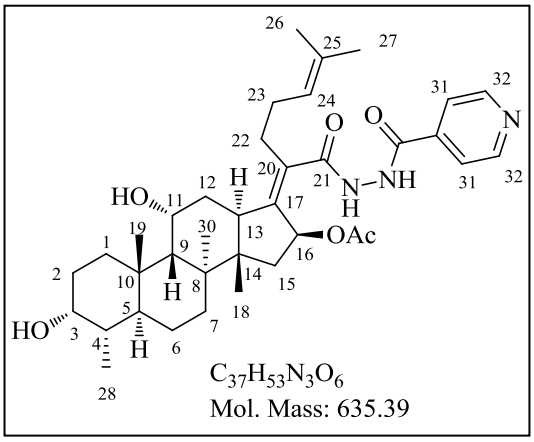

Et_3N (0.12 ml, 0.870 mmol) was added dropwise to a solution of fusidic acid (**3.1**) (0.150 g, 0.290 mmol) and isoniazid (0.039 g, 0.290 mmol) in DCM (5 ml). Resulting reaction mixture was cooled to 0 °C in an ice bath and T3P solution (0.13 ml, 0.435 mmol, 50% w/v in DMF, d = 1.09 g/ml) was added dropwise. Reaction mixture was then slowly warmed to 25 °C and stirred for 5 h. After completion of reaction (TLC), the reaction mixture was diluted with DCM (20 ml) and water (15 ml) and shaken well in a separating funnel. Organic layer was separated, dried over anhydrous sodium sulfate, filtered and concentrated *in vacuo*. The residue was purified by column chromatography on 100-200 silica gel using EtOAc:hexane as eluent affording **3.15** as a white solid (0.084 g, 46%); R_f 0.5 (10% Methanol:DCM); Mp. 189-191 °C; ^{1}H NMR (400 MHz, CD_3OD) δ 8.70 (d, *J* = 6.1 Hz, 2H, 2×H-32), 7.80 (d, *J* = 6.1 Hz, 2H, 2×H-31), 5.75 (d, *J* = 8.2 Hz, 1H, H-16), 5.18 (t, *J* = 7.1 Hz, 1H, H-24), 4.33 (m, 1H, H-11), 3.67 (m, 1H, H-3), 3.11-3.08 (m, 1H, H-13), 2.65-2.57 (m, 1H, H-22), 2.37-2.13 (m, 7H, H-1, H-5, H-12, H-15, H-22, 2×H-23), 1.97 (s, 3H, OAc), 1.92-1.71 (m, 4H, 2×H-2, H-7, H-12), 1.69 (s, 3H, CH_3-27), 1.67 (s, 3H, CH_3-26), 1.64-1.47 (m, 4H, H-1, H-4, H-6 and H-9), 1.41 (s, 3H, CH_3-30), 1.34-1.30 (m, 1H, H-15), 1.19-1.09 (m, 2H, H-6 and H-7), 1.01 (s, 3H, CH_3-19), 0.97 (s, 3H, CH_3-18), 0.90 (d, *J* = 6.8 Hz, 3H, CH_3-28); ^{13}C NMR (100 MHz, CD_3OD) δ 171.6, 171.4, 164.9, 149.5 (2C), 144.1, 140.9, 132.1, 131.8, 123.1, 121.8 (2C), 74.4, 71.0, 67.1, 49.3, 48.3, 43.3, 39.3, 38.9, 36.8, 36.4, 36.0, 35.4, 31.5, 29.6 (2C), 29.5, 27.4, 24.4, 22.4, 22.3, 20.9, 19.9, 16.7, 16.6 and 15.1; LC-MS (ESI): *m/z* 636 $[M+H]^+$, 658 $[M+23]^+$, 576 $[M-OAc]^+$; purity (HPLC): 96% (t_r = 16.74 min).

General synthetic procedure for compounds 3.16-3.17

A solution of fusidic acid hydrazide (**3.13**) (0.150 g, 0.290 mmol) and pyridine-3-carboxaldehyde or pyridine-4-carboxaldehyde (0.040 g, 0.377 mmol) in ethanol (2 ml) was refluxed in a sealed glass tube at 85 °C for 8 h. After completion of reaction (TLC), the reaction mixture was concentrated *in vacuo* and the residue was purified by column

chromatography on 100-200 silica gel using methanol:DCM as eluent affording products **3.16-3.17**.

***N*-(pyridin-3-ylmethylene)fusidic acid hydrazide (3.16)**

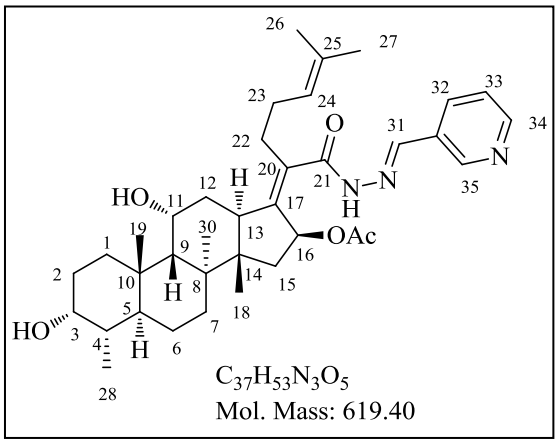

White solid (0.110 g, 63%); R_f 0.2 (8% Methanol:DCM); Mp. 230-232 ^oC; A mixture of E/Z isomers; ^1H NMR (400 MHz, CD_3OD) δ 8.84 (s, 1H, H-35, ***E***/Z), 8.78 (s, 1H, H-35, E/***Z***), 8.56 (d, *J* = 5.2 Hz, 1H, H-34, ***E***/Z), 8.53 (d, *J* = 5.2 Hz, 1H, H-34, E/***Z***), 8.30 (d, *J* = 8.1 Hz, 1H, H-32, ***E***/Z), 8.06 (d, *J* = 8.1 Hz, 1H, H-32, E/***Z***), 8.13 (s, 1H, H-31, ***E***/Z), 7.96 (s, 1H, H-31, E/***Z***), 7.49 (dd, *J* = 8.0 and 4.9 Hz, 1H, H-33), 5.83 (d, *J* = 8.8 Hz, 1H, H-16, ***E***/Z), 5.57 (d, *J* = 8.8 Hz, 1H, H-16, E/***Z***), 5.16 (t, *J* = 7.2 Hz, 1H, H-24), 4.35 (m, 1H, H-11), 3.67 (m, 1H, H-3), 3.14-3.11 (m, 1H, H-13), 2.72-2.64 (m, 1H, H-22), 2.39-2.14 (m, 7H, H-1, H-5, H-12, H-15, H-22 and 2×H-23), 1.94-1.70 (m, 4H, 2×H-2, H-7 and H-12), 1.88 (s, 3H, OAc), 1.67 (s, 3H, CH_3-27), 1.61 (s, 3H, CH_3-26), 1.63-1.47 (m, 4H, H-1, H-4, H-6 and H-9), 1.40 (s, 3H, CH_3-30), 1.22-1.18 (m, 1H, H-15), 1.17 -1.09 (m, 2H, H-6 and H-7), 1.01 (s, 3H, CH_3-19), 0.97 (s, 3H, CH_3-18), 0.90 (d, *J* = 6.8 Hz, 3H, CH_3-28); ^{13}C NMR (100 MHz, CD_3OD) δ 171.0, 169.6, 150.0 (***E***/Z), 149.4 (E/***Z***), 148.3 (***E***/Z), 147.4 (E/***Z***), 145.2, 144.6, 134.5 (***E***/Z), 134.2 (E/***Z***), 132.1 131.5, 130.9, 124.1, 123.2 (***E***/Z), 122.9 (E/***Z***), 74.2 (***E***/Z), 73.6 (E/***Z***), 71.0, 67.1, 49.4, 48.5, 43.4 (***E***/Z), 42.7 (E/***Z***), 39.3, 38.7, 36.9, 36.4, 35.9, 35.4, 31.4, 29.6, 29.5 (***E***/Z), 29.4 (E/***Z***), 28.9, 27.5 (***E***/Z), 27.0 (E/***Z***), 24.5, 22.5, 22.4, 21.0, 19.6 (E/***Z***), 19.3 (***E***/Z), 16.5, 16.4 and 15.0; LC-MS (ESI): *m/z* 620 $[M+H]^+$, 642 $[M+23]^+$, 560 $[M-OAc]^+$; purity (HPLC): 98% (t_r = 16.94 min).

***N*-(pyridin-4-ylmethylene)fusidic acid hydrazide (3.17)**

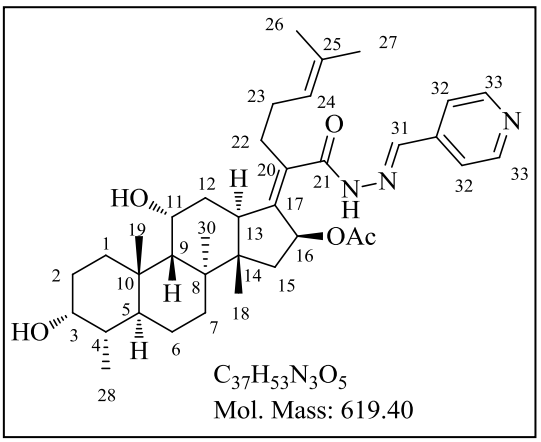

White solid (0.110 g, 63%); R_f 0.2 (8% Methanol:DCM); Mp. 159-161 ^oC; A mixture of E/Z isomers; ^1H NMR (400 MHz, $CDCl_3$) δ 10.18 (s, 1H, NH, ***E***/Z), 9.05 (s, 1H, NH, E/***Z***), 8.66 (br s, 2H, 2×H-33), 8.24 (s, 1H, H-31, ***E***/Z), 7.81 (s, 1H, H-31, E/***Z***), 7.61 (d, *J* = 4.4 Hz, 2H, 2×H-32, ***E***/Z), 7.51 (d, *J* = 4.4 Hz, 2H, 2×H-32, E/***Z***), 5.76 (d, *J* = 8.1 Hz,

1H, H-16, ***E***/Z), 5.63 (d, *J* = 8.1 Hz, 1H, H-16, E/***Z***), 5.10 (m, 1H, H-24), 4.38 (m, 1H, H-11), 3.76 (m, 1H, H-3), 3.12-3.08 (m, 1H, H-13, ***E***/Z), 3.03-2.99 (m, 1H, H-13, E/***Z***), 2.72-2.65 (m, 1H, H-22), 2.57-2.10 (m, 7H, H-1, H-5, H-12, H-15, H-22 and 2×H-23), 1.93-1.73 (m, 4H, 2×H-2, H-7 and H-12), 1.93 (s, 3H, OAc, ***E***/Z), 1.91 (s, 3H, OAc, E/***Z***), 1.67-1.52 (m, 10H, CH_3-27, CH_3-26, H-1, H-4, H-6 and H-9), 1.40 (s, 3H, CH_3-30, ***E***/Z), 1.38 (s, 3H, CH_3-30, E/***Z***), 1.23-1.20 (m, 1H, H-15), 1.16-1.07 (m, 2H, H-6 and H-7), 1.00-0.91 (m, 9H, CH_3-18, CH_3-19 and CH_3-28); ^{13}C NMR (100 MHz, CD_3OD) δ 170.9, 169.8, 149.0 (2C), 145.5, 144.8, 143.0, 132.2, 131.4, 123.2 (***E***/Z), 122.9 (E/***Z***), 121.6 (2C, *E*/Z), 121.1 (2C, *E*/*Z*), 74.2 (***E***/Z), 73.6 (E/***Z***), 71.0, 67.1, 49.4 (***E***/Z), 49.0 (E/***Z***), 48.5, 43.4 (***E***/Z), 42.8 (E/***Z***), 39.3, 38.7, 36.9, 36.4, 35.9, 35.4, 31.4, 29.6, 29.5 (***E***/Z), 29.3 (E/***Z***), 28.9, 27.5 (***E***/Z), 27.1 (E/***Z***), 24.5, 22.5, 22.4, 21.0, 19.5 (***E***/Z), 19.3 (E/***Z***), 16.4 (2C), 15.0; LC-MS (ESI): *m/z* 620 $[M+H]^+$, 642 $[M+23]^+$, 560 $[M-OAc]^+$; purity (HPLC): 98% (t_r = 16.98 min).

General synthetic procedure for compounds 3.18-3.23

To a solution of compound **3.13** (1.0 eq.) in pyridine (2-5 ml), respective sulfonyl chloride (1.0 eq.) was added and reaction mixture was stirred at 25 °C for 1-3 h. After completion of reaction (TLC), reaction mixture was diluted with EtOAc (25 ml) and washed with water (3×15 ml), dried over anhydrous magnesium sulfate, filtered and concentrated *in vacuo*. Purification by flash chromatography on 100-200 silica gel using EtOAc:hexane as eluent afforded products **3.18-3.23.**

***N*-methylsulfonylfusidic acid hydrazide (3.18)**

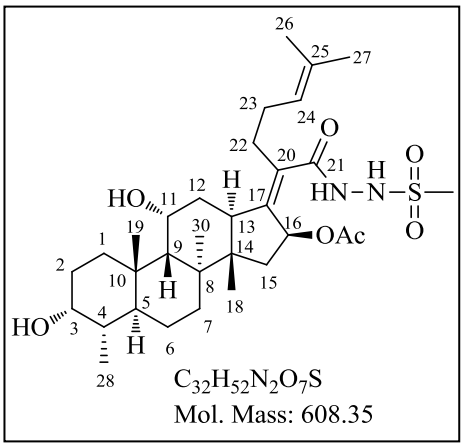

White solid (0.05 g obtained from 0.1 g of **3.13**, 44%); R_f 0.4 (70% EtOAc:hexane); Mp. 125-127 °C; ^{1}H NMR (400 MHz, $CDCl_3$) δ 7.79 (d, *J* = 3.7 Hz, 1H, NH), 6.89 (d, *J* = 4.8 Hz, 1H, NH), 5.74 (d, *J* = 8.1 Hz, 1H, H-16), 5.11 (t, *J* = 7.2 Hz, 1H, H-24), 4.35 (m, 1H, H-11), 3.76 (m, 1H, H-3), 3.07-3.02 (m, 1H, H-13), 3.00 (s, 3H, SO_2CH_3), 2.52-2.45 (m, 1H, H-22), 2.37-2.26 (m, 2H, H-12 and H-22), 2.21-2.09 (m, 5H, H-1, H-5, H-15 and 2×H-23), 2.01 (s, 3H, OAc), 1.91-1.73 (m, 4H, 2×H-2, H-7 and H-12), 1.69 (s, 3H, CH_3-27), 1.62 (s, 3H, CH_3-26), 1.60-1.48 (m, 4H, H-1, H-4, H-6 and H-9), 1.38 (s, 3H, CH_3-30), 1.33-1.27 (m, 1H, H-15), 1.18-1.05 (m, 2H, H-6 and H-7), 0.98 (s, 3H, CH_3-19), 0.95 (s, 3H, CH_3-18), 0.93 (d, *J* = 6.8 Hz, 3H, CH_3-28); ^{13}C NMR (100 MHz, $CDCl_3$) δ 170.8, 170.5, 146.0,

133.1, 131.7, 122.7, 73.8, 71.4, 68.3, 49.4, 48.8, 43.7, 39.6, 39.4, 39.2, 37.0, 36.3, 36.0, 35.4, 32.1, 30.2, 29.8, 29.7, 28.2, 25.6, 24.0, 22.9, 21.1, 20.7, 17.9, 17.8 and 15.8; LC-MS (ESI): *m/z* 609 $[M+H]^+$, 549 $[M-OAc]^+$; purity (HPLC): 96% (t_r = 13.94 min).

_N_-ethylsulfonylfusidic acid hydrazide (3.19)

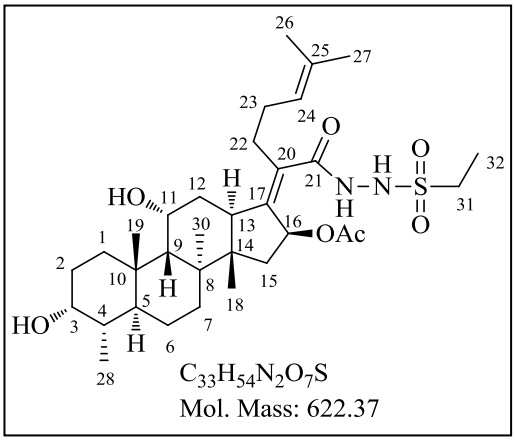

White solid (0.16 g obtained from 0.3 g of **3.13**, 45%); R_f 0.5 (70% EtOAc:hexane); Mp. 127-129 ^oC; ^1H NMR (400 MHz, $CDCl_3$) δ 8.23 (br s, 1H, NH), 7.13 (br s, 1H, NH), 5.74 (d, *J* = 8.2 Hz, 1H, H-16), 5.10 (t, *J* = 6.6 Hz, 1H, H-24), 4.37 (m, 1H, H-11), 3.76 (m, 1H, H-3), 3.17-3.07 (m, 2H, H-31), 3.03-3.00 (m, 1H, H-13), 2.43-2.39 (m, 1H, H-22), 2.33-2.24 (m, 2H, H-12 and H-22), 2.16-2.14 (m, 5H, H-1, H-5, H-15 and 2×H-23), 2.00 (s, 3H, OAc), 1.86-1.80 (m, 4H, 2×H-2, H-7 and H-12), 1.68 (s, 3H, CH_3-27), 1.60 (s, 3H, CH_3-26), 1.57-1.51 (m, 4H, H-1, H-4, H-6 and H-9), 1.43 (t, *J* = 7.3 Hz, 3H, H-32), 1.38 (s, 3H, CH_3-30), 1.28-1.25 (m, 1H, H-15), 1.15-1.09 (m, 2H, H-6 and H-7), 0.97 (s, 3H, CH_3-19), 0.93-0.91 (m, 6H, CH_3-18 and CH_3-28); ^{13}C NMR (100 MHz, $CDCl_3$) δ 171.0, 170.4, 145.3, 132.9, 131.9, 122.8, 73.8, 71.6, 68.3, 49.4, 48.7, 46.4, 43.6, 39.6, 39.2, 36.9, 36.5, 35.8, 35.5, 31.8, 30.1, 29.7, 29.7, 28.2, 25.6, 23.7, 23.1, 21.1, 20.9, 17.7(2C), 15.8 and 7.8; LC-MS (ESI): *m/z* 645 $[M+23]^+$, 563 $[M-OAc]^+$; purity (LC-MS): 96% (t_r = 4.15 min).

_N_-propylsulfonylfusidic acid hydrazide (3.20)

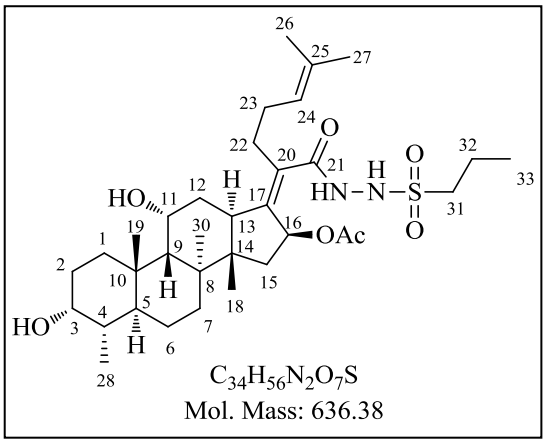

White solid (0.15 g obtained from 0.5 g of **3.13**, 25%); R_f 0.4 (5% Methanol:DCM); Mp. 125-127 ^oC; ^1H NMR (400 MHz, $CDCl_3$) δ 7.95 (br s, 1H, NH), 6.95 (br s, 1H, NH), 5.73 (d, *J* = 8.2 Hz, 1H, H-16), 5.10 (t, *J* = 6.8 Hz, 1H, H-24), 4.36 (m, 1H, H-11), 3.76 (m, 1H, H-3), 3.08-2.99 (m, 3H, 2×H-31 and H-13), 2.49-2.42 (m, 1H, H-22), 2.35-2.25 (m, 2H, H-12 and H-22), 2.17-2.11 (m, 5H, H-1, H-5, H-15 and 2×H-23), 2.01 (s, 3H, OAc), 1.97-1.78 (m, 6H, 2×H-2, H-7, H-12 and 2×H-32), 1.73 (s, 3H, CH_3-27), 1.61 (s, 3H, CH_3-26), 1.58-1.49 (m, 4H, H-1, H-4, H-6 and H-9), 1.38 (s, 3H, CH_3-30), 1.31-1.27 (m, 1H, H-15), 1.14-1.11 (m, 2H, H-6 and H-7),

1.05 (t, J = 7.3 Hz, 3H, H-33), 0.98 (s, 3H, CH_3-19), 0.94 (s, 3H, CH_3-18), 0.93 (d, J = 7.0 Hz, 3H, CH_3-28); ^{13}C NMR (100 MHz, $CDCl_3$) δ 170.8, 170.4, 145.7, 133.1, 131.9, 122.7, 73.8, 71.3, 68.3, 53.4, 49.3, 48.8, 43.7, 39.6, 39.2, 37.0, 36.3, 36.1, 35.5, 32.1, 30.2, 29.8, 29.7, 28.1, 25.5, 23.9, 22.8, 21.1, 20.7, 17.9, 17.7, 17.0, 15.8 and 12.9; LC-MS (ESI): *m/z* 659 $[M+23]^+$, 577 $[M\text{-}OAc]^+$; purity (LC-MS): 99% (t_r = 4.20 min).

_N_-butylsulfonylfusidic acid hydrazide (3.21)

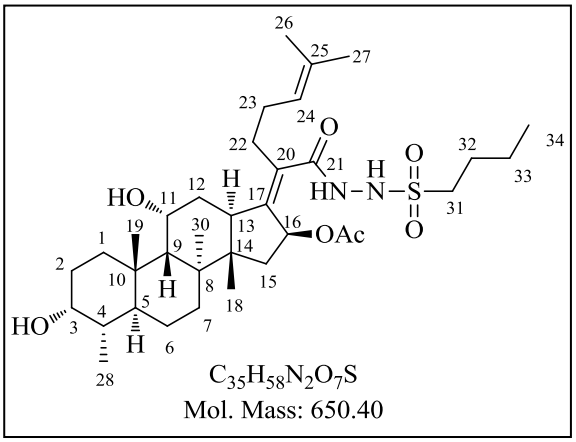

White solid (0.35 g obtained from 0.4 g of **3.13**, 71%); R_f 0.6 (70% EtOAc:hexane); Mp. 121-123 °C; ^{1}H NMR (400 MHz, $CDCl_3$) δ 8.15 (br s, 1H, NH), 7.06 (br s, 1H, NH), 5.74 (d, J = 8.2 Hz, 1H, H-16), 5.10 (t, J = 6.6 Hz, 1H, H-24), 4.36 (m, 1H, H-11), 3.76 (m, 1H, H-3), 3.15-3.00 (m, 3H, 2×H-31 and H-13), 2.45-2.40 (m, 1H, H-22), 2.35-2.24 (m, 2H, H-12 and H-22), 2.16-2.11 (m, 5H, H-1, H-5, H-15 and 2×H-23), 2.01 (s, 3H, OAc), 1.93-1.71 (m, 6H, 2×H-2, H-7, H-12 and 2×H-32), 1.68 (s, 3H, CH_3-27), 1.60 (s, 3H, CH_3-26), 1.59-1.49 (m, 4H, H-1, H-4, H-6 and H-9), 1.47-1.41 (m, 2H, H-33), 1.38 (s, 3H, CH_3-30), 1.29-1.25 (m, 1H, H-15), 1.16-1.07 (m, 2H, H-6 and H-7), 0.97 (s, 3H, CH_3-19), 0.95-0.92 (m, 9H, CH_3-18, CH_3-28 and 3×H-34); ^{13}C NMR (100 MHz, $CDCl_3$) δ 170.9, 170.4, 145.3, 132.9, 131.7, 122.8, 73.7, 71.5, 68.3, 51.6, 49.4, 48.7, 43.6, 39.6, 39.2, 36.9, 36.4, 35.9, 35.5, 31.9, 30.2, 29.7, 28.2, 25.6, 25.1, 23.8, 23.0, 21.5, 21.1, 20.8, 17.8 (C3), 15.8 and 13.4; LC-MS (ESI): *m/z* 673 $[M+23]^+$, 591 $[M\text{-}OAc]^+$; purity (LC-MS): 97% (t_r = 4.47 min).

_N_-(4-Methylphenylsulfonyl)fusidic acid hydrazide (3.22)

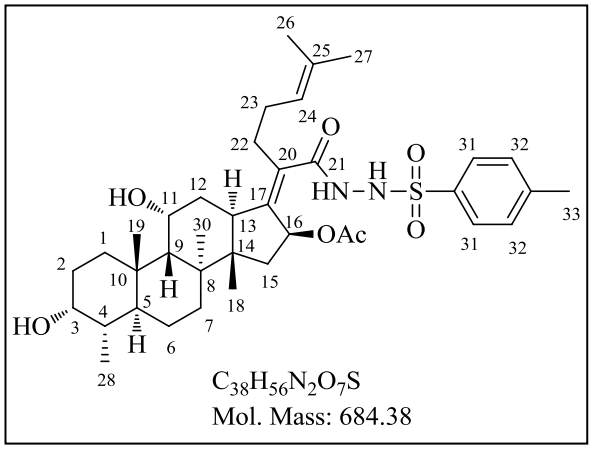

White solid (0.03 g obtained from 0.05 g of **3.13**, 46%); R_f 0.3 (60% EtOAc:hexane); Mp. 220-222 °C; ^{1}H NMR (400 MHz, $CDCl_3$) δ 7.80 (d, J = 8.4 Hz, 2H, H-31), 7.70 (d, J = 6.0 Hz, 1H, NH), 7.32 (d, J = 6.0 Hz, 1H, NH), 7.26 (d, J = 7.9 Hz, 2H, H-32), 5.54 (d, J = 8.2 Hz, 1H, H-16), 4.94 (t, J = 6.8 Hz, 1H, H-24), 4.30 (m, 1H, H-11), 3.75 (m, 1H, H-3), 2.95-2.92 (m, 1H, H-13), 2.38 (s, 3H, H-33),

2.20-2.02 (m, 8H, H-1, H-5, H-12, H-15, 2×H-22 and 2×H-23), 2.00 (s, 3H, OAc), 1.88-1.72 (m, 4H, 2×H-2, H-7 and H-12), 1.70 (s, 3H, CH_3-27), 1.57 (s, 3H, CH_3-26), 1.51-1.47 (m, 4H, H-1, H-4, H-6 and H-9), 1.33 (s, 3H, CH_3-30), 1.27-1.24 (m, 1H, H-15), 1.14-1.04 (m, 2H, H-6 and H-7), 0.96 (s, 3H, CH_3-19), 0.91 (d, J = 6.2 Hz, 3H, CH_3-28), 0.87 (s, 3H, CH_3-18); ^{13}C NMR (100 MHz, $CDCl_3$) δ 170.2, 169.6, 145.9, 144.8, 133.3, 132.7, 131.4, 129.5 (2C), 128.8 (2C), 122.9, 73.9, 71.3, 68.2, 49.3, 48.8, 43.5, 39.5, 39.1, 37.1, 36.2, 36.1, 35.3, 32.4, 30.3, 29.9, 29.5, 28.0, 25.7, 24.1, 22.6, 21.6, 21.0, 20.6, 17.9 (2C) and 15.8; LC-MS (ESI): *m/z* 685 $[M+H]^+$, 625 $[M-OAc]^+$; purity (HPLC): 97% (t_r = 12.56 min).

_N_-(4-chlorophenylsulfonyl)fusidic acid hydrazide (3.23)

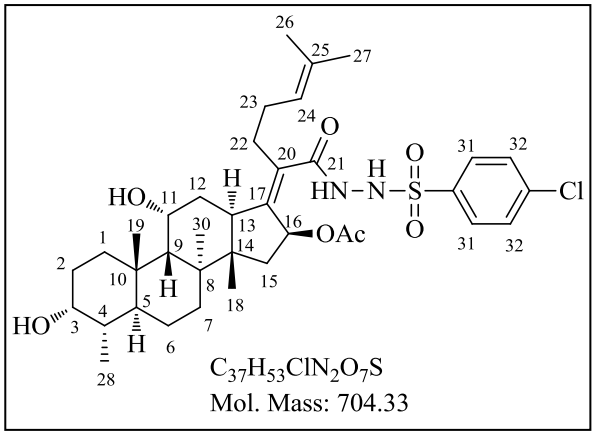

White solid (0.093 g obtained from 0.108 g of **3.13**, 65%); R_f 0.5 (60% EtOAc:hexane); Mp. 230-232 °C; ^{1}H NMR (400 MHz, $CDCl_3$) δ 7.86 (d, J = 8.6 Hz, 2H, H-32), 7.62 (d, J = 5.3 Hz, 1H, NH), 7.45 (d, J = 8.4 Hz, 2H, H-31), 7.31 (d, J = 5.5 Hz, 1H, NH), 5.55 (d, J = 8.4 Hz, 1H, H-16), 4.95 (t, J = 6.8 Hz, 1H, H-24), 4.31 (m, 1H, H-11), 3.75 (m, 1H, H-3), 2.97-2.94 (m, 1H, H-13), 2.18-2.06 (m, 8H, H-1, H-5, H-12, H-15, 2×H-22 and 2×H-23), 2.00 (s, 3H, OAc), 1.91-1.74 (m, 4H, 2×H-2, H-7 and H-12), 1.71 (s, 3H, CH_3-27), 1.58 (s, 3H, CH_3-26), 1.54-1.51 (m, 4H, H-1, H-4, H-6 and H-9), 1.34 (s, 3H, CH_3-30), 1.29-1.26 (m, 1H, H-15), 1.14-1.07 (m, 2H, H-6 and H-7), 0.96 (s, 3H, CH_3-19), 0.92 (d, J = 6.8 Hz, 3H, CH_3-28), 0.89 (s, 3H, CH_3-18); ^{13}C NMR (100 MHz, $CDCl_3$) δ 170.3, 169.7, 146.3, 140.6, 134.9, 133.0, 131.3, 130.2 (2C), 129.2 (2C), 122.6, 73.8, 71.3, 68.1, 49.2, 48.9, 43.6, 39.5, 39.2, 37.1, 36.3, 36.0, 35.3, 32.5, 30.3, 29.9, 29.6, 28.0, 25.7, 24.1, 22.4, 21.1, 20.6, 18.0, 17.9 and 15.8; LC-MS (ESI): *m/z* 722 $[M+NH_4]^+$, 645 $[M-OAc]^+$; purity (HPLC): 98% (t_r = 11.92 min).

General synthetic procedure for compounds 3.24-3.27

EDCI (1.15 eq.) and HOBt (1.20 eq.) were added to a solution of fusidic acid (**3.1**) (1.0 eq.) in acetonitrile (20 ml) and resulting reaction mixture was stirred at 25 °C for 3 h followed by the addition of respective amidoxime (1.10 eq.) and then reaction mixture was heated at 80 °C for 12 h. After completion of reaction (TLC), solvent was removed *in vacuo*. The residue was taken in EtOAc (25 ml), washed with water (3×15 ml), dried over anhydrous magnesium

sulfate, filtered and concentrated *in vacuo*. Without further purification this intermediate and NaOAc (5.0 eq.) were taken in EtOH (20 ml) and irradiated in microwave at 100 °C for 2 h. After completion of reaction (TLC), solvent was removed *in vacuo* and residue was taken in EtOAc (25 ml), washed with water (2×15 ml), dried over anhydrous magnesium sulfate, filtered and concentrated *in vacuo*. Purification by flash chromatography on 100-200 silica gel using EtOAc:hexane as eluent afforded products **3.24-3.27**.

20-Decarboxy-20-(3-methyl-1,2,4-oxadiazol-5-yl)fusidic acid (3.24)

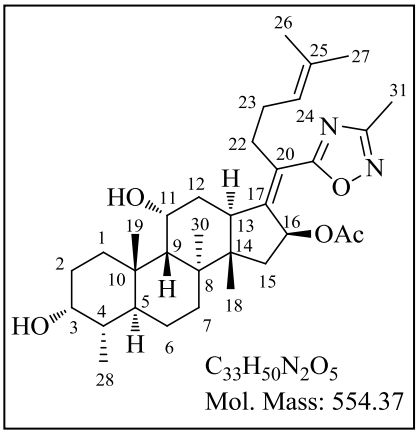

White solid (0.090 g obtained from 0.35 g of **3.1**, 24%); R_f 0.8 (80% EtOAc:hexane); Mp. 152-154 °C; ^{1}H NMR (400 MHz, $CDCl_3$) δ 5.96 (d, *J* = 8.2 Hz, 1H, H-16), 5.06 (t, *J* = 6.8 Hz, 1H, H-24), 4.37 (m, 1H, H-11), 3.76 (m, 1H, H-3), 3.16-3.13 (m, 1H, H-13), 2.70-2.62 (m, 2H, 2×H-22), 2.41-2.37 (m, 1H, H-12), 2.36 (s, 3H, H-31), 2.24-2.06 (m, 5H, H-1, H-5, H-15 and 2×H-23), 1.95-1.76 (m, 4H, 2×H-2, H-7 and H-12), 1.71 (s, 3H, OAc), 1.64 (s, 3H, CH_3-27), 1.60-1.50 (m, 4H, H-1, H-4, H-6 and H-9), 1.57 (s, 3H, CH_3-26), 1.40 (s, 3H, CH_3-30), 1.35-1.32 (m, 1H, H-15), 1.18-1.08 (m, 2H, H-6 and H-7), 0.99 (s, 3H, CH_3-19), 0.93-0.92 (m, 6H, CH_3-18 and CH_3-28); ^{13}C NMR (100 MHz, $CDCl_3$) δ 177.7, 170.0, 166.8, 152.7, 132.8, 123.0, 122.6, 74.6, 71.3, 68.2, 49.2, 48.9, 44.8, 39.5, 39.0, 37.0, 36.2, 36.1, 35.7, 32.5, 30.3, 30.0, 29.8, 28.2, 25.6, 24.2, 22.6, 20.7 (2C), 18.0, 17.7, 15.9 and 11.4; LC-MS (ESI): *m/z* 555 $[M+H]^+$; purity (HPLC): 96% (t_r = 13.91 min).

20-Decarboxy-20-(3-ethyl-1,2,4-oxadiazol-5-yl)fusidic acid (3.25)

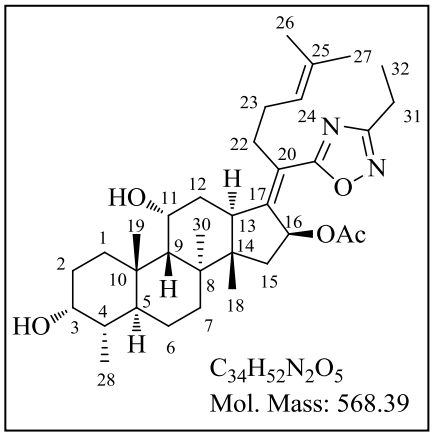

White solid (0.050 g obtained from 0.2 g of **3.1**, 23%); R_f 0.6 (80% EtOAc:hexane); Mp. 126-128 °C; ^{1}H NMR (400 MHz, $CDCl_3$) δ 5.97 (d, *J* = 8.4 Hz, 1H, H-16), 5.07 (t, *J* = 6.8 Hz, 1H, H-24), 4.37 (m, 1H, H-11), 3.76 (m, 1H, H-3), 3.16-3.14 (m, 1H, H-13), 2.72 (q, *J* = 7.5 Hz, 2H, H-31), 2.68-2.63 (m, 2H, 2×H-22), 2.41-2.38 (m, 1H, H-12), 2.24-2.02 (m, 5H, H-1, H-5, H-15 and 2×H-23), 1.98-1.77 (m, 4H, 2×H-2, H-7 and H-12), 1.72 (s, 3H, OAc), 1.64 (s, 3H, CH_3-27), 1.64-1.47 (m, 4H, H-1, H-4, H-6 and H-9), 1.57 (s, 3H, CH_3-26), 1.40 (s, 3H, CH_3-30), 1.32-1.29 (m, 4H, H-15 and 3×H-32), 1.19-1.06 (m, 2H, H-6 and H-7), 0.99 (s, 3H,

CH_3-19), 0.93-0.92 (m, 6H, CH_3-18 and CH_3-28); ^{13}C NMR (100 MHz, $CDCl_3$) δ 177.6, 171.3, 169.9, 152.7, 132.8, 123.0, 122.6, 74.5, 71.3, 68.3, 49.2, 48.9, 44.8, 39.5, 39.0, 37.1, 36.3, 36.1, 35.7, 32.5, 30.3, 30.0, 29.9, 28.2, 25.6, 24.2, 22.6, 20.7 (2C), 19.6, 18.0, 17.7, 15.9 and 11.4; LC-MS (ESI): *m/z* 569 $[M+H]^+$, 509 $[M-OAc]^+$; purity (HPLC): 98% (t_r = 15.38 min).

20-Decarboxy-20-(3-propyl-1,2,4-oxadiazol-5-yl)fusidic acid (3.26)

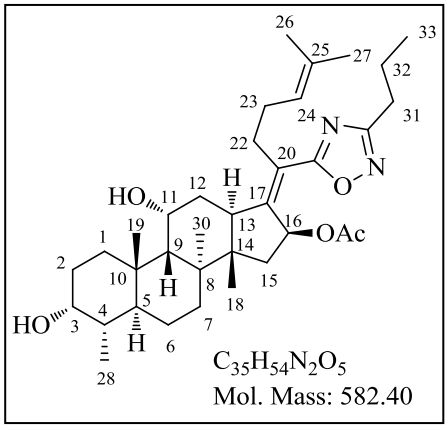

White solid (0.080 g obtained from 0.5 g of **3.1**, 14%); R_f 0.6 (70% EtOAc:hexane); Mp. 110-112 °C; ^1H NMR (400 MHz, $CDCl_3$) δ 5.97 (d, *J* = 8.2 Hz, 1H, H-16), 5.07 (t, *J* = 6.8 Hz, 1H, H-24), 4.37 (m, 1H, H-11), 3.76 (m, 1H, H-3), 3.17-3.14 (m, 1H, H-13), 2.68-2.65 (m, 4H, 2×H-22 and 2×H-31), 2.42-2.38 (m, 1H, H-12), 2.24-2.06 (m, 5H, H-1, H-5, H-15 and 2×H-23), 1.95-1.75 (m, 6H, 2×H-2, H-7, H-12 and 2×H-32), 1.72 (s, 3H, OAc), 1.64 (s, 3H, CH_3-27), 1.60-1.51 (m, 4H, H-1, H-4, H-6 and H-9), 1.57 (s, 3H, CH_3-26), 1.40 (s, 3H, CH_3-30), 1.36-1.33 (m, 1H, H-15), 1.19-1.08 (m, 2H, H-6 and H-7), 1.01-0.97 (m, 6H, CH_3-19 and 3×H-33), 0.93-0.92 (m, 6H, CH_3-28 and CH_3-18); ^{13}C NMR (100 MHz, $CDCl_3$) δ 177.4, 170.2, 169.9, 152.5, 132.7, 123.2, 122.6, 74.6, 71.3, 68.3, 49.2, 48.9, 44.9, 39.5, 39.0, 37.1, 36.3, 36.1, 35.7, 32.5, 30.3, 30.0, 29.9, 28.2, 27.9, 25.6, 24.2, 22.6, 20.7 (2C), 20.4, 18.1, 17.7, 15.9 and 13.7; LC-MS (ESI): *m/z* 583 $[M+H]^+$, 523 $[M-OAc]^+$; purity (LC-MS): 98% (t_r = 4.33 min).

20-Decarboxy-20-(3-(4-fluorophenyl)-1,2,4-oxadiazol-5-yl)fusidic acid (3.27)

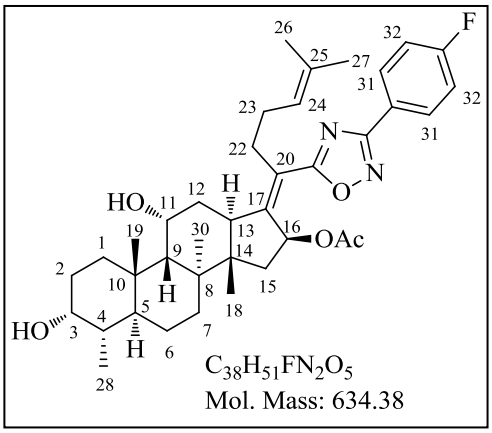

White solid (0.10 g obtained from 0.4 g of **3.1**, 20%); R_f 0.7 (50% EtOAc:hexane); Mp. 86-88 °C; ^1H NMR (400 MHz, $CDCl_3$) δ 8.08 (dd, *J* = 8.8 and 5.3 Hz, 2H, H-32), 7.16 (dd, *J* = 8.6 and 5.5 Hz, 2H, H-31), 6.14 (d, *J* = 8.1 Hz, 1H, H-16), 5.10 (t, *J* = 6.8 Hz, 1H, H-24), 4.39 (m, 1H, H-11), 3.76 (m, 1H, H-3), 3.23-3.20 (m, 1H, H-13), 2.74 (t, *J* = 7.7 Hz, 2H, 2×H-22), 2.46-2.42 (m, 1H, H-12), 2.29-2.08 (m, 5H, H-1, H-5, H-15 and 2×H-23), 1.98-1.75 (m, 4H, 2×H-2, H-7 and H-12), 1.64 (s, 6H, OAc and CH_3-27), 1.58 (s, 3H, CH_3-26), 1.60-1.50 (m, 4H, H-1, H-4, H-6 and H-9), 1.42 (s, 3H, CH_3-

30), 1.40-1.37 (m, 1H, H-15), 1.22-1.09 (m, 2H, H-6 and H-7), 1.00 (s, 3H, CH_3-19), 0.96 (s, 3H, CH_3-18), 0.93 (d, J = 6.8 Hz, 3H, CH_3-28); ^{13}C NMR (100 MHz, $CDCl_3$) δ 177.8, 170.2, 167.3, 165.7, 153.9, 133.0, 129.5, 129.4, 123.2, 122.8, 122.6, 116.1, 115.9, 74.7, 71.3, 68.2, 49.2, 49.1, 45.2, 39.5, 39.0, 37.1, 36.2 (2C), 35.8, 32.4, 30.3, 30.0, 29.6, 28.4, 25.6, 24.2, 22.7, 20.7 (2C), 18.1, 17.7 and 15.9; LC-MS (ESI): *m/z* 635 $[M+H]^+$, 575 $[M-OAc]^+$; purity (HPLC): 97% (t_r = 16.80 min).

20-Decarboxy-20-(5-hydroxy-1,3,4-oxadiazol-2-yl) fusidic acid (3.28)

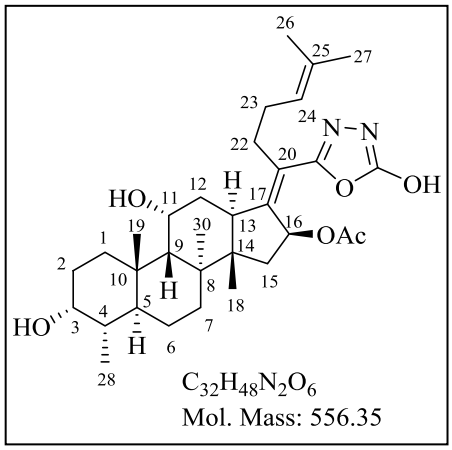

Et_3N (0.1 ml, 0.72 mmol) was added to a solution of compound **3.13** (0.2 g, 0.38 mmol) in THF (10 ml) and reaction mixture was cooled to 0 °C followed by addition of 1,1' carbonyldiimidazole (CDI) (0.092 g, 0.56 mmol). Reaction mixture was stirred at 0 °C for 5 h followed by further addition of Et_3N (0.1 ml, 0.72 mmol) and CDI (0.092 g, 0.56 mmol). Reaction mixture was stirred at 25 °C for 11 h and solvent was removed *in vacuo*. Residue was taken in EtOAc (15 ml) and washed with water (3×15 ml), dried over anhydrous magnesium sulfate, filtered and concentrated *in vacuo*. Purification by flash chromatography on 100-200 silica gel using EtOAc:hexane as eluent afforded product **3.28** as a white solid (0.052 g, 24%); R_f 0.5 (70% EtOAc: hexane); Mp. 137-139 °C; ^{1}H NMR (400 MHz, $CDCl_3$) δ 5.86 (d, J = 8.2 Hz, 1H, H-16), 5.08 (t, J = 6.8 Hz, 1H, H-24), 4.37 (m, 1H, H-11), 3.77 (m, 1H, H-3), 3.12-3.09 (m, 1H, H-13), 2.59-2.52 (m, 1H, H-22), 2.49-2.42 (m, 1H, H-22), 2.38-2.34 (m, 1H, H-12), 2.21-2.11 (m, 5H, H-1, H-5, H-15 and 2×H-23), 1.92 (s, 3H, OAc), 1.89-1.75 (m, 4H, 2×H-2, H-7 and H-12), 1.67 (s, 3H, CH_3-27), 1.62-1.50 (m, 7H, CH_3-26, H-1, H-4, H-6 and H-9), 1.38 (s, 3H, CH_3-30), 1.36-1.33 (m, 1H, H-15), 1.18-1.08 (m, 2H, H-6 and H-7), 0.98 (s, 3H, CH_3-19), 0.93-0.92 (m, 6H, CH_3-18 and CH_3-28); ^{13}C NMR (100 MHz, $CDCl_3$) δ 174.6, 170.3, 154.4, 151.5, 132.9, 122.5, 122.2, 74.5, 71.4, 68.2, 49.2, 48.8, 44.8, 39.5, 39.1, 37.1, 36.2, 36.1, 35.7, 32.4, 30.3, 29.9, 28.5, 28.1, 25.6, 24.2, 22.6, 20.9, 20.7, 18.1, 17.8 and 15.8; LC-MS (ESI): *m/z* 557 $[M+H]^+$; purity (HPLC): 96% (t_r = 12.91 min).

20-Decarboxy-20-(5-thioxo-4,5-dihydro-1,3,4-oxadiazol-2-yl) fusidic acid (3.29)

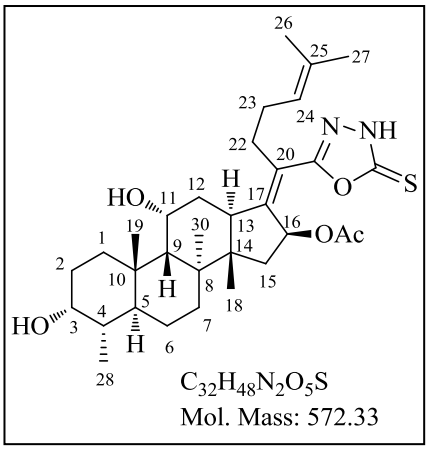

Carbon disulfide (0.03 ml, 0.52 mmol) and KOH (0.026 g, 0.47 mmol) were added to a solution of compound **3.13** (0.25 g, 0.47 mmol) in ethanol (5 ml) at 0 ^{o}C and resulting reaction mixture was shifted to heating at 80 ^{o}C until reaction proceeds to completion. After completion of reaction (TLC, 16 h), solvent was removed *in vacuo* and diluted with EtOAc (15 ml). The organic phase was washed with water (3×15 ml), dried over anhydrous magnesium sulfate, filtered and concentrated *in vacuo*. Purification by flash chromatography on 100-200 silica gel using EtOAc:hexane as eluent afforded product **3.29** as a white solid (0.15 g, 56%); R_f 0.4 (90% EtOAc:hexane); Mp. 130-132 ^{o}C; ^{1}H NMR (400 MHz, $CDCl_3$) δ 11.97 (br s, 1H, NH), 5.86 (d, *J* = 8.2 Hz, 1H, H-16), 5.06 (t, *J* = 6.8 Hz, 1H, H-24), 4.37 (m, 1H, H-11), 3.77 (m, 1H, H-3), 3.14-3.11 (m, 1H, H-13), 2.60-2.54 (m, 2H, 2×H-22), 2.38-2.34 (m, 1H, H-12), 2.20-2.08 (m, 5H, H-1, H-5, H-15 and 2×H-23), 2.02-1.70 (m, 4H, 2×H-2, H-7 and H-12), 1.89 (s, 3H, OAc), 1.65 (s, 3H, CH_3-27), 1.61-1.50 (m, 7H, CH_3-26, H-1, H-4, H-6 and H-9), 1.38 (s, 3H, CH_3-30), 1.35-1.31 (m, 1H, H-15), 1.17-1.07 (m, 2H, H-6 and H-7), 0.98 (s, 3H, CH_3-19), 0.93-0.91 (m, 6H, CH_3-18 and CH_3-28); ^{13}C NMR (100 MHz, $CDCl_3$) δ 170.6 (2C), 153.0 (2C), 133.0, 122.4, 121.0, 74.5, 71.5, 68.1, 49.3, 48.9, 45.1, 39.5, 39.1, 37.0, 36.3, 36.0, 35.7, 32.1, 30.2, 29.8, 29.0, 28.1, 25.6, 24.0, 22.9, 20.9, 20.8, 18.0, 17.8 and 15.9; LC-MS (ESI): *m/z* 595 $[M+23]^+$, 513 $[M\text{-}OAc]^+$; purity (LC-MS): 98% (t_r = 4.55 min).

7.2.1.2 C-3 Fusidic acid derivatives

General synthetic procedure for compounds 3.30 and 3.32

Fusidic acid (**3.1**) (1.0 eq.) was dissolved in a mixture of corresponding acid anhydride (5.5 eq.) and pyridine (6.5 eq.) and the resulting reaction mixture was stirred at 25 ^{o}C for 3 h. After completion of reaction (TLC), water (25 ml) was added to the reaction mixture and aqueous layer was extracted with EtOAc (2×15 ml). Organic layer was washed with aq 0.5 M HCl (2×15 ml) to get rid of excess of pyridine. Organic layer was then dried over anhydrous sodium sulfate, filtered and concentrated *in vacuo*. The residue was purified on 100-200 silica gel using EtOAc: hexane as eluent to afford compound **3.30** and **3.32**.

General synthetic procedure for compounds 3.31 and **3.33-3.35**

T3P (2.0 eq., 50% w/v in DMF, d = 1.09 g/ml) was added dropwise to an ice cooled solution of fusidic acid (**3.1**) (1.0 eq.) and respective carboxylic acid (1.1 eq.) in pyridine. Reaction mixture was then slowly warmed to 25 ^{o}C and stirred for 16 h. After completion of the reaction (TLC), water (25 ml) was added to the reaction mixture and aqueous layer was extracted with EtOAc (2×15 ml). Organic layer was washed with aq 0.5 M HCl (2×15 ml) to remove excess of pyridine. Organic layer was dried over anhydrous sodium sulfate, filtered and concentrated *in vacuo*. The residue was purified by column chromatography on 100-200 silica gel using EtOAc: hexane as eluent to afford compound**3.31** and **3.33-3.35**.

3-Acetoxyfusidic acid (3.30)[3]

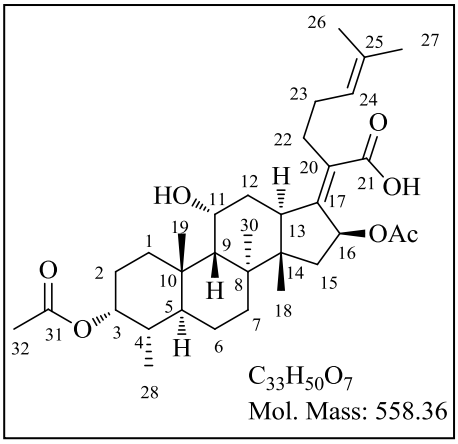

White solid (0.126 g obtained from 0.2 g of **3.1**, 58%); R_f 0.4 (50% EtOAc:hexane); Mp. 112-114 ^{o}C; ^{1}H NMR (400 MHz, $CDCl_3$) δ 5.91 (d, *J* = 8.4 Hz, 1H, H-16), 5.11 (t, *J* =7.2 Hz, 1H, H-24), 4.94 (m, 1H, H-3), 4.34 (m, 1H, H-11), 3.08-3.04 (m, 1H, H-13), 2.53-2.42 (m, 2H, 2×H-22), 2.35-2.30 (m, 1H, H-12), 2.22-2.05 (m, 5H, H-1, H-5, H-15 and 2×H-23), 2.07 (s, 3H, H-32), 1.97 (s, 3H, OAc), 1.91-1.76 (m, 4H, 2×H-2, H-7 and H-12), 1.68 (s, 3H, CH_3-27), 1.63-1.53 (m, 4H, H-1, H-4, H-6 and H-9), 1.61 (s, 3H, CH_3-26), 1.38 (s, 3H, CH_3-30), 1.36-1.32 (m, 1H, H-15), 1.20-1.02 (m, 2H, H-6 and H-7), 0.99 (s, 3H, CH_3-19), 0.93 (s, 3H, CH_3-18), 0.83 (d, *J* = 6.7 Hz, 3H, CH_3-28); ^{13}C NMR (100 MHz, $CDCl_3$) δ 174.3, 170.9, 170.5, 151.1, 132.6, 129.6, 123.0, 74.4, 74.1, 68.3, 49.1, 48.8, 44.3, 39.5, 39.0, 37.8, 36.9, 35.8, 34.8, 32.7, 31.1, 28.7, 28.4, 27.4, 25.7, 24.3, 22.5, 21.3, 20.6 (2C), 18.1, 17.8 and 15.5; LC-MS (ESI): *m/z* 559 $[M+1]^+$, 581 $[M+23]^+$, 499 $[M-OAc]^+$; purity (HPLC): 98% (t_r = 12.56 min).

3-Propionyloxyfusidic acid (3.31)

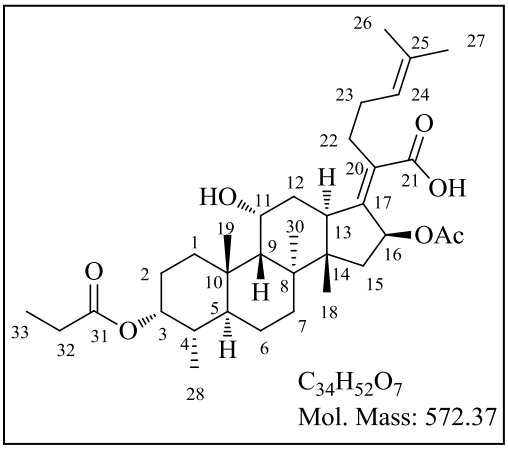

White solid (0.310 g obtained from 0.5 g of **3.1**, 56%); R_f 0.5 (50% EtOAc:hexane); Mp. 93-95 ^{o}C; ^{1}H NMR (400 MHz, $CDCl_3$) δ 5.91 (d, *J* = 8.3 Hz, 1H, H-16), 5.12 (t, *J* = 7.2 Hz, 1H, H-24), 4.95 (m, 1H, H-3), 4.34 (m, 1H, H-11), 3.08-3.04 (m, 1H, H-13), 2.51-2.42 (m, 2H, 2×H-22), 2.36 (q, *J* = 7.6 Hz,

2H, 2×H-32), 2.35-2.30 (m, 1H, H-12), 2.22-2.06 (m, 5H, H-1, H-5, H-15 and 2×H-23), 1.97 (s, 3H, OAc), 1.89-1.78 (m, 4H, 2×H-2, H-7 and H-12), 1.73-1.52 (m, 4H, H-1, H-4, H-6 and H-9), 1.68 (s, 3H, CH_3-27), 1.60 (s, 3H, CH_3-26), 1.38 (s, 3H, CH_3-30), 1.35-1.32 (m, 1H, H-15), 1.19-1.03 (m, 2H, H-6 and H-7), 1.16 (t, J = 7.6 Hz, 3H, H-33), 0.99 (s, 3H, CH_3-19), 0.93 (s, 3H, CH_3-18), 0.83 (d, J = 6.7 Hz, 3H, CH_3-28); ^{13}C NMR (100 MHz, $CDCl_3$) δ 174.1, 173.2, 170.5, 151.0, 132.6, 129.5, 123.0, 74.3, 73.8, 68.2, 49.1, 48.8, 44.3, 39.4, 39.0, 37.8, 37.0, 35.7, 34.8, 32.8, 31.0, 28.8, 28.3, 28.1, 27.4, 25.7, 24.3, 22.5, 20.6, 20.5, 18.1, 17.7, 15.5 and 9.4; LC-MS (ESI): *m/z* 573 $[M+1]^+$, 595 $[M+23]^+$, 513 $[M-OAc]^+$; purity (HPLC): 98% (t_r = 13.20 min).

3-Butyryloxyfusidic acid (3.32)

White solid (3.0 g obtained from 4.0 g of **3.1**, 66%); R_f 0.5 (50% EtOAc:hexane) Mp. 162-164 ^{o}C; ^{1}H NMR (400 MHz, $CDCl_3$) δ 5.90 (d, J = 8.3 Hz, 1H, H-16), 5.10 (t, J = 7.2 Hz, 1H, H-24), 4.95 (m, 1H, H-3), 4.34 (m, 1H, H-11), 3.07-3.03 (m, 1H, H-13), 2.53-2.41 (m, 2H, 2×H-22), 2.35-2.29 (m, 1H, H-12), 2.32 (t, 2H, J = 7.3 Hz, 2×H-32), 2.22-2.03 (m, 5H, H-1, H-5, H-15 and 2×H-23), 1.97 (s, 3H, OAc), 1.91-1.76 (m, 4H, 2×H-2, H-7 and H-12), 1.72-1.52 (m, 6H, H-1, H-4, H-6, H-9 and 2×H-33), 1.68 (s, 3H, CH_3-27), 1.60 (s, 3H, CH_3-26), 1.38 (s, 3H, CH_3-30), 1.35-1.32 (m, 1H, H-15), 1.19-1.05 (m, 2H, H-6 and H-7), 0.99 (s, 3H, CH_3-19), 0.97 (t, J = 7.4 Hz, 3H, 3×H-34), 0.93 (s, 3H, CH_3-18), 0.83 (d, J = 6.7 Hz, 3H, CH_3-28); ^{13}C NMR (100 MHz, $CDCl_3$) δ 174.5, 173.4, 170.4, 151.2, 132.6, 129.6, 123.0, 74.4, 73.8, 68.2, 49.1, 48.8, 44.3, 39.4, 39.0, 37.8, 36.9, 36.7, 35.7, 34.8, 32.7, 31.0, 28.7, 28.3, 27.4, 25.6, 24.3, 22.5, 20.5 (2C), 18.6, 18.0, 17.7, 15.6 and 13.7; LC-MS (ESI): *m/z* 587 $[M+1]^+$, 609 $[M+23]^+$, 527 $[M-OAc]^+$; purity (HPLC): 99% (t_r = 13.94 min).

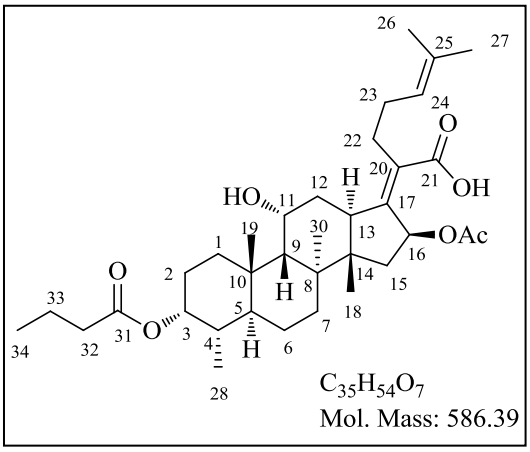

3-Pentanoyloxyfusidic acid (3.33)

White solid (1.3 g obtained from 2.0 g of **3.1**, 56%); R_f 0.6 (50% EtOAc:hexane) Mp. 118-120 ^{o}C; ^{1}H NMR (400 MHz, $CDCl_3$) δ 5.90 (d, J = 8.4 Hz, 1H, H-16), 5.11 (t, J = 7.1 Hz, 1H, H-24), 4.94 (m, 1H, H-3), 4.34 (m, 1H, H-11),

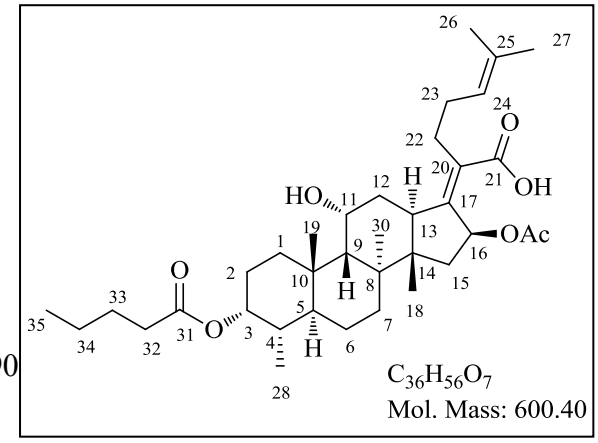

3.07-3.03 (m, 1H, H-13), 2.49-2.45 (m, 2H, 2×H-22), 2.35-2.29 (m, 1H, H-12), 2.33 (t, J = 7.4 Hz, 2H, 2×H-32), 2.22-2.04 (m, 5H, H-1, H-5, H-15 and 2×H-23), 1.96 (s, 3H, OAc), 1.91-1.77 (m, 4H, 2×H-2, H-7 and H-12), 1.64-1.53 (m, 6H, H-1, H-4, H-6, H-9 and 2×H-33), 1.67 (s, 3H, CH_3-27), 1.60 (s, 3H, CH_3-26), 1.40-1.32 (m, 3H, H-15 and 2×H-34), 1.38 (s, 3H, CH_3-30), 1.19-1.04 (m, 2H, H-6 and H-7), 0.99 (s, 3H, CH_3-19), 0.97-0.93 (m, 6H, CH_3-18 and 3×H-35), 0.82 (d, J = 6.7 Hz, 3H, CH_3-28); ^{13}C NMR (100 MHz, $CDCl_3$) δ 174.2, 173.5, 170.4, 151.2, 132.6, 129.5, 123.0, 74.4, 73.8, 68.2, 49.1, 48.8, 44.3, 39.4, 39.0, 37.8, 37.0, 35.7, 34.8, 34.5, 32.8, 31.0, 28.7, 28.3, 27.4, 27.3, 25.6, 24.3, 22.5, 22.3, 20.5 (2C), 18.1, 17.7, 15.6 and 13.7; LC-MS (ESI): *m/z* 601 $[M+1]^+$, 623 $[M+23]^+$, 541 $[M-OAc]^+$; purity (HPLC): 99% (t_r = 14.37 min).

3-Heptanoyloxyfusidic acid (3.34)

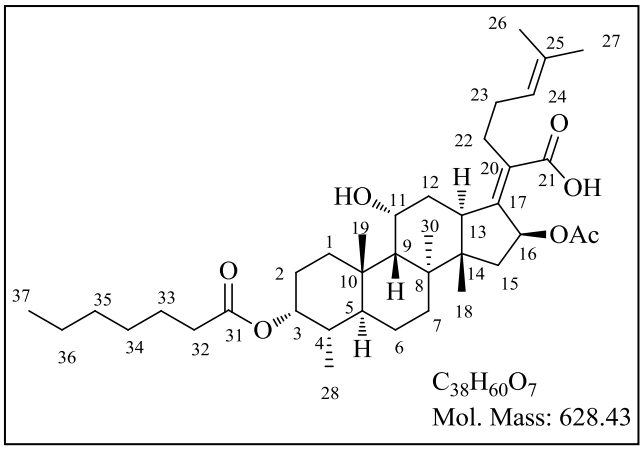

White solid (0.380 g obtained from 0.5 g of **3.1**, 62%); R_f 0.6 (50% EtOAc:hexane); Mp. 167-169 ^oC; ^{1}H NMR (400 MHz, $CDCl_3$) δ 5.91 (d, J = 8.4 Hz, 1H, H-16), 5.11 (t, J = 7.2 Hz, 1H, H-24), 4.95 (m, 1H, H-3), 4.34 (m, 1H, H-11), 3.08-3.04 (m, 1H, H-13), 2.53-2.42 (m, 2H, 2×H-22), 2.36-2.31 (m, 1H, H-12), 2.33 (t, J = 7.4 Hz, 2H, 2×H-32), 2.22-2.05 (m, 5H, H-1, H-5, H-15 and 2×H-23), 1.97 (s, 3H, OAc), 1.89-1.77 (m, 4H, 2×H-2, H-7 and H-12), 1.72-1.53 (m, 6H, H-1, H-4, H-6, H-9 and 2×H-33), 1.68 (s, 3H, CH_3-27), 1.60 (s, 3H, CH_3-26), 1.38 (s, 3H, CH_3-30), 1.39-1.29 (m, 7H, H-15, 2×H-34, 2×H-35 and 2×H-36), 1.19-1.04 (m, 2H, H-6 and H-7), 0.99 (s, 3H, CH_3-19), 0.93 (s, 3H, CH_3-18), 0.89 (t, J = 7.0 Hz, 3H, 3×H-37), 0.83 (d, J = 6.7 Hz, 3H, CH_3-28); ^{13}C NMR (100 MHz, $CDCl_3$) δ 173.5, 173.3, 170.5, 151.0, 132.6, 129.5, 123.0, 74.3, 73.8, 68.2, 49.1, 48.8, 44.3, 39.4, 39.0, 37.9, 37.0, 35.7, 34.8, 34.7, 32.8, 31.5, 31.1, 28.8, 28.7, 28.3, 27.4, 25.6, 25.2, 24.4, 22.4 (2C), 20.6, 20.5, 18.1, 17.7, 15.6 and 14.0; LC-MS (ESI): *m/z* 629 $[M+1]^+$, 651 $[M+23]^+$, 569 $[M-OAc]^+$; purity (HPLC): 99% (t_r = 16.04 min).

3-Decanoyloxyfusidic acid (3.35)

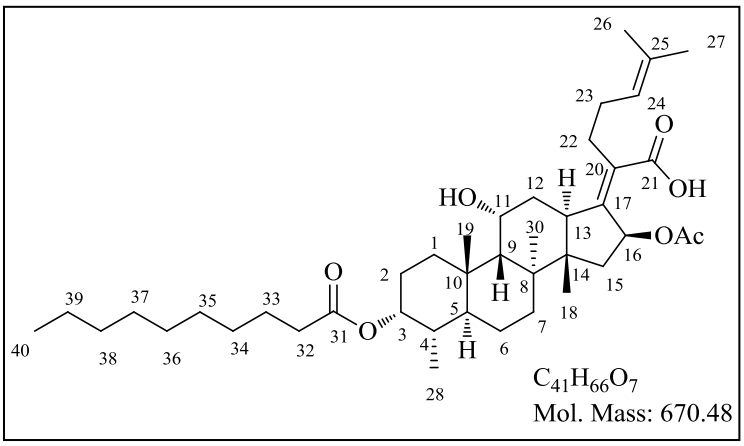

Colourless viscous oil (0.410 g obtained from 0.5 g of **3.1**, 63%); R_f 0.8 (50% EtOAc:hexane); ^{1}H NMR (400 MHz, $CDCl_3$) δ 5.90 (d, *J* = 8.4 Hz, 1H, H-16), 5.10 (t, *J* = 7.2 Hz, 1H, H-24), 4.94 (m, 1H, H-3), 4.34 (m, 1H, H-11), 3.07-3.03 (m, 1H, H-13), 2.51-2.43 (m, 2H, 2×H-22), 2.34-2.30 (m, 1H, H-12), 2.32 (t, *J* = 7.4 Hz, 2H, 2×H-32), 2.21-2.02 (m, 5H, H-1, H-5, H-15 and 2×H-23), 1.96 (s, 3H, OAc), 1.91-1.77 (m, 4H, 2×H-2, H-7, H-12), 1.72-1.52 (m, 6H, H-1, H-4, H-6, H-9 and 2×H-33), 1.68 (s, 3H CH_3-27), 1.60 (s, 3H, CH_3-26), 1.38 (s, 3H, CH_3-30), 1.35-1.27 (m, 13H, H-15, 2×H-34, 2×H-35, 2×H-36, 2×H-37, 2×H-38 and 2×H-39), 1.19-1.04 (m, 2H, H-6 and H-7), 0.99 (s, 3H, CH_3-19), 0.93 (s, 3H, CH_3-18), 0.88 (t, *J* = 6.9 Hz, 3H, 3×H-40), 0.82 (d, *J* = 6.7 Hz, 3H, CH_3-28); ^{13}C NMR (100 MHz, $CDCl_3$) δ 174.1, 173.5, 170.4, 151.0, 132.6, 129.6, 123.0, 74.3, 73.8, 68.2, 49.1, 48.8, 44.3, 39.4, 39.0, 37.8, 37.0, 35.7, 34.8, 34.7, 32.8, 31.8, 31.1, 29.4, 29.3, 29.2, 29.2, 28.7, 28.3, 27.4, 25.6, 25.2, 24.4, 22.6, 22.5, 20.6, 20.5, 18.1, 17.7, 15.6 and 14.0; LC-MS (ESI): *m/z* 671 $[M+1]^+$, 693 $[M+23]^+$, 611 $[M\text{-}OAc]^+$; purity (HPLC): 99% (t_r = 17.48 min).

3-Ketofusidic acid (3.36)[4]

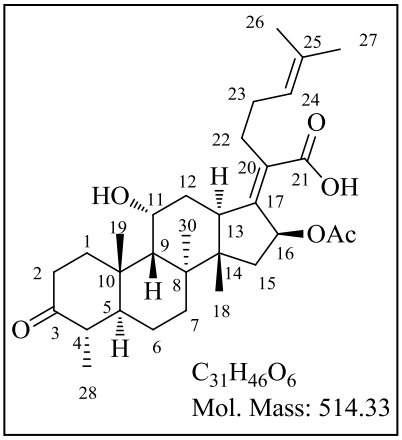

Jones' reagent (0.8 ml) was added dropwise over 30 min to an ice cooled solution of fusidic acid (**3.1**) (2.0 g, 3.87 mmol) in acetone (20 ml). Reaction was monitored by TLC. Reaction mixture was stirred at 0 °C for additional 10 min. Water (40 ml) was then added to the reaction mixture and aqueous layer was extracted with EtOAc (80 ml). Organic layer was then dried over anhydrous sodium sulfate, filtered and concentrated *in vacuo*. The residue was purified by column chromatography on 100-200 silica gel using EtOAc:hexane as eluent, affording **3.36** as a white solid (0.650 g, 33%); R_f 0.4 (60% EtOAc:hexane); Mp. 119-121 °C; ^{1}H NMR (400 MHz, $CDCl_3$) δ 5.91 (d, *J* = 8.3 Hz, 1H, H-16), 5.10 (t, *J* = 7.2 Hz, 1H, H-24), 4.40 (m, 1H, H-11), 3.07-3.03 (m, 1H, H-13), 2.51-2.42 (m, 4H, 2×H-2 and 2×H-22), 2.41-2.04 (m, 7H, H-1, H-4, H-5, H-12, H-15 and 2×H-23), 1.97 (s, 3H, OAc), 2.01-1.86 (m, 3H, H-1, H-7 and H-

12), 1.68 (s, 3H, CH_3-27), 1.67-1.63 (m, 2H, H-6 and H-9), 1.60 (s, 3H, CH_3-26), 1.35-1.33 (m, 1H, H-15), 1.31 (s, 3H, CH_3-30), 1.27-1.13 (m, 2H, H-6 and H-7), 1.16 (s, 3H, CH_3-19), 1.02 (d, J = 6.6 Hz, 3H, CH_3-28), 0.95 (s, 3H, CH_3-18); ^{13}C NMR (100 MHz, $CDCl_3$) δ 212.4, 173.5, 170.4, 151.0, 132.7, 129.7, 122.9, 74.3, 68.1, 48.8, 48.4, 45.7, 45.4, 44.3, 39.4, 39.0, 38.0, 36.9, 36.1, 35.4, 33.5, 28.7, 28.3, 25.7, 24.7, 22.6, 21.9, 20.6, 18.0, 17.7 and 12.3; LC-MS (ESI): *m/z* 515 $[M+H]^+$, 537 $[M+23]^+$, 455 $[M-OAc]^+$; purity (LC-MS): 97% (t_r = 3.89 min).

General synthetic procedure for compounds 3.37-3.39

A mixture of 3-keto fusidic acid **3.36** (1.0 eq.), hydroxyl amine hydrochloride (5 eq.) and ammonium acetate (5 eq.) was taken in ethanol (2-3 ml) in a microwave friendly vessel. The vessel was sealed and the reaction mixture was irradiated in microwave at 80 ^oC for 20 min. After completion of reaction (TLC), the reaction mixture was diluted with water (15 ml) and EtOAc (25 ml). EtOAc layer was separated, dried over anhydrous sodium sulfate, filtered and concentrated *in vacuo*. The residue was purified by column chromatography on 100-200 silica gel using EtOAc:hexane as eluent, affording target compound as a white solid.

3-Hydroxyiminofusidic acid (3.37)

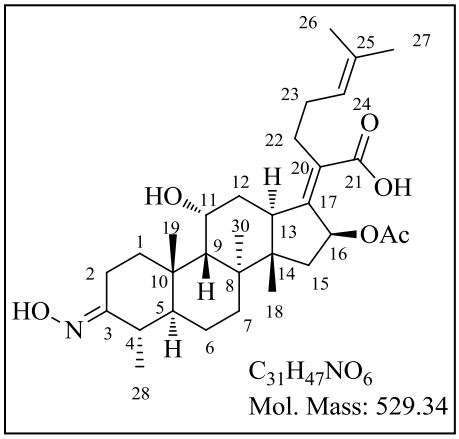

White powder (0.071 g obtained from 0.3 g of **3.36**, 23%); R_f 0.6 (70% EtOAc:hexane); Mp. 149-151 ^oC; A mixture of E/Z isomers; ^{1}H NMR (400 MHz, $CDCl_3$) δ 5.90 (t, J = 8.4 Hz, 1H, H-16), 5.10 (t, J = 7.2 Hz, 1H, H-24), 4.36 (m, 1H, H-11), 3.20-3.15 (m, 1H, H-13, **E**/Z), 3.05-3.02 (m, 1H, H-13, E/**Z**), 2.79-2.69 (m, 1H, H-22), 2.56-2.45 (m, 3H, 2×H-2 and H-22), 2.35-2.00 (m, 7H, H-1, H-4, H-5, H-12, H-15 and 2×H-23), 1.95 (s, 3H, OAc), 1.91-1.54 (m, 5H, H-1, H-6, H-7, H-9 and H-12), 1.67 (s, 3H, CH_3-27), 1.60 (s, 3H, CH_3-26), 1.40-1.30 (m, 4H, H-15 and CH_3-30), 1.20-0.81 (m, 11H, H-6, H-7, CH_3-18, CH_3-19 and CH_3-28); ^{13}C NMR (100 MHz, $CDCl_3$) δ 174.2, 170.6, 164.8, 150.0, 132.6, 130.4, 123.0, 74.2, 68.1, 48.8, 48.5, 46.6, 45.1, 44.0, 39.4, 39.0, 37.3, 36.6, 36.0, 34.1, 33.2, 28.8, 28.3, 25.7, 24.4, 22.7, 21.6, 20.6, 18.3, 17.8 and 14.4; LC-MS (ESI): *m/z* 470 $[M-OAc]^+$, 530 $[M+H]^+$, 552 $[M+23]^+$; purity (LC-MS): 97% (t_r = 3.90 min).

3-Methoxyiminofusidic acid (3.38)

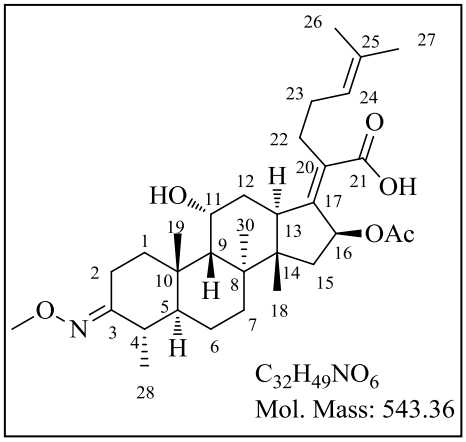

White powder (0.251 g obtained from 0.4 g of **3.36**, 59%); R_f 0.5 (60% EtOAc/Hexane); Mp. 176-178 ^oC; A mixture of E/Z isomers; ^1H NMR (400 MHz, $CDCl_3$) 5.90 (t, *J* = 7.7 Hz, 1H, H-16), 5.09 (t, *J* = 7.2 Hz, 1H, H-24), 4.36 (m, 1H, H-11), 3.83 (s, 1H, =N-OCH_3, ***E***/Z), 3.82 (s, 1H, =N-OCH_3, E/**Z**), 3.05-3.02 (m, 1H, H-13), 2.68-2.56 (m, 1H, H-22), 2.48-2.42 (m, 3H, 2×H-2 and H-22), 2.36-1.99 (m, 7H, H-1, H-4, H-5, H-12, H-15 and 2×H-23), 1.96 (s, 3H, OAc), 1.92-1.44 (m, 5H, H-1, H-6, H-7, H-9 and H-12), 1.67 (s, 3H, CH_3-27), 1.60 (s, 3H, CH_3-26), 1.38-1.34 (m, 4H, H-15 and CH_3-30), 1.20-0.85 (m, 11H, H-6, H-7, CH_3-18, CH_3-19 and CH_3-28,); ^{13}C NMR (100 MHz, $CDCl_3$) δ 174.1, 170.4, 161.9, 151.6, 132.6, 129.9, 122.9, 74.3, 68.1, 61.1, 48.9, 48.5, 46.8, 45.2, 44.3, 39.4, 39.0, 37.0, 36.8, 36.2, 35.4, 33.5, 28.7, 28.3, 25.7, 24.6, 22.5, 21.6, 20.6, 18.0, 17.7 and 14.5; LC-MS (ESI): *m/z* 484 $[M\text{-}OAc]^+$, 544 $[M+H]^+$, 566 $[M+23]^+$; purity (LC-MS): 98% (t_r = 4.47 min).

3-Benzyloxyiminofusidic acid (3.39)

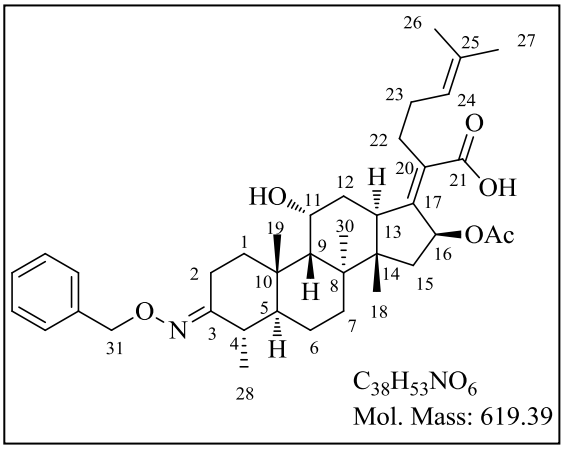

White solid (0.081 g obtained from 0.130 g of **3.36**, 51%); R_f 0.6 (60% EtOAc:hexane); Mp. 176-178 ^oC; A mixture of E/Z isomers; ^1H NMR (400 MHz, $CDCl_3$) δ 7.38-7.25 (m, 5H, ArH), 5.91 (t, *J* = 7.7 Hz, 1H, H-16), 5.10 (t, *J* = 7.3 Hz, 1H, H-24), 5.08 (d, *J* = 5.5 Hz, 2H, 2×H-31), 4.35 (m, 1H, H-11), 3.14-3.08 (m, 1H, H-13, **E**/Z), 3.07-3.02 (m, 1H, H-13, E/**Z**), 2.69-2.61 (m, 1H, H-22), 2.48-2.44 (m, 3H, 2×H-2 and H-22), 2.39-1.99 (m, 7H, H-1, H-4, H-5, H-12, H-15 and 2×H-23), 1.96 (s, 3H, OAc), 1.92-1.44 (m, 5H, H-1, H-6, H-7, H-9 and H-12), 1.67 (s, 3H, CH_3-27), 1.60 (s, 3H, CH_3-26), 1.38-1.30 (m, 4H, H-15 and CH_3-30), 1.20-0.79 (m, 11H, H-6, H-7, CH_3-18, CH_3-19 and CH_3-28,); ^{13}C NMR (100 MHz, $CDCl_3$) δ 174.4, 170.4, 162.6, 151.6, 132.6, 129.9, 128.2, 128.2, 128.1, 127.8, 127.6, 127.5, 123.0, 75.4, 74.3, 68.1, 48.8, 48.5, 46.8, 45.2, 44.3, 39.4, 39.0, 37.1, 36.8, 36.2, 35.4, 33.5, 28.7, 28.3, 25.7, 24.6, 22.5, 21.6, 20.6, 18.0, 17.7 and 14.5;

LC-MS (ESI): *m/z* 560 $[M\text{-}OAc]^+$, 620 $[M+H]^+$, 642 $[M+23]^+$; purity (LC-MS): 98% (t_r = 5.64 min).

3-Epifusidic acid (3.40)[1]

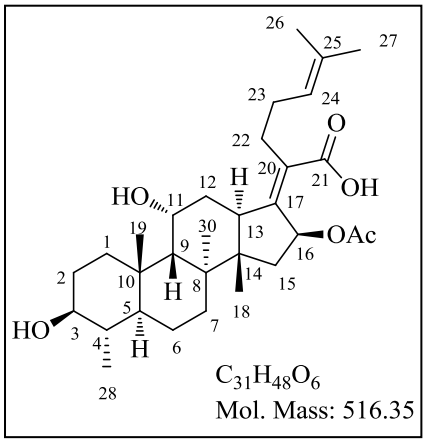

$NaBH_4$ (0.022 g, 0.582 mmol) was added portion wise to a solution of **3.36** (0.1 g, 0.194 mmol) in methanol (3 ml) at 25 °C. Reaction mixture was then stirred for 3 h. After completion of the reaction (TLC), reaction mixture was acidified to pH = 1 by dropwise addition of 1 N aq. HCl. Methanol was then removed *in vacuo* and residue was dissolved in EtOAc (15 ml). The EtOAc layer was washed with water (10 ml), dried over anhydrous sodium sulfate, filtered and concentrated *in vacuo*. The crude product was purified by column chromatography on 100-200 silica gel using EtOAc:DCM as eluent, affording **3.40** as a white solid (0.025 g, 25%); R_f 0.5 (60% EtOAc/DCM); Mp. 211-213 °C; ^{1}H NMR (400 MHz, CD_3OD) δ 5.81 (d, *J* = 8.5 Hz, 1H, H-16), 5.14 (t, *J* = 7.2 Hz, 1H, H-24), 4.31 (m, 1H, H-11), 3.07-2.98 (m, 2H, H-3, H-13), 2.59-2.50 (m, 1H, H-22), 2.42-2.35 (m, 1H, H-22), 2.32-2.27 (m, 1H, H-12), 2.19-2.01 (m, 5H, H-1, H-5, H-15 and 2×H-23), 1.96 (s, 3H, OAc), 1.91-1.72 (m, 4H, 2×H-2, H-7 and H-12), 1.67 (s, 3H, CH_3-27), 1.61 (s, 3H, CH_3-26), 1.61-1.57 (m, 3H, H-1, H-6 and H-9), 1.40-1.29 (m, 1H, H-4), 1.33 (s, 3H, CH_3-30), 1.26-1.22 (m, 1H, H-15), 1.19-1.10 (m, 2H, H-6 and H-7), 1.02 (s, 3H, CH_3-19), 0.94 (d, *J* = 6.5 Hz, 3H, CH_3-28), 0.93 (s, 3H, CH_3-18); ^{13}C NMR (100 MHz, $CDCl_3$) δ 172.8, 171.2, 147.2, 131.9, 130.9, 122.9, 75.9, 74.3, 67.0, 49.0, 48.5, 43.6, 42.6, 39.7, 39.2, 38.6, 36.2, 36.1, 33.7, 32.0, 31.2, 28.5, 27.9, 24.5, 23.0, 22.7, 21.1, 19.3, 16.6, 16.4 and 14.5; LC-MS (ESI): *m/z* 457 $[M\text{-}OAc]^+$, 539 $[M+23]^+$; purity (LC-MS): 98% (t_r = 4.71 min).

General synthetic procedure for compounds 3.41-3.43

Corresponding alcohol (3 eq.) was added dropwise to a solution of $SiCl_4$ (1 eq.) in n-pentane at 25 °C under nitrogen atmosphere. Addition of alcohol was accompanied by frothing in the reaction indicating a rapid reaction between the alcohol and $SiCl_4$. Reaction was stirred for 1 h. The clear solution formed was concentrated *in vacuo* to obtain crude trialkoxychlorosilane which was used as such for next step.

A solution of fusidic acid (**3.1**) (1 eq.) and imidazole (2 eq.) in DMF (5 ml) was cooled to 0 °C under nitrogen atmosphere and trialkoxychlorosilane (3 eq., crude obtained above) was

added. Reaction was stirred at 0 °C for 1 h and monitored by TLC. After completion of reaction (TLC), reaction mixture was diluted with EtOAc (25 ml) and washed with water (3×15 ml). EtOAc layer was then dried over anhydrous sodium sulfate, filtered and concentrated *in vacuo*. Product was purified by column chromatography on 100-200 size silica gel using EtOAc:hexane as eluent, affording target compound as clear liquid (**3.43**) or white solid (**3.41** and **3.42**).

3-Triethoxysilyloxyfusidic acid (3.41)

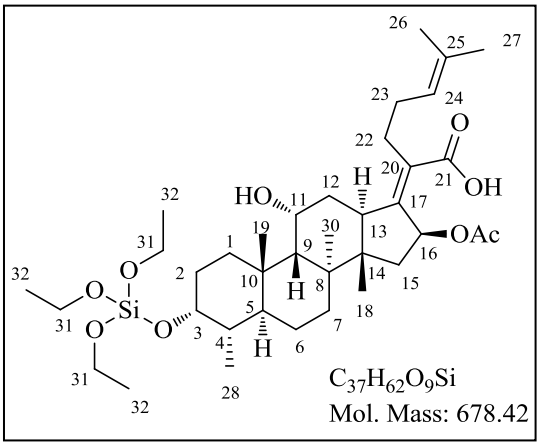

White solid (0.330 g obtained from 0.5 g of **3.1**, 50%); R_f 0.5 (60% EtOAc:hexane); Mp. 72-74 °C; ^{1}H NMR (400 MHz, $CDCl_3$) δ 5.89 (d, *J* = 8.3 Hz, 1H, H-16), 5.10 (t, *J* = 7.2 Hz, 1H, H-24), 4.34 (m, 1H, H-11), 4.00 (m, 1H, H-3), 3.85 (q, *J* = 7.0 Hz, 6H, 6×H-31), 3.07-3.04 (m, 1H, H-13), 2.51-2.42 (m, 2H, 2×H-22), 2.36-2.31 (m, 1H, H-12), 2.25-2.02 (m, 5H, H-1, H-5, H-15 and 2×H-23), 1.96 (s, 3H, OAc), 1.87-1.76 (m, 4H, 2×H-2, H-7 and H-12), 1.67 (s, 3H, CH_3-27), 1.60 (s, 3H, CH_3-26), 1.57-1.45 (m, 4H, H-1, H-4, H-6 and H-9), 1.36 (s, 3H, CH_3-30), 1.34-1.30 (m, 1H, H-15), 1.23 (t, *J* = 7.0 Hz, 9H, 9×H-32), 1.16-1.04 (m, 2H, H-6 and H-7), 0.97 (s, 3H, CH_3-19), 0.92 (s, 3H, CH_3-18), 0.90 (d, *J* = 6.7 Hz, 3H, CH_3-28); ^{13}C NMR (100 MHz, $CDCl_3$) δ 174.3, 170.4, 151.3, 132.6, 129.5, 123.0, 74.4, 73.1, 68.3, 59.2 (3C), 49.1, 48.8, 44.4, 39.4, 39.0, 37.1, 36.4, 36.3, 35.4, 33.0, 30.5, 30.2, 28.7, 28.4, 25.6, 24.2, 22.5, 20.5, 20.4, 18.2(3C), 18.1, 17.7 and 16.2. LC-MS (ESI): *m/z* 619 $[M\text{-}OAc]^+$; purity (LC-MS): 98% (t_r = 5.17 min).

3-Triisopropoxysilyloxyfusidic acid (3.42)

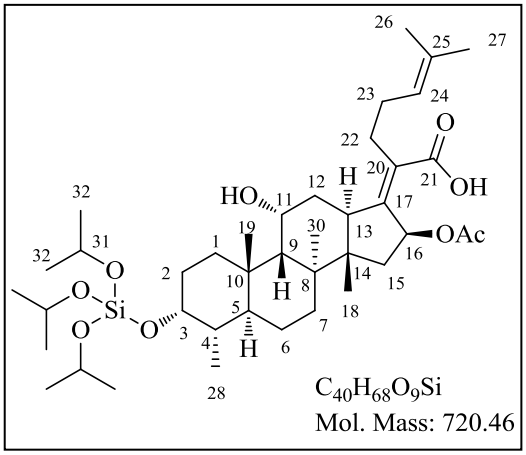

White solid; (0.250 g obtained from 0.5 g of **3.1**, 35%); R_f 0.5 (60% EtOAc:hexane); Mp. 70-72 °C; ^{1}H NMR (400 MHz, $CDCl_3$) δ 5.89 (d, *J* = 8.3 Hz, 1H, H-16), 5.10 (t, *J* = 7.2 Hz, 1H, H-24), 4.34 (m, 1H, H-11), 4.23 (h, *J* = 6.1 Hz, 3H, 3×H-31), 3.99 (m, 1H, H-3), 3.07-3.04 (m, 1H, H-13), 2.51-2.42 (m, 2H, 2×H-22), 2.36-2.31 (m, 1H, H-12), 2.25-2.02 (m, 5H, H-1, H-5, H-15 and 2×H-23), 1.96 (s,

3H, OAc), 1.91-1.73 (m, 4H, 2×H-2, H-7 and H-12), 1.67 (s, 3H, CH_3-27), 1.60 (s, 3H, CH_3-26), 1.57-1.45 (m, 4H, H-1, H-4, H-6 and H-9), 1.36 (s, 3H, CH_3-30), 1.34-1.30 (m, 1H, H-15), 1.19 (d, J = 6.1 Hz, 18H, 18×H-32), 1.14-1.03 (m, 2H, H-6 and H-7), 0.96 (s, 3H, CH_3-19), 0.92 (s, 3H, CH_3-18), 0.90 (d, J = 6.7 Hz, 3H, CH_3-28); ^{13}C NMR (100 MHz, $CDCl_3$) δ 174.2, 170.4, 151.4, 132.6, 129.4, 123.0, 74.4, 72.9, 68.4, 65.7 (3C), 49.2, 48.8, 44.4, 39.4, 39.0, 37.1, 36.4 (2C), 35.3, 33.1, 30.6, 30.0, 28.7, 28.4, 25.6, 25.4 (6C), 24.2, 22.5, 20.6, 20.4, 18.1, 17.7 and 16.3; LC-MS (ESI): *m/z* 661 $[M\text{-}OAc]^+$; purity (LC-MS): 99% (t_r = 6.87 min).

3-Trisoctyloxysilyloxyfusidic acid (3.43)

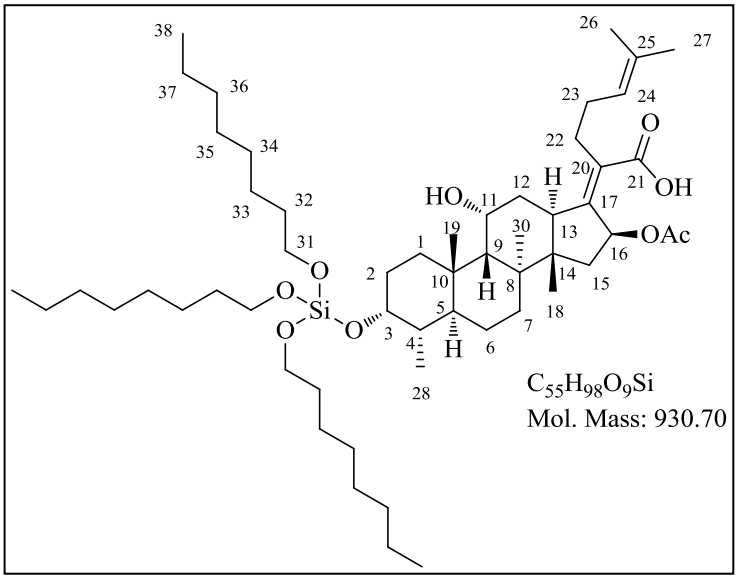

Colourless viscous oil (0.210 g obtained from 0.5 g of **3.1**, 23%); R_f 0.7 (50% EtOAc:hexane); ^{1}H NMR (400 MHz, $CDCl_3$) δ 5.90 (d, J = 8.3 Hz, 1H, H-16), 5.10 (t, J = 7.2 Hz, 1H, H-24), 4.34 (m, 1H, H-11), 3.75 (t, J = 6.7 Hz, 6H, 6×H-31), 3.99 (m, 1H, H-3), 3.07-3.04 (m, 1H, H-13), 2.51-2.42 (m, 2H, 2×H-22), 2.36-2.31 (m, 1H, H-12), 2.22-2.02 (m, 5H, H-1, H-5, H-15 and 2×H-23), 1.96 (s, 3H, OAc), 1.87-1.75 (m, 4H, 2×H-2, H-7 and H-12), 1.67 (s, 3H, CH_3-27), 1.60 (s, 3H, CH_3-26), 1.57-1.45 (m, 10H, H-1, H-4, H-6, H-9 and 6×H-32), 1.36 (s, 3H, CH_3-30), 1.34-1.25 (m, 31H, 30× H-33,34,35, 36, 37 and H-15), 1.14-1.03 (m, 2H, H-6 and H-7), 0.96 (s, 3H, CH_3-19), 0.92 (s, 3H, CH_3-18), 0.90-0.87 (m, 12H, CH_3-28 and 9×H-38); ^{13}C NMR (100 MHz, $CDCl_3$) δ 173.9, 170.4, 151.4, 132.6, 129.4, 123.0, 74.4, 73.0, 68.3, 63.6 (3C), 49.1, 48.8, 44.4, 39.4, 39.0, 37.2, 36.4, 36.3, 35.3, 33.2, 32.4 (3C), 31.8 (3C), 30.6, 30.2, 29.4 (3C), 29.3 (3C), 28.7, 28.4, 25.7 (3C), 25.6, 24.4, 22.6 (3C), 22.4, 20.6, 20.4, 18.1, 17.7, 16.3 and 14.1 (3C).

7.2.1.3 C-16 Fusidic acid derivatives

3-Acetoxy-16-deacetoxy-16α-hydroxyfusidic acid (3.44)[3]

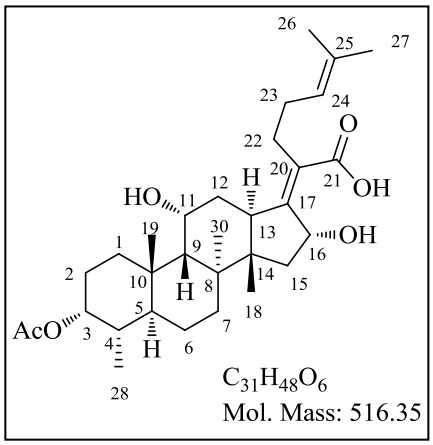

A mixture of **3.30** (0.2 g) and sat. aq. $NaHCO_3$ (2 ml) was irradiated in microwave at 100 °C for 10 min. Reaction mixture was then diluted with water (15 ml) and acidified with 1 N aq. HCl. The acidic layer was extracted with EtOAc (25 ml), dried over anhydrous sodium sulfate, filtered and concentrated *in vacuo*. Product was purified by column chromatography on 100-200 size silica gel using EtOAc:hexane as eluent, affording target compound as a white solid (0.070 g, 37%); R_f 0.3 (50% EtOAc:hexane); ^{1}H NMR (400 MHz, $CDCl_3$) δ 5.12 (t, *J* = 7.2 Hz, 1H, H-24), 4.94 (m, 1H, H-3), 4.83 (t, *J* = 7.3 Hz, 1H, H-16), 4.33 (m, 1H, H-11), 3.34-3.31 (m, 1H, H-13), 2.48-2.44 (m, 2H, 2×H-22), 2.38-2.33 (m, 1H, H-12), 2.25-1.98 (m, 5H, H-1, H-5, H-15 and 2×H-23), 2.07 (s, 3H, OAc), 1.84-1.50 (m, 8H, H-1, 2×H-2, H-4, H-6, H-7, H-9 and H-12), 1.68 (s, 3H, CH_3-27), 1.61 (s, 3H, CH_3-26), 1.45 (s, 3H, CH_3-30), 1.25-1.03 (m, 3H, H-6, H-7 and H-15), 0.97 (s, 3H, CH_3-19), 0.82 (d, *J* = 6.7 Hz, 3H, CH_3-28), 0.75 (s, 3H, CH_3-18); ^{13}C NMR (100 MHz, $CDCl_3$) δ 174.0, 171.0, 164.6, 132.4, 127.6, 123.2, 74.1, 72.1, 68.4, 49.0, 47.4, 43.8, 39.5, 39.2, 37.6, 36.8, 35.9, 34.9, 32.5, 30.9, 29.0, 28.3, 27.3, 25.6, 24.4, 22.6, 21.3, 20.6, 18.3, 17.8 and 15.4; LC-MS (ESI): *m/z* 499 $[M\text{-}OH]^+$, 539 $[M+23]^+$.

3-Acetoxy-16-deacetoxy-16α-hydroxyfusidic acid pivaloyloxymethyl ester (3.45)[3]

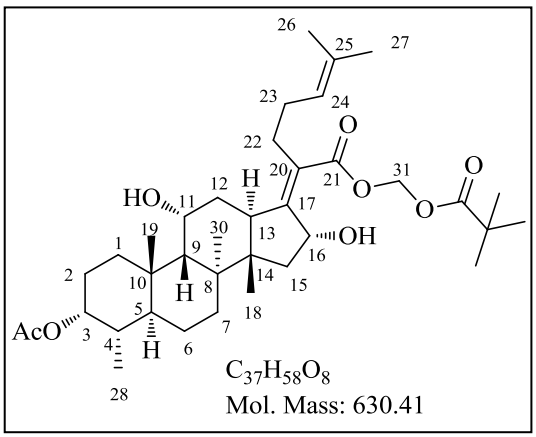

Chloromethyl pivalate (0.19 ml, 1.25 mmol) was added to the solution of compound **3.44** (0.586 g, 1.13 mmol) in DMF (3 ml). This was followed by dropwise addition of Et_3N (0.32 ml, 2.27 mmol). Resulting reaction mixture was stirred at 25 °C for 16 h. After completion of reaction (TLC), reaction mixture was diluted with EtOAc (25 ml) and washed with water (3×15 ml). EtOAc layer was then dried over sodium sulfate, filtered and concentrated *in vacuo*. Crude product was purified by column chromatography on 100-200 size silica gel using EtOAc:hexane as eluent, affording target compound as viscous yellow oil (0.350 g, 49%); R_f 0.6 (40% EtOAc:hexane);

^{1}H NMR (400 MHz, $CDCl_3$) δ 5.88 (d, *J* = 5.4 Hz, 1H, H-31), 5.81 (d, *J* = 5.4 Hz, 1H, H-31), 5.08 (t, *J* = 7.2 Hz, 1H, H-24), 4.94 (m, 1H, H-3), 4.75 (t, *J* = 7.3 Hz, 1H, H-16), 4.31 (m, 1H, H-11), 3.33-3.29 (m, 1H, H-13), 2.45-2.40 (m, 2H, 2×H-22), 2.36-2.28 (m, 1H, H-12), 2.17-1.86 (m, 5H, H-1, H-5, H-15 and 2×H-23), 2.07 (s, 3H, OAc), 1.84-1.49 (m, 8H, H-1, 2×H-2, H-4, H-6, H-7, H-9 and H-12), 1.67 (s, 3H, CH_3-27), 1.59 (s, 3H, CH_3-26), 1.45 (s, 3H, CH_3-30), 1.25-1.03 (m, 3H, H-6, H-7 and H-15), 1.21 (s, 9H, -OCOC(CH_3)$_3$), 0.97 (s, 3H, CH_3-19), 0.82 (d, *J* = 6.7 Hz, 3H, CH_3-28), 0.74 (s, 3H, CH_3-18); LC-MS (ESI): *m/z* 613 [M-OH]$^+$.

3-Acetoxy-16-deacetoxy-16β-bromofusidic acid pivaloyloxymethyl ester (3.46)[5]

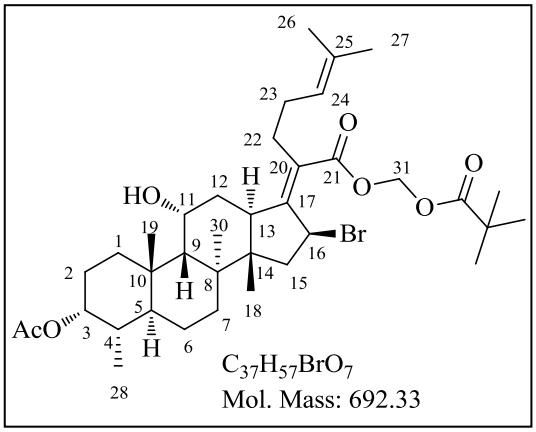

Compound **3.45** (0.4 g, 0.63 mmol) was dissolved in dry benzene (8 ml) and PPh_3 (0.712 g, 2.71 mmol) and CBr_4 (1.13 g, 3.40 mmol) were added at 25 ^oC under nitrogen atmosphere. Resulting reaction mixture was stirred for 1 h. After completion of the reaction (TLC), ether (30 ml) was added and precipitated material was removed by filtration. Filtrate was concentrated *in vacuo* and residue was purified by column chromatography on 100-200 size silica gel using EtOAc:hexane as eluent, affording target compound as viscous yellow oil (0.3 g, 68%); R_f 0.6 (30% EtOAc:hexane); ^{1}H NMR (400 MHz, $CDCl_3$) δ 5.89 (d, *J* = 5.5 Hz, 1H, H-31), 5.84 (d, *J*= 5.5 Hz, 1H, H-31), 5.59 (d, *J* = 8.8 Hz, 1H, H-16), 5.07 (t, *J* = 7.2 Hz, 1H, H-24), 4.95 (m, 1H, H-3), 4.32 (m, 1H, H-11), 3.07-3.03 (m, 1H, H-13), 2.45-2.40 (m, 2H, 2×H-22), 2.36-2.32 (m, 1H, H-12), 2.19-1.97 (m, 5H, H-1, H-5, H-15 and 2×H-23), 2.07 (s, 3H, OAc), 1.91-1.80 (m, 4H, 2×H-2, H-7 and H-12), 1.68 (s, 3H, CH_3-27), 1.63-1.52 (m, 4H, H-1, H-4, H-6 and H-9), 1.59 (s, 3H, CH_3-26), 1.34 (s, 3H, CH_3-30), 1.25-1.03 (m, 3H, H-6, H-7 and H-15), 1.23 (s, 9H, -OCOC(CH_3)$_3$), 1.20 (s, 3H, CH_3-19), 1.00 (d, *J* = 6.7 Hz, 3H, CH_3-28), 0.83 (s, 3H, CH_3-18); ^{13}C NMR (100 MHz, $CDCl_3$) δ 170.8 (2C), 168.3, 152.5, 132.7, 131.7, 122.8, 80.0, 74.1, 68.2, 49.3, 48.6, 48.4, 45.5, 42.6, 39.8, 38.8, 38.0, 37.1, 35.7, 34.4, 33.0, 31.2, 29.3, 28.0, 27.4, 26.9 (3C), 25.7, 24.4, 22.2, 21.3, 20.4, 19.5, 17.8 and 15.5.

3-Acetoxy-16-deacetoxy-16α-bromofusidic acid pivaloyloxymethyl ester (3.47)[5]

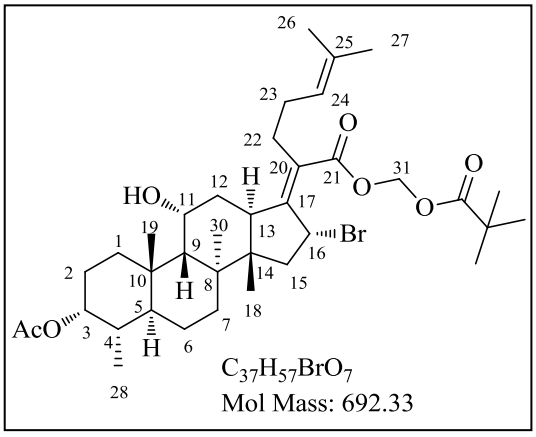

Compound **3.46** (0.3 g, 0.43 mmol) was dissolved in acetonitrile (3 ml) and tetra butyl ammonium bromide (0.3 g, 0.93 mmol) was added. Reaction mixture was then stirred at 25 ^{o}C for 65 h. Acetonitrile was then removed *in vacuo*. Residue was stirred with ether (25 ml) and precipitated tetra butyl ammonium bromide was removed by filtration. Filtrate was concentrated *in vacuo* to afford the target compound as viscous yellow oil, which was used directly for next step without further purification (0.250 g, 83%); R_f 0.6 (30% EtOAc:hexane); ^{1}H NMR (400 MHz, $CDCl_3$) δ 5.90 (d, *J* = 5.4 Hz, 1H, H-31), 5.82 (d, *J* = 5.4 Hz, 1H, H-31), 5.62 (t, *J* = 6.9 Hz, 1H, H-16), 5.08 (t, *J* =7.3 Hz, 1H, H-24), 4.94 (m, 1H, H-3), 4.33 (m, 1H, H-11), 3.45-3.41 (m, 1H, H-13), 2.44-2.40 (m, 2H, 2×H-22), 2.34-2.29 (m, 1H, H-12), 2.15-2.01 (m, 5H, H-1, H-5, H-15 and 2×H-23), 2.07 (s, 3H, OAc), 1.81-1.50 (m, 8H, H-1, 2×H-2, H-4, H-6, H-7, H-9 and H-12), 1.67 (s, 3H, CH_3-27), 1.59 (s, 3H, CH_3-26), 1.45 (s, 3H, CH_3-30), 1.25-1.04 (m, 3H, H-6, H-7 and H-15), 1.23 (s, 9H, -OCOC(CH_3)$_3$), 0.98 (s, 3H, CH_3-19), 0.83 (d, *J* = 6.7 Hz, 3H, CH_3-28), 0.77 (s, 3H, CH_3-18); ^{13}C NMR (100 MHz, $CDCl_3$) δ 170.9 (2C), 167.4, 154.7, 132.6, 129.5, 123.0, 79.8, 74.0, 68.2, 50.6, 49.3, 48.7, 43.5, 41.9, 39.5, 38.8, 37.6, 36.9, 35.8, 35.0, 32.5, 30.9, 28.6, 28.3, 27.3, 26.9 (3C), 25.7, 24.2, 22.8, 21.3, 20.6, 17.8, 17.3 and 15.5.

General synthetic procedure for compounds 3.48 and 3.49

Ag_2CO_3 (2.0 eq.) was added to a solution of compound **3.47** (1.0 eq.) in 2-3 ml of respective alcohol (methanol for **3.48** and ethanol for **3.49**) and reaction mixture was stirred in dark at 25 ^{o}C for 16 h. After completion of reaction (TLC), reaction mixture was filtered to remove excess of Ag_2CO_3. The filtered solid was washed with 1 ml of respective alcohol and filtrates were combined. 5 N aq. NaOH was then added to the combined filtrate and resulting reaction mixture was heated at 80 ^{o}C for 1 h. Reaction mixture was then acidified with 5 N aq. HCl, diluted with water (10 ml) and extracted with EtOAc (25 ml). EtOAc layer was dried over anhydrous sodium sulfate, filtered and concentrated *in vacuo*. Crude product was purified by column chromatography on 100-200 size silica gel using EtOAc:hexane as eluent, affording target compounds as a white solid.

16-Deacetoxy-16β-methoxy fusidic acid (3.48)[5]

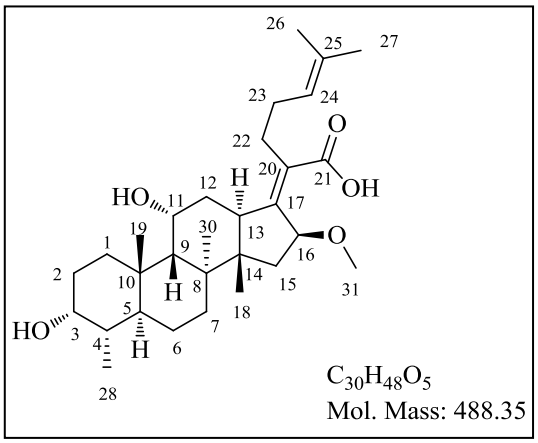

White solid (0.025 g obtained from 0.1 g of **3.47**, 35%); R_f 0.5 (60% EtOAc:hexane); Mp. 139-141 ^{o}C; ^{1}H NMR (400 MHz, $CDCl_3$) δ 5.11 (t, *J* =7.2 Hz, 1H, H-24), 4.37 (d, *J* = 7.1 Hz, 1H, H-16), 4.33 (m, 1H, H-11), 3.76 (m, 1H, H-3), 3.32 (s, 3H, 3×H-31), 3.06-3.02 (m, 1H, H-13), 2.58-2.50 (m, 1H, H-22), 2.47-2.40 (m, 1H, H-22), 2.35-2.30 (m, 1H, H-12), 2.24-2.01 (m, 4H, H-1, H-5 and 2×H-23), 1.92-1.71 (m, 5H, 2×H-2, H-7, H-12 and H-15), 1.67 (s, 3H, CH_3-27), 1.62-1.50 (m, 5H, H-1, H-4, H-6, H-9 and H-15), 1.60 (s, 3H, CH_3-26), 1.38 (s, 3H, CH_3-30), 1.23-1.05 (m, 2H, H-6 and H-7), 0.98 (m, 6H, CH_3-19, CH_3-18), 0.93 (d, *J* = 6.8 Hz, 3H, CH_3-28); ^{13}C NMR (100 MHz, $CDCl_3$) δ 171.5, 150.0, 133.6, 132.3, 123.3, 82.1, 71.4, 68.4, 56.6, 49.3, 49.1, 43.8, 39.7, 37.2, 36.5, 35.9, 35.9, 34.7, 32.9, 30.4, 30.1, 29.6, 28.3, 25.6, 24.4, 22.3, 20.6, 18.4, 17.8 and 15.9; LC-MS (ESI): *m/z* 457 $[M\text{-}OCH_3]^+$, 511 $[M+23]^+$; purity (LC-MS): 98% (t_r = 5.07 min).

16-Deacetoxy-16β-ethoxyfusidic acid (3.49)[5]

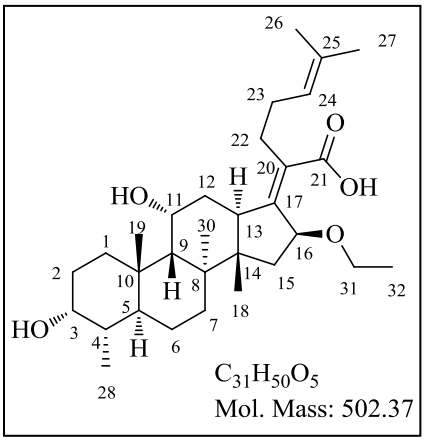

White solid (0.053 g obtained from 0.2 g of **3.47**, 37%); R_f 0.5 (60% EtOAc:hexane); Mp. 177-179 ^{o}C; ^{1}H NMR (400 MHz, $CDCl_3$) δ 5.11 (t, *J* =7.2 Hz, 1H, H-24), 4.45 (d, *J* = 7.1 Hz, 1H, H-16), 4.33 (m, 1H, H-11), 3.76 (m, 1H, H-3), 3.66-3.59 (m, 1H, H-31), 3.42-3.35 (m, 1H, H-31), 3.06-3.02 (m, 1H, H-13), 2.59-2.51 (m, 1H, H-22), 2.46-2.39 (m, 1H, H-22), 2.35-2.30 (m, 1H, H-12), 2.22-2.01 (m, 4H, H-1, H-5, 2×H-23), 1.91-1.71 (m, 5H, 2×H-2, H-7, H-12, H-15,), 1.67 (s, 3H, CH_3-27), 1.64-1.49 (m, 5H, H-1, H-4, H-6, H-9, H-15), 1.60 (s, 3H, CH_3-26), 1.37 (s, 3H, CH_3-30), 1.20 (t, *J* =7.0 Hz, 3H, 3×H-32), 1.22-1.05 (m, 2H, H-6, H-7), 1.00 (s, 3H, CH_3-19), 0.98 (s, 3H, CH_3-18), 0.93 (d, *J* = 6.8 Hz, 3H, CH_3-28); ^{13}C NMR (100 MHz, $CDCl_3$) δ 171.9, 150.1, 133.6, 132.3, 123.3, 80.6, 71.4, 68.5, 64.8, 49.4, 49.1, 43.8, 39.7, 37.2, 36.4, 36.0, 35.9, 35.2, 32.8, 30.4, 30.1, 29.6, 28.3, 25.6, 24.4, 22.3, 20.6, 18.4, 17.8, 15.9 and 14.7; LC-MS (ESI): *m/z* 457 $[M\text{-}OCH_2CH_3]^+$, 525 $[M+23]^+$; purity (LC-MS): 98% (t_r = 5.23 min).

7.2.1.4 Miscellaneous fusidic acid derivatives

24,25-Dihydro methylsulfonyl fusidic acid hydrazide (3.50)

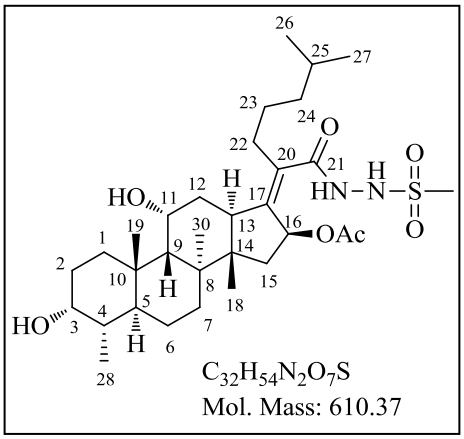

A solution of **3.18** (0.240 g, 0.395 mmol) in ethanol (30 ml) was charged with 10% Pd/C (0.060 g, 50% moisture). The reaction mixture was stirred at 25 ^{o}C for 16 h under a hydrogen atmosphere. Progress of the reaction was monitored by TLC. After completion of reaction, reaction mixture was filtered through a bed of celite and the filtrate was evaporated *in vacuo* to afford compound **3.50** which after trituration with n-pentane delivered a white solid (0.140 g, 58%); R_f 0.3 (90% EtOAc:hexane); Mp. 198-200 ^{o}C; ^{1}H NMR (400 MHz, $CDCl_3$) δ 8.24 (br s, 1H, NH), 7.12 (br s, 1H, NH), 5.73 (d, J = 8.2 Hz, 1H, H-16), 4.37 (m, 1H, H-11), 3.76 (m, 1H, H-3), 3.05-3.01 (m, 1H, H-13), 3.01 (s, 3H, SO_2CH_3), 2.45-2.37 (m, 1H, H-22), 2.32-2.10 (m, 6H, H-1, H-5, H-12, H-15, H-22 and H-25), 2.01 (s, 3H, OAc), 1.89-1.41 (m, 12H, H-1, 2×H-2, H-4, H-6, H-7, H-9, H-12, 2×H-23 and 2×H-24), 1.38 (s, 3H, CH_3-30), 1.29-1.06 (m, 3H, H-6, H-7 and H-15), 0.98 (s, 3H, CH_3-19), 0.94-0.91 (m, 6H, CH_3-18, CH_3-28), 0.87 (d, J = 6.6 Hz, 6H, CH_3-26 and CH_3-27); ^{13}C NMR (100 MHz, $CDCl_3$) δ 170.8, 170.6, 145.1, 132.2, 73.8, 71.6, 68.4, 49.4, 48.7, 43.6, 39.5 (2C), 39.2, 38.8, 36.9, 36.4, 35.8, 35.4, 31.9, 30.2, 29.9, 29.7, 27.7, 27.4, 23.8, 23.1, 22.5 (2C), 21.2, 20.8, 17.8 and 15.8; LC-MS (ESI): *m/z* 633 $[M+23]^+$, 551 $[M\text{-}OAc]^+$; purity (LC-MS): 97% (t_r = 4.41 min)

16-Deacetoxy-16β-hydroxymethanesulfonylfusidic acid hydrazide (3.51)

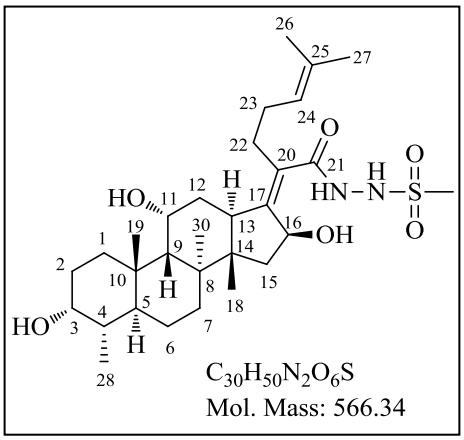

K_2CO_3 (0.460 g, 3.328 mmol) was added to a solution of compound **3.18** (0.1 g, 0.164 mmol) in methanol and the resulting reaction mixture was stirred at 25 ^{o}C for 24 h. After completion of the reaction (TLC), K_2CO_3 was removed by filtration and the resulting filtrate was concentrated *in vacuo*. Residue was purified by column chromatography on 100-200 size silica gel using EtOAc:hexane as eluent, affording target compound as a white solid (0.020 g, 22%); R_f 0.3 (5% Methanol:DCM); Mp. 169-171 ^{o}C; ^{1}H NMR (400 MHz, CD_3OD) δ 5.14 (t, J = 7.2 Hz, 1H, H-24), 4.79 (d, J = 8.5 Hz, 1H, H-16), 4.30 (m, 1H,

H-11), 3.67 (m, 1H, H-3), 3.07 (s, 3H, SO_2CH_3), 3.07-3.02 (m, 1H, H-13), 2.54-2.46 (m, 1H, H-22), 2.36-2.30 (m, 1H, H-22), 2.30-2.07 (m, 6H, H-1, H-5, H-15, H-12 and 2×H-23), 1.89-1.71 (m, 4H, 2×H-2, H-7 and H-12), 1.68 (s, 3H, CH_3-27), 1.62 (s, 3H, CH_3-26), 1.62-1.46 (m, 4H, H-1, H-4, H-6 and H-9), 1.38 (s, 3H, CH_3-30), 1.30-1.27 (m, 1H, H-15), 1.20-1.09 (m, 2H, H-6 and H-7), 1.02 (s, 3H, CH_3-19), 1.00 (s, 3H, CH_3-18), 0.90 (d, J = 6.8 Hz, 3H, CH_3-28); ^{13}C NMR (100 MHz, CD_3OD) δ 172.4, 150.6, 131.8, 130.2, 123.0, 71.2, 71.0, 67.3, 49.2, 48.5, 43.7, 40.6, 39.4 (2C), 36.7, 36.4, 36.1, 35.5, 31.6, 29.6 (2C), 29.0, 27.7, 24.5, 22.5, 22.2, 20.9, 17.3, 16.5 and 15.0; LC-MS (ESI): *m/z* 589 $[M+23]^+$, purity (LC-MS): 96% (t_r = 4.25 min).

General synthetic procedure for compounds 3.52 and 3.53

A solution of fusidic acid (**3.1**) (0.5 g, 0.97 mmol) in DCM (50 ml) was cooled to -78 °C and then ozone was purged through this solution until its colour turns to pale blue. Reaction was then shifted to 25 °C and PPh_3 (0.64 g, 2.42 mmol) was added as a quencher. Reaction mixture was stirred at 25 °C for 2 h. After completion of reaction (TLC), it was washed with water (2×15 ml), dried over anhydrous magnesium sulfate and concentrated *in vacuo*. Purification by column chromatography on 100-200 silica gel using EtOAc:hexane as eluent afforded products **3.52** and **3.53**.

(Z)-2-((3R,4S,5S,8S,9S,10S,11R,13R,14S,16S)-16-acetoxy-3,11-dihydroxy-4,8,10,14-tetramethyldodecahydro-1H-cyclopenta[a]phenanthren-17(2H,10H,14H)-ylidene)-5-oxopentanoic acid (3.52)[6]

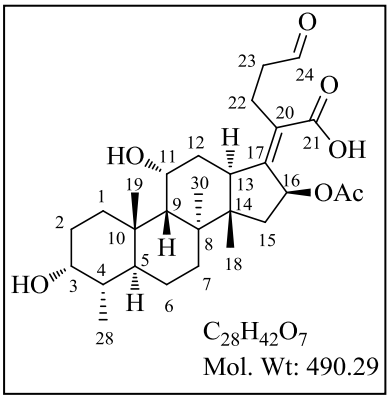

White solid (0.13 g, 27%); R_f 0.1 (100% EtOAc); Mp. 237-239 °C; ^{1}H NMR (400 MHz, $CDCl_3$) δ 9.78 (s, 1H, H-24), 5.90 (d, J = 8.3 Hz, 1H, H-16), 4.34 (m, 1H, H-11), 3.76 (m, 1H, H-3), 3.11-3.08 (m, 1H, H-13), 2.80-2.70 (m, 2H, 2×H-22), 2.61-2.39 (m, 2H, 2×H-23), 2.32-2.27 (m, 1H, H-12), 2.22-2.07 (m, 3H, H-1, H-5 and H-15), 1.98 (s, 3H, OAc), 1.91-1.71 (m, 4H, 2×H-2, H-7 and H-12), 1.63-1.48 (m, 4H, H-1, H-4, H-6 and H-9), 1.38 (s, 3H, CH_3-30), 1.34-1.31 (m, 1H, H-15), 1.23-1.06 (m, 2H, H-6 and H-7), 0.98 (s, 3H, CH_3-19), 0.93-0.91 (m, 6H, CH_3-18 and CH_3-28); ^{13}C NMR (100 MHz, $CDCl_3$) δ 207.0, 170.4 (2C), 156.5, 127.8, 74.5, 71.5, 68.1, 49.3, 48.9, 45.1, 39.5, 39.1, 37.0, 36.3, 36.0, 35.7, 32.1, 30.2, 29.8, 28.7, 28.4, 25.6,

22.9, 20.9, 20.8, 17.8 and 15.9; LC-MS (ESI): *m/z* 490 $[M]^+$, purity (HPLC): 98% (t_r = 15.68 min).

(3*R*,4*S*,5*S*,8*S*,9*S*,10*S*,11*R*,13*R*,14*S*,16*S*)-3,11-dihydroxy-4,8,10,14-tetramethyl-17-oxohexadecahydro-1H-cyclopenta[a]phenanthren-16-yl acetate (3.53)[6]

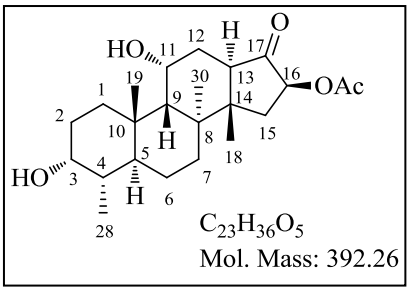

White solid (0.10 g, 26%); R_f 0.5 (100% EtOAc); Mp. 92-94 °C; ^{1}H NMR (400 MHz, $CDCl_3$) δ 5.31 (d, *J* = 7.0 Hz, 1H, H-16), 4.36 (m, 1H, H-11), 3.75 (m, 1H, H-3), 3.05-3.01 (m, 1H, H-13), 2.63-2.56 (m, 1H, H-12), 2.24-2.04 (m, 3H, H-1, H-5 and H-15), 2.11 (s, 3H, OAc), 1.93-1.71 (m, 4H, 2×H-2, H-7 and H-12), 1.65-1.46 (m, 4H, H-1, H-4, H-6 and H-9), 1.49 (s, 3H, CH_3-30), 1.43-1.40 (m, 1H, H-15), 1.27-1.12 (m, 2H, H-6 and H-7), 0.97-0.93 (m, 9H, CH_3-18, CH_3-19 and CH_3-28); ^{13}C NMR (100 MHz, $CDCl_3$) δ 212.1, 170.3, 72.1, 71.3, 67.4, 50.5, 47.5, 46.4, 39.9, 37.1, 36.5, 35.9, 35.8, 30.8, 30.2, 30.0, 29.9, 23.4, 23.1, 20.8 (2C), 17.7 and 15.9; LC-MS (ESI): *m/z* 392 $[M]^+$; purity (LC-MS): 98% (t_r = 5.10 min).

3,11-Diketofusidic acid (3.54)[1]

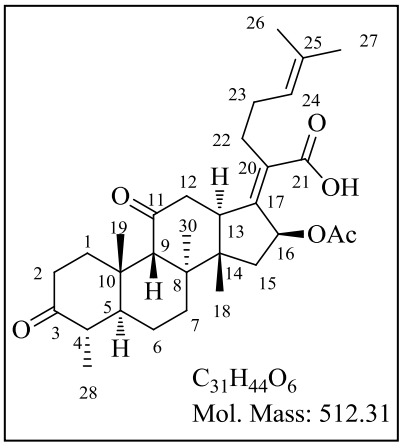

White solid (0.900 g, 45%); R_f 0.3 (60% EtOAc:hexane); Mp. 192-194 °C; ^{1}H NMR (400 MHz, $CDCl_3$) δ 5.93 (d, *J* = 8.3 Hz, 1H, H-16), 5.08 (t, *J* = 7.4 Hz, 1H, H-24), 2.95-2.87 (m, 1H, H-13), 2.77-2.65 (m, 2H, H-9 and H-12), 2.54-2.31 (m, 4H, 2×H-2 and 2×H-22), 2.25-1.96 (m, 8H, 2×H-1, H-4, H-5, H-12, H-15 and 2×H-23), 1.99 (s, 3H, OAc), 1.84-1.78 (m, 1H, H-7), 1.66 (s, 3H, CH_3-27), 1.60-1.56 (m, 4H, H-6 and CH_3-26), 1.47-1.44 (m, 1H, H-15), 1.30-1.10 (m, 2H, H-6 and H-7), 1.20 (s, 3H, CH_3-30), 1.15 (s, 3H, CH_3-19), 1.05 (d, *J* = 6.5 Hz, 3H, CH_3-28), 1.05 (s, 3H, CH_3-18); ^{13}C NMR (100 MHz, $CDCl_3$) δ 215.6, 209.4, 173.6, 170.2, 148.1, 133.1, 130.8, 122.4, 74.1, 58.2, 48.6, 47.0, 46.2, 44.8, 44.3, 40.7, 38.0, 36.6, 36.6, 33.3, 32.4, 28.7, 27.9, 25.6, 23.9, 22.4, 21.2, 20.5, 17.7, 17.0 and 14.0; LC-MS (ESI): *m/z* 453 $[M-OAc]^+$, 535 $[M+23]^+$; purity (LC-MS): 95% (t_r = 4.72 min).

3,11-Diacetoxyfusidic acid (3.55)[1]

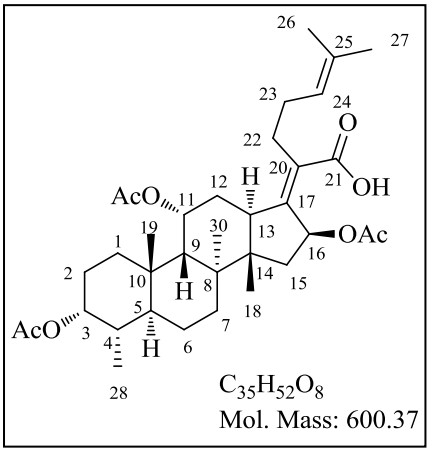

A mixture of fusidic acid (**3.1**) (0.2 g, 0.39 mmol), acetic anhydride (0.4 ml, 3.9 mmol) and pyridine (0.3 ml, 3.9 mmol) was taken in a microwave friendly vessel and irradiated in microwave at 80 ^{o}C for 1.5 h. After completion of the reaction (TLC), water (15 ml) was added to the reaction mixture and aqueous layer was extracted with EtOAc (2×15 ml). Organic layer was washed with aq 0.5 M HCl (2×15 ml) to get rid of excess of pyridine. Organic layer was then dried over anhydrous sodium sulfate, filtered and concentrated *in vacuo*. The residue was purified on 100-200 silica gel using EtOAc: hexane as eluent affording **3.55** as a brown solid (0.082 g, 35%); R_f 0.4 (50% EtOAc:hexane); Mp. 305-307 ^{o}C; ^{1}H NMR (400 MHz, $CDCl_3$) δ 5.88 (d, *J* = 8.4 Hz, 1H, H-16), 5.29 (m, 1H, H-11), 5.06 (t, *J* =7.2 Hz, 1H, H-24), 4.94 (m, 1H, H-3), 2.85-2.81 (m, 1H, H-13), 2.44-2.39 (m, 3H, H-12 and 2×H-22), 2.23-1.99 (m, 5H, H-1, H-5, H-15 and 2×H-23), 2.06 (s, 3H, OAc), 2.03 (s, 3H, OAc), 1.97 (s, 3H, OAc), 1.85-1.60 (m, 8H, H-1, 2×H-2, H-4, H-6, H-7, H-9 and H-12), 1.67 (s, 3H, CH_3-27), 1.57 (s, 3H, CH_3-26), 1.37 (s, 3H, CH_3-30), 1.37-1.03 (m, 3H, H-6, H-7 and H-15), 0.99 (s, 3H, CH_3-19), 0.95 (s, 3H, CH_3-18), 0.82 (d, *J* = 6.7 Hz, 3H, CH_3-28); ^{13}C NMR (100 MHz, $CDCl_3$) δ 173.2, 170.6, 170.4, 170.1, 149.9, 132.9, 129.9, 122.6, 74.2, 74.1, 70.6, 48.6, 48.0, 44.7, 39.6, 38.9, 37.7, 36.8, 34.7, 32.6, 32.1, 29.7, 28.7, 28.1, 27.3, 25.6, 23.9, 22.4, 21.7, 21.2, 20.6, 20.4, 18.0, 17.6 and 15.5; LC-MS (ESI): *m/z* 541 $[M\text{-}OAc]^+$, 623 $[M+23]^+$; purity (LC-MS): 98% (t_r = 5.14 min).

3,11-Diacetoxyfusidic acid methyl ester (3.56)

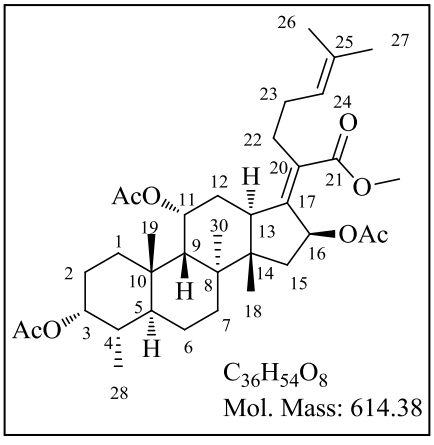

Compound **3.55** (0.1 g, 0.166 mmol) was dissolved in DMF (2 ml) and K_2CO_3 (0.028 g, 0.202 mmol) was added followed by addition of methyl iodide (0.012 ml, 0.202 mmol). Resulting reaction mixture was then heated at 50 ^{o}C for 3 h. After completion of reaction (TLC), reaction mixture was diluted with EtOAc (15 ml) and washed with water (3×10 ml). Organic layer was separated, dried over anhydrous sodium sulfate, filtered and concentrated *in vacuo*. The yellowish product was stirred in n-pentane for 30 min to obtain **3.56** as a white solid (0.074 g, 72%); R_f 0.8 (50% EtOAc:hexane); Mp. 259-261 ^{o}C; ^{1}H NMR (400 MHz,

$CDCl_3$) δ 5.84 (d, *J* = 8.4 Hz, 1H, H-16), 5.28 (m, 1H, H-11), 5.04 (t, *J* =7.3 Hz, 1H, H-24), 4.92 (m, 1H, H-3), 3.64 (s, 3H, OCH_3), 2.84-2.79 (m, 1H, H-13), 2.45-2.34 (m, 3H, H-12 and 2×H-22), 2.22-1.95 (m, 5H, H-1, H-5, H-15 and 2×H-23), 2.05 (s, 3H, OAc), 2.02 (s, 3H, OAc), 1.98 (s, 3H, OAc), 1.85-1.59 (m, 8H, H-1, 2×H-2, H-4, H-6, H-7, H-9 and H-12), 1.66 (s, 3H, CH_3-27), 1.57 (s, 3H, CH_3-26), 1.36 (s, 3H, CH_3-30), 1.33-1.03 (m, 3H, H-6, H-7, H-15), 0.98 (s, 3H, CH_3-19), 0.93 (s, 3H, CH_3-18), 0.82 (d, *J* = 6.6 Hz, 3H, CH_3-28); ^{13}C NMR (100 MHz, CDCl3) δ 170.6, 170.4, 170.3, 170.0, 147.0, 132.7, 131.0, 122.7, 74.1 (2C), 70.6, 51.4, 48.5, 48.0, 44.3, 39.6, 39.0, 37.7, 36.8, 34.7, 32.7, 32.1, 29.7, 28.9, 28.0, 27.3, 25.7, 23.9, 22.4, 21.7, 21.2, 20.9, 20.4, 17.9, 17.6 and 15.5; LC-MS (ESI): *m/z* 555 $[M\text{-}OAc]^+$, 637 $[M+23]^+$; purity (LC-MS): 96% (t_r = 5.42 min).

7.2.2 Chapter 4

7.2.2.1 C-3 Ether derivatives of fusidic acid

Fusidic acid pivaloyloxymethyl ester (4.0)

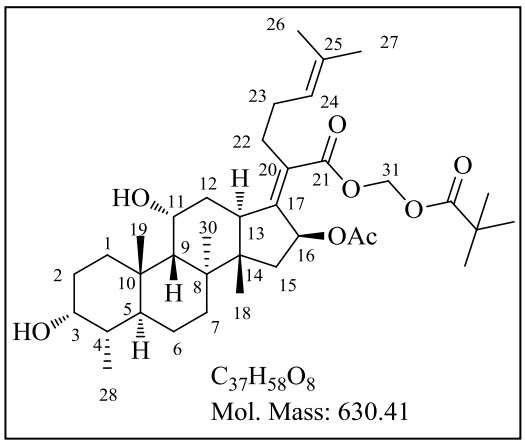

Chloromethyl pivalate (0.17 ml, 1.13 mmol) was added to the solution of compound **3.1** (0.530 g, 1.03 mmol) in DMF (3 ml). This was followed by dropwise addition of Et_3N (0.43 ml, 3.09 mmol). Resulting reaction mixture was stirred at 25 ^oC for 36 h. After completion of reaction (TLC), reaction mixture was diluted with EtOAc (25 ml) and washed with water (3×15 ml). EtOAc layer was then dried over anhydrous sodium sulfate, filtered and concentrated *in vacuo*. Crude product was purified by column chromatography on 100-200 size silica gel using EtOAc:hexane as eluent, affording target compound as a white solid (0.6 g, 93%); R_f 0.6 (60% EtOAc:hexane); ^{1}H NMR (400 MHz, $CDCl_3$) δ 5.85 (d, *J* = 8.4 Hz, 1H, H-16), 5.78 (d, *J* = 5.4 Hz, 1H, H-31), 5.69 (d, *J* = 5.4 Hz, 1H, H-31), 5.07 (t, *J* =7.2 Hz, 1H, H-24), 4.33 (m, 1H, H-11), 3.74 (m, 1H, H-3), 3.06-3.02 (m, 1H, H-13), 2.50-2.37 (m, 2H, 2×H-22), 2.33-2.28 (m, 1H, H-12), 2.21-2.00 (m, 5H, H-1, H-5, H-15 and 2×H-23), 1.97 (s, 3H, OAc), 1.89-1.71 (m, 4H, 2×H-2, H-7 and H-12), 1.66 (s, 3H, CH_3-27), 1.61-1.48 (m, 4H, H-1, H-4, H-6 and H-9), 1.58 (s, 3H, CH_3-26), 1.38 (s, 3H, CH_3-30), 1.31-1.28 (m, 1H, H-15), 1.20 (s, 9H, $OCOC(CH_3)_3$), 1.17-1.03 (m, 2H, H-6 and H-7), 0.97 (s, 3H, CH_3-19), 0.91 (d, *J* = 6.7 Hz, 3H, CH_3-28), 0.90 (s, 3H, CH_3-18); ^{13}C NMR (100 MHz, $CDCl_3$) δ 177.0, 170.2, 168.1, 150.8, 132.6, 129.3, 122.9,

79.8, 74.3, 71.3, 68.2, 49.2, 48.7, 45.8, 44.3, 39.5, 39.0, 38.7, 37.1, 36.2, 35.6, 32.4, 30.3, 30.0, 28.7, 28.2, 26.8 (3C), 25.6, 24.1, 22.7, 20.7 (2C), 17.9, 17.7 and 15.9.

General synthetic procedure for compounds 4.1a-4.3a

A mixture of compound **4.0** (1.0 eq.), respective 4-substitiuted benzyl bromide (3.0 eq.) and DIPEA (5.0 eq.) was heated in a closed vessel at 130 ^{o}C for 16 h. After completion of reaction (TLC), reaction mixture was loaded directly on column containing 100-200 silica gel and purified using DCM: hexane as eluent to afford required products.

3-(4-Chlorobenzyloxy)fusidic acid pivaloyloxymethyl ester (4.1a)

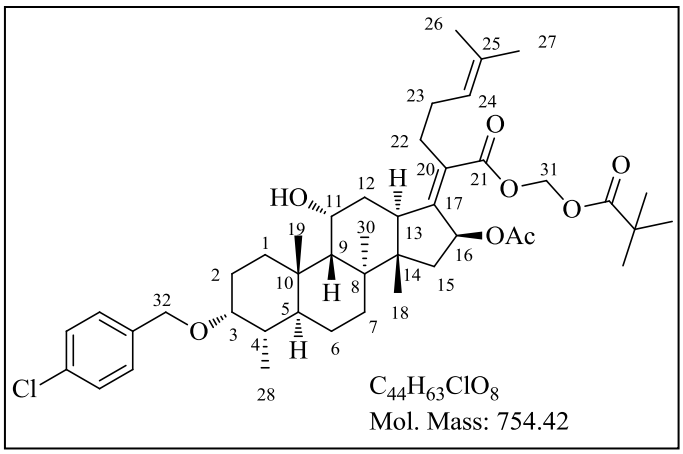

Colourless viscous oil (0.110 g, 45%); R_f 0.6 (25% EtOAc:hexane); ^{1}H NMR (400 MHz, $CDCl_3$) δ 7.31-7.26 (m, 4H, ArH), 5.86 (d, *J* = 8.4 Hz, 1H, H-16), 5.79 (d, *J* = 5.4 Hz, 1H, H-31), 5.70 (d, *J* = 5.4 Hz, 1H, H-31), 5.08 (t, *J* =7.2 Hz, 1H, H-24), 4.57 (d, *J* = 12.3 Hz, IH, H-32), 4.32 (d, *J* = 12.3 Hz, 1H, H-32), 4.32 (m, 1H, H-11), 3.36 (m, 1H, H-3), 3.06-3.02 (m, 1H, H-13), 2.51-2.38 (m, 2H, 2×H-22), 2.34-2.29 (m, 1H, H-12), 2.25-2.01 (m, 5H, H-1, H-5, H-15 and 2×H-23), 1.97 (s, 3H, OAc), 1.94-1.73 (m, 4H, 2×H-2, H-7 and H-12), 1.67 (s, 3H, CH_3-27), 1.63-1.46 (m, 4H, H-1, H-4, H-6 and H-9), 1.59 (s, 3H, CH_3-26), 1.36 (s, 3H, CH_3-30), 1.32-1.28 (m, 1H, H-15), 1.21 (s, 9H, $OCOC(CH_3)_3$), 1.17-1.03 (m, 2H, H-6 and H-7), 0.97 (s, 3H, CH_3-19), 0.91 (s, 3H, CH_3-18), 0.90 (d, *J* = 6.7 Hz, 3H, CH_3-28); ^{13}C NMR (100 MHz, $CDCl_3$) δ 177.0, 170.2, 168.1, 150.8, 138.1, 132.8, 132.6, 129.3, 128.6 (2C), 128.3 (2C), 122.9, 79.8, 78.7, 74.3, 69.9, 68.3, 49.2, 48.8, 44.3, 39.4, 39.0, 38.7, 37.1, 37.0, 36.2, 35.5, 32.7, 30.9, 28.8, 28.2, 26.9 (3C), 25.7, 25.4, 24.3, 22.6, 20.8, 20.6, 18.0, 17.7 and 16.2.

3-(4-Methoxybenzyloxy)fusidic acid pivaloyloxymethyl ester (4.2a)

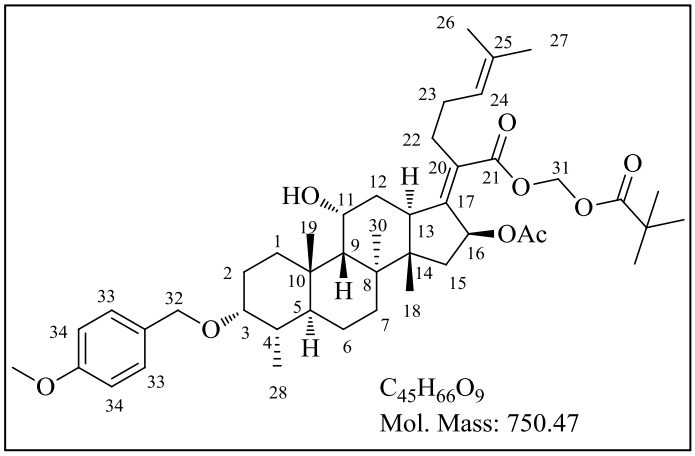

Colourless viscous oil (0.075 g, 31%); R_f 0.6 (25% EtOAc:hexane); ^{1}H NMR (400 MHz, $CDCl_3$) δ 7.26 (d, *J* = 8.7 Hz, 2H, 2×H-34), 6.86 (d, *J* = 8.7 Hz, 2H, 2×H-33), 5.86 (d, *J* = 8.4 Hz, 1H, H-16), 5.79 (d, *J* = 5.3 Hz, 1H, H-31), 5.70 (d, *J* = 5.3 Hz, 1H, H-31), 5.08 (t, *J* = 7.2 Hz, 1H, H-24), 4.55 (d, *J* = 11.8 Hz, 1H, H-32), 4.32 (m, 1H, H-11), 4.30 (d, *J* = 11.8 Hz, 1H, H-32), 3.80 (s, 3H, OCH_3), 3.36 (m, 1H, H-3), 3.06-3.02 (m, 1H, H-13), 2.51-2.38 (m, 2H, 2×H-22), 2.35-2.30 (m, 1H, H-12), 2.24-2.01 (m, 5H, H-1, H-5, H-15 and 2×H-23), 1.97 (s, 3H, OAc), 1.92-1.66 (m, 4H, 2×H-2, H-7 and H-12), 1.67 (s, 3H, CH_3-27), 1.58-1.45 (m, 4H, H-1, H-4, H-6 and H-9), 1.59 (s, 3H, CH_3-26), 1.36 (s, 3H, CH_3-30), 1.32-1.28 (m, 1H, H-15), 1.21 (s, 9H, $OCOC(CH_3)_3$), 1.18-1.00 (m, 2H, H-6 and H-7), 0.97 (s, 3H, CH_3-19), 0.90 (s, 3H, CH_3-18), 0.89 (d, *J* = 6.7 Hz, 3H, CH_3-28); ^{13}C NMR (100 MHz, $CDCl_3$) δ 177.0, 170.2, 168.1, 158.8, 150.9, 132.6, 131.7, 129.3, 128.8 (2C), 122.9, 113.6 (2C), 79.8, 78.0, 74.3, 70.2, 68.3, 55.2, 49.2, 48.8, 44.3, 38.7, 39.4, 39.0, 37.1 (2C), 36.2, 35.4, 32.7, 30.9, 28.7, 28.2, 26.8 (3C), 25.6, 25.4, 24.3, 22.6, 20.8, 20.6, 18.0, 17.7 and 16.1.

3-(4-Methylbenzyloxy)fusidic acid pivaloyloxymethyl ester (4.3a)

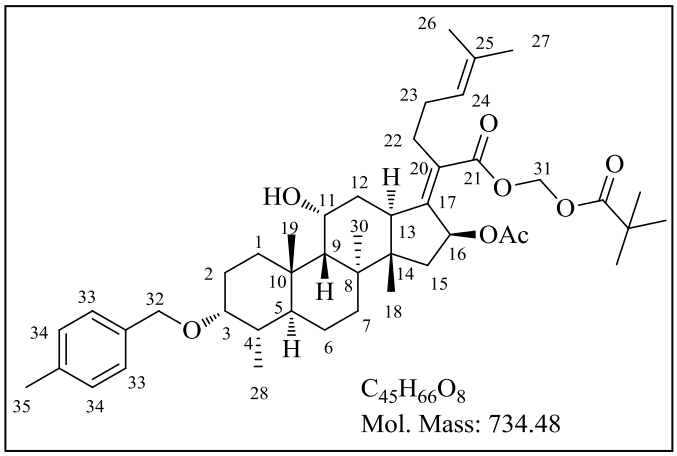

Colourless viscous oil (0.288 g, 62%); R_f 0.7 (25% EtOAc:hexane); ^{1}H NMR (400 MHz, $CDCl_3$) δ 7.23 (d, *J* = 8.0 Hz, 2H, 2×H-34), 7.13 (d, *J* = 8.0 Hz, 2H, 2×H-33), 5.86 (d, *J* = 8.4 Hz, 1H, H-16), 5.79 (d, *J* = 5.4 Hz, 1H, H-31), 5.70 (d, *J* = 5.4 Hz, 1H, H-31), 5.08 (t, *J* =7.2 Hz, 1H, H-24), 4.58 (d, *J* = 12.0 Hz, H-32), 4.33 (d, *J* = 12.0 Hz, H-32), 4.32 (m, 1H, H-11), 3.36 (m, 1H, H-3), 3.06-3.02 (m, 1H, H-13), 2.51-2.38 (m, 2H, 2×H-22), 2.35-2.30 (m, 1H, H-12), 2.34 (s, 3H, 3×H-35), 2.26-2.02 (m, 5H, H-1, H-5, H-15 and 2×H-23), 1.97 (s, 3H, OAc), 1.94-1.70 (m, 4H, 2×H-2, H-7 and H-12), 1.67 (s, 3H, CH_3-27), 1.65-

1.45 (m, 4H, H-1, H-4, H-6 and H-9), 1.59 (s, 3H, CH_3-26), 1.36 (s, 3H, CH_3-30), 1.32-1.28 (m, 1H, H-15), 1.21 (s, 9H, $OCOC(CH_3)_3$), 1.16-1.01 (m, 2H, H-6 and H-7), 0.97 (s, 3H, CH_3-19), 0.91 (s, 3H, CH_3-18), 0.90 (d, J = 6.7 Hz, 3H, CH_3-28); ^{13}C NMR (100 MHz, $CDCl_3$) δ 177.0, 170.2, 168.1, 150.9, 136.7, 136.6, 132.6, 129.3, 128.8 (2C), 127.4 (2C), 123.0, 79.8, 78.2, 74.3, 70.5, 68.3, 49.2, 48.8, 44.3, 38.7, 39.4, 39.0, 37.1(2C), 36.2, 35.4, 32.8, 30.9, 28.8, 28.2, 26.9 (3C), 25.7, 25.4, 24.3, 22.6, 21.1, 20.8, 20.6, 18.0, 17.7 and 16.1.

General synthetic procedure for compounds 4.1-4.3

K_3CO_3 (1.5 eq.) was added to the solution of compound (**4.1a-4.3a**) (1.0 eq.) in methanol (2 ml) and reaction mixture was stirred at 25 ^oC for 2.5 h. After completion of reaction (TLC), reaction mixture was acidified to pH = 1 with 1 N aq. HCl and concentrated to remove methanol. Residue was diluted with DCM (25 ml) and water (15 ml). DCM layer was separated, dried over anhydrous sodium sulfate, filtered and concentrated *in vacuo*. Compound was stirred in n-pentane for 30 min and filtered to obtain pure product as a white solid.

3-(4-Chlorobenzyloxy)fusidic acid (4.1)

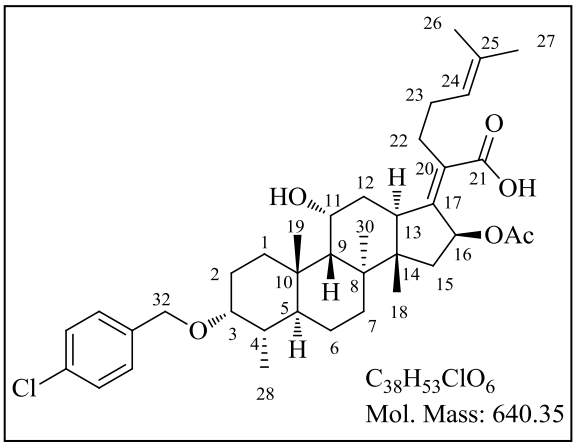

White solid (0.083 g obtained from 0.110 g of **4.1a**, 89%); R_f 0.2 (30% EtOAc:hexane); Mp. 301-303 ^oC; ^{1}H NMR (400 MHz, $CDCl_3$) δ 7.31-7.27 (m, 4H, ArH), 5.89 (d, J = 8.3 Hz, 1H, H-16), 5.10 (t, J = 7.3 Hz, 1H, H-24), 4.58 (d, J = 12.3 Hz, 1H, H-32), 4.32 (d, J = 12.3 Hz, 1H, H-32), 4.34 (m, 1H, H-11), 3.36 (m, 1H, H-3), 3.07-3.03 (m, 1H, H-13), 2.53-2.41 (m, 2H, 2×H-22), 2.36-2.31 (m, 1H, H-12), 2.25-2.02 (m, 5H, H-1, H-5, H-15 and 2×H-23), 1.96 (s, 3H, OAc), 1.95-1.74 (m, 4H, 2×H-2, H-7 and H-12), 1.68 (s, 3H, CH_3-27), 1.65-1.47 (m, 4H, H-1, H-4, H-6 and H-9), 1.60 (s, 3H, CH_3-26), 1.37 (s, 3H, CH_3-30), 1.34-1.30 (m, 1H, H-15), 1.18-1.01 (m, 2H, H-6 and H-7), 0.98 (s, 3H, CH_3-19), 0.92 (s, 3H, CH_3-18), 0.90 (d, J = 6.7 Hz, 3H, CH_3-28); ^{13}C NMR (100 MHz, $CDCl_3$) δ 173.8, 170.4, 151.3, 138.1, 132.8, 132.6, 129.4, 128.6 (2C), 128.3 (2C), 123.0, 78.7, 74.4, 69.9, 68.4, 49.2, 48.8, 44.4, 39.4, 39.0, 37.1, 37.0, 36.2, 35.5, 32.7, 30.9, 28.7, 28.4, 25.7, 25.4, 24.3, 22.6, 20.6, 20.6, 18.0, 17.7 and 16.2; LC-MS (ESI): *m/z* 581 $[M\text{-}OAc]^+$; purity (LC-MS): 98% (t_r = 6.18 min).

3-(4-Methoxybenzyloxy)fusidic acid (4.2)

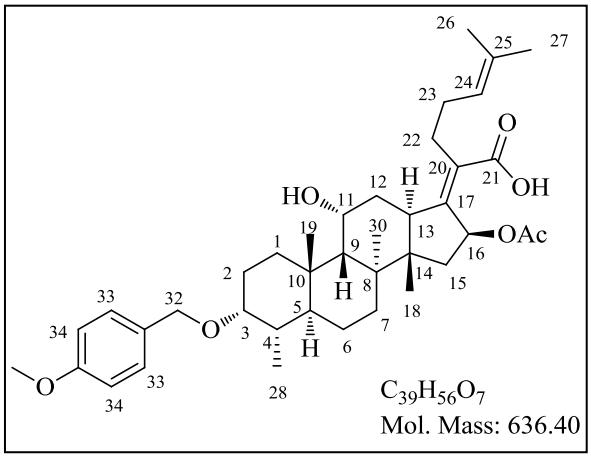

White solid (0.050 g obtained from 0.075 g of **4.2a**, 78%); R_f 0.2 (30% EtOAc:hexane); Mp. 271-273 ^oC; ^1H NMR (400 MHz, $CDCl_3$) δ 7.26 (d, *J* = 8.7 Hz, 2H, 2×H-34), 6.87 (d, *J* = 8.7 Hz, 2H, 2×H-33), 5.89 (d, *J* = 8.3 Hz, 1H, H-16), 5.10 (t, *J* = 7.2 Hz, 1H, H-24), 4.55 (d, *J* = 11.8 Hz, 1H, H-32), 4.33 (m, 1H, H-11), 4.30 (d, *J* = 11.8 Hz, 1H, H-32), 3.80 (s, 3H, OCH_3), 3.36 (m, 1H, H-3), 3.06-3.03 (m, 1H, H-13), 2.53-2.41 (m, 2H, 2×H-22), 2.36-2.31 (m, 1H, H-12), 2.24-2.02 (m, 5H, H-1, H-5, H-15 and 2×H-23), 1.95 (s, 3H, OAc), 1.93-1.72 (m, 4H, 2×H-2, H-7 and H-12), 1.67 (s, 3H, CH_3-27), 1.64-1.46 (m, 4H, H-1, H-4, H-6 and H-9), 1.60 (s, 3H, CH_3-26), 1.37 (s, 3H, CH_3-30), 1.33-1.29 (m, 1H, H-15), 1.16-1.02 (m, 2H, H-6 and H-7), 0.97 (s, 3H, CH_3-19), 0.91 (s, 3H, CH_3-18), 0.89 (d, *J* = 6.7 Hz, 3H, CH_3-28); ^{13}C NMR (100 MHz, $CDCl_3$) δ 174.7, 170.5, 158.8, 151.1, 132.6, 131.7, 129.6, 128.8 (2C), 123.0, 113.6 (2C), 78.0, 74.4, 70.2, 68.4, 55.2, 49.2, 48.7, 44.3, 39.4, 38.9, 37.0 (2C), 36.2, 35.4, 32.7, 30.9, 28.7, 28.4, 25.7, 25.4, 24.3, 22.7, 20.7, 20.6, 18.0, 17.7 and 16.1; LC-MS (ESI): *m/z* 577 $[M\text{-}OAc]^+$; purity (LC-MS): 96% (t_r = 5.91 min).

3-(4-Methylbenzyloxy)fusidic acid (4.3)

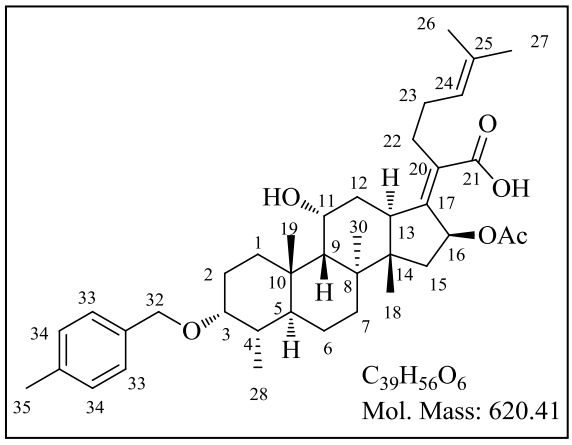

White solid (0.200 g obtained from 0.288 g of **4.2a**, 82%); Mp. 206-208 ^oC; R_f 0.2 (30% EtOAc:hexane); ^1H NMR (400 MHz, $CDCl_3$) δ 7.24 (d, *J* = 7.8 Hz, 2H, 2×H-34), 7.14 (d, *J* = 7.8 Hz, 2H, 2×H-33), 5.89 (d, *J* = 8.3 Hz, 1H, H-16), 5.11 (t, *J* =7.2 Hz, 1H, H-24), 4.58 (d, *J* = 12.0 Hz, 1H, H-32), 4.33 (d, *J* = 12.0 Hz, 1H, H-32), 4.34 (m, 1H, H-11), 3.37 (m, 1H, H-3), 3.07-3.04 (m, 1H, H-13), 2.51-2.41 (m, 2H, 2×H-22), 2.38-2.30 (m, 1H, H-12), 2.34 (s, 3H, 3×H-35), 2.26-2.03 (m, 5H, H-1, H-5, H-15 and 2×H-23), 1.96 (s, 3H, OAc), 1.94-1.73 (m, 4H, 2×H-2, H-7 and H-12), 1.68 (s, 3H, CH_3-27), 1.63-1.47 (m, 4H, H-1, H-4, H-6 and H-9), 1.60 (s, 3H, CH_3-26), 1.37 (s, 3H, CH_3-30), 1.34-1.30 (m, 1H, H-15), 1.17-1.01 (m, 2H, H-6 and H-7), 0.98 (s, 3H, CH_3-19), 0.92-0.90 (m, 6H, CH_3-18 and CH_3-28); ^{13}C NMR (100 MHz,

$CDCl_3$) δ 174.6, 170.4, 151.4, 136.7, 136.6, 132.6, 129.5, 128.8 (2C), 127.4 (2C), 123.0, 78.2, 74.4, 70.4, 68.4, 49.2, 48.7, 44.4, 39.4, 39.0, 37.0 (2C), 36.2, 35.4, 32.7, 30.9, 28.7, 28.4, 25.6, 25.4, 24.3, 22.6, 21.1, 20.6, 20.5, 18.0, 17.7 and 16.1; LC-MS (ESI): *m/z* 561 $[M\text{-}OAc]^+$; purity (LC-MS): 97% (t_r = 6.24 min).

7.2.2.2 C-21 Amide derivatives of fusidic acid

General synthetic procedure for compounds 4.4-4.8

Et_3N (3 eq.) was added dropwise to a solution of fusidic acid (**3.1**) (1 eq.) and respective amine (1.2 eq.) in DCM (5 ml). Resulting reaction mixture was cooled to 0 °C in an ice bath and T3P solution (1.5 eq., 50% w/v in DMF, d = 1.09 g/ml) was added dropwise. Reaction mixture was then slowly warmed to 25 °C and stirred for 5 h. After completion of reaction (TLC), the reaction mixture was diluted with DCM (20 ml) and water (15 ml) and shaken well in a separating funnel. Organic layer was separated, dried over anhydrous sodium sulfate, filtered and concentrated *in vacuo*. The residue was purified by column chromatography on 100-200 silica gel using EtOAc:hexane as eluent, affording target compound as a white solid.

***N*-(4-chlorobenzyl)fusidic acid amide (4.4)**

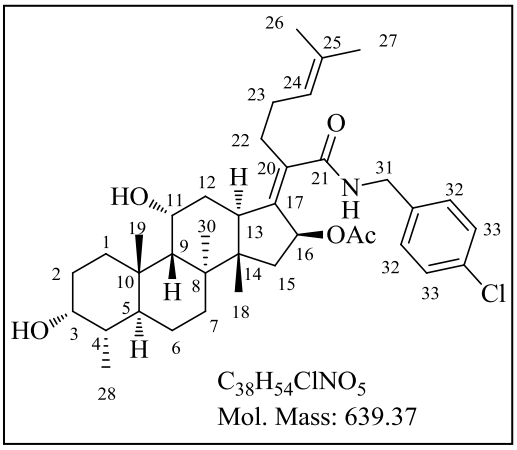

White solid (0.183 g obtained from 0.2 g of **3.1**, 74%); R_f 0.3 (60% EtOAc:hexane); Mp 195-197 °C; ^{1}H NMR (400 MHz, $CDCl_3$) δ 7.29 (d, *J* = 8.6 Hz, 2H, 2×H-33), 7.21 (d, *J* = 8.6 Hz, 2H, 2×H-32), 5.74 (d, *J* = 8.2 Hz, 1H, H-16), 5.67 (dd, *J* = 6.8, 4.5 Hz, 1H, NH), 5.06 (t, *J* =7.2 Hz, 1H, H-24), 4.57 (dd, *J* = 14.5, 6.8 Hz, 1H, H-31), 4.32 (m, 1H, H-11), 4.06 (dd, *J* = 14.5, 6.8 Hz, 1H, H-31), 3.74 (m, 1H, H-3), 2.98-2.95 (m, 1H, H-13), 2.55-2.2.47 (m, 1H, H-22), 2.40-2.33 (m, 1H, H-22), 2.29-2.24 (m, 1H, H-12), 2.18-2.06 (m, 5H, H-1, H-5, H-15 and 2×H-23), 1.98 (s, 3H, OAc), 1.90-1.70 (m, 4H, 2×H-2, H-7 and H-12), 1.63 (s, 3H, CH_3-27), 1.62-1.48 (m, 4H, H-1, H-4, H-6 and H-9), 1.55 (s, 3H, CH_3-26), 1.36 (s, 3H, CH_3-30), 1.29-1.25 (m, 1H, H-15), 1.16-1.08 (m, 2H, H-6 and H-7), 0.97 (s, 3H, CH_3-19), 0.94 (s, 3H, CH_3-18), 0.91 (d, *J* = 6.8 Hz, 3H, CH_3-28); ^{13}C NMR (100 MHz, $CDCl_3$) δ 171.1, 170.7, 142.0, 136.5, 135.5, 133.5, 132.5, 129.4 (2C), 128.9 (2C), 123.2, 73.6, 71.3, 68.3, 49.2, 48.7, 43.3, 43.1, 39.5, 39.3, 37.1, 36.3,

36.1, 35.6, 32.6, 30.3, 30.0, 29.4, 28.0, 25.6, 24.2, 22.6, 21.0, 20.7, 17.8, 17.8 and 15.9; LC-MS (ESI): *m/z* 580 $[M\text{-}OAc]^+$, 662 $[M+23]^+$; purity (LC-MS): 99% (t_r = 5.51 min).

_N_-(4-methoxybenzyl)fusidic acid amide (4.5)

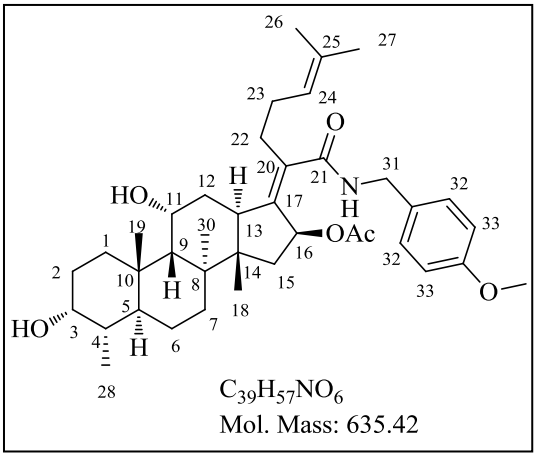

White solid (0.173 g obtained from 0.2 g of **3.1**, 70%); R_f 0.3 (60% EtOAc:hexane); Mp 106-108 ^oC; ^1H NMR (400 MHz, $CDCl_3$) δ 7.20 (d, *J* = 7.9 Hz, 2H, 2×H-33), 6.86 (d, *J* = 8.0 Hz, 2H, 2×H-32), 5.72 (d, *J* = 8.2 Hz, 1H, H-16), 5.61 (t, *J* = 4.7 Hz, 1H, NH), 5.06 (t, *J* = 7.2 Hz, 1H, H-24), 4.51 (dd, *J* = 14.1, 5.8 Hz, 1H, H-31), 4.32 (m, 1H, H-11), 4.06 (dd, *J* = 14.1, 5.8 Hz, 1H, H-31), 3.79 (s, 3H, OCH_3), 3.74 (m, 1H, H-3), 2.98-2.95 (m, 1H, H-13), 2.55-2.47 (m, 1H, H-22), 2.40-2.33 (m, 1H, H-22), 2.29-2.24 (m, 1H, H-12), 2.18-2.06 (m, 5H, H-1, H-5, H-15 and 2×H-23), 1.99 (s, 3H, OAc), 1.89-1.71 (m, 4H, 2×H-2, H-7 and H-12), 1.63 (s, 3H, CH_3-27), 1.62-1.48 (m, 4H, H-1, H-4, H-6 and H-9), 1.56 (s, 3H, CH_3-26), 1.35 (s, 3H, CH_3-30), 1.29-1.26 (m, 1H, H-15), 1.16-1.05 (m, 2H, H-6 and H-7), 0.96 (s, 3H, CH_3-19), 0.94 (s, 3H, CH_3-18), 0.91 (d, *J* = 6.7 Hz, 3H, CH_3-28); ^{13}C NMR (100 MHz, $CDCl_3$) δ 171.0, 170.8, 159.1, 141.6, 135.7, 132.4, 129.9, 129.4 (2C), 123.3, 114.2 (2C), 73.7, 71.3, 68.3, 55.3, 49.2, 48.7, 43.3, 43.2, 39.5, 39.3, 37.1, 36.2, 36.1, 35.6, 32.5, 30.3, 30.0, 29.4, 28.0, 25.6, 24.1, 22.6, 21.0, 20.7, 17.8, 17.8 and 15.9; LC-MS (ESI): *m/z* 576 $[M\text{-}OAc]^+$, 658 $[M+23]^+$; purity (LC-MS): 97% (t_r = 5.13 min).

_N_-(4-methylbenzyl)fusidic acid amide (4.6)

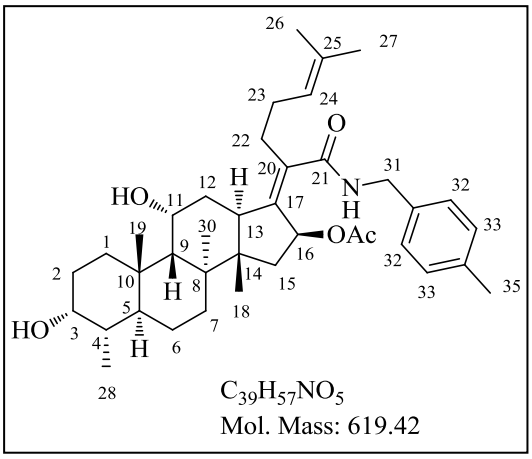

White solid (0.168 g obtained from 0.2 g of **3.1**, 70%); R_f 0.3 (60% EtOAc:hexane); Mp. 110-112 ^oC; ^1H NMR (400 MHz, $CDCl_3$) δ 7.16 (d, *J* = 8.2 Hz, 2H, 2×H-33), 7.12 (d, *J* = 8.0 Hz, 2H, 2×H-32), 5.72 (d, *J* = 8.2 Hz, 1H, H-16), 5.63 (dd, *J* = 6.4, 4.3 Hz, 1H, NH), 5.07 (t, *J* =7.2 Hz, 1H, H-24), 4.54 (dd, *J* = 14.3, 6.3 Hz, 1H, H-31), 4.32 (m, 1H, H-11), 4.06 (dd, *J* = 14.3, 6.3 Hz, 1H, H-31), 3.74 (m, 1H, H-3), 2.97-2.94 (m, 1H, H-13), 2.55-2.47 (m, 1H, H-22), 2.40-2.33 (m, 1H, H-22), 2.32 (s, 3H, 3×H-35), 2.29-2.24 (m, 1H, H-12), 2.18-2.06 (m, 5H,

H-1, H-5, H-15 and 2×H-23), 1.98 (s, 3H, OAc), 1.89-1.69 (m, 4H, 2×H-2, H-7 and H-12), 1.63 (s, 3H, CH_3-27), 1.61-1.47 (m, 4H, H-1, H-4, H-6 and H-9), 1.56 (s, 3H, CH_3-26), 1.36 (s, 3H, CH_3-30), 1.29-1.25 (m, 1H, H-15), 1.16-1.08 (m, 2H, H-6 and H-7), 0.96 (s, 3H, CH_3-19), 0.94 (s, 3H, CH_3-18), 0.91 (d, J = 6.8 Hz, 3H, CH_3-28); ^{13}C NMR (100 MHz, $CDCl_3$) δ 171.0, 170.7, 141.6, 137.3, 135.7, 134.8, 132.4, 129.4 (2C), 128.1 (2C), 123.3, 73.7, 71.3, 68.3, 49.2, 48.7, 43.6, 43.2, 39.5, 39.3, 37.1, 36.2, 36.1, 35.6, 32.5, 30.3, 30.0, 29.4, 28.0, 25.6, 24.1, 22.6, 21.0 (2C), 20.7, 17.8, 17.7 and 15.9; LC-MS (ESI): *m/z* 560 $[M\text{-}OAc]^+$, 642 $[M+23]^+$; purity (LC-MS): 98% (t_r = 5.39 min).

***N*-(1-(4-Chlorophenyl)ethyl)fusidic acid amide (4.7)**

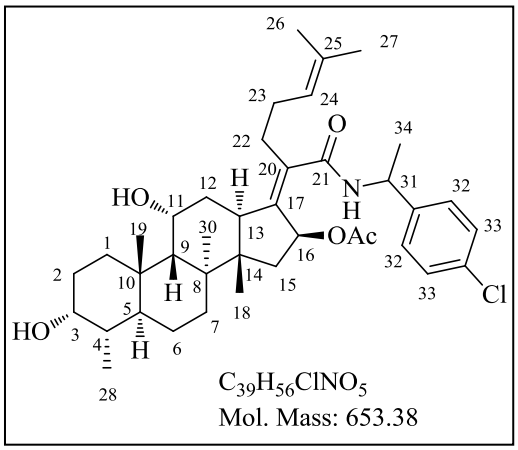

White powder (0.100 g obtained from 0.4 g of **3.1**, 20%); R_f 0.4 (60% EtOAc:hexane); Mp 127-129 °C; ^{1}H NMR (400 MHz, $CDCl_3$) δ 7.30 (d, J = 8.4 Hz, 2H, 2×H-33), 7.22 (d, J = 8.4 Hz, 2H, 2×H-32), 5.71 (d, J = 8.2 Hz, 1H, H-16), 5.52 (d, J = 7.9 Hz, 1H, NH), 5.08 (t, J =6.8 Hz, 1H, H-24), 5.04-4.92 (m, 1H, H-31), 4.31 (m, 1H, H-11), 3.73 (m, 1H, H-3), 2.99-2.94 (m, 1H, H-13), 2.51-2.40 (m, 1H, H-22), 2.35-2.29 (m, 1H, H-22), 2.27-2.24 (m, 1H, H-12), 2.19-1.98 (m, 5H, H-1, H-5, H-15 and 2×H-23), 1.95 (s, 3H, OAc), 1.87-1.70 (m, 4H, 2×H-2, H-7 and H-12), 1.66 (s, 3H, CH_3-27), 1.59-1.41 (m, 4H, H-1, H-4, H-6 and H-9), 1.45 (d, J = 6.9 Hz, 3H, H-34). 1.57 (s, 3H, CH_3-26), 1.34 (s, 3H, CH_3-30), 1.30-1.25 (m, 1H, H-15), 1.15-1.03 (m, 2H, H-6 and H-7), 0.96 (s, 3H, CH_3-19), 0.93-0.89 (m, 6H, CH_3-18 and CH_3-28); ^{13}C NMR (100 MHz, $CDCl_3$) δ 170.8, 170.3, 142.0, 141.3, 135.7, 133.2, 132.5, 128.8 (2C), 127.8 (2C), 123.3, 74.4, 71.3, 68.3, 49.2, 48.5, 48.4, 43.2, 39.5, 39.3, 37.0, 36.2, 36.1, 35.7, 32.4, 30.2, 30.0, 29.5, 28.0, 25.7, 24.0, 22.7, 21.7, 21.3, 20.7, 18.0, 17.8 and 15.9; LC-MS (ESI): *m/z* 594 $[M\text{-}OAc]^+$; purity (LC-MS): 96% (t_r = 5.36 min).

***N*-(4-chlorophenyl)fusidic acid amide (4.8)**

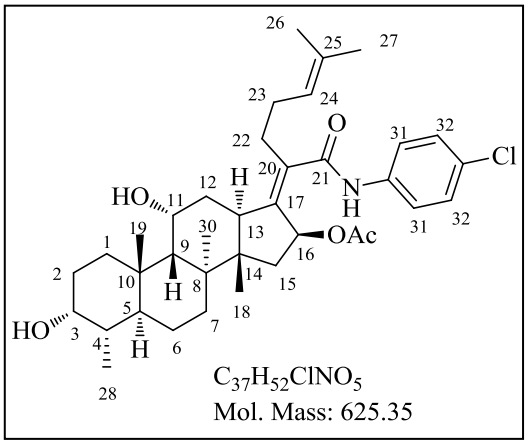

White solid (0.060 g obtained from 0.2 g of **3.1**, 25%); R_f 0.3 (60% EtOAc:hexane); Mp. 250-252 °C; ^{1}H NMR (400 MHz, $CDCl_3$) δ 7.46 (d, J = 8.9 Hz, 2H, 2×H-32), 7.26 (d, J = 8.9 Hz, 2H, 2×H-31), 7.15 (br s, 1H, NH), 5.76 (d, J = 8.5 Hz, 1H,

H-16), 5.11 (t, *J* =7.2 Hz, 1H, H-24), 4.36 (m, 1H, H-11), 3.74 (m, 1H, H-3), 3.06-3.03 (m, 1H, H-13), 2.61-2.54 (m, 1H, H-22), 2.45-2.39 (m, 1H, H-22), 2.33-2.28 (m, 1H, H-12), 2.26-2.09 (m, 5H, H-1, H-5, H-15 and 2×H-23), 1.91-1.72 (m, 4H, 2×H-2, H-7 and H-12), 1.73 (s, 3H, OAc), 1.66 (s, 3H, CH_3-27), 1.62-1.49 (m, 4H, H-1, H-4, H-6 and H-9), 1.59 (s, 3H, CH_3-26), 1.39 (s, 3H, CH_3-30), 1.28-1.24 (m, 1H, H-15), 1.17-1.08 (m, 2H, H-6 and H-7), 0.98 (s, 3H, CH_3-19), 0.94 (s, 3H, CH_3-18), 0.92 (d, *J* = 6.8 Hz, 3H, CH_3-28); ^{13}C NMR (100 MHz, $CDCl_3$) δ 170.6, 169.4, 142.9, 136.5, 135.0, 132.8, 129.1, 129.0 (2C), 123.2, 120.6 (2C), 73.7, 71.3, 68.3, 49.4, 48.7, 43.2, 39.5, 39.3, 37.1, 36.3, 36.2, 35.6, 32.4, 30.3, 29.9, 29.3, 28.1, 25.7, 24.1, 22.8, 20.8, 20.7, 17.9, 17.8 and 15.9; LC-MS (ESI): *m/z* 566 $[M\text{-}OAc]^+$, 648 $[M+23]^+$; purity (LC-MS): 98% (t_r = 5.66 min).

7.2.3 Chapter 5 (Metergoline derivatives)

(5*R*,8*S*,10*R*)-1,6-Dimethyl-8-aminomethyl-ergoline (5.2)[7]

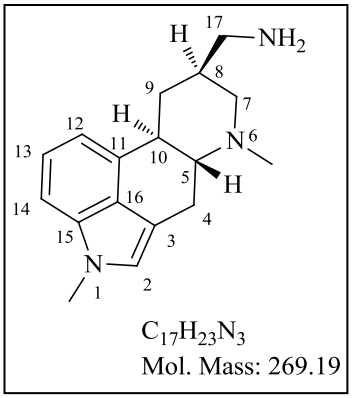

$C_{17}H_{23}N_3$
Mol. Mass: 269.19

A suspension of metergoline (**5.1**) (1.0 g, 3.712 mmol) in methanol (30 ml) was charged with 10% Pd/C (50% moisture). The reaction mixture was stirred at 25 °C for 16 h under a hydrogen atmosphere. Progress of the reaction was monitored by TLC. After completion of reaction, reaction mixture was filtered through a bed of celite and the filtrate was evaporated *in vacuo* to afford compound **5.2** as yellow viscous oil which solidified on long standing in refrigerator. Yellow solid (0.630 g, 95%); Mp. 151-153 °C; ^{1}H NMR (400 MHz, $CDCl_3$): δ 7.18 (t, *J* = 7.1 Hz, 1H, H-13), 7.10 (d, *J* = 8.2 Hz, 1H, H-12), 6.92 (d, *J* = 7.1 Hz, 1H, H-14), 6.72 (s, 1H, H-2), 3.74 (s, 3H, N1-CH_3), 3.38 (dd, *J* = 14.7, 4.3 Hz, 1H, H-4), 3.22-3.18 (m, 1H, H-7), 3.06-2.99 (m, 1H, H-10), 2.80-2.69 (m, 4H, 2×H-17, H-4 and H-9), 2.52 (s, 3H, N6-CH_3), 2.37 (br s, 2H, NH_2), 2.24-2.18 (m, 1H, H-5), 2.14-2.04 (m, 1H, H-8), 2.00 (t, *J* = 11.3 Hz, 1H, H-7), 1.12 (q, *J* = 12.2 Hz, 1H, H-9); ^{13}C NMR (100 MHz, $CDCl_3$) δ 134.6, 133.7, 126.7, 122.7, 122.4, 112.6, 111.0, 106.6, 67.7, 61.8, 46.6, 43.2, 40.6, 39.2, 32.6, 32.2 and 27.0; LC-MS (ESI): *m/z* 270 $[M+H]^+$; purity (HPLC): 99% (t_r = 4.75 min).

General Synthetic procedure for metergoline derivatives

Procedure A

Compound **5.2** (1.0 eq.), respective carboxylic acid (1.2 eq.) and HOBt (1.2 eq.) were dissolved in DCM. Diisopropylethylamine (3.0 eq.) was then added dropwise followed by

addition of EDCI (1.2 eq.). Reaction mixture was stirred at 25 ^{o}C for 24 h. After completion of reaction (TLC), reaction mixture was diluted with DCM and washed with water. Organic layer was separated, dried over anhydrous sodium sulfate, filtered and concentrated *in vacuo*. Crude product was purified by column chromatography on 60-120 silica gel using methanol:DCM as eluent.

Procedure B (for compounds 5.6, 5.7, 5.15, 5.20 and 5.22)

A solution of compound **5.2** (1.0 eq.) and respective acid chloride (1.5 eq.) in DCM was stirred at 25 ^{o}C for 3 h. After completion of reaction (TLC), reaction mixture was diluted with DCM and washed with water. Organic layer after drying over anhydrous sodium sulfate was concentrated *in vacuo*. Crude product was purified by column chromatography on 60-120 silica gel using methanol:DCM as eluent.

(5*R*,8*S*,10*R*)-1,6-Dimethyl-8-(4-chlorobenzoyl)aminomethyl-ergoline (5.3)

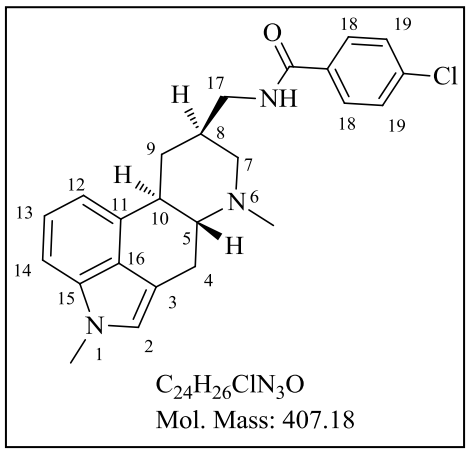

$C_{24}H_{26}ClN_3O$
Mol. Mass: 407.18

Off-white solid (0.070 g obtained from 0.130 g of **5.2**, 35%); R_f 0.5 (10% Methanol:DCM); Mp. 224-226 ^{o}C; ^{1}H NMR (400 MHz, $CDCl_3$): δ 7.74 (d, *J* = 8.6 Hz, 2H, 2×H-18), 7.41 (d, *J* = 8.6 Hz, 2H, 2×H-19), 7.18 (t, *J* = 7.1 Hz, 1H, H-13), 7.11 (d, *J* = 8.2 Hz, 1H, H-12), 6.89 (d, *J* = 7.1 Hz, 1H, H-14), 6.73 (s, 1H, H-2), 6.37 (t, *J* = 5.4 Hz, 1H, NH), 3.75 (s, 3H, N1-CH_3), 3.52-3.42 (m, 2H, 2×H-17), 3.38 (dd, *J* = 14.7, 4.3 Hz, 1H, H-4), 3.12-3.08 (m, 1H, H-7), 3.03-2.97 (m, 1H, H-10), 2.74-2.67 (m, 2H, H-4 and H-9), 2.48 (s, 3H, N6-CH_3), 2.31-2.22 (m, 1H, H-8), 2.22-2.16 (m, 1H, H-5), 2.06 (t, *J* = 11.3 Hz, 1H, H-7), 1.23 (q, *J* = 12.2 Hz, 1H, H-9); ^{13}C NMR (100 MHz, $CDCl_3$) δ 166.7, 137.7, 134.4, 133.1, 133.0, 128.8 (2C), 128.3 (2C), 126.4, 122.7, 122.5, 112.5, 110.5, 106.9, 67.4, 61.5, 43.8, 43.2, 40.4, 36.7, 32.7, 32.1 and 26.9; LC-MS (ESI): *m/z* 408 $[M+H]^+$; purity (LC-MS): 99% (t_r = 3.71 min).

(5*R*,8*S*,10*R*)-1,6-Dimethyl-8-(2-chlorobenzoyl)aminomethyl-ergoline (5.4)

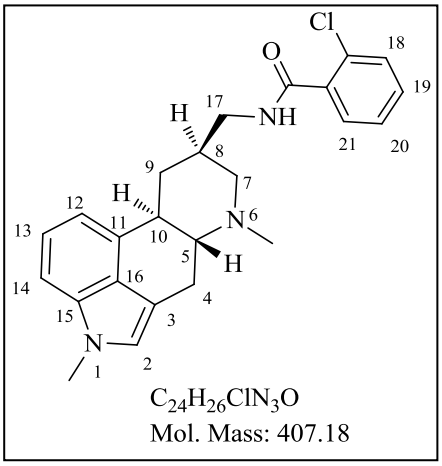

White solid (0.150 g obtained from 0.150 g of **5.2**, 66%); R_f 0.5 (10% Methanol:DCM); Mp. 180-182 ^oC; ^1H NMR (400 MHz, $CDCl_3$): δ 7.71-7.69 (m, 1H, H-18), 7.43-7.41 (m, 1H, H-21), 7.39-7.32 (m, 2H, H-19 and H-20), 7.19 (t, *J* = 7.1 Hz, 1H, H-13), 7.11 (d, *J* = 8.2 Hz, 1H, H-12), 6.90 (d, *J* = 7.1 Hz, 1H, H-14), 6.73 (s, 1H, H-2), 6.31 (t, *J* = 5.4 Hz, 1H, NH), 3.76 (s, 3H, N1-CH_3), 3.53-3.50 (m, 2H, 2×H-17), 3.39 (dd, *J* = 14.7, 4.3 Hz, 1H, H-4), 3.19-3.15 (m, 1H, H-7), 3.04-2.98 (m, 1H, H-10), 2.79-2.68 (m, 2H, H-4 and H-9), 2.50 (s, 3H, N6-CH_3), 2.34-2.23 (m, 1H, H-8), 2.22-2.16 (m, 1H, H-5), 2.10 (t, *J* = 11.3 Hz, 1H, H-7), 1.26 (q, *J* = 12.3 Hz, 1H, H-9); ^{13}C NMR (100 MHz, $CDCl_3$): δ 166.6, 135.2, 134.4, 133.1, 131.3, 130.5, 130.3, 130.2, 127.1, 126.5, 122.7, 122.5, 112.5, 110.6, 106.8, 67.4, 61.5, 43.9, 43.3, 40.5, 36.6, 32.7, 32.2 and 26.9; LC-MS (ESI): *m/z* 408 $[M+H]^+$; purity (HPLC): 99% (t_r = 12.89 min).

(5*R*,8*S*,10*R*)-1,6-Dimethyl-8-(3-chlorobenzoyl)aminomethyl-ergoline (5.5)

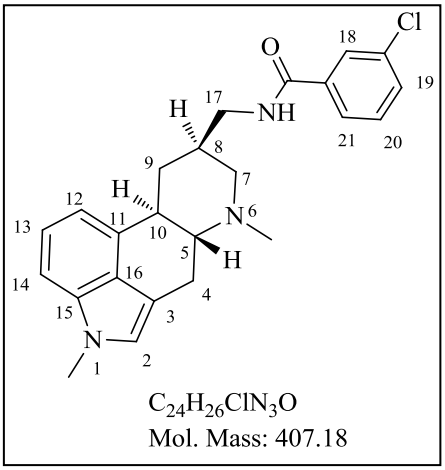

White solid (0.143 g obtained from 0.150 g of **5.2**, 63%); R_f 0.5 (10% Methanol:DCM); Mp. 183-185 ^oC; ^1H NMR (400 MHz, $CDCl_3$): δ 7.81 (t, *J* = 1.8 Hz, 1H, H-18), 7.68 (ddd, *J* = 7.7, 1.7, 1.1 Hz, 1H, H-21), 7.46 (ddd, *J* = 8.0, 2.1, 1.1 Hz, 1H, H-19), 7.36 (t, *J* = 7.8 Hz, 1H, H-20), 7.18 (t, *J* = 7.1 Hz, 1H, H-13), 7.11 (d, *J* = 8.2 Hz, 1H, H-12), 6.88 (d, *J* = 7.1 Hz, 1H, H-14), 6.73 (s, 1H, H-2), 6.48 (t, *J* = 5.4 Hz, 1H, NH), 3.75 (s, 3H, N1-CH_3), 3.50-3.46 (m, 2H, 2×H-17), 3.39 (dd, *J* = 14.7, 4.3 Hz, 1H, H-4), 3.18-3.14 (m, 1H, H-7), 3.11-3.04 (m, 1H, H-10), 2.81-2.69 (m, 2H, H-4 and H-9), 2.53 (s, 3H, N6-CH_3), 2.38-2.30 (m, 1H, H-8), 2.30-2.23 (m, 1H, H-5), 2.14 (t, *J* = 11.3 Hz, 1H, H-7), 1.25 (q, *J* = 12.3 Hz, 1H, H-9); ^{13}C NMR (100 MHz, $CDCl_3$): δ 166.3, 136.5, 134.8, 134.4, 133.1, 131.5, 129.9, 127.3, 126.5, 124.9, 122.7, 122.5, 112.5, 110.6, 106.8, 67.4, 61.5, 43.9, 43.3, 40.6, 36.8, 32.7, 32.2 and 27.0; LC-MS (ESI): *m/z* 408 $[M+H]^+$; purity (HPLC): 98% (t_r = 14.09 min).

(5*R*,8*S*,10*R*)-1,6-Dimethyl-8-(3,4-dichlorobenzoyl)aminomethyl-ergoline (5.6)

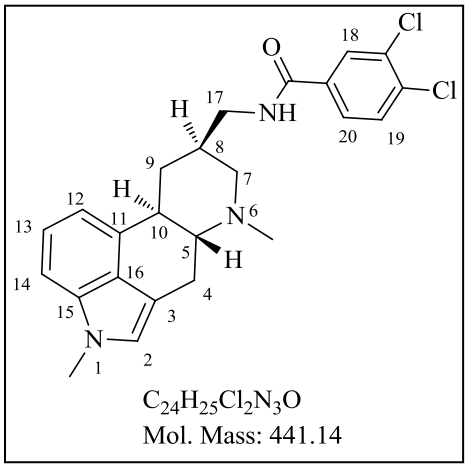

$C_{24}H_{25}Cl_2N_3O$
Mol. Mass: 441.14

Off-white solid (0.070 g obtained from 0.080 g of **5.2**, 53%); R_f 0.6 (10% Methanol:DCM); Mp. 139-141 ^oC; ^1H NMR (400 MHz, CD_3OD): δ 8.03 (d, *J* = 2.0 Hz, 1H, H-18), 7.78 (dd, *J* = 8.4, 2.1 Hz, 1H, H-20), 7.64 (d, *J* = 8.4 Hz, 1H, H-19), 7.13-7.11 (m, 2H, H-12 and H-13), 6.88 (d, *J* = 7.1 Hz, 1H, H-14), 6.84 (s, 1H, H-2), 3.74 (s, 3H, N1-CH_3), 3.57-3.41 (m, 4H, 2×H-17 and H-4), 3.25-3.23 (m, 1H, H-7), 3.03-2.97 (m, 1H, H-10), 2.80-2.68 (m, 2H, H-4 and H-9), 2.63 (s, 3H, N6-CH_3), 2.47-2.40 (m, 1H, H-5), 2.36-2.27 (m, 2H, H-7 and H-8), 1.25 (q, *J* = 12.3 Hz, 1H, H-9); ^{13}C NMR (100 MHz, CD_3OD): δ 166.6, 135.4, 134.6, 134.3, 130.9, 130.4, 129.6, 129.2, 126.7, 125.9, 123.0, 122.4, 112.4, 107.7, 107.1, 67.3, 59.8, 42.7, 40.8, 39.0, 35.1, 31.4, 30.8 and 25.0; LC-MS (ESI): *m/z* 442 $[M+H]^+$; purity (HPLC): 97% (t_r = 14.16 min).

(5*R*,8*S*,10*R*)-1,6-Dimethyl-8-(2,4-dichlorobenzoyl)aminomethyl-ergoline (5.7)

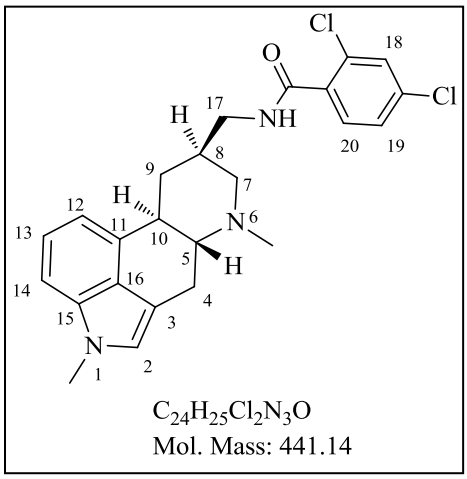

$C_{24}H_{25}Cl_2N_3O$
Mol. Mass: 441.14

Off-white solid (0.120 g obtained from 0.180 g of **5.2**, 41%); R_f 0.6 (10% Methanol:DCM); Mp. 160-162 ^oC; ^1H NMR (400 MHz, $CDCl_3$): δ 7.67 (d, *J* = 8.3 Hz, 1H, H-20), 7.44 (d, *J* = 2.0 Hz, 1H, H-18), 7.33 (dd, *J* = 8.3, 2.0 Hz, 1H, H-19), 7.19 (t, *J* = 7.1 Hz, 1H, H-13), 7.12 (d, *J* = 8.2 Hz, 1H, H-12), 6.89 (d, *J* = 7.0 Hz, 1H, H-14), 6.73 (s, 1H, H-2), 6.34 (t, *J* = 5.4 Hz, 1H, NH), 3.76 (s, 3H, N1-CH_3), 3.52-3.47 (m, 2H, 2×H-17), 3.39 (dd, *J* = 14.7, 4.3 Hz, 1H and H-4), 3.17-3.13 (m, 1H, H-7), 3.03-2.97 (m, 1H, H-10), 2.77-2.67 (m, 2H, H-4 and H-9), 2.50 (s, 3H, N6-CH_3), 2.34-2.24 (m, 1H, H-8), 2.23-2.16 (m, 1H, H-5), 2.09 (t, *J* = 11.3 Hz, 1H, H-7), 1.26 (q, *J* = 12.2 Hz, 1H, H-9); ^{13}C NMR (100 MHz, $CDCl_3$): δ 166.3, 136.8, 134.4, 133.4, 131.6, 130.9, 130.5, 130.0, 127.5, 125.9, 123.0, 122.9, 112.9, 108.0, 107.5, 67.6, 60.3, 42.9, 41.8, 38.7, 35.0, 32.8, 31.1 and 25.3; LC-MS (ESI): *m/z* 442 $[M+H]^+$; purity (HPLC): 98% (t_r = 14.12 min).

(5*R*,8*S*,10*R*)-1,6-Dimethyl-8-(4-chloro-3-trifluoromethybenzoyl)aminomethyl-ergoline (5.8)

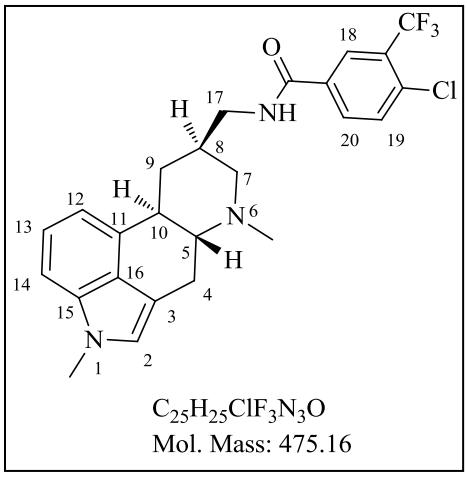

$C_{25}H_{25}ClF_3N_3O$
Mol. Mass: 475.16

White solid (0.192 g obtained from 0.150 g of **5.2**, 72%); R_f 0.5 (10% Methanol:DCM); Mp. 192-194 ^oC; ^1H NMR (400 MHz, $CDCl_3$): δ 8.20 (d, *J* = 2.1 Hz, 1H, H-18), 7.97 (dd, *J* = 8.3, 2.0 Hz, 1H, H-20), 7.54 (d, *J* = 8.3 Hz, 1H, H-19), 7.19 (t, *J* =7.1 Hz, 1H, H-13), 7.12 (d, *J* = 8.2 Hz, 1H, H-12), 6.95 (t, *J* = 5.4 Hz, 1H, NH), 6.87 (d, *J* = 7.1 Hz, 1H, H-14), 6.74 (s, 1H, H-2), 3.76 (s, 3H, N1-CH_3), 3.58-3.45 (m, 2H, 2×H-17), 3.40 (dd, *J* = 14.7, 4.3 Hz, 1H, H-4), 3.30-3.26 (m, 1H, H-7), 3.24-2.18 (m, 1H, H-10), 2.94-2.87 (m, 1H, H-4), 2.77-2.72 (m, 1H, H-9), 2.61 (s, 3H, N6-CH_3), 2.54-2.41 (m, 2H, H-5 and H-8), 2.29 (t, *J* = 11.5 Hz, 1H, H-7), 1.28 (q, *J* = 12.2 Hz, 1H, H-9); ^{13}C NMR (100 MHz, $CDCl_3$) δ 165.5, 135.6, 134.4, 133.1, 131.7 (3C), 131.3 (2C), 126.6, 126.2, 122.8 (2C), 112.7, 109.3, 107.2, 67.5, 61.1, 43.6, 42.5, 39.7, 35.9, 32.8, 31.8 and 26.2; LC-MS (ESI): *m/z* 476 $[M+H]^+$; purity (LC-MS): 99% (t_r = 4.16 min).

(5*R*,8*S*,10*R*)-1,6-Dimethyl-8-(4-nitro-3-trifluoromethylbenzoyl)aminomethyl-ergoline (5.9)

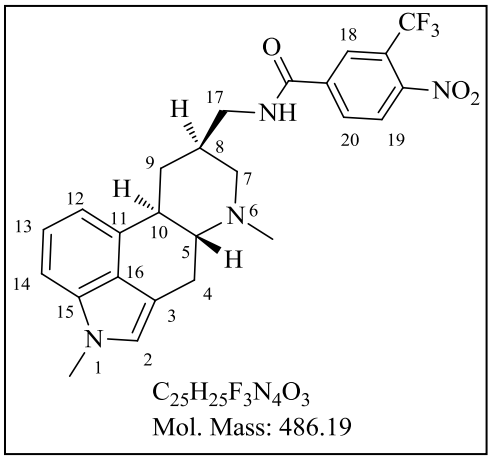

$C_{25}H_{25}F_3N_4O_3$
Mol. Mass: 486.19

Yellow solid (0.050 g obtained from 0.108 g of **5.2**, 26%); R_f 0.5 (10% Methanol:DCM); Mp. 195-197 ^oC; ^1H NMR (400 MHz, $CDCl_3$): δ 8.30 (d, *J* = 1.5 Hz, 1H, H-18), 8.15 (dd, *J* = 8.3, 1.6 Hz, 1H, H-20), 7.86 (d, *J* = 8.3 Hz, 1H, H-19), 7.16 (t, *J* = 7.1 Hz, 1H, H-13), 7.11 (d, *J* = 8.2 Hz, 1H, H-12), 7.01 (t, *J* = 5.4 Hz 1H, NH), 6.86 (d, *J* = 7.1 Hz, 1H, H-14), 6.74 (s, 1H, H-2), 3.75 (s, 3H, N1-CH_3), 3.56-3.44 (m, 2H, 2×H-17), 3.38 (dd, *J* = 14.7, 4.3 Hz, 1H, H-4), 3.17-3.13 (m, 1H, H-7), 3.08-3.01 (m, 1H, H-10), 2.76-2.70 (m, 2H, H-4 and H-9), 2.52 (s, 3H, N6-CH_3), 2.43-2.32 (m, 1H, H-8), 2.28-2.22 (m, 1H, H-5), 2.12 (t, *J* = 11.4 Hz, 1H, H-7), 1.24 (q, *J* = 12.4 Hz, 1H, H-9); ^{13}C NMR (100 MHz, $CDCl_3$) δ 164.3, 149.4, 138.4, 134.4, 132.3, 131.7 (2C), 127.2, 126.3, 125.2 (2C), 122.7 (2C), 112.5, 109.9, 107.1, 67.4, 61.2, 44.2, 43.0, 40.2, 36.2, 32.7, 32.0 and 26.6; LC-MS (ESI): *m/z* 487 $[M+H]^+$; purity (LC-MS): 97% (t_r = 3.49 min).

(5*R*,8*S*,10*R*)-1,6-Dimethyl-8-(nicotinoyl)aminomethyl-ergoline (5.10)[8]

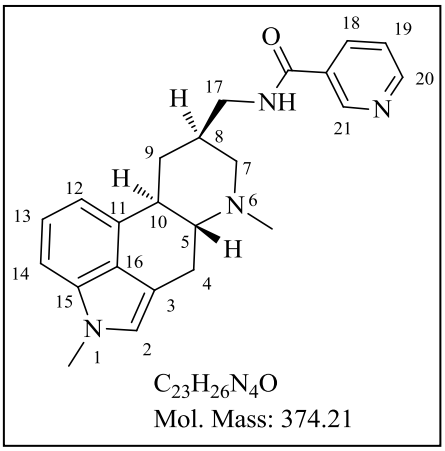

$C_{23}H_{26}N_4O$
Mol. Mass: 374.21

Light-yellow solid (0.050 g obtained from 0.080 g of **5.2**, 45%); R_f 0.5 (20% Methanol:DCM); Mp. 178-180 °C; ^{1}H NMR (400 MHz, $CDCl_3$): δ 9.05 (s, 1H, H-21), 8.72 (d, *J* = 4.8 Hz, 1H, H-20), 8.16 (dt, 1H, *J* = 8.0, 1.9 Hz, 1H, H-18), 7.38 (dd, *J* = 7.9, 4.8 Hz, 1H, H-19), 7.18 (t, *J* = 7.1 Hz, 1H, H-13), 7.11 (d, *J* = 8.2 Hz, 1H, H-12), 6.89 (d, *J* = 7.1 Hz, 1H, H-14), 6.77 (t, *J* = 5.4 Hz, 1H, NH), 6.73 (s, 1H, H-2), 3.75 (s, 3H, N1-CH_3), 3.59-3.45 (m, 2H, 2×H-17), 3.40 (dd, *J* = 14.6, 4.3 Hz, 1H, H-4), 3.25-3.21 (m, 1H, H-7), 3.16-3.10 (m, 1H, H-10), 2.85-2.72 (m, 2H, H-4 and H-9), 2.57 (s, 3H, N6-CH_3), 2.46-2.31 (m, 2H, H-5 and H-8), 2.21 (t, *J* = 11.5 Hz, 1H, H-7), 1.28 (q, *J* = 12.4 Hz, 1H, H-9); ^{13}C NMR (100 MHz, $CDCl_3$): δ 165.9, 152.2, 148.0, 135.1, 134.4, 132.3, 130.2, 126.3, 123.5, 122.8, 122.7, 112.6, 109.8, 107.0, 67.5, 61.2, 43.6, 42.8, 40.0, 36.3, 32.7, 31.9 and 26.5; LC-MS (ESI): *m/z* 375 $[M+H]^+$; purity (HPLC): 98% (t_r = 10.67 min).

(5*R*,8*S*,10*R*)-1,6-Dimethyl-8-(isonicotinoyl)aminomethyl-ergoline (5.11)[8]

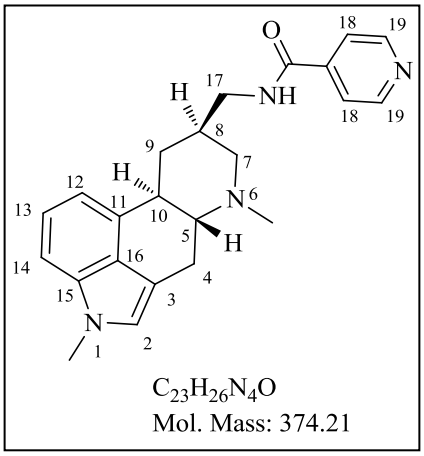

$C_{23}H_{26}N_4O$
Mol. Mass: 374.21

Off-white solid (0.032 g obtained from 0.1 g of **5.2**, 23%); R_f 0.4 (15% Methanol:DCM); Mp. 218-220 °C; ^{1}H NMR (400 MHz, $CDCl_3$): δ 8.75 (d, *J* = 4.5 Hz, 2H, 2×H-19), 7.65 (d, *J* = 4.5 Hz, 2H, 2×H-18), 7.18 (t, *J* = 7.1 Hz, 1H, H-13), 7.12 (d, *J* = 8.2 Hz, 1H, H-12), 6.88 (d, *J* = 7.0 Hz, 1H, H-14), 6.74 (s, 1H, H-2), 6.57 (t, *J* = 5.4 Hz, 1H, NH), 3.76 (s, 3H, N1-CH_3), 3.58-3.46 (m, 2H, 2×H-17), 3.40 (dd, *J* = 14.7, 4.4 Hz, 1H, H-4), 3.20-3.16 (m, 1H, H-7), 3.13-3.06 (m, 1H, H-10), 2.82-2.71 (m, 2H, H-4 and H-9), 2.54 (s, 3H, N6-CH_3), 2.41-2.34 (m, 1H, H-8), 2.33-2.27 (m, 1H, H-5), 2.16 (t, *J* = 11.4 Hz, 1H, H-7), 1.27 (q, *J* = 12.3 Hz, 1H, H-9); ^{13}C NMR (100 MHz, $CDCl_3$): δ 165.8, 150.6 (2C), 141.5, 134.4, 132.4, 126.3, 122.7 (2C), 120.9 (2C), 112.5, 110.0, 107.0, 67.4, 61.3, 43.8, 43.0, 40.2, 36.4, 32.7, 32.0 and 26.6; LC-MS (ESI): *m/z* 375 $[M+H]^+$; purity (HPLC): 98% (t_r = 10.70 min).

(5*R*,8*S*,10*R*)-1,6-Dimethyl-8-(picolinoyl)aminomethyl-ergoline (5.12)[8]

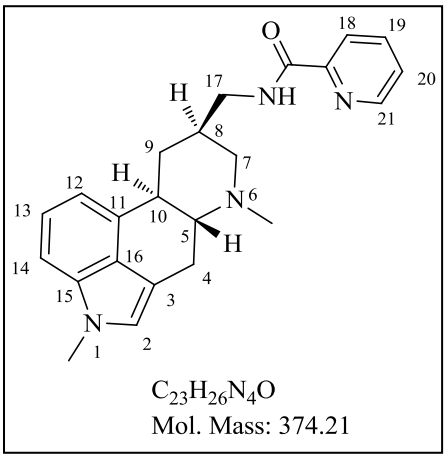

$C_{23}H_{26}N_4O$
Mol. Mass: 374.21

Pale-yellow solid (0.070 g obtained from 0.100 g of **5.2**, 50%); R_f 0.5 (10% Methanol:DCM); Mp. 168-170 °C; ^{1}H NMR (400 MHz, $CDCl_3$): δ 8.57 (ddd, *J* = 4.8, 1.7, 0.9 Hz, 1H, H-21), 8.22 (dt, *J* = 7.8, 1.1 Hz, 1H, H-18), 8.22 (br s, 1H, NH), 7.86 (td, *J* = 7.7, 1.7 Hz, 1H, H-19), 7.43 (ddd, *J* = 7.6, 4.8, 1.2 Hz, 1H, H-20), 7.18 (t, *J* = 7.1 Hz, 1H, H-13), 7.11 (d, *J* = 8.2 Hz, 1H, H-12), 6.92 (d, *J* = 7.4 Hz, 1H, H-14), 6.72 (s, 1H, H-2), 3.75 (s, 3H, N1-CH_3), 3.54-3.50 (m, 2H, 2×H-17), 3.39 (dd, *J* = 14.7, 4.3 Hz, 1H, H-4), 3.18-3.13 (m, 1H, H-7), 3.09-3.02 (m, 1H, H-10), 2.79-2.71 (m, 2H, H-4 and H-9), 2.51 (s, 3H, N6-CH_3), 2.38-2.28 (m, 1H, H-8), 2.26-2.20 (m, 1H, H-5), 2.12 (t, *J* = 11.3 Hz, 1H, H-7), 1.28 (q, *J* = 12.3 Hz, 1H, H-9); ^{13}C NMR (100 MHz, $CDCl_3$): δ 164.5, 149.9, 148.1, 137.3, 134.4, 133.0, 126.4, 126.1, 122.7, 122.5, 122.2, 112.6, 110.5, 106.8, 67.4, 61.4, 43.1 (2C), 40.4, 36.5, 32.7, 32.1 and 26.8; LC-MS (ESI): *m/z* 375 $[M+H]^+$; purity (HPLC): 98% (t_r = 11.51 min).

(5*R*,8*S*,10*R*)-1,6-Dimethyl-8-(pyrazinoyl)aminomethyl-ergoline (5.13)

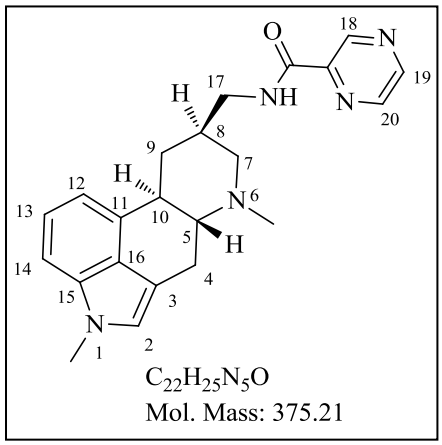

$C_{22}H_{25}N_5O$
Mol. Mass: 375.21

Off-white solid (0.070 g obtained from 0.100 g of **5.2**, 51%); R_f 0.5 (10% Methanol:DCM); Mp. 202-204 °C; ^{1}H NMR (400 MHz, $CDCl_3$): δ 9.43 (d, *J* = 1.4 Hz, 1H, H-18), 8.76 (d, *J* = 2.4 Hz, 1H, H-20), 8.54 (dd, *J* = 2.4, 1.4 Hz, 1H, H-19), 7.96 (t, *J* = 5.5 Hz, 1H, NH), 7.18 (t, *J* = 7.1 Hz, 1H, H-13), 7.11 (d, *J* = 8.2 Hz, 1H, H-12), 6.90 (d, *J* = 7.1 Hz, 1H, H-14), 6.73 (s, 1H, H-2), 3.75 (s, 3H, N1-CH_3), 3.55-3.52 (m, 2H, 2×H-17), 3.39 (dd, *J* = 14.7, 4.3 Hz, 1H, H-4), 3.16-3.12 (m, 1H, H-7), 3.10-3.03 (m, 1H, H-10), 2.78-2.72 (m, 2H, H-4 and H-9), 2.51 (s, 3H, N6-CH_3), 2.39-2.28 (m, 1H, H-8), 2.27-2.21 (m, 1H, H-5), 2.13 (t, *J* = 11.3 Hz, 1H, H-7), 1.28 (q, *J* = 12.3 Hz, 1H, H-9); ^{13}C NMR (100 MHz, $CDCl_3$): δ 163.1, 147.3, 144.5, 144.4, 142.5, 134.4, 132.9, 126.4, 122.7, 122.6, 112.5, 110.3, 106.9, 67.4, 61.3, 43.1 (2C), 40.3, 36.5, 32.7, 32.0 and 26.8; LC-MS (ESI): *m/z* 376 $[M+H]^+$; purity (HPLC): 97% (t_r = 10.67 min).

(5*R*,8*S*,10*R*)-1,6-Dimethyl-8-(pyrimidine-4-carbonyl)aminomethyl-ergoline (5.14)

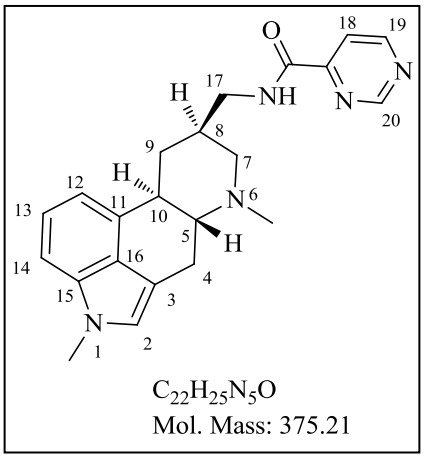

Pale-yellow solid (0.050 g obtained from 0.100 g of **5.2**, 35%); R_f 0.5 (10% Methanol:DCM); Mp. 168-170 ^oC; ^1H NMR (400 MHz, $CDCl_3$): δ 9.26 (d, *J* = 1.3 Hz, 1H, H-20), 8.98 (1H, d, *J* = 5.0 Hz, 1H, H-18), 8.15 (br s, 1H, NH), 8.14 (dd, *J* = 5.0, 1.4 Hz, 1H, H-19), 7.18 (t, *J* = 7.1 Hz, 1H, H-13), 7.11 (d, *J* = 8.2 Hz, 1H, H-12), 6.90 (d, *J* = 7.0 Hz, 1H, H-14), 6.73 (s, 1H, H-2), 3.75 (s, 3H, N1-CH_3), 3.54-3.51 (m, 2H, 2×H-17), 3.39 (dd, *J* = 14.7, 4.3 Hz, 1H, H-4), 3.15-3.11 (m, 1H, H-7), 3.09-3.03 (m, 1H, H-10), 2.78-2.71 (m, 2H, H-4 and H-9), 2.51 (s, 3H, N6-CH_3), 2.40-2.28 (m, 1H, H-8), 2.27-2.20 (m, 1H, H-5), 2.12 (t, *J* = 11.4 Hz, 1H, H-7), 1.28 (q, *J* = 12.4 Hz, 1H, H-9); ^{13}C NMR (100 MHz, $CDCl_3$): δ 162.8, 159.2, 157.8, 156.1, 134.4, 132.9, 126.4, 122.7, 122.6, 118.5, 112.5, 110.4, 106.9, 67.4, 61.3, 43.3, 43.1, 40.3, 36.4, 32.7, 32.0 and 26.8; LC-MS (ESI): *m/z* 376 $[M+H]^+$; purity (HPLC): 98% (t_r = 10.83 min).

(5*R*,8*S*,10*R*)-1,6-Dimethyl-8-(acetyl)aminomethyl-ergoline (5.15)[8]

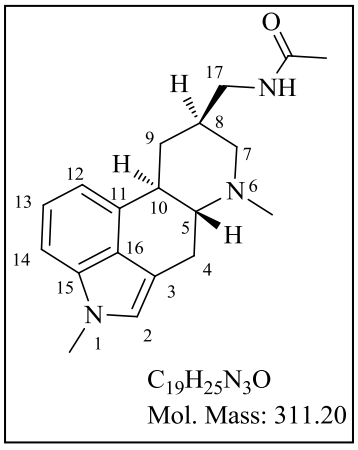

Off-white solid (0.040 g obtained from 0.080 g of **5.2**, 43%); R_f 0.4 (10% Methanol:DCM); Mp. 191-193 ^oC; ^1H NMR (400 MHz, CD_3OD): δ 7.14-7.10 (m, 2H, H-12 and H-13), 6.87-6.83 (m, 2H, H-2 and H-14), 3.71 (s, 3H, N1-CH_3), 3.43 (dd, *J* = 14.5, 4.4 Hz, 1H, H-4), 3.27-3.23 (m, 1H, H-7), 3.22-3.15 (m, 2H, 2×H-17), 3.05-2.99 (m, 1H, H-10), 2.80-2.73 (m, 1H, H-4), 2.70-2.65 (m, 1H, H-9), 2.68 (s, 3H, N6-CH_3), 2.53-2.46 (m, 1H, H-5), 2.31 (t, *J* = 11.8 Hz, 1H, H-7), 2.25-2.16 (m, 1H, H-8), 2.00 (s, 3H, $COCH_3$), 1.13 (q, *J* = 12.1 Hz, 1H, H-9); ^{13}C NMR (100 MHz, CD_3OD): δ 172.1, 134.6, 131.7, 126.2, 122.6, 122.2, 112.1, 109.0, 106.6, 67.3, 60.5, 42.6, 41.6, 39.6, 35.5, 31.5, 31.4, 25.7 and 21.1; LC-MS (ESI): *m/z* 312 $[M+H]^+$; purity (HPLC): 96% (t_r = 12.98 min).

(5*R*,8*S*,10*R*)-1,6-Dimethyl-8-(propanoyl)aminomethyl-ergoline (5.16)[8]

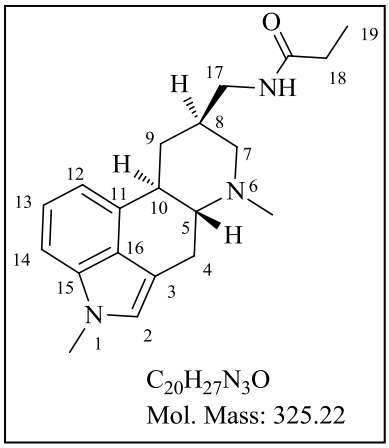

Off-white solid (0.129 g obtained from 0.160 g of **5.2**, 67%); R_f 0.4 (10% Methanol:DCM); Mp. 185-187 °C; ^{1}H NMR (400 MHz, $CDCl_3$): δ 7.18 (t, *J* = 7.1 Hz, 1H, H-13), 7.11 (d, *J* = 8.2 Hz, 1H, H-12), 6.88 (d, *J* = 7.1 Hz, 1H, H-14), 6.73 (s, 1H, H-2), 5.67 (t, *J* = 5.4 Hz, 1H, NH), 3.75 (s, 3H, N1-CH_3), 3.39 (dd, *J* = 14.7, 4.3 Hz, 1H, H-4), 3.35-3.24 (m, 2H, 2×H-17), 3.12-3.04 (m, 2H, H-7 and H-10), 2.82-2.75 (m, 1H, H-4), 2.70-2.64 (m, 1H, H-9), 2.53 (s, 3H, N6-CH_3), 2.29-2.15 (m, 4H, H-5, H-8 and 2×H-18), 2.09 (t, *J* = 11.3 Hz, 1H, H-7), 1.23-1.14 (m, 4H, H-9 and 3×H-19); ^{13}C NMR (100 MHz, $CDCl_3$): δ 173.9, 134.4, 132.7, 126.4, 122.7, 122.6, 112.6, 110.1, 106.9, 67.4, 61.3, 43.0 (2C), 40.1, 36.4, 32.7, 31.9, 29.8, 26.6 and 9.9; LC-MS (ESI): *m/z* 326 $[M+H]^+$; purity (HPLC): 99% (t_r = 10.34 min).

(5*R*,8*S*,10*R*)-1,6-Dimethyl-8-(butanoyl)aminomethyl-ergoline (5.17)

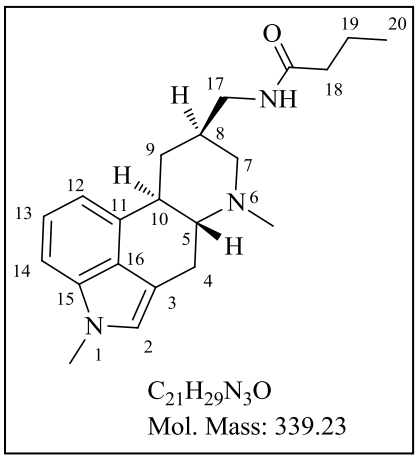

Off-white solid (0.090 g obtained from 0.100 g of **5.2**, 71%); R_f 0.5 (10% Methanol:DCM); Mp. 169-171 °C; ^{1}H NMR (400 MHz, $CDCl_3$): δ 7.18 (t, *J* = 7.1 Hz, 1H, H-13), 7.11 (d, *J* = 8.2 Hz, 1H, H-12), 6.88 (d, *J* = 7.1 Hz, 1H, H-14), 6.73 (s, 1H, H-2), 5.58 (t, *J* = 5.4 Hz, 1H, NH), 3.75 (s, 3H, N1-CH_3), 3.39 (dd, *J* = 14.7, 4.3 Hz, 1H, H-4), 3.35-3.25 (m, 2H, 2×H-17), 3.11-3.03 (m, 2H, H-7 and H-10), 2.81-2.74 (m, 1H, H-4), 2.70-2.64 (m, 1H, H-9), 2.53 (s, 3H, N6-CH_3), 2.28-2.14 (m, 4H, H-5, H-8 and 2×H-18), 2.08 (t, *J* = 11.3 Hz, 1H, H-7), 1.74-1.65 (m, 2H, 2×H-19), 1.19 (q, *J* = 12.2 Hz, 1H, H-9), 0.98 (t, *J* = 7.4 Hz, 3H, 3×H-20); ^{13}C NMR (100 MHz, $CDCl_3$): 173.1, 134.4, 132.7, 126.4, 122.7, 122.6, 112.5, 110.2, 106.9, 67.4, 61.3, 43.0 (2C), 40.2, 38.8, 36.5, 32.7, 31.9, 26.6, 19.2 and 13.8; LC-MS (ESI): *m/z* 340 $[M+H]^+$; purity (HPLC): 97% (t_r = 11.16 min).

(5*R*,8*S*,10*R*)-1,6-Dimethyl-8-(*tert*-butanoyl)aminomethyl-ergoline (5.18)

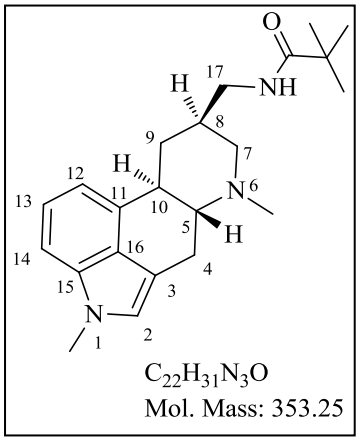

Yellow solid (0.066 g obtained from 0.100 g of **5.2**, 50%); R_f 0.5 (10% Methanol:DCM); Mp. 102-104 °C; ^{1}H NMR (400 MHz, $CDCl_3$): δ 7.18 (t, *J* = 7.1 Hz, 1H, H-13), 7.11 (d, *J* = 8.2 Hz, 1H, H-12), 6.88 (d, *J* = 7.1 Hz, 1H, H-14), 6.73 (s, 1H, H-

2), 5.77 (t, *J* = 5.4 Hz, 1H, NH), 3.75 (s, 3H, N1-CH_3), 3.39 (dd, *J* = 14.7, 4.3 Hz, 1H, H-4), 3.31-3.27 (m, 2H, 2×H-17), 3.08-3.00 (m, 2H, H-7 and H-10), 2.78-2.71 (m, 1H, H-4), 2.68-2.62 (m, 1H, H-9), 2.51 (s, 3H, N6-CH_3), 2.26-2.12 (m, 2H, H-5 and H-8), 2.04 (t, *J* = 11.3 Hz, 1H, H-7), 1.23 (s, 9H, 3×CH_3), 1.19 (q, *J* = 12.2 Hz, 1H, H-9); ^{13}C NMR (100 MHz, $CDCl_3$): δ 178.5, 134.4, 132.9, 126.4, 122.7, 122.5, 112.5, 110.3, 106.9, 67.4, 61.4, 43.1 (2C), 40.3, 38.8, 36.6, 32.7, 31.9, 27.7 (3C) and 26.7; LC-MS (ESI): *m/z* 354 $[M+H]^+$; purity (HPLC): 98% (t_r = 12.19 min).

(5*R*,8*S*,10*R*)-1,6-Dimethyl-8-(pentanoyl)aminomethyl-ergoline (5.19)

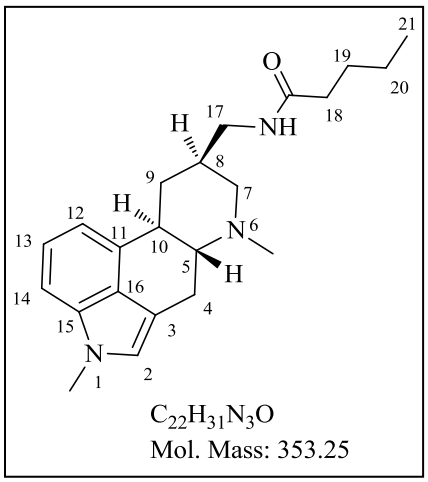

$C_{22}H_{31}N_3O$
Mol. Mass: 353.25

Off-white solid (0.120 g obtained from 0.100 g of **5.2**, 91%); R_f 0.5 (10% Methanol:DCM); Mp. 166-168 °C; ^{1}H NMR (400 MHz, $CDCl_3$): δ 7.18 (t, *J* = 7.1 Hz, 1H, H-13), 7.11 (d, *J* = 8.2 Hz, 1H, H-12), 6.88 (d, *J* = 7.1 Hz, 1H, H-14), 6.73 (s, 1H, H-2), 5.54 (t, *J* = 5.2 Hz, 1H, NH), 3.75 (s, 3H, N1-CH_3), 3.38 (dd, *J* = 14.7, 4.3 Hz, 1H, H-4), 3.31-3.27 (m, 2H, 2×H-17), 3.06-2.95 (m, 2H, H-7 and H-10), 2.74-2.64 (m, 2H, H-4 and H-9), 2.48 (s, 3H, N6-CH_3), 2.22 (t, *J* = 7.4 Hz, 2H, 2×H-18), 2.18-2.07 (m, 2H, H-5 and H-8), 2.01 (t, *J* = 11.3 Hz, 1H, H-7), 1.69-1.61 (m, 2H, 2×H-19), 1.43-1.34 (m, 2H, 2×H-20), 1.17 (q, *J* = 12.2 Hz, 1H, H-9), 0.94 (t, *J* = 7.3 Hz, 3H, 3×H-21); ^{13}C NMR (100 MHz, $CDCl_3$): δ 173.2, 134.4, 133.1, 126.5, 122.7, 122.5, 112.5, 110.5, 106.8, 67.4, 61.5, 43.2, 43.1, 40.4, 36.7, 36.6, 32.7, 32.0, 27.9, 26.9, 22.4 and 13.8; LC-MS (ESI): *m/z* 354 $[M+H]^+$; purity (HPLC): 97% (t_r = 12.05 min).

(5*R*,8*S*,10*R*)-1,6-Dimethyl-8-(hexanoyl)aminomethyl-ergoline (5.20)

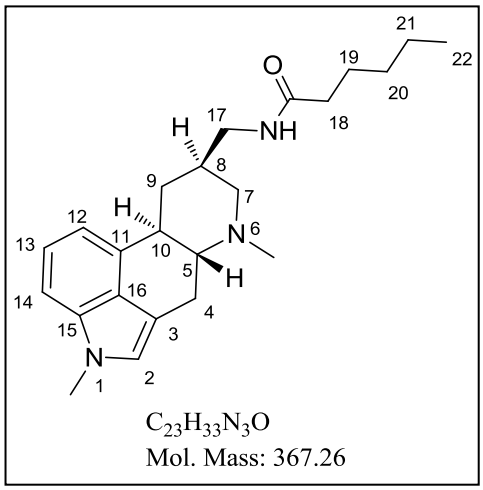

$C_{23}H_{33}N_3O$
Mol. Mass: 367.26

White solid (0.050 g obtained from 0.070 g of **5.2**, 52%); R_f 0.5 (10% Methanol:DCM); Mp. 133-135 °C; ^{1}H NMR (400 MHz, $CDCl_3$): δ 7.18 (t, *J* = 7.1 Hz, 1H, H-13), 7.11 (d, *J* = 8.2 Hz, 1H, H-12), 6.88 (d, *J* = 7.1 Hz, 1H, H-14), 6.73 (s, 1H, H-2), 5.67 (t, *J* = 5.4 Hz, 1H, NH), 3.76 (s, 3H, N1-CH_3), 3.39 (dd, *J* = 14.7, 4.3 Hz, 1H, H-4), 3.35-3.24 (m, 2H, 2×H-17), 3.14-3.06 (m, 2H, H-7 and H-10), 2.85-2.78 (m, 1H, H-4), 2.70-2.64 (m, 1H, H-9), 2.55 (s, 3H, N6-CH_3), 2.32-2.18

(m, 2H, H-5 and H-8), 2.21 (t, *J* = 7.4 Hz, 2H, 2×H-18), 2.11 (t, *J* = 11.4 Hz, 1H, H-7), 1.68-1.61 (m, 2H, 2×H-19), 1.38-1.26 (m, 4H, 2×H-20 and 2×H-21), 1.19 (q, *J* = 12.3 Hz, 1H, H-9), 0.90 (t, *J* = 6.9 Hz, 3H, 3×H-22); ^{13}C NMR (100 MHz, $CDCl_3$): δ 174.0, 134.4, 130.0, 125.8, 123.1, 122.9, 112.9, 107.7, 107.4, 67.8, 60.2, 42.1, 41.6, 38.2, 36.6, 34.8, 32.8, 31.5, 30.9, 25.3, 24.9, 22.4 and 13.9; LC-MS (ESI): *m/z* 368 $[M+H]^+$; purity (HPLC): 99% (t_r = 13.07 min).

(5*R*,8*S*,10*R*)-1,6-Dimethyl-8-(heptanoyl)aminomethyl-ergoline (5.21)

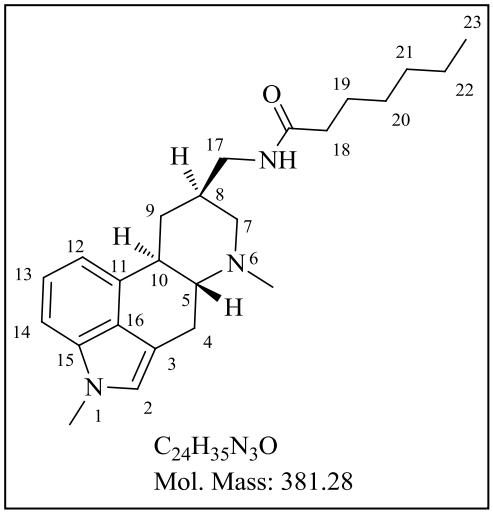

White solid (0.070 g obtained from 0.100 g of **5.2**, 49%); R_f 0.6 (10% Methanol:DCM); Mp. 146-148 ^{o}C; ^{1}H NMR (400 MHz, $CDCl_3$): δ 7.18 (t, *J* = 7.1 Hz, 1H, H-13), 7.11 (d, *J* = 8.2 Hz, 1H, H-12), 6.88 (d, *J* = 7.1 Hz, 1H, H-14), 6.73 (s, 1H, H-2), 5.67 (t, *J* = 5.4 Hz, 1H, NH), 3.75 (s, 3H, N1-CH_3), 3.39 (dd, *J* = 14.7, 4.3 Hz, 1H, H-4), 3.35-3.24 (m, 2H, 2×H-17), 3.14-3.06 (m, 2H, H-7 and H-10), 2.85-2.78 (m, 1H, H-4), 2.70-2.64 (m, 1H, H-9), 2.55 (s, 3H, N6-CH_3), 2.33-2.19 (m, 2H, H-5 and H-8), 2.21 (t, *J* = 7.4 Hz, 2H, 2×H-18), 2.11 (t, *J* = 11.4 Hz, 1H, H-7), 1.69-1.62 (m, 2H, 2×H-19), 1.38-1.26 (m, 6H, 2×H-20, 2×H-21 and 2×H-22), 1.19 (q, *J* = 12.3 Hz, 1H, H-9), 0.89 (t, *J* = 6.9 Hz, 3H, 3×H-23); ^{13}C NMR (100 MHz, $CDCl_3$): δ 173.3, 134.4, 132.5, 126.3, 122.7, 122.6, 112.6, 110.0, 107.0, 67.4, 61.2, 42.9 (2C), 40.0, 36.9, 36.3, 32.7, 31.8, 31.5, 29.0, 26.5, 25.8, 22.5 and 14.0; LC-MS (ESI): *m/z* 382 $[M+H]^+$; purity (HPLC): 99% (t_r = 13.74 min).

(5*R*,8*S*,10*R*)-1,6-Dimethyl-8-(Octanoyl)aminomethyl-ergoline (5.22)

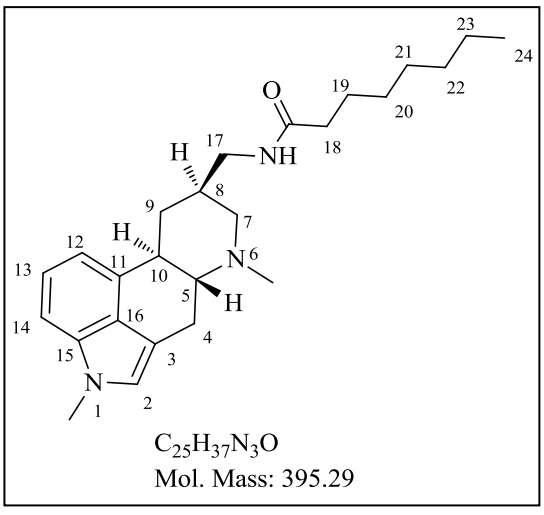

Off-white solid (0.078 g obtained from 0.100 g of **5.2**, 53%); R_f 0.5 (10% Methanol:DCM); Mp. 141-143 ^{o}C; ^{1}H NMR (400 MHz, $CDCl_3$): δ 7.18 (t, *J* = 7.1 Hz, 1H, H-13), 7.10 (d, *J* = 8.2 Hz, 1H, H-12), 6.88 (d, *J* = 7.1 Hz, 1H, H-14), 6.72 (s, 1H, H-2), 5.60 (t, *J* = 5.4 Hz, 1H, NH), 3.74 (s, 3H, N1-CH_3), 3.38 (dd, *J* = 14.7, 4.3 Hz, 1H, H-4), 3.30-3.26 (m, 2H, 2×H-17), 3.06-2.95 (m, 2H, H-7 and H-10), 2.74-2.63 (m, 2H, H-4 and H-9),

2.48 (s, 3H, N6-CH_3), 2.21 (t, J = 7.4 Hz, 2H, 2×H-18), 2.19-2.08 (m, 2H, H-5 and H-8), 2.01 (t, J = 11.3 Hz, 1H, H-7), 1.70-1.62 (m, 2H, 2×H-19), 1.36-1.25 (m, 8H, 2×H-20, 2×H-21, 2×H-22 and 2×H-23), 1.17 (q, J = 12.3 Hz, 1H, H-9), 0.88 (t, J = 6.9 Hz, 3H, 3×H-24); ^{13}C NMR (100 MHz, $CDCl_3$): δ 173.2, 134.4, 133.1, 126.5, 122.7, 122.5, 112.5, 110.5, 106.8, 67.4, 61.4, 43.2, 43.1, 40.4, 36.9, 36.6, 32.7, 32.0, 31.7, 29.3, 29.0, 26.8, 25.8, 22.6 and 14.0; LC-MS (ESI): *m/z* 396 $[M+H]^+$; purity (HPLC): 99% (t_r = 14.56 min).

(5*R*,8*S*,10*R*)-1,6-Dimethyl-8-(decanoyl)aminomethyl-ergoline (5.23)

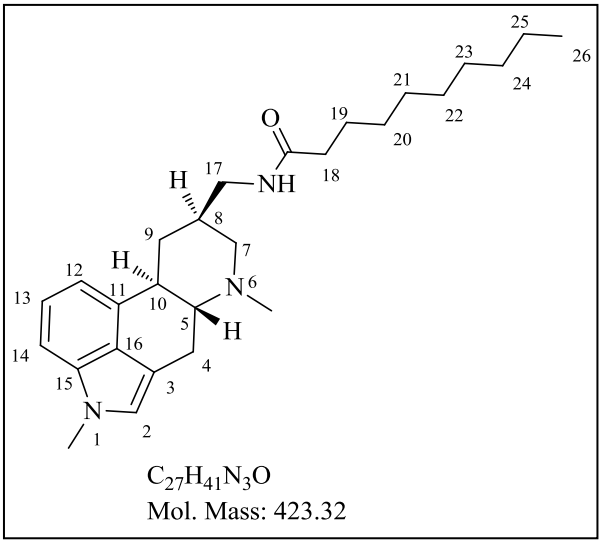

Light-yellow solid (0.050 g obtained from 0.050 g of **5.2**, 64%); R_f 0.5 (10% Methanol:DCM); Mp. 138-140 ^oC; ^{1}H NMR (400 MHz, $CDCl_3$): δ 7.18 (t, J = 7.1 Hz, 1H, H-13), 7.11 (d, J = 8.2 Hz, 1H, H-12), 6.88 (d, J = 7.0 Hz, 1H, H-14), 6.73 (s, 1H, H-2), 5.56 (br s, 1H, NH), 3.75 (s, 3H, N1-CH_3), 3.39 (dd, J = 14.7, 4.3 Hz, 1H, H-4), 3.33-3.26 (m, 2H, 2×H-17), 3.10-3.01 (m, 2H, H-7 and H-10), 2.80-2.73 (m, 1H, H-4), 2.68-2.65 (m, 1H, H-9), 2.52 (s, 3H, N6-CH_3), 2.27-2.15 (m, 4H, H-5, H-8 and 2×H-18), 2.06 (t, J = 11.3 Hz, 1H, H-7), 1.69-1.62 (m, 2H, 2×H-19), 1.38-1.14 (m, 13H, H-9, 2×H-20, 2×H-21, 2×H-22, 2×H-23, 2×H-24 and 2×H-25), 0.88 (t, J = 6.9 Hz, 3H, 3×H-26); ^{13}C NMR (100 MHz, $CDCl_3$): δ 173.3, 134.4, 132.8, 126.4, 122.7, 122.6, 112.5, 110.2, 106.9, 67.4, 61.3, 43.1 (2C), 40.2, 36.9, 36.5, 32.7, 31.9, 31.8, 29.4, 29.3 (2C), 29.2, 26.7, 25.8, 22.6 and 14.0; LC-MS (ESI): *m/z* 424 $[M+H]^+$; purity (HPLC): 99% (t_r = 15.80 min).

(5*R*,8*S*,10*R*)-1,6-Dimethyl-8-(cyclopentanoyl)aminomethyl-ergoline (5.24)

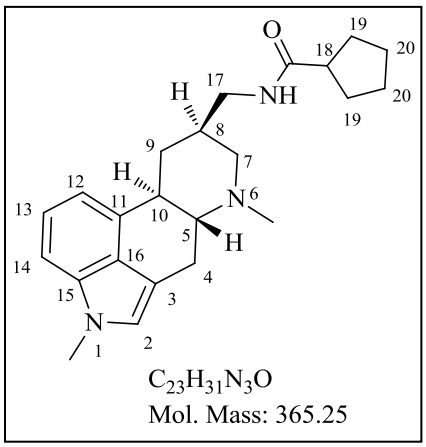

Light-yellow solid (0.060 g obtained from 0.070 g of **5.2**, 63%); R_f 0.5 (10% Methanol:DCM); Mp. 145-147 ^oC; ^{1}H NMR (400 MHz, $CDCl_3$): δ 7.18 (t, J = 7.1 Hz, 1H, H-13), 7.11 (d, J = 8.2 Hz, 1H, H-12), 6.88 (d, J = 7.1 Hz, 1H, H-14), 6.73 (s, 1H, H-2), 5.57 (t, J = 5.4 Hz, 1H, NH), 3.75 (s, 3H, N1-CH_3), 3.39 (dd, J = 14.7, 4.3 Hz, 1H, H-4), 3.31-3.27 (m, 2H, 2×H-17), 3.09-3.00 (m, 2H, H-7 and H-10), 2.78-2.72 (m, 1H, H-4), 2.69-2.63 (m, 1H, H-9), 2.58-

2.48 (m, 1H, H-18), 2.51 (s, 3H, N6-CH_3), 2.25-2.12 (m, 2H, H-5 and H-8), 2.05 (t, J = 11.3 Hz, 1H, H-7), 1.93-1.71 (m, 6H, 2×H-19 and 4×H-20), 1.65-1.54 (m, 2H, 2×H-19), 1.19 (q, J = 12.2 Hz, 1H, H-9); ^{13}C NMR (100 MHz, $CDCl_3$): δ 176.3, 134.4, 132.9, 126.4, 122.7, 122.5, 112.5, 110.3, 106.9, 67.4, 61.4, 46.0, 43.1(2C), 40.3, 36.6, 32.7, 31.9, 30.5, 30.5, 26.7, 25.9 (2C); LC-MS (ESI): *m/z* 366 $[M+H]^+$; purity (HPLC): 97% (t_r = 12.28 min).

(5*R*,8*S*,10*R*)-1,6-Dimethyl-8-(2-piperidinoyl)aminomethyl-ergoline (5.25)

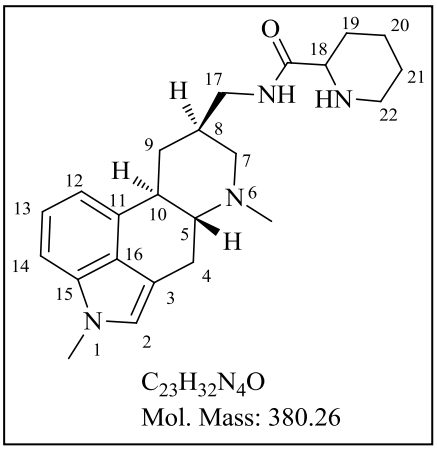

$C_{23}H_{32}N_4O$
Mol. Mass: 380.26

Yellow solid (0.117 g obtained from 0.200 g of **5.2**, 41%); R_f 0.8 (20% Methanol:DCM); Mp. 124-126 ^oC; ^{1}H NMR (400 MHz, $CDCl_3$): 7.18 (t, J = 7.1Hz, 1H, H-13), 7.11 (d, J = 8.2 Hz, 1H, H-12), 7.08 (br s, 1H, NH), 6.89 (d, J = 7.0 Hz, 1H, H-14), 6.72 (s, 1H, H-2), 3.75 (s, 3H, N1-CH_3), 3.38 (dd, J = 14.7, 4.3 Hz, 1H, H-4), 3.34-3.19 (m, 3H, 2×H-17 and H-18), 3.12-3.05 (m, 2H, H-7 and H-22), 3.03-2.97 (m, 1H, H-10), 2.76-2.57 (m, 4H, H-4, H-9, H-19 and H-22), 2.51 (s, 3H, N6-CH_3), 2.25-2.11 (m, 2H, H-5 and H-8), 2.07-2.00 (m, 2H, H-7 and H-19), 1.85-1.78 (m, 1H, H-20), 1.64-1.57 (m, 1H, H-20), 1.52-1.39 (m, 2H, 2×H-21), 1.18 (q, J = 12.4 Hz, 1H, H-9); ^{13}C NMR (100 MHz, $CDCl_3$): δ 173.9, 134.4, 132.9, 126.4, 122.7, 122.5, 112.6, 110.3, 106.9, 67.4, 61.4, 60.3, 45.8, 43.1, 42.6, 40.4, 36.5, 32.7, 31.9, 30.0, 26.7, 25.8 and 24.9; LC-MS (ESI): *m/z* 381 $[M+H]^+$; purity (HPLC): 98% (t_r = 8.45 min).

7.3 The biological assays procedures for target compounds

7.3.1 Antimycobacterial evaluation protocol

All the target compounds were evaluated against the H37Rv strain of *Mtb* using the broth microdilution method.[9] This method allows a range of compound concentrations to be tested on a single 96-well microtitre plate in order to determine the minimum inhibitory concentration (MIC).

A 10 ml culture of *Mtb* (H37RvMa)[10,11] was grown to an OD_{600} of 0.6 - 0.7. The culture was then diluted 1:100 in GAST/Fe medium. In a 96-well microtitre plate, 50 µl of GAST/Fe medium was added to all wells from Rows 2-12. The compound to be tested was added to Row 1 in duplicate, at a final concentration of 640 µM (stock was made up to a concentration of 12.8 mM in DMSO, and diluted to 640 µM in GAST/Fe medium). A two-fold serial

dilution was prepared, by transferring 50 µl of the liquid in Row 1 to Row 2 and aspirated to mix. 50 µl of the liquid in Row 2 was then transferred to Row 3 and aspirated, and so on. This procedure was repeated until Row 12 was reached, from which 50 µl of the liquid was discarded so as to bring the final volume in all wells to 50 µl. Finally, 50 µl of the 1:100 diluted *Mtb* cultures was added to all wells in Rows 2-12. Cells were not added to Row 1, as this serves as a contamination control. Controls include media only, 5% DMSO, rifampicin and kanamycin. The microtitre plate was stored in secondary container and incubated at 37 °C with humidifier to prevent evaporation of liquid. The lowest concentration of compound that inhibits growth of more than 99% of the bacterial population was considered to be the MIC_{99}. MIC_{99} values were scored visually at 7-days and 14-days post inoculation.

GAST/Fe media: 1L in distilled water contains:
0.3 g of Bacto Casitone (Difco)
4.0 g of dibasic potassium phosphate
2.0 g of citric acid
1.0 g of L-alanine
1.2 g of magnesium chloride hexahydrate
0.6 g of potassium sulfate
2.0 g of ammonium chloride
1.80 ml of 10 M sodium hydroxide
10.0 ml of glycerol
$Tween_{80}$ was added to 0.05%.
0.05 g of ferric ammonium citrate

Dissolve above components in distilled water. Adjust pH to 6.6 if necessary, then filter sterilize (0.2 µM filter) and store at 37 °C.

7.3.2 Antiplasmodial evaluation protocol

The *in vitro* antiplamodial testing of compounds was performed against the NF54 strain of *P. falciparum* using method as described by Desjardins *et al*.[12] Uptake of [^{3}H]-hypoxanthine was used as a marker of parasite growth. Chloroquine and artesunate were used as positive controls.

Materials: Screening Medium: RPMI 1640 (10.44 g/l) (no hypoxanthine) supplemented with HEPES (5.94 g/l), $NaHCO_3$ (2.1 g/l), Neomycin (100 microg/ml) + Albumax II (5 g/l);

Human red blood cells: 50% haematocrit; [^{3}H]-hypoxanthine: dilute stock (5mCi/5ml) ½ with 50% EtOH. 1ml aliquots were then diluted 1/50 with screening medium ready to use.

Plates: Falcon 96-well microtiter plates (No. 353072)
Gas: 37 °C; 93% N_2, 4% CO_2, 3% O_2

Preparation of stock solution: Compounds were dissolved in DMSO at 10 mg/ml. The stocks were kept at 4 °C. For the assays, fresh 4X dilutions of all compounds in screening medium were prepared.

Assay procedure: Blood smears of stock cultures of the NF54 strain were prepared and parasitemia was determined (parasitemia < 3% should not be used). Compound stock solutions were diluted with screening medium to the right start concentrations. Infected red cells solution was prepared as parasitemia (p) of 0.3%, and hematocrit (h) of 2.5%, therefore the final concentration of p and h in the assay were 0.3 and 2.5%, respectively.

Calculation example for one 96-well plate:
Goal: 10 ml of 0.3% parasitemia / 2.5% hematocrit
Start solutions:
- Human erythrocytes (50% hematocrit)
- Continuous culture with 5% parasitemia (with 5% hematocrit)
1. 0.3% parasitemia = (x ml * 5% p)/ (10 ml /2); x= 0.3 ml of infected culture
2. 2.5% hematocrit = [(0.3 ml*5% hematocrit) + (x ml*50% hematocrit)]/10 ml; x = 0.47 ml of blood
3. 10 ml – 0.3 ml – 0.47 ml = 9.23 ml of screening medium
Mix these three volumes to obtain 10 ml of 0.3% parasitemia / 2.5% hematocrit solution
1 ml of un-infected red cells solution was prepared (no parasites, 2.5% hematocrit) by mixing 50 µl of washed human erythrocytes (50% hematocrit) with 950 µl screening medium. 100 µl of this were added to each well of the microtiter plate (multipette). 100 µl of screening medium, containing 4x the highest compound concentration, were added to wells in row B. Serial drug dilutions were prepared with a multichannel pipette. 100 µl were taken from wells of row B and transferred, after gentle mixing, to wells of row C. After mixing, 100 µl were transferred from wells of row C to wells of row D and so forth to row H. The 100 µl removed from wells of row H were discarded. A two-fold serial dilution of compounds was thus

obtained. For too active compounds the highest concentration was appropriately lowered. Wells of rows A served as controls without drug.

100 µl of infected blood (parasitemia of 0.3%, 2.5% hematocrit) were added to all wells with a multipette. Only the control wells (A9-12) got uninfected blood of 2.5% hematocrit. The plates were incubated in an incubation chamber at 37 °C in an atmosphere containing the special gas mixture (93% N_2, 4% CO_2, 3% O_2). After 48 hours 50 µl [^{3}H]-hypoxanthine (= 0.5 µCi) solution were added to each well of the plate. The plates were incubated for another 24 hours. The plates then were harvested with a BetaplateTM cell harvester (Wallac, Zurich, Switzerland), which transfers the red blood cells onto a glass fiber filter and washes with distilled water. The dried filters were inserted into a plastic foil with 10 ml of scintillation fluid and counted in a BetaplateTM liquid scintillation counter (Wallac, Zurich, Switzerland). The results were recorded as counts per minute (cpm) per well at each compound concentration.

Finally, Data were transferred into a graphic programme and expressed as percentage of the untreated controls. The 50% inhibitory concentration (IC_{50}) value is evaluated by Logit regression analysis.

7.3.3 Cytotoxicity evaluation protocol

Compounds were screened for *in vitro* cytotoxicity against a mammalian cell-line, Chinese Hamster Ovarian (CHO) using the 3-(4,5-dimethylthiazol-2-yl)-2,5-diphenyltetrazoliumbromide (MTT)-assay. The MTT-assay is used as a colorimetric assay for cellular growth and survival, and compares well with other available assays.[13,14] The tetrazolium salt MTT was used to measure all growth and chemosensitivity. Compounds were tested in triplicate on one occasion.

The test compounds were prepared to a 20 mg/ml stock solution in 100% DMSO and stored at -20 ºC until use. Dilutions were prepared on the day of the experiment. Emetine was used as the reference drug in all experiments. The initial concentration of emetine was 100 µg/ml, which was serially diluted in complete medium with 10-fold dilutions to give 6 concentrations, the lowest being 0.001 µg/ml. The same dilution technique was applied to the all test compounds. The 50% inhibitory concentration (IC_{50}) values were obtained from full dose-response curves, using a non-linear dose-response curve fitting analysis via GraphPad Prism v.4 software.

7.3.4 *In vivo* pharmacokinetic evaluation protocol

7.3.4.1 Compound administration and samples collection

The studied compounds were administered via 2 routes: per oral (p.o) and intravenous (i.v) administration. For oral administration, compounds were prepared in 0.5% (hydroxypropyl) methyl cellulose in 10% DMSO and administered via oral gavage to three female C57BL/6 mice to achieve a single dose of 20 mg/kg body weight, while compounds administered intravenously were prepared in the mixture [10% DMSO, 30% polyethylene glycol (PEG), 60% of the mixture (10% Ethanol, 80% Propylene Glycol, 10% Tween20)] and injected through the penile vein of three male C57BL/6 mice to achieve a single dose of 5 mg/kg body weight. Mice whole blood was collected at 30 min, 1, 3, 5, 7 and 24 h for oral and 5 min, 30 min, 1, 3, 5, 7 and 24 h for intravenous administration. Collected blood samples were mixed using a vortex and stored at -80 °C until analysis.

7.3.4.2 Quantification of compounds plasma level

(a) Calibration standard

Stock solutions of tested compounds were prepared in DMSO at a concentration of 1 mg/mL. The solutions were then diluted in mice blood to obtain standard (S) 1 at a concentration of 4000 ng/mL. Subsequently, S2 (2000 ng/mL), S3 (1000 ng/mL), S4 (500 ng/mL), S5 (250 ng/mL), S6 (125 ng/mL), S7 (62.5 ng/mL), S8 (31.25 ng/mL) and S9 (15.625 ng/mL) were prepared by serial dilution. The calibration standards were briefly mixed by vortexing and stored at −80 °C until analysis. The calibration standards were analysed in duplicate in each study sample batch.

(b) Compounds and standards extraction

To extract compounds, 20 µL of standards and whole blood samples were thawed on ice. The internal standard, prednisolone, was diluted in acetonitrile at the final concentrations of 1200 ng/ml. One hundred (100) µL of internal standard solution were then added to 20 µL of blood samples and mixed by vortexing for 1 min, then centrifuged at 1500*g* for 5 min at room temperature (25 ^{o}C). The supernatant (approximately 80 µL) was transferred to a clean tube. A “blank” and a “double blank” were equally included in the analysis; these two samples consisted of whole blood containing none of the tested compounds. The difference between the blank and the double blank is that the first sample is extracted using the solvent containing the internal control while the latter is only extracted with the solvent.

(c) Chromatography and mass spectrometry

Compounds were quantified using an Agilent 1100 HPLC (Agilent technologies, USA) connected in tandem to an AB Sciex API 2000 mass spectrometer (AB SCIEX, 110 Marsh Drive, Foster City, California, USA) equipped with a turbo ion spray (ESI) source. The software Analyst 1.5.1 was used to control both, the liquid chromatogram and the mass spectrometer. The Gemini 3u C18 110A (50 × 2.0 mm, 5 µm) column (Phenomenex, USA) was used for compounds separation. The mobile phases consisted of a gradient of acetronitrile and 0.1% formic acid or a gradient of acetonitrile and 5 mM ammonium acetate. The system operated at a flow rate of 0.4 ml/min and the volume of injection was 5 µL. The ESI interface was used in positive mode and the turbo ion spray source was heated to 300 °C. The AB Sciex API 2000 mass spectrometer was operated at unit resolution in the multiple reaction monitoring (MRM) mode, monitoring the transition of the protonated molecular ions to the product ions.

(d) Calculation of pharmacokinetic parameters

The normalized plasma concentrations were plotted as a function of sampling time. The pharmacokinetic parameters of each compound were determined using the PK Solutions 2.0, non-compartment Data Analysis software (Ashland OH, USA).

7.4 References

(1) Godtfredsen, W. O.; Daehne, V. W.; Tybring, L.; Vangedal, S. Fusidic Acid Derivatives. I. Relationship between Structure and Antibacterial Activity. *J. Med. Chem.* **1966**, *9*, 15–22.

(2) Acornley, J. E.; Bessell, C. J.; Bynoe, M. L.; Godtfredsen, W.; Knoyle, J. M. Antiviral Activity of Sodium Fusidate and Related Compounds. *Br. J. Pharmac. Chemother.* **1967**, *31*, 210–220.

(3) Duvold, T.; Bretting, C. A. S.; Rasmussen, P. A. ; Bouerat, L.; Thorhauge, J. Novel Fusidic Acid Derivatives. WO2005007669 A1, 2005.

(4) Duvold, T. Novel Polyaminated Fusidic Acid Derivatives. WO2002077007 A2, 2002.

(5) Von Daehne, W.; Rasmussen, P. R. l6-Ethers Of Fusidic Acid Derivatives. US4060606, 1977.

(6) Janssen, G.; Vanderhaeghe, H. Modification of the Side Chain of Fusidie Acid (Ramycin). *J. Med. Chem.* **1967**, *10*, 205–208.

(7) Dosa, P. I.; Ward, T.; Walters, M. A.; Kim, S. W. Synthesis of Novel Analogs of Cabergoline: Improving Cardiovascular Safety by Removing 5-HT2B Receptor Agonism. *ACS Med. Chem. Lett.* **2013**, *4*, 254–258.

(8) Camerino, B.; Patelli, B.; Glaesser, A. Derivatives of 6-Methyl and 1,6-Dimethyl Ergoline. U.S. Patent 3238211, 1966.

(9) Collins, L. A.; Franzblau, S. G. Microplate Almar Blue Assay versus BACTEC 460 System for High-Throughput Screeing of Compunds against Mycobacterium Tuberculosis and Mycobacterium Avium. *Antimicrob. Agents Chemother.* **1997**, *41*, 1004–1009.

(10) Collins, L. A.; Torrero, M. N.; Franzblau, S. G. Green Fluorescent Protein Reporter Microplate Assay for High-Throughput Screening of Compounds against Mycobacterium Tuberculosis. *Antimicrob. Agents Chemother.* **1998**, *42*, 344–347.

(11) Ioerger, T. R.; Feng, Y.; Ganesula, K.; Chen, X.; Dobos, K. M.; Fortune, S.; Jacobs, W. R.; Mizrahi, V.; Parish, T.; Rubin, E.; Sassetti, C.; Sacchettini, J. C. Variation among Genome Sequences of H37Rv Strains of Mycobacterium Tuberculosis from Multiple Laboratories. *J. Bacteriol.* **2010**, *192*, 3645–3653.

(12) Desjardins, R. E.; Canfield, C. J.; Haynes, J. D.; Chulay, J. D. Quantitative Assessment of Antimalarial Activity In Vitro by a Semiautomated Microdilution Technique. *Antimicrob. Agents Chemother.* **1979**, *16*, 710–718.

(13) Rubinstein, L. V; Shoemaker, R. H.; Paull, K. D.; Simon, R. M.; Tosini, S.; Skehan, P.; Scudiero, D. a; Monks, A.; Boyd, M. R. Comparison of In Vitro Anticancer-Drug-Screening Data Generated With a Tetrazolium Assay Versus a Protein Assay against a Diverse Panel of Human Tumor Cell Lines. *J. Natl. cancer Inst.* **1990**, *82*, 1113–1118.

(14) Mosmann, T. Rapid Colorimetric Assay for Cellular Growth and Survival: Application to Proliferation and Cytotoxicity Assays. *J. Immunol. Methods* **1983**, *65* (1), 55–63.